Multidrug Resistance in Breast and Bladder Cancer Cell lines

A thesis submitted for the degree of

Doctor of Philosophy

in

The Faculty of Clinical Sciences

University College London Medical School

University of London

by

Claire Louise Davies

August 1998

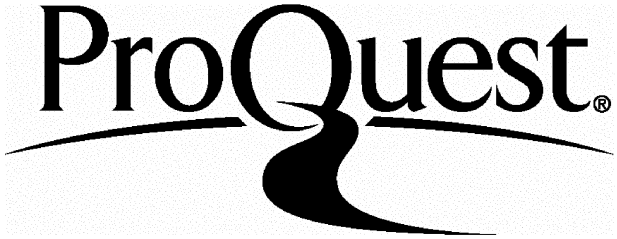

ABSTRACT

Multidrug resistance (MDR) in cancer cells defines a phenotype of cellular cross-resistance to a broad spectrum of structurally and functionally unrelated cytotoxic drugs. This phenomenon leads to lowered cellular drug uptake and therefore lowered cell death. To try and reverse or circumvent MDR many different types of MDR modulator are being produced and investigated, including essential fatty acids (EFA).

This study investigated chemotherapeutic drug uptake and intracellular localisation within drug sensitive and MDR human breast and bladder cancer cell lines. In general a difference in drug uptake, accumulation and intracellular localisation was observed between sensitive and resistant cells. The sensitive cells showed predominantly nuclear localisation of the drugs with little in the cytoplasm. The resistant cells displayed mainly cytoplasmic intracellular drug distribution with reduced overall drug accumulation compared to the sensitive cells.

The presence and location of proteins believed to be involved with drug efflux from the cells and hence cellular resistance were investigated in the cell lines and breast and bladder cancer tissue. The drug efflux pumps studied were P-glycoprotein (Pgp), lung resistance protein (LRP) and multidrug resistance associated protein (MRP). From this study Pgp was shown to be present and believed to be the main mechanism of drug efflux functioning in these resistant cells lines.

Finally, the thesis was concerned with one method of increasing drug uptake in the resistant cells by using the EFA γ-linolenic acid (GLA). Modulation of drug uptake and intracellular localisation in resistant cells due to GLA incorporation was drug dependent. The addition of GLA to these cell lines did not affect the profile of the resistance proteins.

The field of MDR is changing continually with new mechanisms being discovered. This study gives an insight into cellular MDR and efflux pumps. As the way forward clinically appears to be with adjuvant therapy, the modulation of MDR, such as with GLA, warrants further investigations.

ACKNOWLEDGMENTS

I would like to express my thanks to Scotia Pharmaceuticals and Prof. Taylor, the former who funded this project and the latter who gave me the chance to undertake it.

I offer a most sincere and grateful thanks to:

Marilena, not only a supervisor but dear friend,
without whose help this thesis would not have been penned,
The two Alans in my life,
who could have done without my trouble and my strife,
Many friends who have kept me sane,
Amanda, Saskia, Tracey, Gyorgyi, Jenny and Jane,
All of those who, my research aided and abetted
for from flow to confocal, cell assays and staining they vetted,
Without peoples help, time and wits being pitted
this thesis could not have been completed and submitted,
But above all the person I thank the most
without whose support this thesis I could not boast
is the one with whom I share my fate
and to whom this thesis I do dedicate.

For Stewart,

Est foris veritis,

ABBREVIATIONS

AA	Arachidonic acid
AD	Actinomycin D
ATP	Adenosine triphosphate
ABC	ATP binding cassette
BSA	Bovine serum albumin
cDNA	complementary deoxyribonucleic acid
CCD	Charge-coupled device
CHO	Chinese hamster ovarian
CLSM	Confocal and laser scanning microscopy
Cy 3	Cyanine 3
DMEM	Dulbecco's Modified Eagle's Medium
DHA	Docosahexanoic acid
DMSO	Dimethyl sulphoxide
DNA	Deoxyribonucleic acid
DOX	Doxorubicin
EDTA	Ethylene diamine tetra-acetic acid
EFA	Essential fatty acid
EPA	Eicosapentanoic acid
EPI	Epirubicin
FA	Fatty acid
FBS	Foetal bovine serum
FCS	Forward scatter
FITC	Fluorescein isothiocyanate
GLA	Gamma linolenic acid
HEPES	N-2-Hydroxyethylpiperazine-N'-2-ethanesulfonic acid
HLA	Human leukocyte antigen
ICRF	Imperial Cancer Research Fund
IDA	Idarubicin
Ig	Immunoglobulin
LA	Linolenic acid
LiGLA	Lithium GLA

LRP	Lung resistance protein
LUT	Look-up table
MDR	Multidrug resistance
MHC	Major histocompatibility complex
mRNA	Messenger ribonucleic acid
MRP	Multidrug-resistance associated protein
MTT	3-(4,5-dimethylthlazol-2-yl)-2,5-diphenyl tetrazolium
MTZ	Mitozantrone
NPC	Nuclear pore complex
PBS	Phosphate buffered saline
PG	Prostaglandins
Pgp	P-glycoprotein
PKC	Protein kinase C
PLC	Prelysosomal sorting compartment
PUFA	Polyunsaturated fatty acid
SSC	Side scatter
TAP	Transporter associated with antigen presentation
topoI / II	Topoisomerase I / II
TRITC	Tetramethyl rhodamine isothiocyanate

CONTENTS

2.B. Methods

Chapters 3-6. RESULTS

3. Differences in Anthracycline Uptake Between Sensitive and Resistant Cells

4. Intracellular Incorporation of GLA

LIST OF FIGURES, GRAPHS AND TABLES

Graphs 3.2f-k. Drug dose response curves:

Figs. 3.1-3.16. Patterns of intracellular drug localisation:

INTRODUCTION

As a high percentage of cancers are not curable by conventional methods of treatment, such as surgery, radiation therapy and chemotherapy, new methods for successful cancer treatment are constantly being sought. These include ways of enhancing cancer cell death by increasing the success of existing therapies. One of the major obstacles in the use of chemotherapy against cancer is the onset of cellular multidrug resistance (MDR). This phenomenon leads to lowered cellular drug uptake and, therefore, lowered cancer cell death. To try and reverse or circumvent MDR many different types of modulators are being produced and investigated, including the use of essential fatty acids (EFA).

EFAs have been found to be selectively cytotoxic to human cancer cells compared to normal human cells *in vitro*. In some cases, when EFAs are added to cancer cells which are being treated with chemotherapeutic drugs there is an increase in cell death. This increase may be through additive or synergistic cell killing by the two cytotoxics. The exact mechanism of cellular modulation by the EFAs leading to increased cellular drug uptake and cell death are still not fully understood.

This study investigated the presence of MDR and the use of an EFA in enhancing the effectiveness of chemotherapy drugs against human breast and bladder cancer cell lines.

1.1. MULTIDRUG RESISTANCE IN CANCER

Multidrug resistance (MDR) defines a phenotype of cellular cross resistance to a broad spectrum of structurally and functionally unrelated cytotoxic drugs[1]. There are two fundamental types of resistance i) inherent resistance: where there is no significant response to chemotherapy by the cancer and more commonly, ii) acquired resistance: where the cancer initially responds to chemotherapy but then acquires resistance during the course of therapy. Both lead to a lowering of bioactive drug levels within the cancer cells and hence decreased cell death.

Of approximately 1,000,000 new patients per year with cancer about 50%

can be cured by surgery and radiation therapy as their tumours have not spread. Of the remaining 50%, about 10%, including choriocarcinoma, acute lymphocytic leukaemia, Hodgkins disease and testicular cancer are curable with systemic chemotherapy. However, the majority of metastatic cancers are not currently curable by chemotherapy or any other kind of therapy[2]. One group of cancers falling into the MDR category are the solid tumours, such as colon, breast and bladder cancer. The occurrence of drug resistance in tumours has been observed and discussed since 1946, the time of first clinical use of cancer chemotherapy[3].

Multidrug resistance was first described in 1970 after the selection of Chinese hamster ovarian (CHO) cancer cells exposed to increasing concentrations of actinomycin D (AD)[4]. Increase in resistance to AD in a series of cell lines was accompanied by a proportional decrease in sensitivity to vincristine and daunomycin; furthermore several daunomycin-resistant cell lines also exhibited increased resistance to AD. In general, the higher molecular weight drugs produce greater cross-resistance to an agent[4]. Thus, these cells proved to be resistant to a range of clinically important anti-cancer drugs, including the anthracyclines (such as doxorubicin), the Vinca alkaloids and colchicine, although originally they had been selected by a single agent.

Several unrelated mechanisms have been identified that mediate biologically unrelated forms of tumour multidrug resistance[5] and other mechanisms are being investigated continually. As there appears to be no clear cut universal mechanism for multidrug resistance, there is also no direct method of reversal. The classical form of MDR, which was the first to be discovered and the most thoroughly investigated, involves the overexpression of a membrane glycoprotein (Pgp)[6], which is an energy-dependent multidrug efflux pump. Several other transporter molecules have been implicated in MDR including non-Pgp protein pumps, multidrug resistance-associated protein (MRP)[7, 8], vault related MDR (lung resistance protein, LRP)[9] and transporters associated with antigen presentation (TAP)[10]. There are other mechanisms including atypical MDR and those involving the anti-metabolism drugs such as cisplatin.

Although these mechanisms of resistance are not mutually exclusive and several different mechanisms may be operating concurrently to confer resistance to the cells, usually only one MDR protein is inducing drug resistance in cell lines. As

an example, the breast cancer cell line MCF-7 which is drug sensitive contains no Pgp, partial MRP and LRP whilst its MDR counterpart also contains partial MRP and LRP but mainly Pgp which is believed to produce the observed MDR phenotype[10].

The phenomenon of MDR is very intricate and the methods of conferring resistance to cells not completely understood with new mechanisms, in particular those involving transporter molecules, being discovered continually.

1.1.1. RESISTANCE MECHANISMS

This section will mainly deal with the protein pump mechanisms of MDR as those are the ones investigated in this thesis.

P-GLYCOPROTEIN

This was the first MDR mechanism to be described. In 1976, Juliano and Ling showed that overexpression of a membrane protein of 170kDa was responsible for the MDR in cells that had a drug accumulation defect[11]. At first, the accumulation defect was believed to be a fault in the permeability of the cell's membrane, hence the name P (for permeability) -glycoprotein. This was later found to confer resistance, at least in part, through enhanced drug efflux from the cells rather than decreased drug influx[12]. The presence of an energy-dependent efflux system was first demonstrated in experiments producing metabolic inhibition as a result of rendering the medium glucose-free, by addition of 2-deoxyglucose, and adding uncouplers of oxidative phosphorylation, *e.g.* sodium azide[13]. By blocking the supply of energy (ATP) in the cell in this way, the drug resistant cell became indistinguishable from a drug sensitive cell, with the same initial rate of drug uptake and final drug accumulation as found in a sensitive cell.

P-glycoprotein belongs to a superfamily of adenosine triphosphate (ATP) binding cassette (ABC) transporters and functions as an energy-dependent drug efflux pump. Mammalian Pgps are encoded by small *mdr* gene families. These homologous *mdr*-like genes are ubiquitous with three found in mouse, three found in rat[14], and they have also been found in lower eukaryotes *e.g. Drosophila*

melanogaster[15]. A bacterial analogue of the gene has been found to be expressed by *Streptomyces peucetius* but only during anthracycline antibiotic production by this organism[16]. Two highly homologous members have been identified in humans, *mdr1* and *mdr2* or *mdr3*. The latter two genes are identical in sequence but were located and named by two different research groups[17], for future reference the second *mdr* gene will be referred to as *mdr3*. In humans, the *mdr* gene families are localised in a cluster on chromosome 7q21.1 and are linked within 230 kilobases[18]. Mammalian *mdr* genes can be subdivided into different classes: class1A includes the human *mdr1* gene and class 2 includes the human *mdr3* gene. The 2 isoforms of the P-glycoprotein are functionally distinct but with a very high degree of amino acid sequence identity (76%). Direct proof for the role of *mdr1* in MDR was obtained by transfection experiments. Expression of a full length cDNA clone of the human *mdr1* gene in a drug sensitive cell conferred the MDR phenotype[19]. Transfection studies with *mdr3* did not produce evidence for multidrug transporter activity[20]. However, due to the degree of homology between these two proteins it is believed that both classes of Pgp act as ATP-dependent efflux pumps. Like Class1 proteins, Class 2 (*mdr3*) are present in the plasma membranes of various specialised cells in normal tissues such as the liver but in a more restricted distribution[21]. Coexpression of *mdr1* and *mdr3* occurs in the liver, kidney and adrenal gland and spleen[22]. The substrates for class 2 pumps are largely unknown, however in mouse, the equivalent *mdr2* Pgp transports the phospholipid, phosphatidylcholine, from liver hepatocytes into bile ducts[23]. As class 2 pumps are probably not associated with MDR, as they are believed not to transport drugs[20], the rest of this section is devoted to the Class1 Pgp pumps and their involvement in conferring MDR to cancer cells.

It has been shown by many researchers that the gene *mdr*1 encodes for a single peptide chain with a molecular weight of 170kDa [18, 19]. The nucleotide sequence analysis of full-length *mdr* cDNAs indicates that the two halves of the protein are highly homologous[24]. This protein is both phosphorylated, mainly by protein kinase C (PKC) which may regulate its biological activity[25] and glycosylated[2] and known as the P170 glycoprotein (Pgp). It is an integral plasma membrane protein consisting of 1280 amino acids with 12 putative transmembrane regions and two ATP binding sites per molecule duplex, Fig.1.1a.[26].

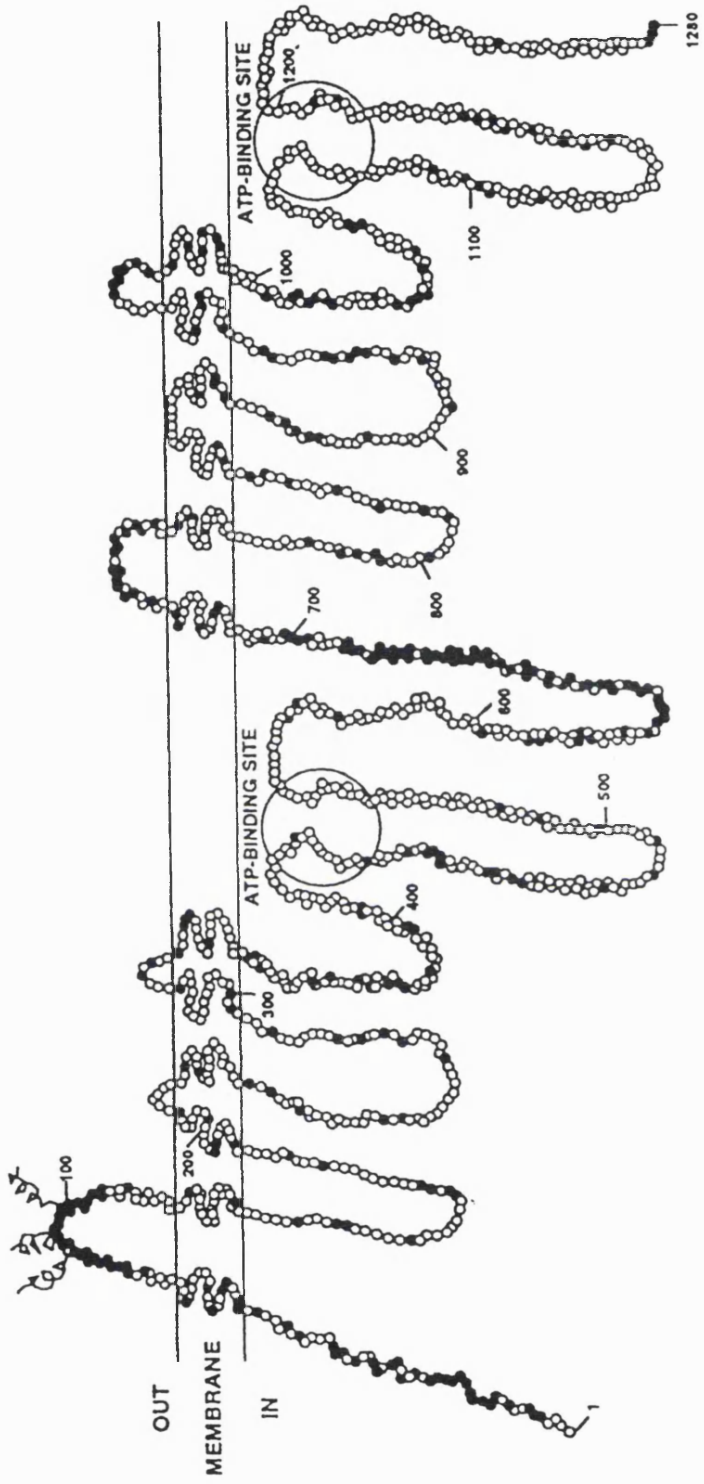

Fig. 1.1a. Two-dimensional model of the human multi-drug transporter polypeptide chain (Pgp) inserted within the cell membrane. The two ATP binding sites are circled.

Taken without permission from Ref. 26.

The orientation of the molecule is such that both the amino- and carboxy-terminus are located on the cytoplasmic side of the plasma membrane. The first extracellular loop carries the carbohydrate portion and is believed to contain several N-linked glycosylation sites. According to this model the two putative nucleotide-binding regions are located intracellularly which is consistent with the postulated ATP-dependent transport activity. These ATP binding sites represent the most conserved regions in P-glycoproteins from the different classes. This probably indicates that they play a pivotal role in the functioning of Pgps[26] as membrane efflux pumps. The transport activity of drugs out of MDR cells requires constant energy provided by either ATP or GTP and although the actual mechanism of drug transport by Pgp is unknown there are two theories. One proposed by Gottesman (1988) is that the two halves of P-glycoprotein come together to form a single channel for drug transport. The major function for the multidrug transporter is to detect drug within the plasma membrane and extrude it from the cell. In this way, when an amphiphilic drug enters a cell by diffusion, the multidrug transporter within the plasma membrane can, using energy transduced from the two essential ATP binding / utilisation sites, remove the drug substrates from the cell through a single channel-like structure[2] Fig.1.1b.

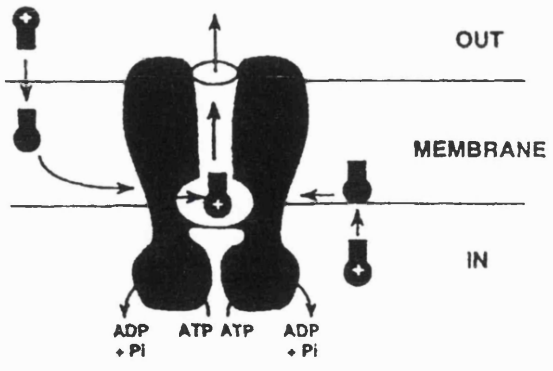

Fig. 1.1b. Hypothetical model for the mechanism of drug transport by Pgp. Showing a single channel-like structure with two ATP binding / utilisation sites. Taken without permission from Ref. 27

The other theory suggests that the pump acts as a flippase and flips the drug from the inner leaflet of the membrane onto the outer leaflet[27]. Pgp is not only associated with plasma membranes at the cell surface but small amounts of it are located in intracellular organelles, such as on the luminal side of Golgi stack

membranes[28]. This observation has led to other speculations about the removal of cytotoxics from the cell. Gervasoni hypothesises that the P-glycoprotein migrates with the recycling plasma membrane vesicles[29]. Various different models depicting endocytotic pathways have been described usually involving transport of lipids *via* a perinuclear compartment to the Golgi then in vesicles to the plasma membrane[30, 31]. One theory involves a structure that has been termed the prelysosomal sorting compartment (PLC) which is located in the perinuclear region and may contain migrating membranous Pgp[29]. As the Pgp would be in the correct orientation it would pump the drug into the vesicles or into the PLC. Once inside the drug would be trapped until the vesicles fused with the plasma membrane and effluxed out of the cell[29]. As anthracyclines are weak bases, and passive diffusion of non-charged molecules across membranes is faster than for protonated forms, net cellular anthracycline accumulation is dependent on pH-gradients across the plasma membrane and in intracellular compartments. So another mechanism for anthracycline efflux could be based on drug-trapping in the acidic endosomal / lysosomal system or the Golgi complex followed by extrusion of the concentrated drug *via* exocytosis[32, 33, 34]. It may be that all these mechanisms are connected and that Pgp requires the drug to be protonated before removal. A calcium channel has been detected in close relationship with the Pgp. Its function, if any, in the removal of drugs is as yet unknown. Drug efflux mediated by Pgp can be specifically tested for as it is competitively inhibited by other drug substrates and by reversing agents, such as Pgp modulation by the calcium channel blocker verapamil[35].

The resistance conferred by this protein includes cross resistance to anticancer drugs such as the anthracyclines, the Vinca alkaloids and mitomycin C but not to alkylating agents and antimetabolites (*e.g.* 5-fluorouracil), or cisplatin[26]. Analysis of the drugs that MDR cells are resistant to, show them to have no strong chemical similarities but they do have physical properties in common. All the drugs are relatively hydrophobic (*i.e.* lipid soluble), amphipathic and many are cationic. None of the drugs affected by the MDR phenotype are anionic, as negatively charged drugs do not appear to be substrates for this multidrug transport system[2]. These drugs also cause many tumours to acquire MDR; for example doxorubicin (DOX) caused the activation of *mdr1* gene at the transcription level[36] leading to overexpression of Pgp and cross resistance.

The physiological role of Pgp is a matter of speculation with the protein being expressed in a cell- and tissue-specific manner[37]. Substantial expression of the *mdr1* gene has been reported in normal adrenal, jejunal, rectal, liver and lung tissues[38, 39]. Other organs and tissues, such as skin, muscle and heart had low or undetectable levels of *mdr1*. Using immunohistochemical techniques, expression of Pgp was found on the biliary surface of the hepatocytes and small biliary ductules in the liver, on the luminal surface of the epithelial cells of the small ductules in the pancreas and on the brush borders of the proximal tubules in the kidney. The colon and jejunum both show high levels of P-glycoprotein on the luminal surface of the mucosa[39]. Hence it is mainly found in specialised epithelial cells with secretory or excretory functions where it is likely to be involved in transport. Lower amounts of Pgp are present in the endothelial cells of the capillary blood vessels at blood-tissue barrier sites, such as in the blood-brain barrier, suggesting that Pgp also exerts a general protective function[40].

From clinical studies, it has been shown that those tumours which are intrinsically resistant *i.e.* have a very low response rate to chemotherapy are usually those which developed from tissues normally expressing high *mdr1* levels, though exceptions have been noted[37]. In a study on normal intestinal cells and the intrinsic drug resistance of colon tumours, it was suggested that enhanced drug efflux is a property of normal cells which may be retained by the tumours. In normal intestinal cells this enhanced outward transport of drug is probably one of the mechanisms involved in the protection of the intestinal epithelium from plant alkaloids and other xenobiotic agents ingested in the diet[41]. This role for Pgp in the protection of normal epithelium from a variety of local and systemic toxins, possibly including carcinogens, has also been suggested for normal bladder urothelium containing high levels of this protein. In one report, approximately 50% of the normal urinary epithelium studied had levels of *mdr*1 mRNA comparable to those found in the highest expressing tissues in the body. However, the levels of *mdr*1 mRNA in these tissues did vary over a 60-fold range between individuals[42].

The *mdr*1 gene appears to be regulated by an distal and proximal promoter[43]. The former has been found in normal tissues such as, liver, kidney and adrenal, whereas the latter is activated in drug-selected cells[44]. The downstream promoter appears to be stimulated by products of both the c-Ha-*Ras* oncogene and

the mutant *p53* supressor gene, two genes that are commonly associated with tumour progression[45]. In drug sensitive human breast cancer cells (MCF-7), wild type p53 protein is sequestered in the cytoplasm, whereas in the MDR clone of this cell line (MCF-7/Adr) the protein was localised within the nucleus. p53 in the resistant cells was also shown to be mutated in one of the protein's four conserved regions within the conformational domain. In addition the half-life of p53 in MCF-7 cells was less than 30 min while the mutated protein was more stable; with a half-life of about 4h in MCF-7/Adr cells. This increased stability, overexpression and nuclear localisation of the protein in MDR cells suggested that mutated p53 might be involved in the development of multidrug resistance in this cell line[46].

The Pgp drug transporter has been located, using immunohistochemical studies, on a wide variety of human tumours, most commonly in colon, renal and adrenal carcinomas[40]. Many other tumours, such as breast and bladder, tend to express Pgp during a course of chemotherapy due to acquired MDR[2]. In one study, high level expression of Pgp was observed more frequently in chemotherapy treated breast cancers than in untreated breast cancers[47], and the same was seen in bladder cancers[48]. As Pgp was found to be more frequently expressed in breast cancers that had metastasised compared to primary breast cancers, this led to speculation that Pgp may be an indicator of the aggressiveness of the tumour[49, 50]. This was also found in bladder cancers where high grade tumours expressed higher levels of MDR1 mRNA than low grade tumours[42]. This was further supported by suggestions that co-expression of p53 and Pgp was a strong prognostic factor for shorter survival[51]. Following this reasoning, reports have suggested that Pgp expression in breast tumours leads to a poor response to chemotherapy[52]. However, whether Pgp and the other resistance proteins could be used as predictors for a tumours' response to chemotherapy remains a subject of debate. In one study, none of the known proteins related to multidrug resistance predicted an individuals response to chemotherapy in breast cancer. The authors of this study also concluded that the resistant clones left behind after treatment generally had a low proliferation rate[53]. The presence of Pgp before chemotherapy was shown not to predict the clinical outcome of the treatment in patients with bladder cancer[54].

Pgp has been detected in many MDR human cancer cell lines from different histological backgrounds, including breast[55], colon[56] and bladder. In many cell

lines, the protein conferring MDR on the cells, *i.e.* Pgp, LRP or MRP appears to be dependent on which drug the resistant cells are raised against. For example, two drug resistant variants of the MCF-7 human breast cancer cell line produced by chronic *in vitro* exposure to doxorubicin (MCF-7/D40) and mitoxantrone (MCF-7/Mitox) had different mechanisms of decreased drug accumulation. MCF-7/D40 displayed a classical MDR phenotype expressing Pgp whereas the MCF-7/Mitox line exhibited the MDR phenotype without expression of Pgp[57, 58].

One positive side to MDR in cancer is that the *mdr1* gene may be used in gene therapy. This gene was able to confer the multidrug resistant phenotype on mouse bone marrow supporting the hypothesis that it may be possible to protect normal human bone marrow during intensive chemotherapy[2].

MULTIDRUG-RESISTANCE ASSOCIATED PROTEIN (MRP)

Overexpression of MRP, with amplification of the *mrp* gene, was first described by Cole *et al*[7] and has been found in several, but not all, non Pgp MDR cell lines[59]. cDNA sequencing and *in situ* hybridisation techniques demonstrated that the gene encoding for MRP has a single open reading frame of 1531 amino acids[60] and is located on chromosome 16 at band p13.1[7]. From the gene sequence it was found that MRP is another member of the ABC superfamily of transport systems[61], though MRP is only distantly related to the P-glycoproteins known to transport hydrophobic cationic drugs[7]. MRP is most related to the ABC-transporter encoded by the *pgp*A gene of *Leishmania tarentolae*[7]. This *Leishmania* protein is known to be involved in low level arsenite resistance, rather than hydrophobic drug resistance[62]. In resistant cells, loss of *mrp* gene amplification and decreased mRNA expression led to a reversion to drug sensitivity[7].

The protein MRP has a molecular weight of 190kDa (P190) with highly phosphorylated serine residues (more than Pgp) and a cycle of dephosphorylation and rephosphorylation occurs which may be important in its biological activity[63]. MRP has been shown by immunocytochemistry to be located primarily in the endoplasmic reticulum with lower levels in the plasma membrane[64].

This protein conferred cross-resistance to cells for a range of drugs similar to those excreted by Pgp, *i.e.* they are cationic or neutral and lipophilic. However,

there was no increased expression of Pgp or its cognate mRNA in these cell lines, which include the small cell lung cancer cell line HL69AR. Although exhibiting MDR, net drug accumulation and efflux appeared unchanged in this cell line[65]. This raises the possibility that sequestration of drugs in these resistant cells may be modified so that the drugs are less able to reach their intracellular sites of action. MRP may participate directly in the active transport of drugs into subcellular organelles or influence drug distribution indirectly. If MRP is involved in ion transport, its overexpression could alter cytoplasmic or intra-organelle pH. A relative decrease in intra-organelle pH would result in greater trapping of drugs, such as the anthracyclines which are protonated under acidic conditions[66]. In non-Pgp resistant cells, believed to contain the P190 protein, perinuclear localisation of drug has been observed in the Golgi and lysosomes[67]. This may represent the transport pathway away from the prime site of action for these drugs, the nucleus, via a site which possibly represents the PLC[29, 68] and out of the cell. Studies by Hindenburg *et al* on non-Pgp MDR cells suggested that using the protein as a pump, drug was diverted away from the nucleus, and accumulated into membranes and the Golgi apparatus or other membranous organelles. This was followed by a shift to lysosomes or mitochondria and was accompanied by reduced net drug accumulation and increased cytotoxic resistance[69]. Confocal microscopic analysis of intracellular daunorubicin in MRP transfectants revealed both reduced intracellular drug concentration and an altered pattern of intracellular drug distribution. The latter being characterised by an initial accumulation of drug in a perinuclear location, followed by the subsequent development of a punctate pattern of drug localisation throughout the cytoplasm[70]. Again this observed punctate pattern suggests drug sequestration and vesicular transport to be involved in the MDR phenotype.

It has also been observed that P190 is capable of binding to and transporting leukotrine glutathione conjugate into isolated vesicles, again raising the possibility that P190 may transport anionic drug conjugates[63]. Another feature that distinguishes MRP lines from cell lines overexpressing Pgp is the inability of cyclosporin A and several other chemosensitising agents to reverse this resistance[71, 8]. Although verapamil and cyclosporin A do cause a modest increase in drug accumulation in MDR cells they do not restore levels to those of the sensitive

cells[71, 72].

However, Zaman *et al* reported that MRP is similar to Pgp in its mode of action, exhibiting resistance to a range of hydrophobic drugs, being predominantly located in the plasma membrane and increasing the efflux of drugs from the cells. This has led them to the conclusion that MRP acts as a drug pump, like Pgp, extruding hydrophobic compounds from cells against a concentration gradient using the two ATP binding motifs to hydrolyse ATP for active transport[8]. It has been speculated that non-Pgp mediated resistance precedes Pgp expression during *in vitro* selection for MDR cancer cell lines[73]. The most likely candidate for this role is MRP. Short exposure of a myeloid leukaemic cell line to doxorubicin has shown overexpression of the *mrp* gene but not the increased MDR1 expression. However, prolonged exposure of these cells to DOX had little effect on MRP RNA levels but increased MDR1 expression. There were other indications, such as vesicular drug accumulation which was not abolished by treatment with verapamil indicating that induction of MRP overexpression occurred before that of the MDR1 gene[74].

Many normal tissues have been found to contain MRP but in particular the spleen and adrenal gland (MDR cells contain very high levels of MRP even compared to these tissues). That these particular normal tissues contained increased levels of MRP leads to the suggestion that the protein relates to the handling of exogenous and endogenous toxic compounds[75].

As with Pgp, reports have suggested the prognostic significance of MRP in clinical treatment. It has been reported that, in primary breast cancer, immunohistochemically detected MRP might be related to altered cell biological behaviour, including a more aggressive phenotype and resistance to adjuvant systemic chemotherapy. In this study, MRP expression was not related to tumour size, differentiation grade or lymph node involvement[76].

Enhanced MRP expression is also believed to be correlated with decreased expression of the topoisomerase II gene[77] and altered DNA topoisomerase II drug sensitivity[78]. This loss of topoisomerase II can also lead to cells expressing MDR (see Atypical MDR).

LUNG RESISTANCE PROTEIN (LRP)

This protein was so called because it was first identified in a lung cancer MDR cell line[79] but has since been discovered in other MDR cell lines of different origins (such as breast cancer and myeloma cell lines). The *lrp* gene is located on the short arm of chromosome 16, a region which seems to be critically involved in MDR, close to the genes encoding for the MRP[9]. The *lrp* gene encodes for a 110kDa unglycosylated protein of 896 amino acids. The deduced amino acid sequence of the protein shows 87.7% homology with the 104kDa rat major vault protein strongly suggesting that LRP is the human major vault protein[9]. Vaults are barrel-like cytoplasmic ribonucleoprotein organelles (probably associated with vesicles) that are highly conserved and broadly distributed among eukaryotes ranging from humans to *Dictyostelium*[80]. They consist of four proteins and a small RNA; 75% of the mass of the vault comes from the major vault protein alone, which is 95-104kDa depending on the species. A single vault barrel opens into two flower-like structures in which eight rectangular petals are joined by hooks to a central ring[81]. This structure is similar to that proposed for the central plug (or transporter) of the nuclear pore complex (NPC) and it has been demonstrated, by immunoblotting and immunofluorescence techniques, that the vaults specifically associate with the nuclear envelope in tissue sections and with NPC's of isolated nuclei[82]. Immunohistochemical staining with a p110 specific monoclonal antibody (LRP 56) has shown the protein to be primarily cytoplasmic, in a coarsely granular fashion indicating that it is closely associated with vesicular / lysosomal structures[79]. This evidence leads to the theory that LRP / vaults mediate drug resistance through vesicular and nucleocytoplasmic transport of drugs, Fig.1.1c.[83].

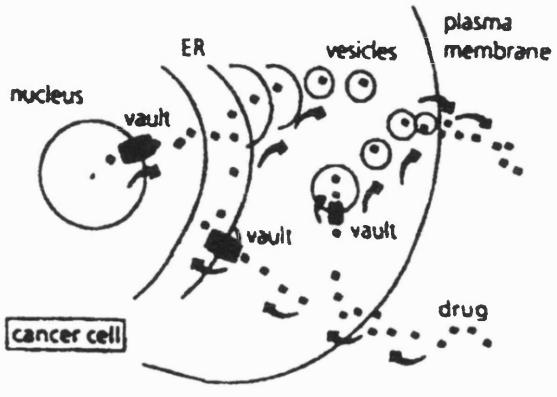

Fig. 1.1c. Functional hypothesis for LRP in multidrug resistance. LRP / vaults mediate nucleocytoplasmic and vesicular transport of drug. Taken without permission from Ref. 83.

LRP has a high expression in normal epithelial cells and tissues chronically exposed to xenobiotics and potentially toxic agents, such as bronchial cells, cells lining the intestines and kidney tubules[79]. These cells have an excretory or secretory function.

TRANSPORTER ASSOCIATED WITH ANTIGEN PRESENTATION (TAP)

This transporter protein is believed to transport molecules, *e.g.* cytotoxic drugs, into vesicles. It specialises in transporting peptides, in particular from foreign proteins into vesicles onto the major histocompatibility complex (MHC1) molecule then to the cell surface to display the foreign peptide. Co-upregulation of TAP / human leucocyte antigen (HLA)-1 occurs in MDR cells selected after drug treatment. As HLA is presented on the surface of the cell, this expression may make the cells more susceptible to immuno-therapy[10].

Since none of the other resistance mechanisms are directly related to this thesis, I have summarised them into two sections, atypical or topoisomerase associated MDR and other MDR mechanisms.

ATYPICAL MDR

A second form of phenotypic MDR has been shown to be associated with drugs that interfere with topoisomerase II activity[84]. Topoisomerases are ubiquitous enzymes, which are present in the nuclei of mammalian cells, and regulate the topological state of DNA. Essentially two major forms of topoisomerases have been described, topoisomerase I (topoI) and topoisomerase II (topoII)[85]. Although, there are several differences between the two enzymes both form cleavable complexes with DNA which allows cutting and resealing DNA strands. The resulting conformational changes release DNA supercoiling and twisting and allow changes in the conformation of the DNA helix to occur. These changes are essential for several physiological cellular functions such as DNA synthesis, replication and RNA transcription[49]. Topoisomerases are important enzymes for antineoplastic therapy as they are the targets for several antineoplastic agents[86], for

example, anthracyclines are topoII inhibitors. The anti-topoisomerase II drugs are thought to exert their cytotoxic effects by binding the topoII - DNA cleavable complex. This stabilisation essentially interrupts the housekeeping role of topoII and leads to DNA damage and cell death[84].

It is believed that MDR occurs as a result of loss of topoisomerase II activity, with decreased levels or altered catalytic properties of topoisomerases II in drug resistant cells. These qualitative changes in topoII are believed to alter the interaction of drug with this enzyme or enzyme-DNA complex[87]. Altered topoII confers cross-resistance to the anthracyclines and drugs closely related to the group but not to the Vinca alkaloids or the anti-metabolites[49]. This is supported in part by a study on a non-Pgp expressing adriamycin-resistant human small cell lung carcinoma cell line. Here, topoII catalytic activity was two- to three-fold lower than in the sensitive cell line between comparable cellular and nuclear extracts, with topoI activities being almost equal in extracts from both lines. Thus, the differences in topoII catalytic activity were not due to an overall decrease of nuclear proteins (detected in cellular extracts) or to a decrease of topoI and II activities in nuclear activities in the resistant cell line[88]. In human and murine cells two isoenzymes (α and β) of DNA topoisomerase II have been discovered[89]. In a cell line exhibiting an atypical MDR phenotype, including expression of drug resistant topoII activity, deletion of one of topoIIβ alleles was observed. This mutation may interfere with drug induced trapping of the topoII-DNA cleavable complex or could exert a loss of functional phenotype[90]. It has also been indicated that changes in topoII may have a role in the resistance phenotype of another resistant small cell lung cancer cell line, H69AR. However, the changes observed in this enzyme alone cannot explain the resistance of these cells to such drugs as the Vinca alkaloids[65].

OTHER MECHANISMS OF MDR

These involve cellular resistance against the anti-metabolites, such as cisplatin and alkylating agents, *e.g.* mustard gas, usually following exposure to these compounds. Almost all these drugs interact with DNA by intercalating in the major groove, though the newer compounds are DNA minor groove alkylators,

with the different alkylating agents causing different DNA lesions[91].

The mechanisms of resistance produced by the cells against these drugs include: i) methylation of DNA; where cells produce methyl-transferase to mend gene damage, caused by the drug, and halting cell death. The production of the enzyme could therefore be said to confer resistance to cells. ii) increased levels of other enzymes, such as glutathione transferase which conjugate with the drugs rendering them inactive[27]. Glutathione-related mechanisms mediate a variety of normal detoxification reactions in cells, and may represent potential drug resistance mechanisms in neoplastic cells. For example, part of the cytotoxicity of anthracyclines is due to the free radical intermediates produced which would be reduced by glutathione-dependent mechanisms[92]. Increased expression of glutathione has been documented in some anthracycline resistant breast cancer cell lines[93].

Furthermore, an increase in production of heat shock proteins was observed in association with the induction of resistance to doxorubicin in some breast cancer cell lines. This resistance was not associated with increased levels of MDR proteins, but only with a several-fold increase in the levels of heat shock proteins[94]. Other mechanisms by which a cell may protect itself , such as decrease in the ability of cells, particularly aberrant ones, to undergo programmed cell death (apoptosis) may also confer relative resistance to a chemotherapeutic agent[92].

1.1.2. CIRCUMVENTION AND REVERSAL OF MDR

As MDR in cancer is such a major clinical problem, ways of reversing or circumventing the effect are continually being investigated. Novel drugs, such as annamycin were shown not to be affected by Pgp mediated MDR in some cell lines, *e.g.* the Pgp positive human leukaemia cell line (HL-60)[95]. The calcium channel blocker Verapamil, a known reverser of Pgp resistance[96], did not alter drug sensitivity in most other non-Pgp resistant cell lines[71]. The immunosuppressive agent, cyclosporin A also reversed Pgp MDR as did novel modulator S 9788[97]. In comparison tests between these three modulators cyclosporin A was the most potent, then S 9788, followed by verapamil, in increasing DOX accumulation in rat-hepatocyte primary cultures[98]. Verapamil, cyclosporin A and other agents

known to reverse resistance (quinidine, trifluoperazine and diltiazem) inhibited drug efflux from MDR cells by competitively binding to Pgp[35, 99]. Tamoxifen, which can also reverse MDR, appeared to have a mechanism different from that of verapamil[100]. Drug accumulation in MCF-7/ADR cells could be increased by sphingosine isomers (not substrates of Pgp), in a manner associated with the inhibition of PKC-mediated phosphorylation of Pgp[101]. In some non-Pgp mediated MDR cell lines, including MCF-7/Mitox, genistein increased drug accumulation[102]. The drug estramustine is a conjugate of *nor*-nitrogen and estradiol and has cytotoxic activity as an antimicrotubule agent[103]. It has also been shown to be a modulator of MDR, increasing drug uptake in resistant human ovarian carcinoma cells *in vitro* by 12-fold which was less effective than verapamil in this study[104]. Estramustine as a cytotoxic did not induce overexpression of the *mdr* gene but interacted with the Pgp efflux pump altering intracellular drug accumulation[103]. Cytotoxic drugs complexed with fatty acids have been shown to increase drug uptake in cells compared to free drug[105]. This method of encapsulating drug in liposomes has also been used to try and circumvent MDR both successfully[106] and unsuccessfully[107]. This theory has been extended to the addition of fatty acids to alter membrane fluidity causing a lowering in the level of resistance[108] (see section 1.3).

Notwithstanding experimental reversal of resistance, additional problems arise when these reversing agents are considered clinically. Often the necessary amounts or just the nature of the agent *e.g.* verapamil which is a calcium channel blocker, would render it dangerous to use in most clinical situations. Therefore, the possible use of fatty acids, which can be administered at high quantities without biological damage to healthy tissues, is both attractive and feasible.

1.2. ANTHRACYCLINE CHEMOTHERAPY

Chemicals from the anthracycline family are widely used in the treatment of patients with cancer. Of the numerous anthracyclines that have been isolated or synthesised since the discovery of daunorubicin (DNR), only a few molecules have been brought to clinical trials and even fewer have entered clinical use.

Doxorubicin remains the most widely used anthracycline and is the benchmark against which all new compounds of this series are compared[109]. However, severe side effects including cardiotoxicity and development of drug resistance continue to place limits on the effectiveness of these agents.

The discovery of the first anthracycline, daunorubicin, occurred simultaneously in France and Italy in the early 1960's. In Italy, a soil sample was taken from near the Adriatic coast, and an organism, *Streptomyces peucetius*, was cultured from it. These colonies produced a solid red substance which had anti-tumour activity against Ehrlich carcinoma, Sarcoma 180 and Yoshida hepatoma in animal models. It was also intensely active against haematological tumours in humans[110]. The rest of the anthracyclines are similar glycoside antibiotics either isolated from various mutants of the fungus, *S. peucetius*, such as doxorubicin (DOX), modified from other anthracyclines such as epirubicin (EPI), or completely synthetic such as idarubicin (IDA). Microbial synthesis with subsequent biochemical modification still remains the primary source of anthracycline production[111].

Four drugs, belonging to or closely related to the anthracycline family, were used to investigate drug uptake and intracellular localisation by MDR cells with or without the addition of an EFA. These drugs were doxorubicin, epirubicin, idarubicin and mitozantrone and the structures are shown in Fig.1.2a.

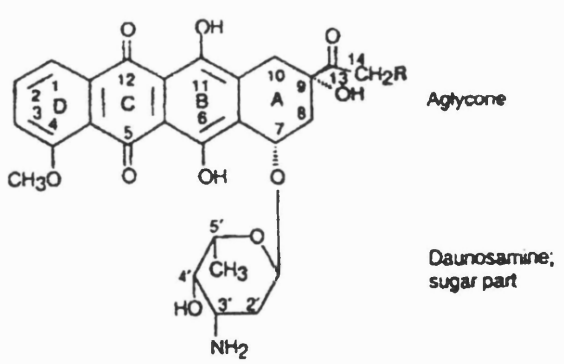

Daunorubicin:	**R** = H
Doxorubicin (adriamycin):	**R** = OH
Epirubicin:	4'-epi isomer of doxorubicin
Idarubicin:	4-demethoxy-daunorubicin

Fig. 1.2a. Anthracycline chemical structures.

The anthracyclines were chosen for this study not only because they are the most commonly used chemotherapeutic agents, hence often associated with MDR, but also because they exhibit natural fluorescence. This fluorescence is in the red / far red band of the spectrum allowing detection and quantification of intracellular drug localisation, in both drug sensitive and MDR cell lines, using established techniques, such as flow cytometry and fluorescence microscopy.

DOXORUBICIN (DOX)

This antibiotic was originally isolated from the mutant *Streptomyces peucetius var.caesius* again as a red pigment which diffused from the mycelium of colonies. The DOX molecule differs from daunorubicin by a single hydroxyl group on carbon-14[112] Fig.1.2a. DOX has a broad spectrum of antitumour activity, extending to all solid tumours as well as haematological and lymphoid malignancies[110]. However, many clinically common tumours such as colorectal, pancreatic and lung cancers are generally unresponsive or acquire resistance to DOX[113].

EPIRUBICIN (EPI)

This drug is the stereoisomer of DOX; the molecular modification does not substantially modify the antitumour efficacy compared to the original drug[113]. It is also used to treat the same spectrum of tumours especially bladder cancer with the same type of response rates and problems with MDR. EPI appears to be significantly better tolerated by patients and less cardiotoxic than DOX[113].

IDARUBICIN (IDA)

IDA is a totally synthetic compound commercially available since the early 1990's. It is much more lipophilic than the other anthracyclines Fig.1.2a. and therefore enters the cells much quicker. IDA is an orally active drug believed to be absorbed via the jejunum and perhaps the ileum[110]. It has been shown that the major circulating metabolite of IDA, idarubicinol is more effective in inducing

DNA damage than the metabolites of DOX and EPI. This was shown using an *in vitro* system against human tumour leukaemia cell lines where the ability of the drugs and their metabolites to induce DNA single strand breaks were assessed[114].

MITOZANTRONE (MTZ)

This drug is a bis(alkylamino)anthraquinone and is structurally related to the anthracyclines[115]. As the modes of action and physical properties of the anthracyclines and anthraquinones are very similar, no further distinction will be made between the chemical class, for the purpose of this thesis. MTZ shows activity against breast cancer and against the acute leukaemias[116], but many cancers including colorectal, lung and melanoma are particularly poor responders to MTZ treatment.

1.2.1 MECHANISM OF ACTION OF THE ANTHRACYCLINES

The anthracyclines produce a wide range of biochemical effects that have potentially toxic results for mammalian cells (see table 1.1).

Table 1.1. Biological actions of the anthracyclines.

Inhibition of:

- *Mitochondrial oxidative phosphorylation*
- *DNA polymerases*
- *RNA polymerases*
- *DNA repair enzymes*
- *Helicases*

Free radical production

Membrane modulation

Endonucleolytic cleavage

This complexity has made it difficult to assign a given biochemical action to specific host-tissue toxicity or to tumour-cell killing despite extensive study[112]. They are believed to cause cytotoxicity by one or more mechanisms, and the four most likely are discussed here: direct DNA intercalation, inhibition of the enzyme topoisomerase II, effects on the cell membrane, generation of free radicals.

DNA INTERCALATION

The largest proportion of drug entering the sensitive cell is taken up into the nucleus with DNA being the primary target. Drug uptake occurs throughout the cell cycle reaching a maximum during DNA replication[117]. The anthracycline inserts itself into the DNA double helix with the aminosugar portion of the drug binding strongly, through ionic processes, with the sugar phosphate backbone of DNA[112]. This binding has several consequences for the DNA; there is a local relaxation-unwinding of the DNA helix by 15°[118], disruption of the ability of the nucleic acid to act as a template for polymerases blocking DNA synthesis and repair and fragmentation of DNA[119]. However, all these assaults on the DNA do not always work and the cells survive the treatment. Furthermore, any altered cells that come through these DNA interactions could be potentially more dangerous to the patient, as it has been shown in *in vivo* models that anthracyclines can act as mutagens and carcinogens[120].

TOPOISOMERASE INHIBITION

Topoisomerase enzymes (I and II) are responsible for conformational changes in DNA. The enzymes form a complex with the DNA and are able to break, rearrange and amend the DNA strands, resulting in DNA relaxation (uncoiling), decatenation (unlinking) and unknotting. Therefore, topoisomerase enzymes aid the orderly progression of DNA replication, gene transcription and the separation of daughter chromosomes at cell division. Anthracyclines affect topoisomerase II action by binding to the enzyme-DNA complex which leads to lethal lesions appearing in the DNA. There is still some speculation about the detailed mechanism of this process, including whether the nucleic acid, the enzyme

or a novel binding site on the DNA-topoisomerase complex is the direct target for the drug[120]. However, the most probable target is the DNA-topoisomerase complex. Current findings indicate that both isozymes of topoII (α and β) may be *in vivo* targets of these antitumour poisons[121] (also see section 'Atypical MDR' in section 1.1.1).

MEMBRANE DAMAGE

For any intracellular mechanism of drug action, the anthracyclines must initially bind and be transported across the plasma membrane. However, it is also possible that the plasma membrane itself is a primary site of drug action. Studies have shown that immobilised DOX shows significant cytotoxicity, without uptake, in several cell types in culture[122]. The drugs partition into the liquid phase of the membrane causing alterations in its fluidity (producing changes in ion permeability), function, *e.g.* transport through protein channels, and interferes with membrane based signalling systems, *e.g.* phosphatidylinositol. These alterations of membrane function and morphology are caused by drug concentrations below those necessary for DNA damage but high enough to inhibit cell growth[122].

FREE RADICAL FORMATION

The ability of anthracyclines to trigger formation of oxygen radicals was first noted by Handa *et al*[123]. They demonstrated that the microsomal enzyme P_{450} reductase was able to catalyse the reduction of either daunorubicin or doxorubicin to semiquinone free radicals in microsomes from cancer cells and rat liver *in vitro*. The semiquinone, in turn, reduced molecular oxygen to the superoxide ion which can be found in drug treated cells. Evidence that free-radical reactions might account for some of the effects of anthracycline[124] led to a proposal that oxygen-radical -mediated membrane damage in cardiac tissue was the mechanism of DOX cardiomyopathy. However, there is no evidence linking the role of free radicals in the mutagenicity and cardiotoxicity with the tumour cell killing capacity of the anthracyclines[112]. Also MTZ does not generate significant levels of radicals but retains the capacity to alter membrane fluidity, bind directly to DNA, trap DNA

topoisomerase II complexes and therefore, kill tumour cells[125].

1.2.2 DRUG TARGETING

New drugs are continually being investigated in an effort to produce the ideal chemotherapeutic agent and to overcome MDR. Alongside this, drug delivery systems are also of importance to maximise tumour cell death and to circumvent MDR. One method of targeting the drug to tumour cells by encapsulation of drug is considered here briefly.

The initial aim of anthracycline encapsulation in liposomes or other nanoparticulate carriers was originally to divert the drug from some highly sensitive targets, such as the heart. In addition, it has been suggested that some carriers could be useful by altering drug recognition by the drug efflux pumps of MDR cells[109] (see section 1.1.2.) Liposomes consist of synthetic phospholipid membranes organised as either unilamellar or multilamellar vesicles that temporarily trap and transport the drug. Variations of the phospholipid composition increase the flexibility of the physiochemical properties of these carriers making it possible to tailor their formulation so as to obtain the pharmaceutical properties required in terms of stability or bioavailablity[109]. An increase in encapsulated drug entering tumour cells compared to free drug has been reported[126, 127] in *in vivo* systems, as has circumvention of MDR by DOX loaded nanospheres in an *in vitro* system[106].

1.3. ESSENTIAL FATTY ACIDS

Fatty acids are amphipathic substances comprising of a hydrophobic lipid soluble hydrocarbon chain and a hydrophilic acidic carboxyl group. The common range of carbon atoms is between 12 to 22 and when double bonds occur between carbon atoms the resulting fatty acids are referred to as unsaturated. Those with more than one double bond, like the essential fatty acids, are called polyunsaturated (PUFA). Using proper chemical nomenclature, fatty acids are designated as number of carbons : number of double bonds with 'n' indicating the position of the

first double bond, *e.g.* γ- linolenic acid is 18 : 3n6.

$CH_3(CH_2)_4CH=CHCH_2CH=CHCH_2CH=CH(CH_2)_4COOH$

Fig. 1.3a. Chemical formula of the essential fatty acid, γ- linolenic acid (GLA)[128].

Essential fatty acids (EFAs) are characterised by the presence of several double bonds in the carbon skeleton and are essential dietary requirements because they cannot be synthesised *de novo* in the human body. The n-3 series are derived from fish oils and the n-6 series, commencing with linolenic acid, from plant sources. Linolenic acid (LA) is present in many of the polyunsaturated vegetable oils but its metabolite, γ- linolenic acid (GLA), is relatively scarce, being found in abundance in relatively few plants such as evening primrose oil (10% GLA), blackcurrant seed oil (15-20% GLA) and borage (20-25% GLA)[128, 129]. The main way GLA is ingested is *via* LA which is converted to GLA by the enzyme delta-6-desaturase. This is further desaturated to produce arachidonic acid (AA) which is the precursor of series-1 prostaglandins (PG). By further desaturations, precursors for other PG and leukotrienes series are produced. This chain of events of fatty acid desaturation and elongation to produce different biochemical intermediates occurs in the n-3 EFA family using similar (or even identical) desaturating enzymes[130].

Fatty acids, including the EFAs, are an important source of energy for animals. They are stored in the cytoplasm of many cells in the form of droplets of triglyceride molecules, which consist of three fatty acid chains each joined to a glycerol molecule. But the most important function of the fatty acids is in the construction of cell membranes which are composed largely of phospholipids; constructed mostly from fatty acids and glycerol. The fatty acid composition of the membrane is very important to the cells as it dictates the fluidity of the membrane and therefore, the ease of entry and exit of molecules into the cell[131]. Hence EFA's are important structural components of all cell membranes and give rise to a variety of intermediates, such as prostaglandins and leukotrienes, which are believed to have wide-ranging influences on the immune system, autocrine-paracrine growth regulation and the mediation of inflammation[129].

1.3.1. CELLULAR CYTOTOXICITY OF EFA's

PUFA's have been shown to be cytotoxic to many cancer cell lines and tended to kill human cancer cells at concentrations which had no adverse effects on normal human cells, such as fibroblasts, or on normal animal cell lines[132]. Although the normal cells were not killed, their rate of growth was slowed down[133]. These results have been repeated on a variety of human cancer cell lines from different histological origins such as breast, lung and prostate tumours. The most effective and selective results were gained from fatty acids with 3, 4 or 5 double bonds compared to those with 2 or 6 double bonds[134], from either n-3 or n-6 families. When human cancer cells and normal fibroblasts were co-cultured the malignant cells overgrew the normal ones, but when GLA was added to the medium this was reversed with the normal cells outgrowing the malignant ones[132]. Experiments on human breast cancer cells showed that these cells did not demonstrate resistance to the cytotoxic effects induced by the fatty acids at any concentrations[134].

These PUFA induced differential effects may be due to various factors, including increased PUFA uptake and /or unusual distribution or an ability of the PUFA's to alter free radical generation in tumour but not normal cells. Comparison of three labelled EFA's, LA (18:2n-6), AA (20:4n-6) and eicosapentanoic acid (EPA) (20:5n-3) showed labelled LA was taken up in similar quantities by normal cells and tumour cells, whereas AA and EPA were taken up substantially more by normal compared to resistant tumour cells[135]. Free radical generation was observed to occur selectively in the tumour cells. Tumour cells incorporate major portions of the fatty acids in the ether lipid and phospholipid fractions, whereas normal cells incorporate the fatty acids primarily into the phospholipid fraction. These results suggested that there were significant differences between normal and tumour cells in fatty acid uptake and distribution, and in the ability of fatty acids to generate free radicals[135].

To try and understand the mechanism of EFA cytotoxicity, the contribution of lipid peroxidation to the killing of human breast cancer cells by GLA has been examined and other EFAs of different cytotoxic potential were tested for comparison. It was found that the cytotoxic potential varied with the ability of the

EFAs to stimulate the production of superoxide radicals. The addition of EFAs with 3,4, or 5 double bonds in the cancer cells induced the production of superoxide radicals with the extent of lipid peroxidation being EFA specific in cancer cells. Tumour cells supplemented with GLA produced more superoxide radicals than unsupplemented cells and cells containing EFAs with lower cytotoxic potential[136]. LA, AA and EPA also selectively increased free radical generation in tumour cells compared to other EFAs[135]. The effectiveness of an EFA in inhibiting cell growth and killing cancer cells appeared to be correlated with the extent of lipid peroxidation of the added FA in the cells. The presence of PUFA's in a cell membrane made the cells susceptible to lipid peroxidation which can occur by a number of different enzymatic mechanisms[136, 137]. This suggests that the addition of GLA stimulates the initiation of its own peroxidation by increasing the amount of superoxide radicals and by increasing the substrate available for lipid peroxidation. Consequently, cancer cells are thought to be killed as a result of an elevation of toxic peroxidation products generated by the PUFA's[136]. This theory is supported by the detection of peroxidation degradation products and the ability of antioxidants, such as Vitamin E, which scavenge free radicals, to block the PUFA's cytotoxic effects[129, 136]. Since the cytotoxicity was enhanced by the addition of iron to the culture medium[136], an alteration in the intracellular iron concentration may be necessary to promote autocatalytic lipid peroxidation[138]. However, it is important to bear in mind that the cytotoxic effect may be due to an oxidative process other than lipid peroxidation or one specific metabolite formed by lipid peroxidation. Furthermore, the *in vivo* effects of the PUFA's are likely to be far more complex and influenced by other factors[139].

There is still alot of controversy over the EFAs cytotoxicity and therapeutic effects, including increased chemotherapy drug uptake, by EFAs and this is partly reviewed in the next section.

1.3.2. EFA's AND CANCER

The membrane fatty acid composition of cancer cells can be modified either in culture or during growth in animals without disrupting basic membrane or cellular integrity. These changes in lipid composition may alter the cells' growth

pattern, increase its sensitivity to certain forms of therapy, alter pathways involved in membrane transduction of external signals and may consequently modulate the response of tumour cells to growth factors, thereby modifying the evolution of cancer[140]. In breast cancer, the combined amount of LA and AA was significantly lower in tumours that gave rise to systemic metastasis than those tumours which did not[141]. Cancer cells have been reported to have reduced concentrations of desaturated metabolites of LA, such as GLA and AA, probably due to reduced activity of delta -6-desaturase[142, 143]. In another study LA, the precursor EFA, was at similar concentrations in both malignant and benign prostatic tissue, whilst AA, its metabolite was found to be at significantly lower in malignant tissue. However, this was suggested to be due to an increase in AA metabolism, possibly to form prostaglandins, high concentrations of which are often found in this malignant tissue[144].

As mentioned above the type of EFA which is involved in the selective cytotoxicity of cancer cells is subject of debate. It has been found that n-3 and n-6 fatty acids killed breast, lung and prostate cancer cells selectively compared with human fibroblasts *in vitro*[133]. Another study found inhibition of MCF-7 breast cancer cell growth occurred with n-3 FA's but not with n-6 FA's, such as GLA or LA[145]. Other reports suggest that although high doses of PUFA's are cytotoxic, lower doses can stimulate cancer cell growth. LA and AA at doses between 18-33μM stimulated growth of two murine adenocarcinoma cell lines in serum depleted medium[146]. Also, LA stimulated the proliferation of human breast cancer cells when they were cultured in serum free medium[147]. In a model mouse system, transplantable mouse mammary tumour cells were inoculated into the mammary pads of athymic nude mice. The effects of feeding the mice diets high in LA (8 or 12%) or low in LA (1 or 2 or 4%) were then observed. Whilst the level of dietary LA did not enhance the growth rate of primary mammary tumours, the diet high in LA did stimulate the spread and growth of these tumour cells in the lungs and at other sites as metastatic tumours[148]. From one study, it was observed that n-3 FAs, such as EPA inhibited growth in the cultured human breast cells and those injected into the thoracic mammary fat pad in a model mouse system[149]. Using the same model mouse system, the inhibitory effects of dietary fish oil were noted and ascribed, from the above results, to its high EPA and docosahexaenoic acid (DHA)

content. The mechanism of inhibition is likely to involve the suppression of tumour eicosanoid biosynthesis[150]. These lipoxygenase products are involved in breast cancer progression with eicosanoid 12- hydroxyeicosatetraenoic acid, a metabolite of AA, having a role at several levels in the metastatic cascade[151]. The growth of human colon cancer cells *in vivo* has also been restricted on a diet high in n-3 lipids[152].

Addition of different fatty acids, including LA, to the diet of tumour bearing mice led to modifications in the fatty acid composition in the plasma membranes of these tumour cells[153, 154]. However, there were no appreciable changes in membrane cholesterol or phospholipid content, including phospholipid head composition[154]. Therefore, what occurred is a substitution of fatty acyl chains without any disruption in the usual lipid bilayer[153]. The fatty acid composition of the nuclear membrane was also modified[153]. This enrichment of cell membranes with PUFAs resulted in an increase in membrane fluidity as measured by electron spin resonance techniques[154]. As enhanced fluidity in model systems leads to an increase in permeability with changes in bi-directional flux across the cell's plasma membrane this should affect the influx of drugs, such as DOX and MTZ[155].

The synergistic effects of increased cell killing may also be through augmented drug-induced free radical production and subsequent heightened lipid peroxidation. For example, anthracyclines, such as DOX are known to generate free radicals[155, 156] and to be more effective in killing cells enriched in polyunsaturated fatty acids[157]. This increased sensitivity could be in part the result of augmented lipid peroxidation[155]. Murine leukaemia cells, L1210, grown in medium supplemented with DHA (22:6n-3) increased their sensitivity to DOX compared to unsupplemented cells. This sensitivity increased with increasing concentrations of DHA in the medium and was apparent over a range of drug concentrations. However, there was no change in the growth rate or cloning ability of the cells when only DHA was present[157]. This effect of DHA to enhance the toxic action of chemotherapeutic agents has also been shown on cultured lymphoma cells, although in this study the PUFA alone reduced cell proliferation[158].

A variety of EFAs, such as GLA and EPA have been shown to potentiate the cytotoxicity of anti-cancer drugs, by a mechanism which does not appear to be

due to an increase in lipid peroxidation[159, 160, 161, 162]. Hence, EFAs could be used in conjunction with chemotherapeutic agents to increase cell death or manipulate MDR by increasing cell permeability allowing more drug to enter. Certain MDR cancer cell lines are more sensitive to EFAs, including EPA and GLA, than their non-MDR parental lines making them a potential alternative for cancer patients with resistance to conventional anticancer drugs[163]. Studies have shown increased cell death by incubating cells with both PUFAs and cytotoxic drugs cell death is probably due to additive toxicity rather than manipulation of MDR by the fatty acids[164]. The use of lipids in anticancer therapy offers a new avenue of approach. A combination of fatty acid based therapy with traditional modalities such as drug chemotherapy may be required for eliminating cancer cells. This combination may be through additive or synergistic cell killing. In summary, the possible clinical implications of the use of dietary lipids in cancer therapy are shown in Table 1.2.[155].

Table 1.2. Potential clinical implications of dietary lipids

Increase sensitivity of tumours to anticancer drugs due to membrane lipid modification by:

Increased drug uptake

Increased free radical generation and lipid peroxidation

Accelerated differentiation

Direct toxicity of high concentrations of fatty acids in the diet or infused to influence growth rate of established tumours

Increase the toxicity of anticancer drugs to normal tissues

Modulation of carcinogenesis in cancer prevention

1.4. AIMS OF THE THESIS

To investigate the modulatory effects of GLA on chemotherapeutic drug uptake in sensitive and MDR cancer cell lines.

MATERIALS AND METHODS

A. MATERIALS

All materials were obtained from Imperial Laboratories, Andover, England, unless otherwise stated.

2.A.1. CELL CULTURE

The cell lines used in the studies were the MCF-7 breast cancer cell line and the MGH-U1 urothelial cancer cell line. Both these parental cell lines are anthracycline sensitive and were used as a comparison to their MDR counterparts. Both resistant cell lines were raised by exposing the parental cell lines to increasing doses of Adriamycin (Doxorubicin).

The MCF-7 human breast adenocarcinoma cell line was obtained from the European Collection of Animal Cell Cultures (ECACC No:86012803, Porton Down, England). This cell line was originally established from the pleural effusion of a 69 year old female Caucasian. The cells will form tumours in nude mice and show some of the features of differentiated mammary epithelium, such as oestradiol synthesis and hence are oestrogen receptor positive[165]. The MCF-7 cell line can be separated into several different sub-populations with different characteristics including rate of growth[166]. The MCF-7/R cell line was produced and kindly donated to us by Dr. John Masters, Institute of Urology, University College London.

The MGH-U1 human bladder cancer cell line is believed to be a multi-clonal cell line. It was originally derived in America from a T3 bladder cancer metastasis which has since been cross contaminated with the T24 clone[167]. The MGH-U1 cell line and its resistant sub-line (MGH-U1/R)[168] were also kindly donated by Dr. John Masters.

All cell lines were grown in Dulbecco's Modified Eagle's Medium (DMEM) with 2mM L-glutamine, foetal bovine serum (FBS at 10% v/v), and 100μg/ml each penicillin / streptomycin solution. The MCF-7 and MCF-7R cell lines needed to be fed every 48/72h. The cells became confluent, thus needing to be

passaged, approximately every 7 days. These cell lines were not allowed to become supra-confluent otherwise a single cell suspension after disaggregation became hard to achieve. The MGH-U1 and MGH-U1/R cell lines grew much faster and needed to be passaged every 48/72h. As reported by other researchers, our resistant cells had a slower growth rate than the sensitive[168]. Stocks of the cell lines were maintained by viably freezing the cells down regularly.

After thorough washing in phosphate buffered saline (PBS) with EDTA, the cells were harvested using a disaggregating solution of 1mg/ml trypsin in PBS / EDTA. The PBS removes any serum which might inhibit trypsin action whilst the EDTA helps release cellular connections by removing the calcium. The disaggregating solution was kept frozen in ampoules until required. For experiments all cells were harvested after becoming visually 90% confluent.

All cultures were grown from frozen stocks and kept in a humidifying incubator with 5% CO_2 at 37°C. The stock of cell lines was continually replenished by freezing the cells down into ampoules containing 1ml of freezing medium, which is, L-15 medium with dimethylsulphoxide (DMSO, 10%) and FBS (10%).

2.A.2. PATIENT SAMPLES

The tissues used were resection specimens from patients with breast cancer (n=10) or bladder cancer (n=11), snap frozen and stored in liquid nitrogen. Frozen sections (5μm) were cut on a microtome (5030 microtome, Bright Instruments Co. Ltd, Huntingdon, England), mounted on slides and allowed to air dry at room temperature, after which they were stored at -20°C.

2.A.3. EFAs and CHEMOTHERAPEUTIC AGENTS

The essential fatty acid used in all experiments was γ – linolenic acid (GLA). This was provided by Scotia Pharmaceuticals (Stirling, Scotland) as the clinical formulation Lithium GLA (LiGLA). This came as a solution in 5ml vials at a concentration of 140mg/ml GLA and all subsequent dilutions were made using DMEM (with additives, as described previously). The vials of LiGLA were stored

in a cool, dark place and only used if the solution was a pale straw colour. Exposure to air for a period of time was shown to adversely effect the LiGLA, therefore opened vials were discarded after being used once. A time period of 24h was long enough to change the liquid from a pale yellow to a darkish brown colour. Furthermore, a series of pilot experiments were conducted comparing the cytotoxicity of fresh (newly opened vial) with 24h and 48h old GLA on two cell lines: MCF-7 and MCF-7/R. The potency of GLA had deteriorated for the aged samples.

The chemotherapy drugs studied were anthracyclines or related compounds, hence they all have very similar structures and endogenous fluorescence in the red / far red band of the visible light spectrum. Doxorubicin (Adriamycin™), Epirubicin (Pharmorubicin™) and Idarubicin (Zavedos™) were obtained in dry pellet form from Pharmacia (Milton Keynes, England) and were rehydrated in sterile water to a concentration of 2mg/ml. These drugs were aliquoted into ampoules and kept at -20°C. Mitozantrone (Novantrone™) is an anthraquinone and was obtained in solution from Lederle Laboratories (Gosport, England) at a concentration of 2mg/ml which was stored in a dark cool place. All subsequent dilutions of these four drugs were made using complete DMEM.

2.A.4. MONOCLONAL ANTIBODIES

The antibodies used in these experiments were originally kindly donated by Dr.Flens and Prof. Rik Scheper (Free University Hospital of Holland, Amsterdam) and then ordered from TCS Biologicals, Aylesbury, England and from Harlan-Sera Labs, Crawley Down, England.

As the most well documented form of MDR is associated with P-glycoprotein (Pgp), several monoclonal antibodies have been raised against this protein. The antibody chosen for these experiments was JSB-1, mouse anti-human Pgp. JSB-1 reacts with the conserved cytoplasmic epitope of the plasma membrane-associated transporter, 170kDa Pgp. JSB-1 detects Pgp overexpression in human tumour cells of all different derivations. The secondary antibody was a

sheep anti-mouse IgG immunoglobulin, human serum absorbed and conjugated with fluorescein isothiocyanate (FITC).

The monoclonal antibody raised to the MDR-related Lung Resistance Protein, was LRP-56 (mouse-anti human LRP antibody). This antibody reacts with an epitope of the LRP-protein (110kDa). This protein is believed to be overexpressed in various human non-P-glycoprotein MDR tumour cell lines. The secondary antibody was the same as above.

The third protein studied was the MDR-related Protein (MRP). MRP is an 180-105 kDa transmembrane transporter protein overexpressed in various human non-P-glycoprotein MDR tumour cell lines. Two different clones of antibody were used; MRPm6 produced in mouse cells and MRPr1 produced in rat cells. MRPm6 and MRPr1 react with different internal epitopes of the MRP. MRPm6 was raised against a bacterial fusion of MRP, containing a segment of 170 amino acids in the carboxy terminal end and part of the carboxy proximal nucleotide binding domain of the protein. MRPr1 was raised against a bacterial fusion protein of MRP, containing a segment of 168 amino acids in the amino-proximal half of the protein. Neither MRPm6 or MRPr1 cross react with the human MDR1 and MDR3 gene products. For viewing the MRPm6 the same sheep anti-mouse FITC conjugated secondary antibody as used for viewing Pgp and LRP was used. As MRPr1 was produced from rat not mouse, a different secondary antibody was employed, this was rabbit anti-rat IgG, human serum absorbed and conjugated with FITC. Some of the staining for LRP/MRP was performed in three layers to enhance intensity. In this case the secondary antibody was a biotinylated bridge linking to the third antibody which was streptavidin conjugated with Cy3. The methodology is fully described in the appropriate section (2.B.3). All secondary antibodies were obtained from Dako, High Wycombe, England or Sigma, Poole, England.

B. METHODS

2.B.1. DETECTION OF CELLULAR ANTHRACYCLINE UPTAKE

i. FLOW CYTOMETRY

Flow cytometry was used for studying dynamics of drug uptake in sensitive and resistant cells.

This technique allows us to measure and record the fluorescence intensity, size and granularity of any particle, normally whole cells or nuclei. The flow cytometer used in these studies was the Becton Dickinson FACScan (fluorescence activated cell sorting device) combined with an Apple Macintosh Quadra 650 running CellQuest software. The instrument is equipped with a single 15mW air cooled argon ion laser emitting light at 488nm. The main experiments were done at the Imperial Cancer Research Fund (ICRF), London, with the kind permission and help of Derek Davies.

The mechanics are as follows: as a particle *i.e.* an event, passes through the laser beam of the instrument, it scatters laser light and its attached fluorochromes emit light. In this case, the cells (events) scatter the laser light whilst the anthracycline within them emits light, *i.e.* fluorescence. Photodetectors collect forward scattered light (FSC), side scattered light (SSC), emitted green fluorescence (FL1, 530 ± 15nm), orange fluorescence (FL2, 585 ± 21nm) and red fluorescence (FL3, above 620nm). FSC is related to the size of event and SSC is related to the internal complexity (granularity) of the particle. The three FL channels pick up emitted fluorescence within their respective ranges. The drugs used in this study all have their photon absorption maximum close to 488nm and emit fluorescence in the red / far red range which is detected by FL3. The detection of scattered and emitted light results in a pulse of electrical energy, which is converted to a digital signal for each measured parameter of each cell. These values can be stored for a requested number of events, usually 10000 cells[169].

The computer displays these digital signals on the screen. Two different types of data plots are displayed of the events as they are being acquired, dual

parameter dot plots and single parameter histograms. Forward scatter signals are read on a linear scale of 1024 channels with a default threshold level set at 52, *i.e.* for an event to be recorded its measurement must be greater than the threshold level. This allows much of the cellular debris to be excluded from the measurements. To reduce further acquisition of events other than single live cells, an inclusion gate or region is drawn around the main population of live cells, shown on the dot plot of FSC and SSC and only cells within that region are acquired and recorded (see Appendix 2). The main population of live cells is determined by running a control containing propidium iodide, a dye detected in FL2 which only enters the nuclei of dead cells, before each series of experiments. PI cannot be used simultaneously with the anthracyclines due to spectral overlap of the two emission spectra. The nature of the inclusion polygon gate meant that large clumps of cells are also excluded. This method means a defined distinct population of mainly live single cells was acquired producing more accurate results recorded as clumped cells had increased levels of drug.

For analysis, both dot plots and histograms of the total events acquired are displayed along with a statistical analysis. The amount of fluorescence emitted by each cell, which is proportional to the amount of drug within the cell, is recorded and the mean fluorescence intensity per 10000 cells displayed along with the median and the peak channel of fluorescence. All data is shown as arbitrary units. The parameters and detector values were saved on the hard disc drive and kept as constant as possible. Slight variation, such as adjusting the forward scatter and FL3 channel, was necessary depending on the cells' condition and the anthracycline being investigated so the dot plot of the control cells fell completely within the inclusion gate .

A standard procedure was maintained (unless otherwise stated) for all flow cytometry experiments regardless of cell line or anthracycline used. A 12.5cm^2 flask of cells >90% confluent per cell line was used for each drug dose per experiment with or without pre-incubation with GLA. For dose response uptake curves, the cells were incubated in 5mls of medium, each flask containing a different drug dilution. This resulted in 7 flasks of 7 different drug concentration per cell line per experiment. Each flask contained similar numbers of cells. This

meant dose response curves could be repeated for each cell line using different cell passage numbers. A wide variation in cell numbers and confluence drastically changed the amount of cellular drug uptake; depending on the type of drug incubation protocol, *i.e.* whether the cells were in suspension or attached to flasks. The effect of GLA on drug uptake was also studied using flow cytometry for only 3 different drug concentrations: i) no drug, ii) a drug concentration taken from the uptake part of the dose response curve and iii) a drug concentration taken from the plateau region of the dose response curve. The cells were incubated on the flasks with a set dose of GLA for 24h before the addition of anthracycline, while negative controls were not exposed to GLA.

For all drug uptake studies, the cells were incubated at 37°C with the drug. From previous experiments it was noted that it was preferable to use HEPES (N-2-hydroxyethylpiperazine-N'-2-ethanesulfonic acid) buffered medium. HEPES buffered medium was used to help maintain pH levels and cell integrity in the flasks during travel to the ICRF. The cells were then harvested and the amount of drug uptake per cell recorded on the FACScan. This method produced reliable and consistent results with an easily defined main cell population. Previously the cells were incubated in suspension with the drug medium but this proved to be damaging to their integrity giving inconsistent results. The latter method also gave a more realistic comparison to the *in vivo* situation where cells are layered and cellular connections are still intact.

ii. CONFOCAL MICROSCOPY

Confocal microscopy was used for visualising either the intracellular distribution of drugs or the fluorescent profile of resistance proteins (also see 2.B.3).

In conventional light or fluorescence microscopy, two dimensional images of the object are formed. This is also true of confocal microscopy but each image represents only part of the thickness of the sample. This is possible because the microscope optics exclude features outside the plane of focus. A series of images at different positions through the thickness of the object can be obtained by changing

the plane of focus or moving the object. Such a series of images can be reconstructed to a three dimensional representation of the object produced by optical (as opposed to physical) sectioning. This is the main feature and major advantage of confocal microscopy over conventional microscopy (Fig.2.1). The confocal principle is effectively implemented when combined with a point scanning system using a laser light source. This builds up an image by scanning a point of laser light across the sample in the X and Y directions in a raster pattern. The detector in the laser scanning system is usually a photomultiplier tube. An image is displayed by using a computer to store the intensity value of each point from the detector and then presenting these in the correct order on a high resolution video monitor. To collect a series of images the computer then shifts the focus by a fixed amount and the object is scanned again to produce the next image at a different Z position. This image is stored and the process repeated to build the 3D data set. The combination of confocal microscopy and laser scanning microscopy (CLSM) was implemented in the drug localisation studies using the Leica TCS 4D confocal microscope system Fig. 2.2.

As mentioned a digital record of the image is produced by recording the brightness of each pixel in the image as it is scanned. In the case of the Leica TCS each point is allocated a value between 0 (black) and 255 (white). Therefore the image is stored in black and white, although often displayed in 'false' colour. On the monitor each point of the image is displayed in the correct position and is allocated a colour using a 'look-up' table (LUT). The scanning laser source in this system is an air cooled, mixed gas (Argon / Krypton) 3 micron fibre-optic. The endogenous fluorescence of the drug localised within the cells could be directly viewed using a mercury vapour light source and a filter. The microscope used was the Leitz DMR BE research microscope. This is a high resolution, light microscope with semi-automatic focusing controls and a galvanometric stage facilitating automatic specimen scanning in both the X/Y and X/Z directions. A variety of objectives of both water and oil immersion type allow 'wet' preparations as well as permanently mounted specimens to be examined at low and high power magnifications up to 1000 times life size[170].

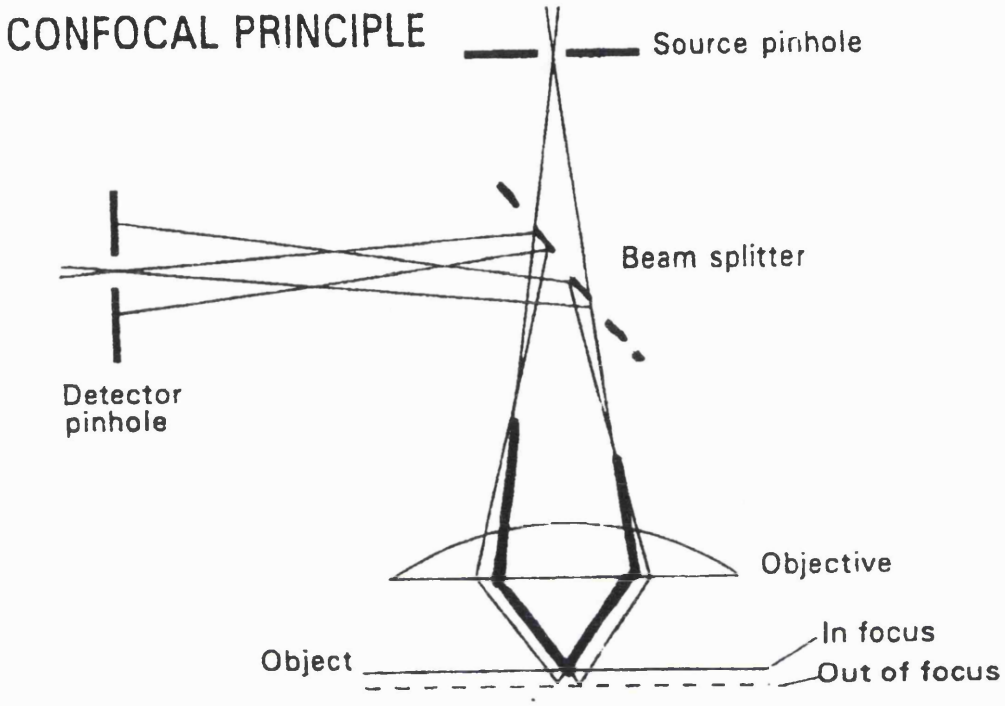

Fig. 2.1. Principle of the confocal microscope.

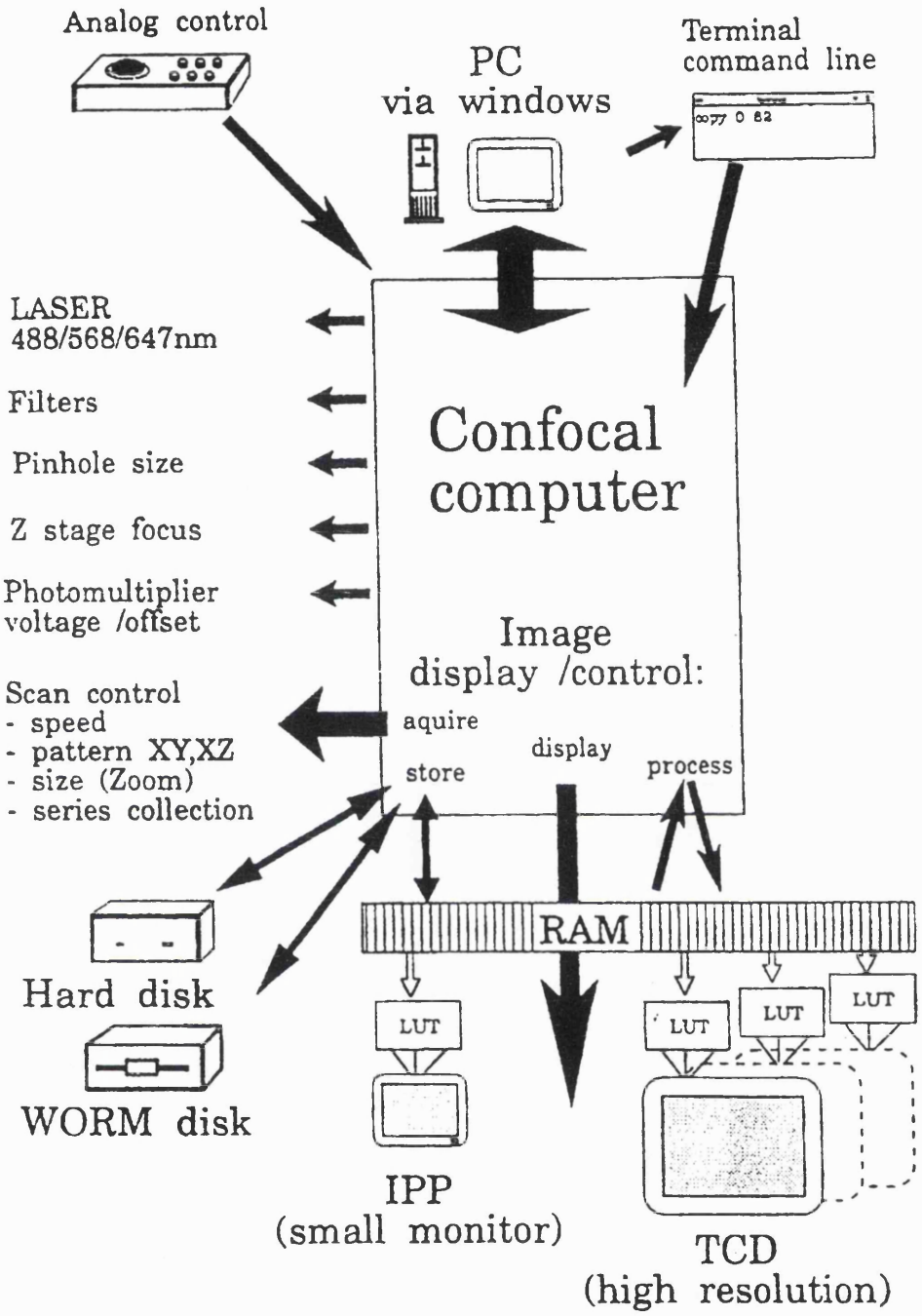

Fig. 2.2. Confocal Microscope Set-up.

The cells were grown on 15mm easy grip style petri dishes. They were incubated with medium containing drug and viewed under the confocal microscope in the dishes. For these experiments a X50 water immersion lens was used and this allowed the cell preparations to be viewed still in the drug incubation medium. Viewing the cells in medium allowed longer time periods for the fluorescent images to be formed as the cells were prevented from drying out. HEPES buffered medium was also used to help maintain medium pH levels.

Direct fluorescence viewing was necessary to find suitable fields of view (*i.e.* where the individual cells could be seen clearly) for scanning. A green filter was used to detect the fluorescence of the anthracyclines and the filter in the confocal system set for rhodamine isothiocyanate (TRITC) *i.e.* red fluorescence, *via* the computer. This set the excitation wavelength from the argon / krypton laser at 568nm. The setting up of the confocal microscope was made even easier by the 'quick-start' facility. Once the image had been scanned the zoom could be used to orientate particular features or cells within the image. Following this the top and bottom of the chosen image were set and a series of images through the sample collected. This series was then displayed as averages removing the majority of background fluorescence. The recorded images were displayed with false colour added, using the 'glow' LUT, and saved on optical disc. Quantification of the amount of fluorescence, which corresponds to the amount of drug within the cells, in a field of view could also be recorded. This was done by plotting a gradient chart of drug concentration over the cells.

iii. CHARGE - COUPLE DEVICE CAMERA

The charge-coupled device camera was used for visualisation and semi-quantitation of intracellular drug distribution.

Like the confocal microscope this technique allows one to visualise the fluorescence of the drug localised within the cell. An inverted microscope (Olympus IMT-2) with epifluorescence and phase-contrast attachments was used for the microscopy. The drugs fluorescence was excited by an 1.8mW helium-neon laser (633nm) coupled to a liquid light guide with the beam directed *via* a band-pass

filter at 630nm (to remove extraneous light) into the dichroic mirror housing for epifluorescence studies. Fluorescence was detected between 660nm and 710nm using a combination of band-pass and long-pass filters. The fluorescence was imaged quantitatively using a highly sensitive cryogenically cooled charge-coupled device (CCD) camera fitted to the microscope. Owing to the high signal intensity of the anthracyclines found in sensitive cells a relatively short exposure time of 10s was employed; however the resistant cells having incorporated less drug needed an exposure time of 25s. Negligible photobleaching by the laser was confirmed by repeating a few images using 90s exposure when the image intensity decreased proportionally with increased exposure. The signal was processed by an IBM personal computer into a falsely colour-coded microscopic image of the cells depicting the mean counts per pixel. The software also allowed quantitative analysis of the signal by calculating the mean fluorescence count and standard deviation within any chosen area on the fluorescence image[171].

Using a 10X objective, a phase contrast view of the cells was recorded. These cellular compartments were usually readily discernible on the fluorescence image but where necessary conventional light microscopy of the cells also helped to enable accurate identification of the various structures. Both fluorescence image and the light microscopic image of the field of view were recorded for comparison and analysis. Using this technique the image of the cells in phase contrast could be viewed while analysing the fluorescent drug distribution within them. Representative areas over the nucleus, cytoplasm and the whole cell were chosen for analysis on each section. By drawing around these cellular compartments in phase contrast, the computer automatically recorded the amount of mean fluorescence within them which corresponds to the amount of drug within that compartment. For these experiments, the cells were grown on coverslips and were exposed to the drug when still sub-confluent, when it was easier to discern individual cells, then placed on slides for viewing under the microscope.

Although the resolution of the CCD was probably as good as the confocal microscope and it is an excellent technique for analysing fluorescent drug location within fixed tissue sections it did not play an integral part in these studies. Although both could be used for cellular drug localisation and limited

quantification of the amount of drug, the CCD camera only allowed squares to be drawn around the cellular compartments for fluorescence analysis (Fig. 2.3). Also the cells tended to dry out whilst being viewed under the microscope connected to the CCD. This problem could be avoided by preparing a suitable fixative to maintain the integrity of the cell and the drug within them. Hence, it was decided that all cellular drug localisation experiments would be carried out using the confocal microscope which proved to be the more appropriate machine to use.

The incubation times of the drugs were the same for all experiments, MTZ and IDA for 1h and DOX for 2h. The optimum incubation time for each drug was found by timing drug uptake and plotting the results of the experiments. The time when drug uptake just began to plateau out, *i.e.* when the maximum amount of drug was taken up by the cells, was used as the optimum incubation time.

2.B.2. CELLULAR INCORPORATION AND CYTOTOXICITY OF EFA's

i. ISOTOPE INCORPORATION

Radioactivity was used to assess the uptake over time of GLA. The EFA used was a radiolabelled LiGLA. This was labelled using radioactive ^{14}C which allowed the GLA to be detected using established methods of tracking the radioactivity.

Cells were incubated in solution with the labelled LiGLA and carrier LiGLA. The carrier GLA was the same LiGLA used in all the other studies. Its role was to saturate cell uptake of GLA and therefore only a small amount of labelled GLA had to be used for detection to occur. Carrier GLA was used at 20μg/ml and radioactive GLA at 0.05μCi/ml. The uptake of GLA was stopped at various time intervals and the amount of cellular GLA at each time analysed by counting the amount of radioactivity. Uptake was stopped by centrifuging the cells, removing the medium containing labelled GLA, solubilising the cells with 0.5ml of Solvable™ for 1min then adding 15ml of scintillation fluid. This scintillation fluid transduces β emission energy to light pulses which are detected by a photomultiplier tube. Samples were set to count automatically for six minutes in a scintillation counter set

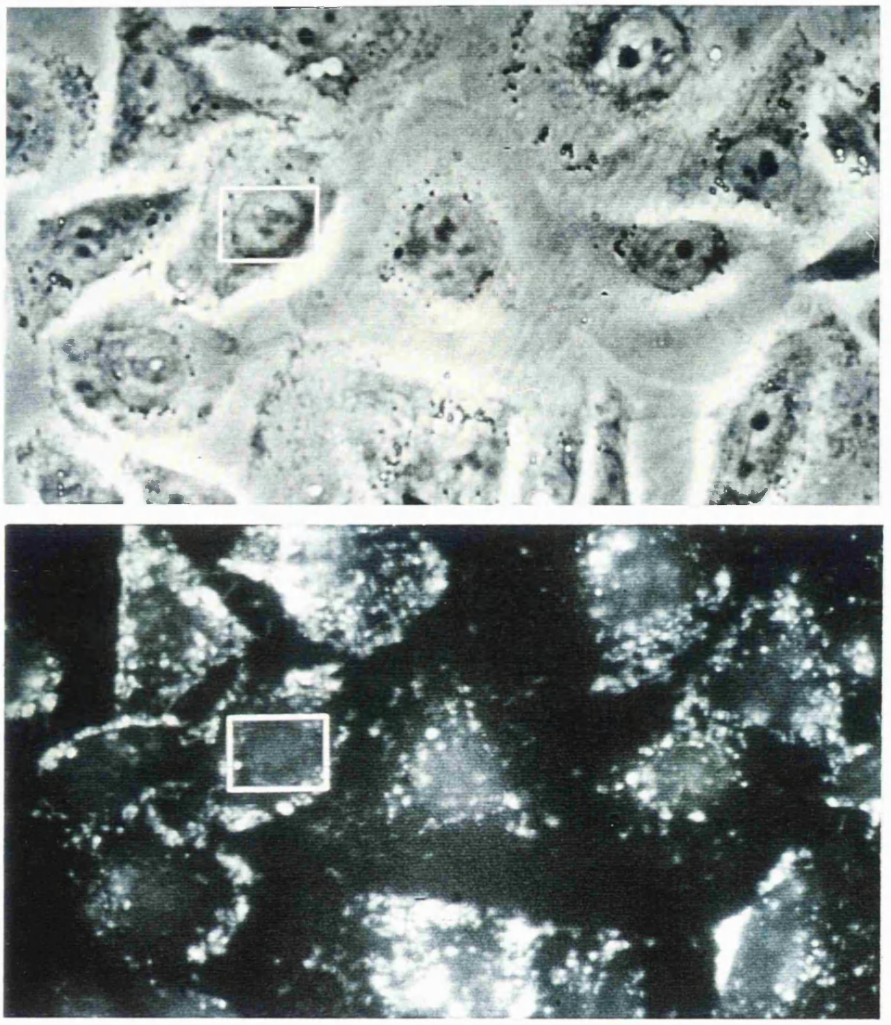

Fig. 2.3. **Analysis of drug uptake within intracellular compartments, using the CCD camera. Cells were visualised as phase contrast and fluorescent images.**
(X 750)

to detect ^{14}C emission products. Backgrounds were automatically subtracted using vials containing scintillation fluid only. The results were produced as mean counts per minute per vial.

ii) AUTORADIOGRAPHY

Radiolabelled LiGLA was also used to detect the intracellular localisation and distribution of GLA. Here the cells were grown on chamber slides, resistant cells in one chamber and sensitive cells in the other, allowing comparison in uptake. The cells were incubated with the same doses of ^{14}C LiGLA and LiGLA as above (see 2.B.2i). After 24h the chambers were removed, the cells fixed and the slides dipped in Kodak autoradiography emulsion, NTB-2, to allow silver grains to appear where radioactivity was present. It was important that the emulsion coated the slides smoothly leaving a layer of uniform thickness. This and all the following stages were done in the dark room with the aid of a red safety light. The slides were exposed to the emulsion in dark refrigerated conditions for 72h. The emulsion was then developed using Kodak Dektol developer and fixed using Kodak fixer. The resulting silver grains showed over where the GLA was situated intracellularly. The slides were counterstained using heamatoxylin to enable the cells' features to be easily identified and were viewed under an ordinary light microscope.

iii. CYTOTOXICITY ASSAY

The direct cytotoxicity of the GLA was analysed by a cell viability study using the MTT (3-(4,5-dimethylthlazol-2-yl)-2,5-diphenyl tetrazolium) assay[172]. This is a colourimetric dye assay based on the ability of viable cells to reduce MTT to a blue/purple formazan product. Cells were seeded in 96 well plates at a density of 1000 cells per well and left to settle and grow for 48h. Different doses of GLA between 10-40μg/ml were then added to each row of wells, including 2 control rows with no GLA. These plates were then left for different time periods between 24-72h. After a pre-determined time, 50μl of MTT in PBS at a dose of 2mg/ml was added to each well (containing cells and 200μl of medium). The plates were then wrapped in foil and incubated for 3h at 37C. After this incubation period, the

medium and MTT were removed and 200μl of DMSO immediately added to each well. This dissolved the purple formazan crystals which had formed in the viable cells only. The optical density of the purple liquid formed in the wells was then read using a spectrophotometer plate reader set to read at 570nm.

2.B.3 IMMUNOCYTOCHEMISTRY

This technique allows detection of any antigenic molecule of interest (generally a protein) in cell preparations. Monoclonal antibodies have the ability to recognise and bind to specific combining sites (epitopes) on the corresponding antigens and this forms the basis of immunocytochemistry. Once the antibody has bound to its epitope a number of methods are available for detection of the antigen-antibody complex[173]. These methods tend to involve more than one layer of molecules (indirect staining), each specifically binding to the previous one and thus amplifying the antibody signal. Visual detection falls into two categories: either an enzyme tagged to the last of the molecules in the staining complex, which is then exposed to a substrate leading to a precipitation of colour visible under light; or a fluorescent moiety again conjugated to the end layer which is visible under fluorescence. The latter method was chosen to determine whether and where the resistance related proteins, Pgp, LRP and MRP were localised in the cells and tissue sections.

i). PROTOCOL FOR BREAST AND BLADDER CANCER CELL LINES

The cell lines were grown on 13mm diameter coverslips in well plates (24 wells) to different levels of confluence although near confluence tended to give the clearest results. The cells were washed in PBS to remove all traces of medium, fixed in acetone for 6 mins at room temperature and stored in PBS at 4°C until used. This fixation procedure allowed cell integrity to be maintained whilst permitting antibodies to penetrate the cell membrane to bind to internal epitopes. The cells were not allowed to dry out at any time during the fixing or subsequent staining procedures, to avoid cellular damage.

Immunofluorescence was performed for the detection of Pgp, LRP and MRP as follows: all antibodies were diluted in L-15 containing 10% FCS. The primary antibodies were incubated on the cells for 1.5h at room temperature, on a roller to ensure uniform exposure. Following a thorough washing in PBS (3 x 5 mins) to remove any unbound primary antibody, the secondary (FITC) conjugated antibody was added for another hour and again incubated on a roller .

For viewing, all the coverslips were given a third wash then inverted and mounted on slides using Citiflour™ mounting fluid. The coverslips were then securely attached to the slides using nail polish and kept refrigerated in the dark until required. All cells were viewed under a fluorescence microscope. As the proteins were stained using a fluorescence conjugate, they were also viewed and photographed using the confocal microscope (see section 2.B.1ii).

ii). PROTOCOL FOR BREAST AND BLADDER CANCER SECTIONS

Slides were removed from -20°C storage, allowed to reach room temperature and fixed by immersion in 100% acetone at 4°C for 7 minutes. They were washed three times for five minutes in PBS. The slides were arranged in a humidity chamber, and 2% rabbit albumin was applied for five minutes to block any non-specific staining. Pgp expression was investigated by indirect immunofluorescence. The primary JSB antibody was diluted 1:20 in 1% BSA in PBS and applied on the slides for a 1h incubation after which the secondary antibody, goat anti-mouse IgG-FITC, was applied to all sections at a 1:100 dilution with PBS. The slides were covered in tin foil to prevent moisture loss and exposure to light, and incubated for 1 hour at room temperature. Three PBS washes were carried out as before, and excess moisture around the sections removed.

MRP and LRP expression was investigated by immunohistochemistry using an avidin-biotin complex method. The primary antibody used was mouse anti-human MRPm6 or mouse anti-human LRP-56, diluted 1:20 in 10% foetal calf serum in PBS for 1h 30 min. Preparation of all antibodies in 10% FCS/PBS produced much lower backgrounds compared with using 1% BSA/PBS. The sections were washed in PBS (3x5 min). The secondary antibody used was goat

anti-mouse biotinylated IgG1 at a 1:100 dilution in 10% FCS/PBS for 1h. The sections were then washed in PBS (3x5 min). This was followed by incubation with the tertiary layer, streptavidin Cy3 diluted at 1:100 in PBS for 30 min at room temperature. The slides were covered with tin foil for the final incubation. A three layer method of staining was chosen for the MRP and LRP proteins as it resulted in a stronger signal being produced.

Following the staining procedure all sections were washed with PBS (3x5 min) before being mounted with Citifluor™ and observed under a fluorescent microscope (Leitz).

A number of methodological variations in fixing and blocking were carried out both on cell lines and tissue sections to determine the protocol which gave the 'cleanest' staining: i) fixation using acetone for 6min at room temperature gave good staining with slightly less background compared to acetone: chloroform (50:50) or acetone: ethanol (50:50) or paraformaldehyde: formaldehyde (50:50) at room temperature for 20 min. Furthermore, preincubation with any amount of BSA in PBS or human serum in PBS gave considerably more background than 5% rabbit albumin which still produced a higher background than medium containing 10% FCS. Therefore, the antibody dilutions were performed mainly in air-buffered L-15 medium containing 10% FCS.

RESULTS

3. DIFFERENCES IN ANTHRACYCLINE UPTAKE BETWEEN SENSITIVE AND RESISTANT CELLS

3.1. TIMED DRUG UPTAKE CURVES

In this subsection, the uptake of drug by the cells over a period of time was observed using flow cytometry. This gave an indication of the time the cells would need for incubation with the drug for optimum intracellular drug uptake to occur. Optimum cellular drug uptake was perceived as the time when drug uptake slowed down considerably, even if maximum uptake had not yet occurred; longer drug incubation would endanger the cells integrity or produce anomalous results (see Appendix 2.1). For all these experiments the amount of drug taken up by the cells was recorded as the amount of fluorescence per cell (arbitrary fluorescent units) then presented as a mean (± s.d.) using the FACScan. The graphs for this section are presented on pages 66 to 71. The drug dose used in all experiments was 10μg/ml, this was decided upon as a suitable dose to observe drug uptake over time from similar studies by other researchers. The exception was IDA which has been shown to have significantly higher accumulation levels than other anthracyclines in both sensitive and resistant cell lines[174] so that a dose of 5μg/ml was sufficient to record the uptake of this drug over a timed period.

3.1.i). MGH-U1 AND MGH-U1/R CELLS

DOXORUBICIN: Maximum drug uptake in MGH-U1 cells, producing the largest difference between sensitive and resistant cells, occurred after 90 min DOX incubation. At this point there was a difference between drug uptake in sensitive cells compared to resistant cells of approximately 5 fold (47.5 ± 10 vs 10 ± 1.0) (Graph 3.1a).

EPIRUBICIN: Although drug uptake in sensitive cells continued rising until 120 min the two final points at 90 and 120 min appeared anomalous with very high drug

uptake at these points (278.4 ± 16.2 and 388.0 ± 16.0). The cells primarily appeared to reach saturation after 60 min (135.9 ± 13.5). The sudden increase in drug uptake by the sensitive cells at 90 min could be a result of the cells becoming stressed due to incubation with the drug as time increased. After all, cells which are damaged in any way are known to take up increased quantities of drug, (see Appendix 2.1). However, there was no observable difference in the dot plots of the cells at either of these incubation times and any change in the state of cells, such as death, is usually visible on the SSC plot. The optimum uptake time was decided to be 60 min, where high uptake occurred and the cells were considered healthier than at 90 or 120 min. The difference in drug uptake between sensitive and resistant at 60 min was approximately 6 fold (135.9 ± 13.5 vs 21.0 ± 2.5) (Graph 3.1b).

IDARUBICIN: The sensitive cells reached saturation of IDA uptake at around 60 min, after which the uptake of the drug slowed down considerably. At this point there was over a 4 fold difference in IDA uptake between sensitive and resistant cells (685.5 ± 80.0 vs 140.9 ± 20.0) (Graph 3.1c).

3.1.ii) MCF-7 AND MCF-7/R CELLS

DOXORUBICIN: Both the sensitive and resistant cells continued taking up drug over the full 120 min, however, both showed aberrant points on the graph for 120 min (especially the MCF-7 cells). These points of high drug uptake are likely to be due to the cells becoming stressed. Therefore, the optimum incubation time for the MCF-7 and MCF-7/R cells with DOX was taken as 90 min. At this point the difference in drug uptake between sensitive and resistant cells was approximately 3 fold (107.8 ± 8.0 vs 35.7 ± 7.0) (Graph 3.1d).

MITOZANTRONE: The maximum difference in drug uptake between sensitive and resistant cells occurred after 120 min of MTZ incubation. However, the rapid phase of drug uptake appeared to stop at 60 min (sensitive vs resistant, 66.7 ± 8.0 vs 49.0 ± 10.0) (Graph 3.1e).

IDARUBICIN: There was not much difference in drug uptake between sensitive and resistant cells over the 120 min of incubation. Over the first 40 min, the resistant cells took up the same amount of IDA as the sensitive cells, after this the gap between drug uptake by the resistant cells and the sensitive cells widened slightly, but never more than by a factor of 0.5. In both cell lines drug uptake slowed down after 60 min making this the optimum incubation period for these cells with this drug (sensitive vs resistant, 265.3 ± 18 vs 206.1 ± 20.0) (Graph 3.1f).

3.2.DRUG DOSE RESPONSE CURVES

3.2.1. METHOD OF INCUBATING CELLS WITH DRUG

This subsection illustrates differences in uptake of the same drug by the same cell lines using different drug incubation methods. The two methods investigated were drug uptake by the cells incubated in suspension with drug spiked medium or cells incubated with drug spiked medium while still in a monolayer and adherent to the flasks. Both methods of drug uptake by the cells were recorded using flow cytometry. The graphs for this section are presented on pages 72 to 76.

3.2.1.i) MGH-U1 AND MGH-U1/R CELLS

DOXORUBICIN: DOX uptake by cells in suspension was much higher compared to adherent cells for both resistant and sensitive cells. There was much better separation between drug uptake in sensitive and resistant cells, particularly at 15μg/ml, in adherent cells (134.0 ± 15.0 vs 16.0 ± 1.3) than between the two cell lines incubated with DOX in suspension (224.38 ± 37.5 vs 280.6 ± 25.0). When the cells were incubated with DOX in suspension the resistant cells took up more drug or at least similar quantities of drug than the sensitive cells over all drug doses (Graph 3.2a).

IDARUBICIN: Drug uptake by both the resistant and sensitive cells in suspension was much higher than for the same cells incubated with the same amount of drug

but in a monolayer and adherent. Separations between IDA uptake in sensitive and resistant cells differed depending on their method of incubation. At 10μg/ml the fluorescence detected (arbitrary units) in adherent sensitive vs resistant cells was 939.0 ± 40.0 vs 120.0 ± 20.0 an approximately 8 fold difference and for the cells in suspension sensitive vs resistant was 1619.0 ± 200.0 vs 648.0 ± 70.0 an approximately 3 fold difference (Graph 3.2 b).

3.2.1.ii) MCF-7 AND MCF-7/R CELLS

DOXORUBICIN: Sensitive and resistant cells incubated with DOX in suspension displayed much higher drug uptake than the identical cells incubated whilst adherent. There was no clear difference in drug uptake between sensitive and resistant cells incubated in suspension with the resistant cells taking up more DOX than sensitive cells at some drug concentrations.

There was a much clearer separation in DOX uptake between sensitive and resistant cells incubated with drug whilst in a monolayer, the sensitive cells took up 2.1 fold more DOX than the resistant cells (Graph 3.2c).

MITOZANTRONE: This was the only drug were the method of incubation did not drastically influence drug uptake by the cells. Although the cells incubated with MTZ in suspension showed higher MTZ uptake, sensitive cells took up 2.9 fold more drug than resistant cells at 15μg/ml. Incubating the cells with drug in monolayers produced a similar difference in MTZ uptake between sensitive and resistant cells, sensitive cells took up 2.8 fold more MTZ than the resistant at 15μg/ml, but at lower levels of fluorescent intensity (Graph 3.2d).

IDARUBICN: Cells incubated with drug in suspension had much higher levels of fluorescence compared to cells incubated in monolayers. However, there was no significant difference between drug uptake by sensitive and resistant cells for either incubation method (Graph 3.2e).

In summary the two main points from these experiments were drug uptake in suspension was higher and the separation between sensitive and resistant cells was better in adherent cells for most drugs. This led to the decision that all cells would be incubated with the drug in monolayers whilst adhered to the flasks (due to this EPI was not incubated with cells in suspension).

3.2.2. CELLULAR DRUG UPTAKE

The cellular drug uptake at different drug doses was recorded using flow cytometry. This allowed comparison between drug uptake in sensitive cell lines and their resistant counterparts at varying drug concentrations. As with the above experiments (Section 3.1), unless otherwise stated the cells were incubated with drug while attached to the flasks. The graphs for this section are presented on Pages 77 to 82.

3.2.2.i) MGH-U1 AND MGH-U1/R CELLS

DOXORUBICIN: The sensitive cells took up more drug than their resistant counterparts at all concentrations. At the lower doses there was not such a pronounced difference in DOX uptake between the two cell lines, about 2 fold. At higher DOX doses the resistant cells reached a plateau (15.0 ± 4.0), starting at 10μg/ml, while the sensitive cells continued to take up DOX. DOX uptake by the sensitive cells began to plateau at 15μg/ml (87.0 ± 4.0). A maximum difference in DOX uptake between sensitive and resistant cells of 6 fold was reached at 20μg/ml (91.4 ± 25.0 vs 17.8 ± 3.5). A statistically significant difference in drug uptake between sensitive and resistant cells was first observed at 10μg/ml using the Welch alternate t-test (Graph 3.2f).

EPIRUBICIN: The resistant cells took up very little EPI at any concentration but practically none at the lower doses. The sensitive cells took up EPI in an exponential curve with uptake beginning to plateau at 10μg/ml (172.0 ± 40.0). After 5μg/ml there was a difference in EPI uptake by sensitive and resistant cells of approximately 30 fold which was increased over the last three EPI concentrations.

A statistically significant difference in drug uptake between sensitive and resistant cells was first observed at 5μg/ml using the Welch alternate t-test (Graph 3.2g).

IDARUBICIN: Unlike the two drugs above, IDA was taken up by the sensitive cells in an almost linear fashion. This was also true for the IDA uptake by resistant cells but at much lower rate compared to the sensitive cells. There was a difference in fluorescence intensity between sensitive and resistant cells at all IDA doses but particularly at 5 and 10μg/ml. At these concentrations the sensitive cells took up about 6-9 times more IDA than the resistant cells (594.0 ± 30.0 vs 62.0 ± 6.0 at 5μg/ml and 939.0 ± 40.0 vs 120.0 ± 10.0 at 10μg/ml). A statistically significant difference in drug uptake between sensitive and resistant cells was first observed at 2μg/ml using the Welch alternate t-test (Graph 3.2h).

3.2.2.ii). MCF-7 AND MCF-7/R CELLS

DOXORUBICIN: As the concentration of DOX increased so did the difference in DOX uptake between sensitive and resistant cells. From 10μg/ml through to 20μg/ml there was a constant difference in drug uptake between the two cell lines with sensitive cells taking up 2 fold more DOX than resistant cells (40.0 ± 4.0 vs 19.1 ± 3.1). Drug uptake by the resistant cells began to slow down at 10μg/ml, whilst the sensitive cells only began to plateau after 15μg/ml. A statistically significant difference in drug uptake between sensitive and resistant cells was first observed at 10μg/ml using the Welch alternate t-test (Graph 3.2i).

MITOZANTRONE: There was a difference in MTZ uptake between the two cell lines at all concentrations. Both cell lines showed a slowing down in MTZ uptake from about 10μg/ml for sensitive cells and 5μg/ml for resistant cells only to increase slightly again at 20μg/ml. This could be as the cells, of both cell lines, became slightly unhealthy at this concentration of MTZ. The maximum difference between MTZ uptake in sensitive and resistant cells was 3 fold at 10μg/ml (105.3 ± 10.0 vs 29.9 ± 2.0). A statistically significant difference in drug uptake between

sensitive and resistant cells was first observed at 10μg/ml using the Welch alternate t-test (Graph 3.2j).

IDARUBICIN: The two cell lines followed a very similar pattern of IDA uptake and were also very similar in the amount of IDA they took up. At no point on the graph did the sensitive cells take up any more than 0.5 times more IDA than the resistant cells. So the sensitive and resistant cells took up similar amounts IDA with both cell lines appearing to be 'sensitive' in their IDA uptake for 10μg/ml, sensitive cells read at 648.1 ± 15.0 and resistant cells 534.0 ± 27.0. No statistically significant difference in drug uptake between sensitive and resistant cells was observed in these cells with IDA using the Welch alternate t-test (Graph 3.2k).

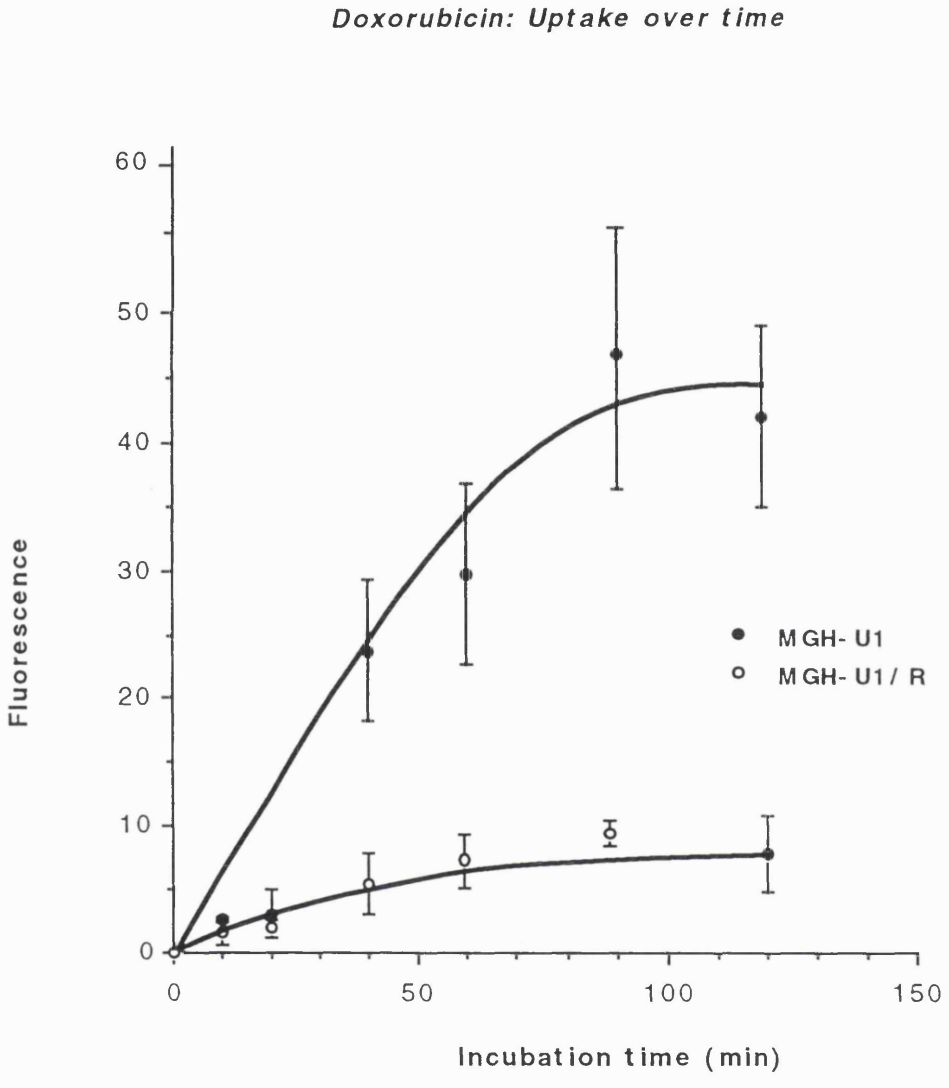

Graph 3.1a. **Uptake of doxorubicin over time by MGH-U1 and MGH-U1/R cells. Means ± standard deviations (SD) of intracellular drug fluorescence as arbritary units from the FACScan.**

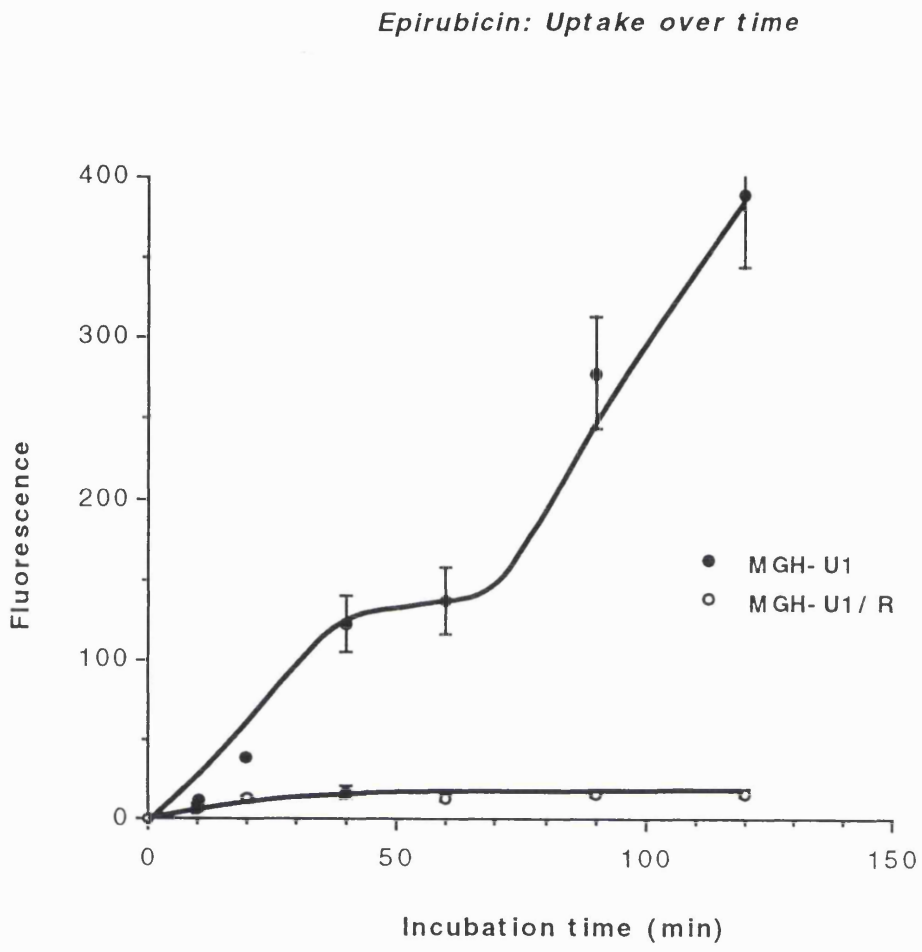

Graph 3.1b. **Uptake of epirubicin over time by MGH-U1 and MGH-U1/R cells. Means ± standard deviations (SD) of intracellular drug fluorescence as arbritary units from the FACScan.**

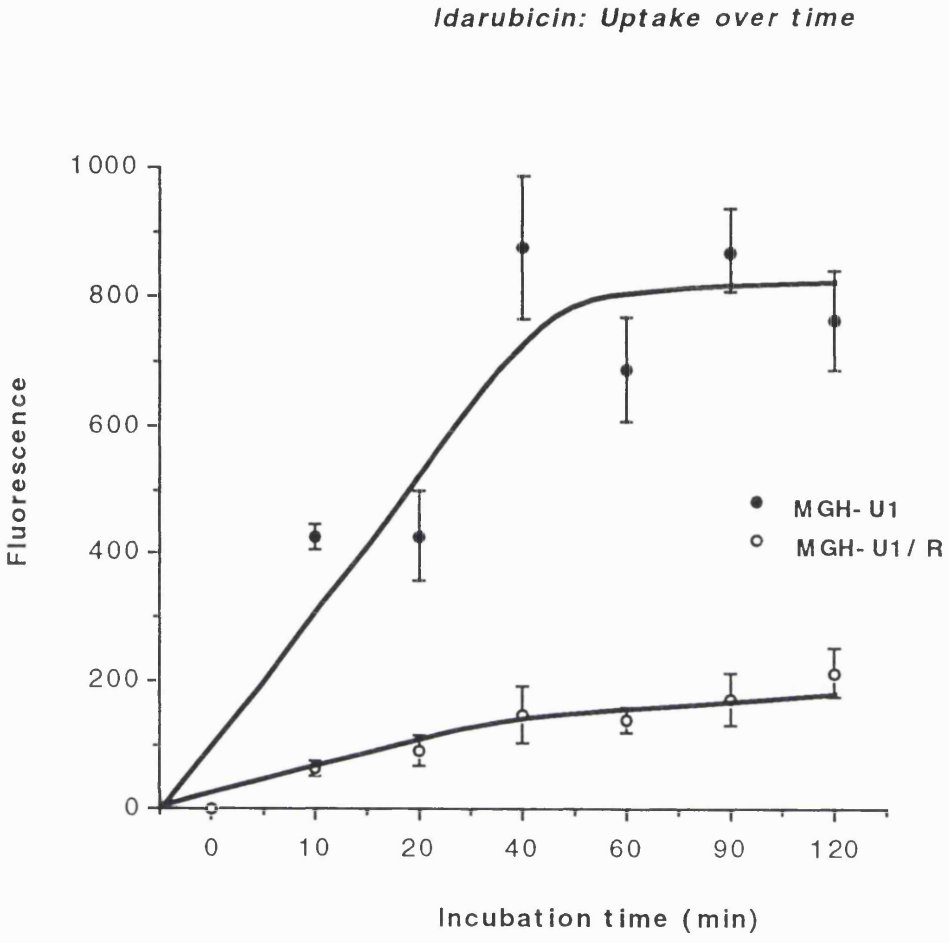

Graph 3.1c. **Uptake of idarubicin over time by MGH-U1 and MGH-U1/R cells. Means ± standard deviations (SD) of intracellular drug fluorescence as arbritary units from the FACScan.**

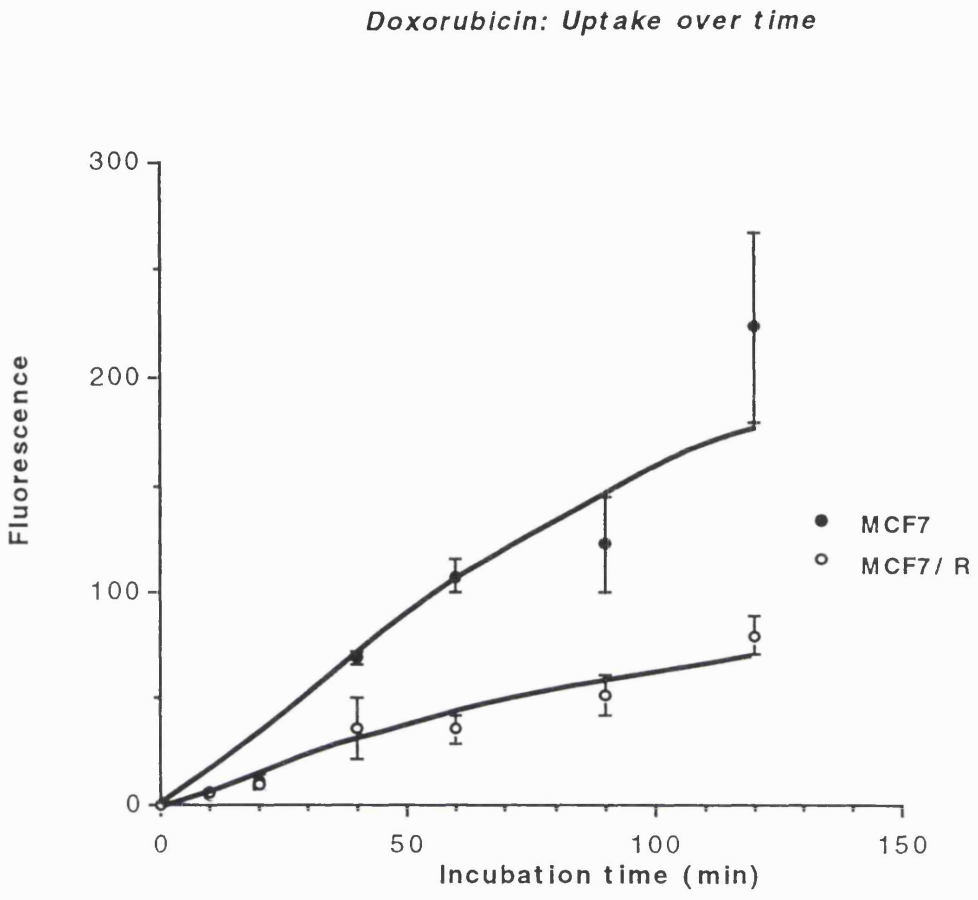

Graph 3.1d. **Uptake of doxorubicin over time by MCF-7 and MCF-7/R cells. Means ± standard deviations (SD) of intracellular drug fluorescence as arbritary units from the FACScan.**

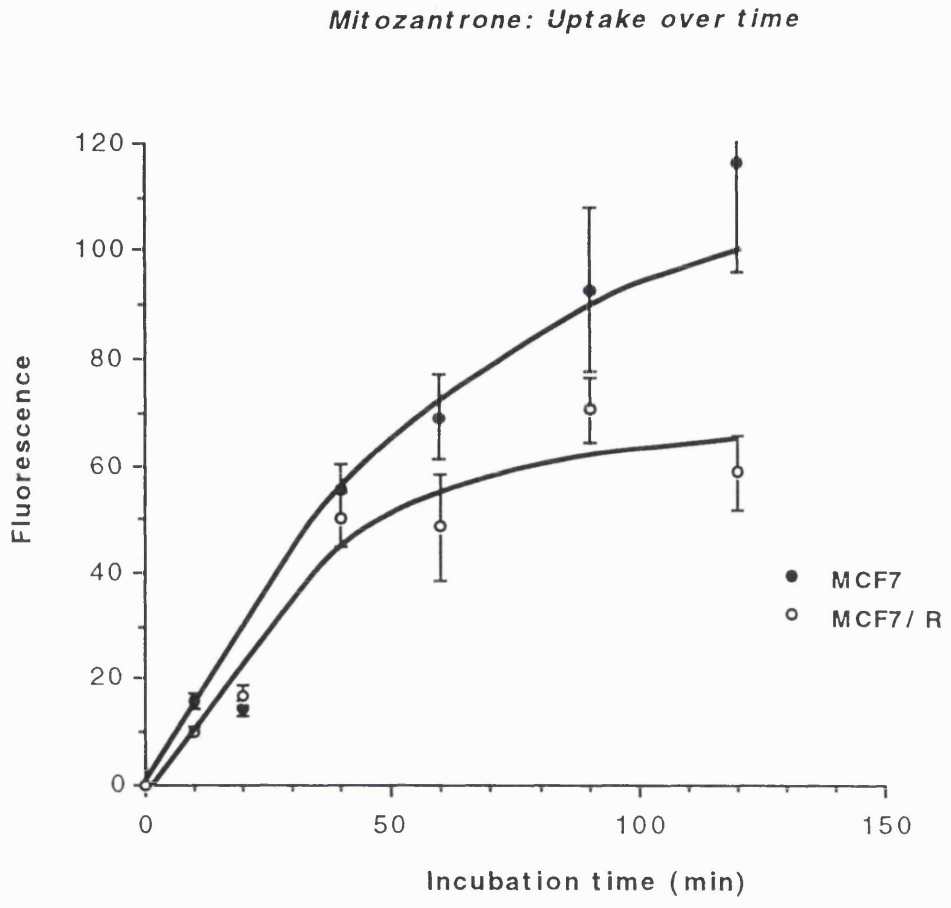

Graph 3.1e. **Uptake of mitozantrone over time by MCF-7 and MCF-7/R cells. Means ± standard deviations (SD) of intracellular drug fluorescence as arbritary units from the FACScan.**

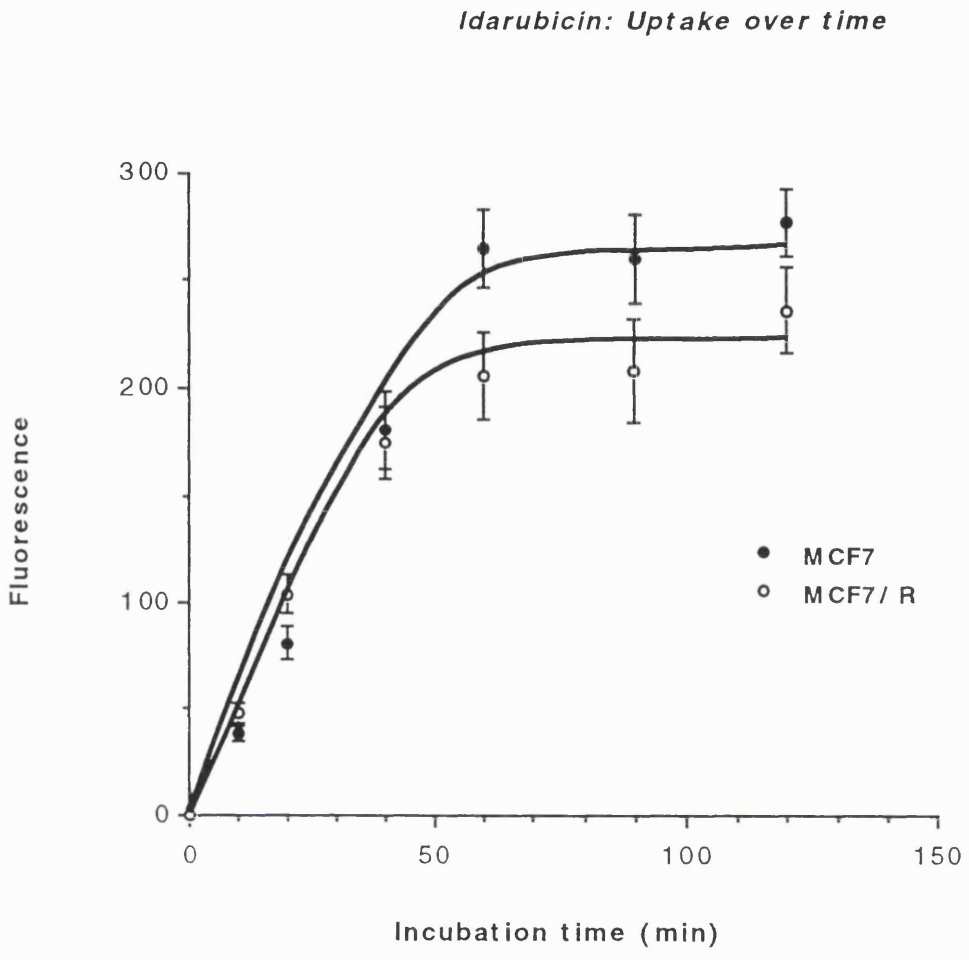

Graph 3.1f. **Uptake of idarubicin over time by MCF-7 and MCF-7/R cells. Means ± standard deviations (SD) of intracellular drug fluorescence as arbritary units from the FACScan.**

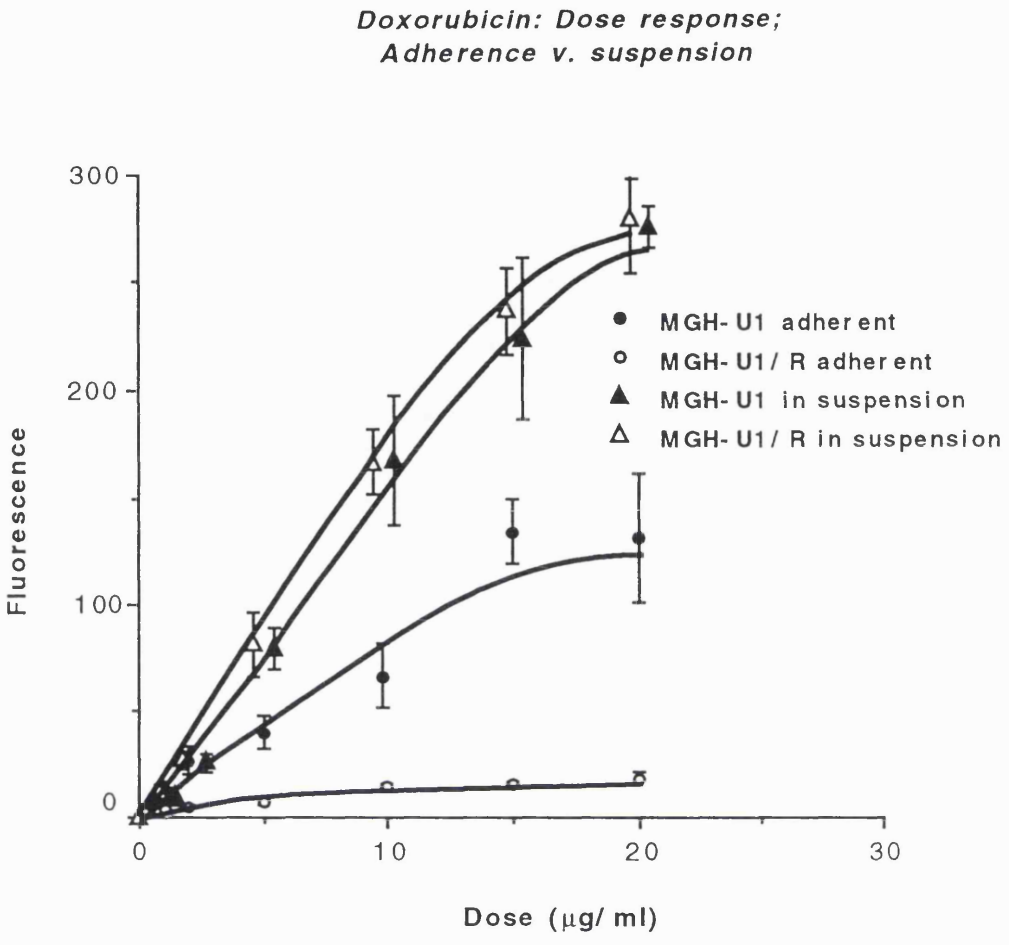

Graph 3.2a. **Doxorubicin uptake by MGH-U1 and MGH-U1/R cells incubated with drug when attached to the flask compared with DOX uptake by cells in suspension. Means ± standard deviations (SD) of intracellular drug fluorescence as arbritary units from the FACScan.**

Idarubicin: Dose response;
Adherence v. suspension

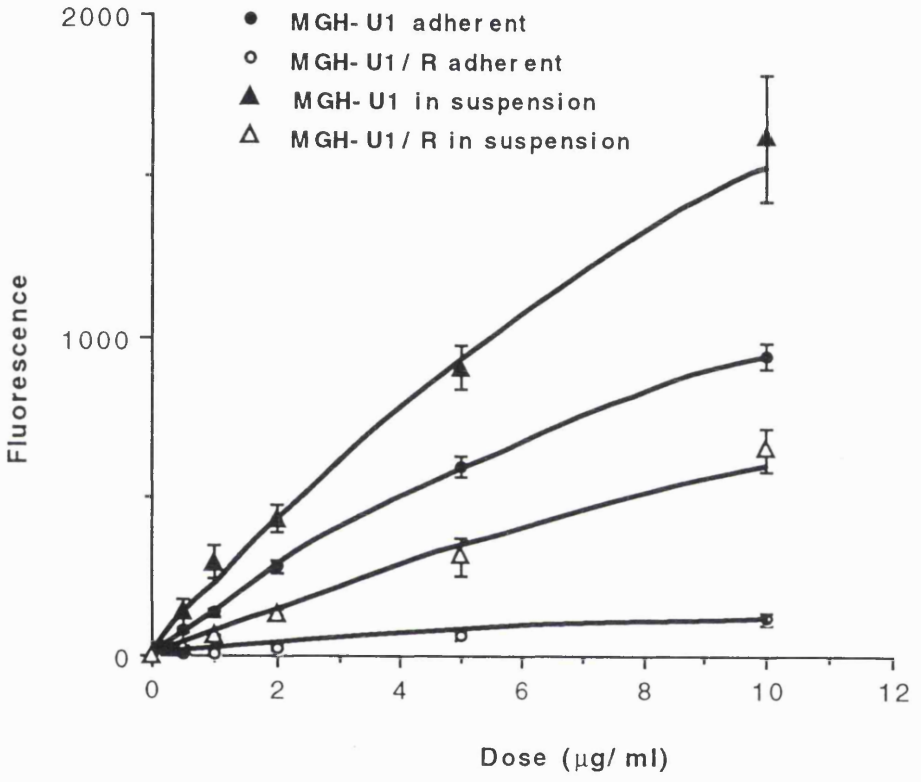

Graph 3.2b. **Idarubicin uptake by MGH-U1 and MGH-U1/R cells incubated with drug when attached to the flask compared with DOX uptake by cells in suspension. Mean ± standard deviations (SD) of intracellular drug fluorescence as arbritary units from the FACScan.**

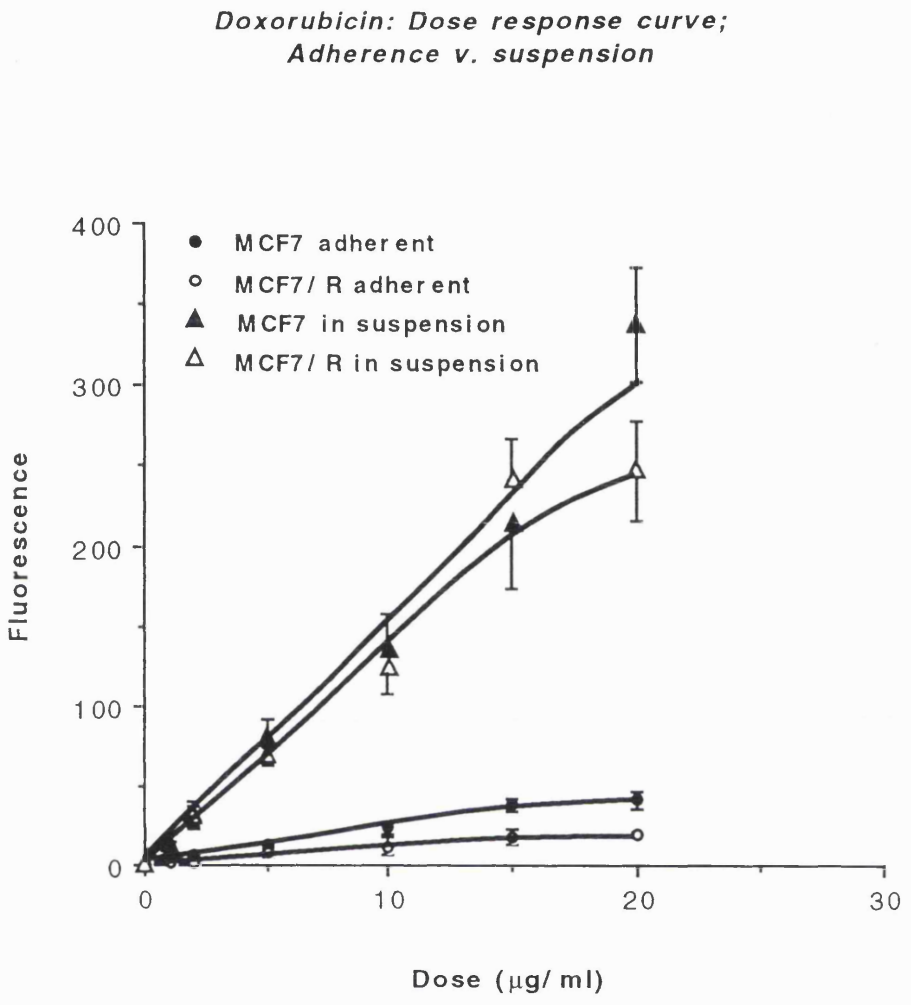

Graph 3.2c. **Doxorubicin uptake by MCF-7 and MCF-7/R cells incubated with drug when attached to the flask compared with DOX uptake by cells in suspension. Mean ± standard deviations (SD) of intracellular drug fluorescence as arbritary units from the FACScan.**

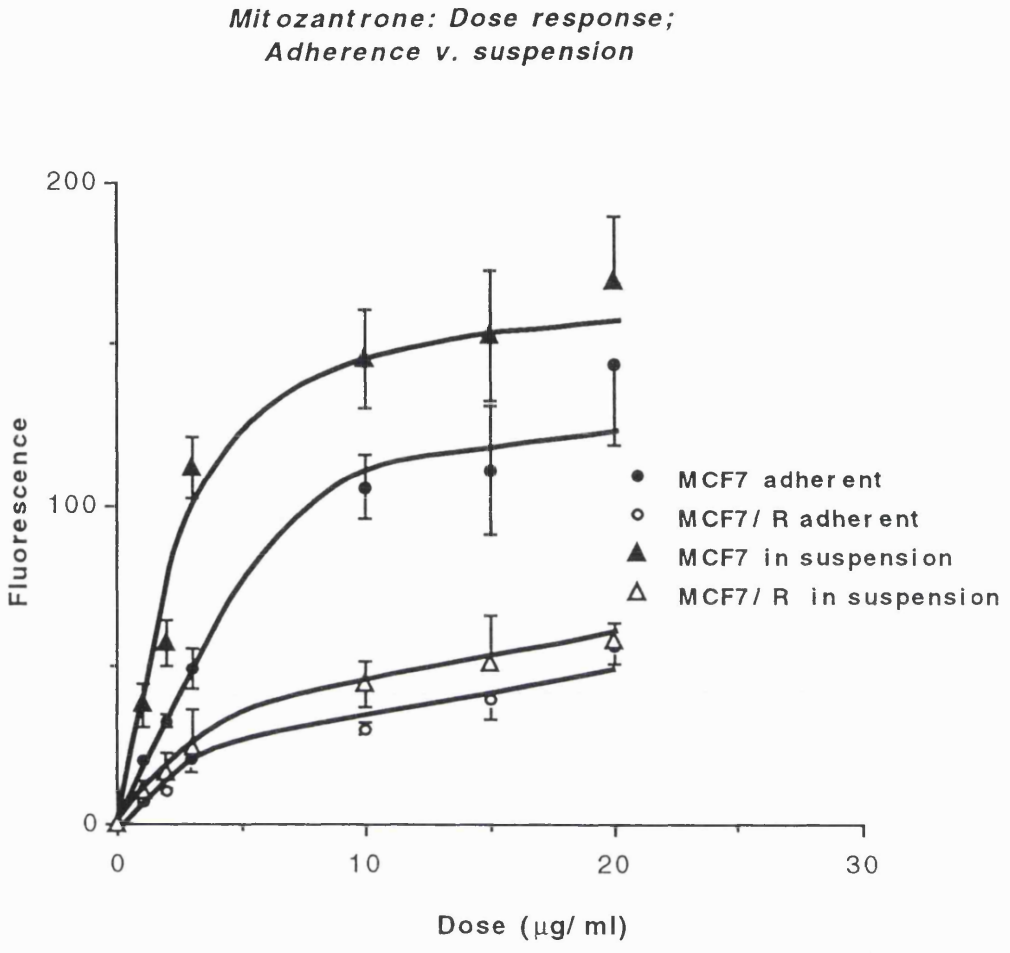

Graph 3.2d. **Mitozantrone uptake by MCF-7 and MCF-7/R cells incubated with drug when attached to the flask compared with DOX uptake by cells in suspension. Means ± standard deviations (SD) of intracellular drug fluorescence as arbritary units from the FACScan.**

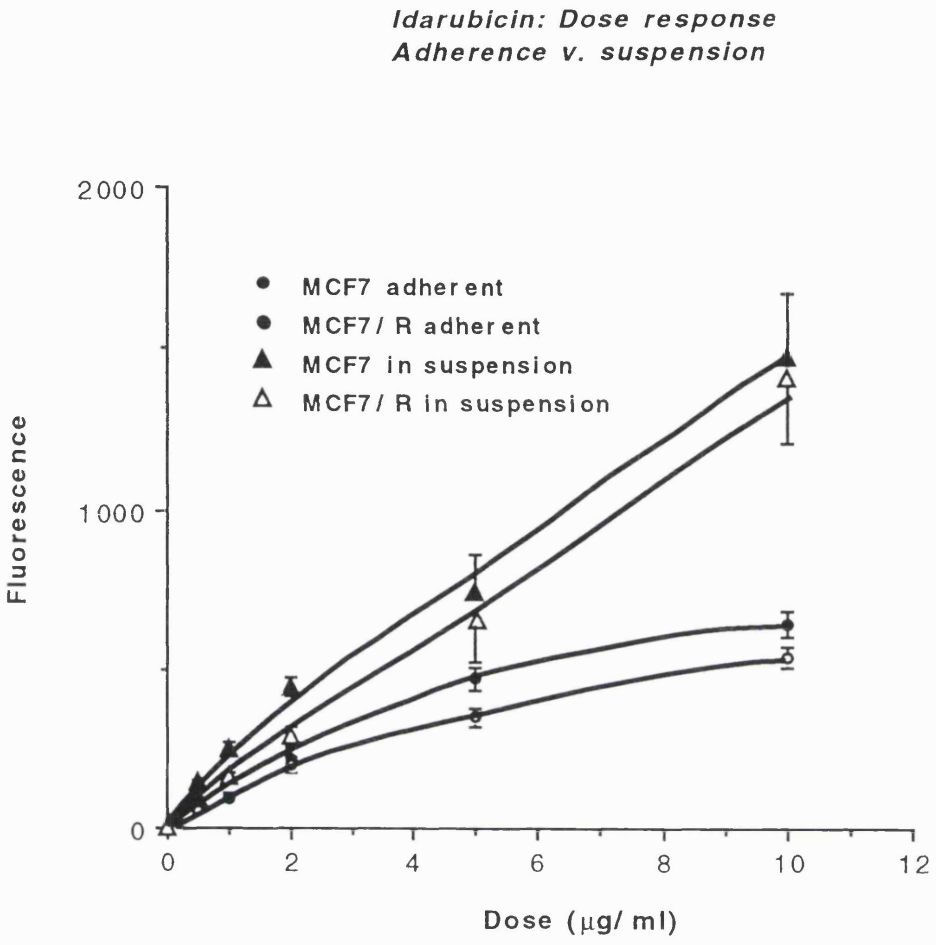

Graph 3.2e. **Idarubicin uptake by MCF-7 and MCF-7/R cells incubated with drug when attached to the flask compared with DOX uptake by cells in suspension. Mean ± standard deviations (SD) of intracellular drug fluorescence as arbritary units from the FACScan.**

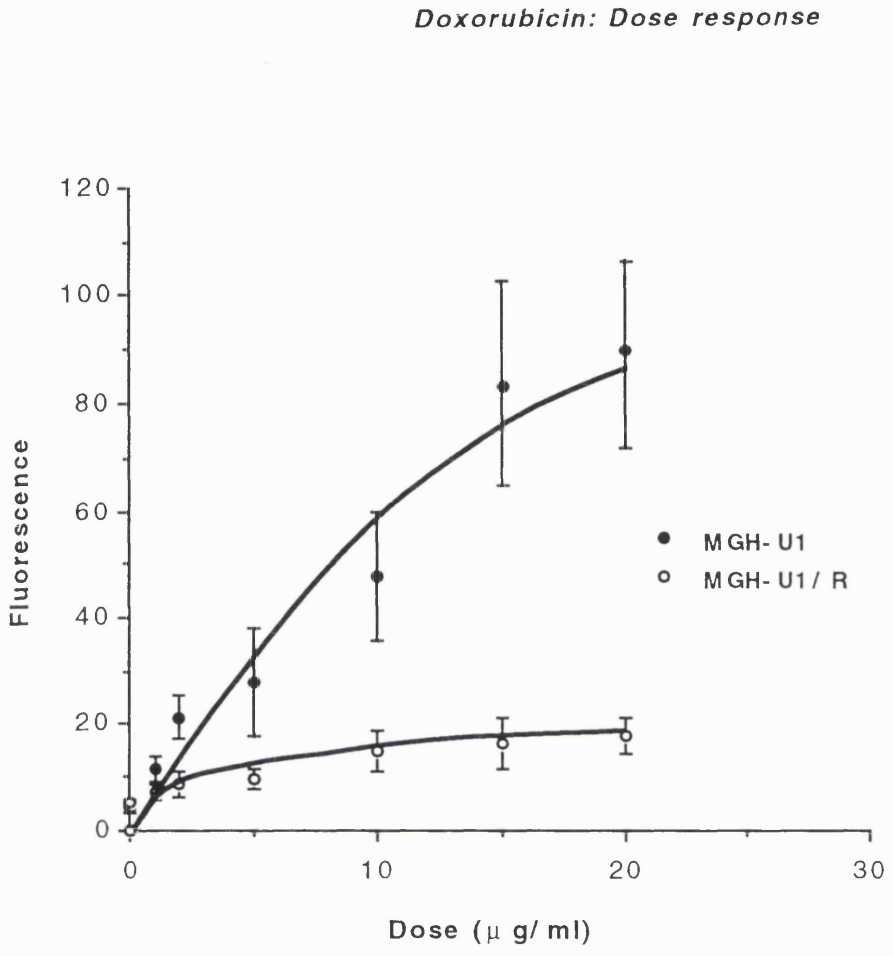

Graph 3.2f. **Doxorubicin dose response by MGH-U1 and MGH-U1/R cells. Cells incubated with DOX for 90 min. Means ± standard deviations (SD) of intracellular drug fluorescence as arbritary units from the FACScan. A statistically significant difference in drug uptake between sensitive and resistant cells was first observed at 10μg/ml using the Welch alternate t-test.**

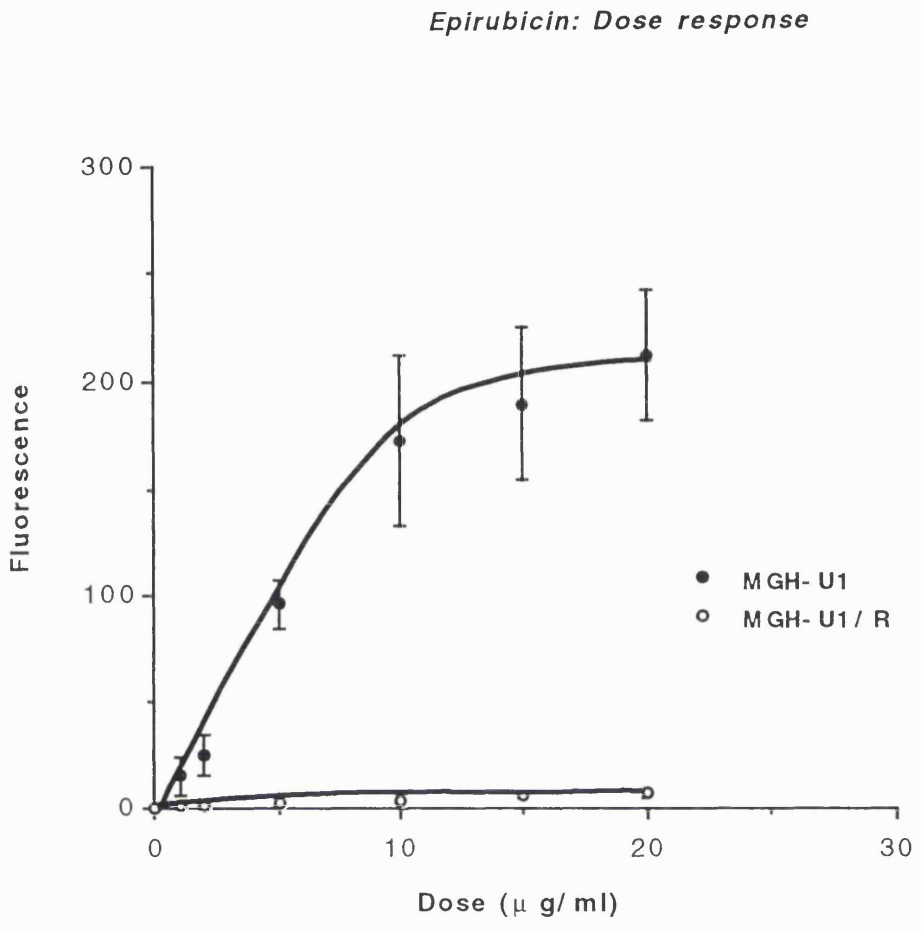

Graph 3.2g. **Epirubicin dose response by MGH-U1 and MGH-U1/R cells. Cells incubated with EPI for 60 min. Means ± standard deviations (SD) of intracellular drug fluorescence as arbritary units from the FACScan. A statistically significant difference in drug uptake between sensitive and resistant cells was first observed at 5μg/ml using the Welch alternate t-test.**

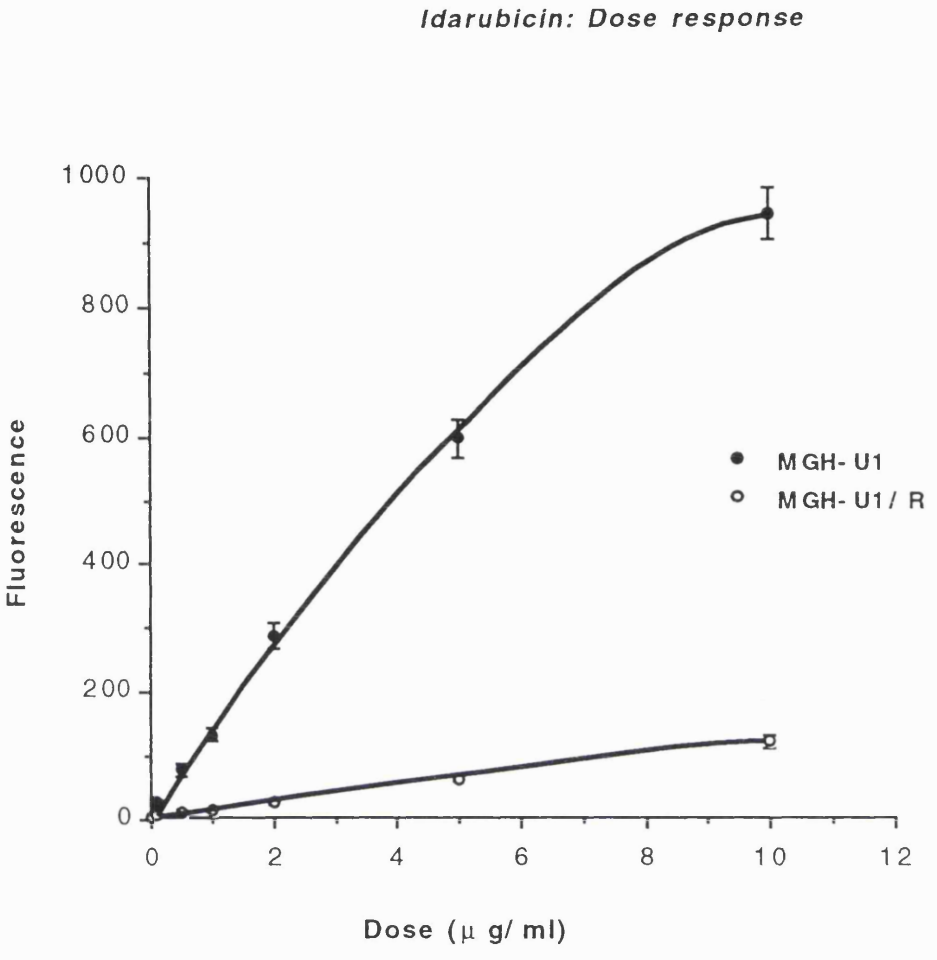

Graph 3.2h. **Idarubicin dose response by MGH-U1 and MGH-U1/R cells. Cells incubated with IDA for 60 min. Means ± standard deviations (SD) of intracellular drug fluorescence as arbritary units from the FACScan. A statistically significant difference in drug uptake between sensitive and resistant cells was first observed at 2μg/ml using the Welch alternate t-test.**

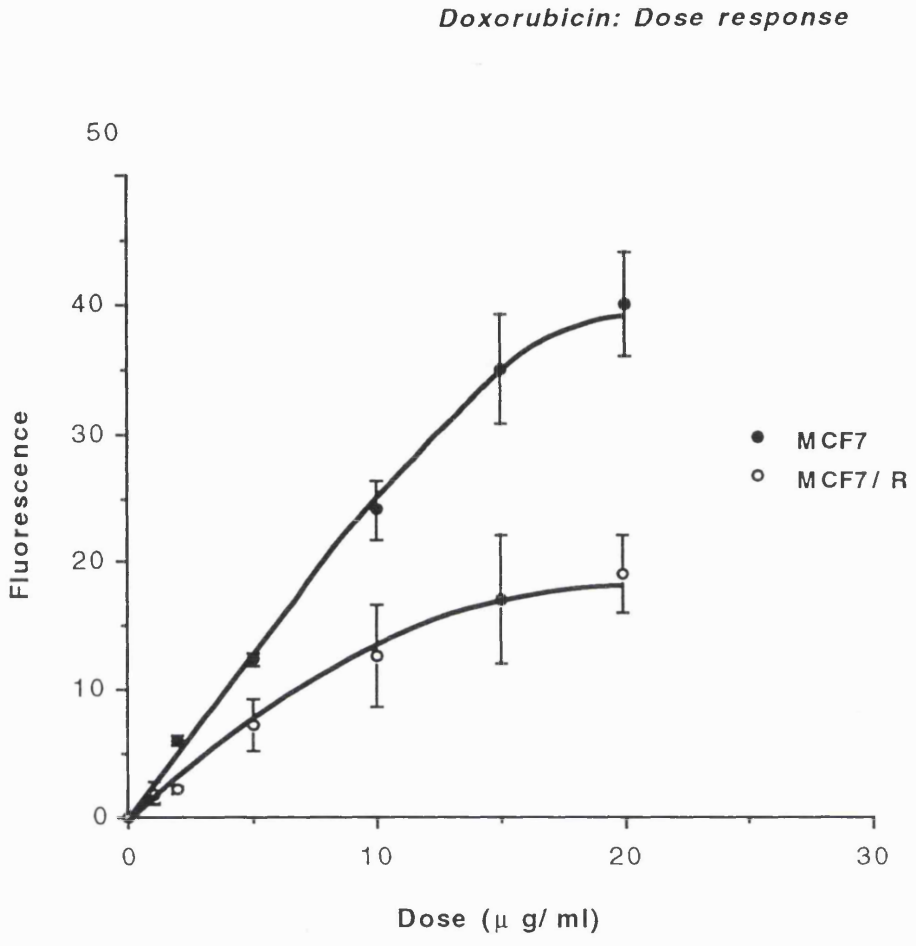

Graph 3.2i. **Doxorubicin dose response by MCF-7 and MCF-7/R cells. Cells incubated with DOX for 90 min. Means ± standard deviations (SD) of intracellular drug fluorescence as arbritary units from the FACScan. A statistically significant difference in drug uptake between sensitive and resistant cells was first observed at 10μg/ml using the Welch alternate t-test.**

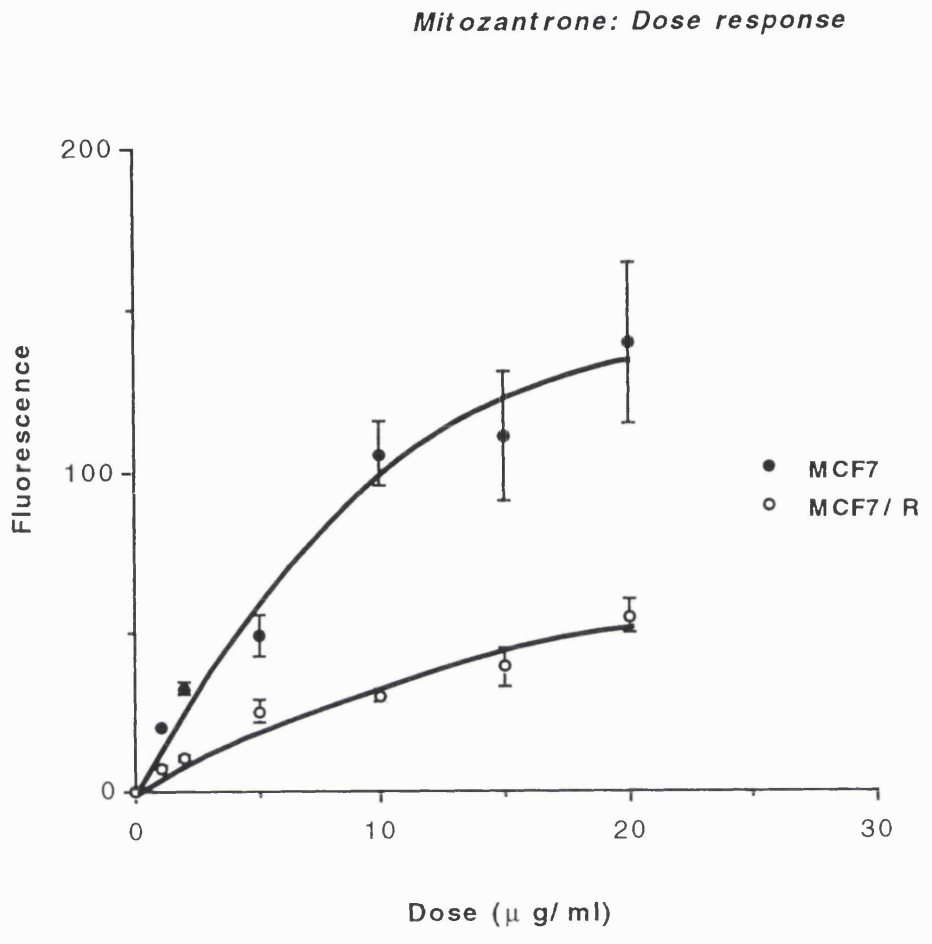

Graph 3.2j. Mitozantrone dose response by MCF-7 and MCF-7/R cells. Cells incubated with MTZ for 60 min. Means ± standard deviations (SD) of intracellular drug fluorescence as arbritary units from the FACScan. A statistically significant difference in drug uptake between sensitive and resistant cells was first observed at 10μg/ml using the Welch alternate t-test.

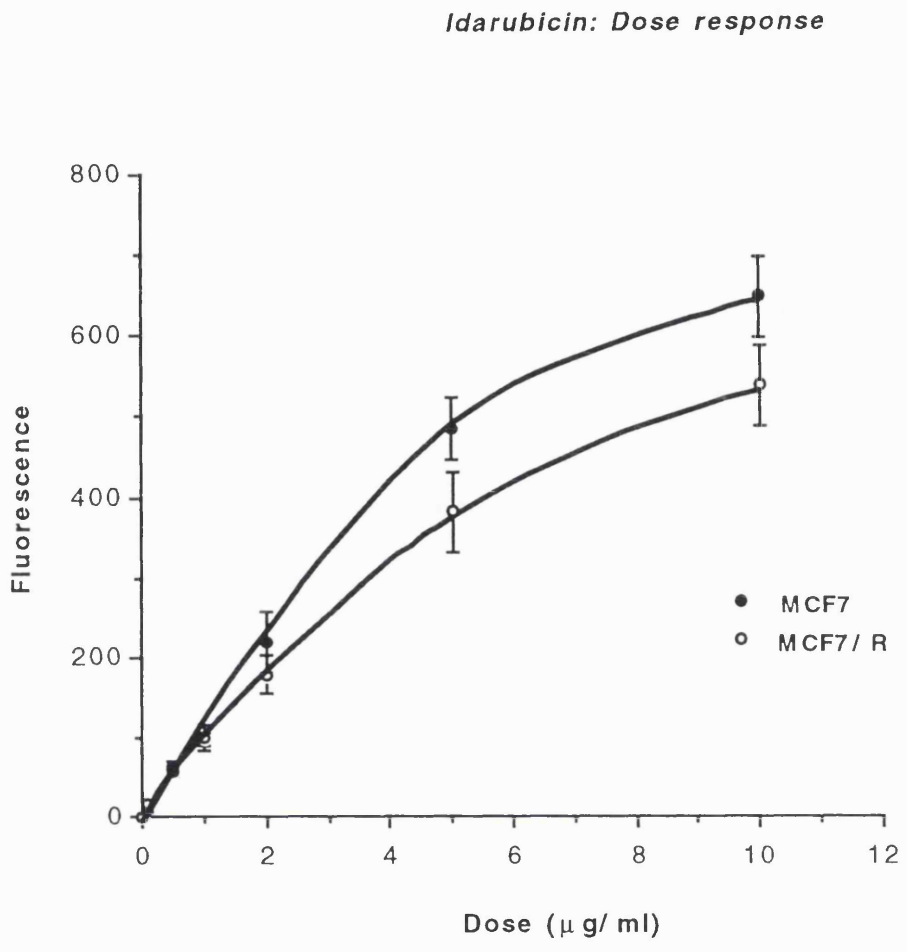

Graph 3.2k. **Idarubicin dose response by MCF-7 and MCF-7/R cells. Cells incubated with IDA for 60 min. Means ± standard deviations (SD) of intracellular drug fluorescence as arbritary units from the FACScan. No statistically significant difference in drug uptake between sensitive and resistant cells was observed using the Welch alternate t-test.**

3.3. PATTERNS OF INTRACELLULAR DRUG DISTRIBUTIONS

3.3.1. DETECTION BY CONFOCAL MICROSCOPY

As the drugs are naturally fluorescent, their intracellular localisation could be detected and recorded using the confocal microscope. The confocality of the microscope allowed better observation of the location and concentration of drug within cellular compartments, such as the nuclei, than conventional fluorescent microscopy. This machine also allowed semi-quantification of the amount of drug, directly related to the amount of fluorescence within the cell or section. As many of the drug uptake experiments, using the FACScan, were achieved using the drug dose at 10μg/ml (see section 5.3), the confocal studies of intracellular drug distribution were also undertaken at this dose. However, some of the drugs were not clearly detected and produced high background fluorescence at this concentration. These drugs were EPI and in particular DOX which was noted to be "sticky" on the plastic petri dishes leading to high background fluorescence especially in the resistant cells (see section 3.3.ii MCF-7/R + DOX). Therefore, for DOX and EPI the experiments were repeated using higher concentrations to overcome the background and observe clearly the intracellular drug localisation patterns. The drug concentration used is recorded with each figure. The intensity graphs were produced by drawing a line through the displayed field of view and letting the computer automatically record the intensity of the fluorescence on an arbitrary scale. These intensity graphs were to give some indication of the differing patterns of fluorescence between sensitive and resistant cells but not used as numerical indications of the amount of drug uptake between cell lines. The figures for this section are presented on pages 88 to 99.

3.3.1.i) MGH-U1 AND MGH-U1/R CELLS

DOXORUBICIN: In sensitive cells, at 10μg/ml, there was mainly nuclear fluorescence, containing points of increased fluorescence which could correlate to increased DOX uptake by the nucleoli or chromatin (Fig.3.1A). These increased points of fluorescence could only be detected using the confocality of the

microscope. These points of increased nuclear fluorescence were not detected at the higher drug dose due to the very high overall nuclear DOX accumulation (Fig. 3.2A). At 20μg/ml, areas of less intense fluorescence spots, compared to the nuclei, in the perinuclear region of some cells could be observed. There was some cytoplasmic fluorescence but at a much lower level than the nuclei. From the intensity graphs, recorded from the 20μg/ml drug dose, the nuclei can clearly be observed as having high peaks of fluorescence, steeply dropping when the line cuts through the cytoplasm (Fig.3.2A).

The resistant cells compared to the sensitive cells took up less DOX, the intensity graph indicating less than half, and had a different intracellular drug localisation pattern. The DOX uptake pattern was most clearly shown at 20 μg/ml (Fig.3.2B) where the fluorescence was located in the cytoplasm with very little in the nucleus producing an effect termed 'nuclear holes'. The heaviest fluorescence was in the perinuclear region with the cytoplasmic fluorescence being coarsely punctate. There were the odd cells with some nuclear staining which was similar to the high spots of fluorescence seen in sensitive cells and may correspond to nucleolar activity.

EPIRUBICIN: In sensitive cells, at both drug concentrations but especially at 20μg/ml (Fig. 3.4A), there was obvious nuclear EPI accumulation especially within the nucleoli and / or chromatin which was highly fluorescent. Very little cytoplasmic fluorescence was discernible (Figs. 3.3A and 3.4A).

The intracellular pattern of EPI uptake in resistant cells produced nuclear holes with very high points of perinuclear fluorescence which may correspond to the Golgi apparatus (Fig. 3.3B and 3.4B).

The soft zoom from the confocal microscope allows us to enlarge sections of the field of view and closely observe the differences in intracellular EPI distribution patterns in sensitive and resistant cells, whilst the intensity graphs records the peaks and troughs of the fluorescence i.e. the drug localisation. Fig.3.5B is a good example of nuclear holes in resistant cells where the drug was excluded from the nucleus. The sensitive cells showed an opposite pattern of intracellular EPI localisation with the nuclei taking up the most drug.

IDARUBICIN: Compared to the two aforementioned drugs IDA was brightly fluorescent at 10 μg/ml. The intracellular drug distribution for this drug was unusual as the sensitive and resistant cells (Fig. 3.6A and B) produced similar patterns of drug localisation, although the resistant cells took up a lot less drug (Fig. 3.6B). Both cell lines showed low nuclear fluorescence but high perinuclear staining with the rest of the cytoplasm weakly fluorescent.

3.3.ii) MCF-7 AND MCF-7/R CELLS

DOXORUBICIN: At both drug concentrations the sensitive cells showed mainly nuclear fluorescence (Figs. 3.7A and 3.8A). The intracellular pattern of DOX fluorescence at the higher drug concentrations indicates that within the nucleus there was more drug sequestered in the nucleolar and/or chromatin regions (Fig 3.8A).

As mentioned before (section 3.2) at 10 μg/ml DOX the fluorescence within the resistant cells was very difficult to record due to the very high background. This was speculated to be due to the drug 'sticking' to the plastic petri dish. Because of the low fluorescence of the resistant cells with this drug, and the interference from the high background, the intensity of the image had to be increased. Hence, in this particular figure the intracellular fluorescence of the resistant cells appeared to be as bright as that in the sensitive cells at 10 μg/ml (Fig. 3.7B). At 20 μg/ml there was a large difference in the amount of intracellular fluorescence, i.e. the amount of drug, between sensitive and resistant cells (Fig. 3.8). At this drug dose EPI in resistant cells was observed to localise mainly in the perinuclear region of the cytoplasm with little in the nuclei producing nuclear holes.

MITOZANTRONE: Both cell lines showed a 'nuclear hole' fluorescence pattern of intracellular drug uptake with the sensitive cells taking up more MTZ overall than the resistant cells (Fig. 3.9). The sensitive cells displayed rings of fluorescence around the nuclei (Fig. 3.9A) whilst the resistant cells showed a small localised area of perinuclear drug distribution (Fig.3.9B). Cytoplasmic fluorescence was low for both cell lines with a few cells having a more punctate pattern of bright

fluorescence within the cytoplasm. This pattern was more discernible in the sensitive cells but could also be detected in the resistant cells.

The sensitive cells on the edges of the colonies were more fluorescent than the more central cells which suggested they had taken up more drug. This phenomenon was observed in all experiments with this drug. In some sensitive cells, the nucleoli / chromatin stood out as brightly fluorescent, from sequestering MTZ, within the nuclear hole (Fig. 3.9A). These cellular organelles could have taken up most of the drug within the nucleus or simply retained the drug they had taken up while the remaining MTZ was excluded from the nucleus. There was also staining of the nuclear membrane in some of the sensitive cells.

IDARUBICIN: A similar pattern of intracellular drug distribution was observed in both sensitive and resistant cells with the sensitive cells taking up more IDA overall than the resistant cells. Both displayed low cytoplasmic staining and an obvious ring of perinuclear staining, where most of the drug was localised (Fig. 3.10).

There was heterogeneity in the IDA uptake in sensitive cells with some cells taking up much more IDA than others, regardless of their positioning within the cell colony. Unlike MTZ uptake by sensitive cells where the cells on the fringes of the colony take up more drug consistently; this was not the case with IDA uptake by sensitive cells. This heterogeneity in drug uptake was only observed in the sensitive cell lines, MGH-U1 and MCF-7, and with the drugs IDA and MTZ. MGH-U1 sensitive cells show a slight heterogeneity in IDA uptake. The resistant cells display more uniform drug uptake with all the drugs as do the sensitive cells with DOX and EPI.

3.3.2. CCD Images of MTZ Uptake in MGH-U1 and MGH-U1/R Cells

The CCD camera allowed us to capture the cells in phase as well as image the fluorescence drug (MTZ) within them. For these experiments, the MGH-U1 and MGH-U1/R cell lines were used with the drug MTZ. The figures for this section are presented on pages 98 and 99.

3.3.2.i) MGH-U1 AND MGH-U1/R CELLS

MITOZANTRONE: The sensitive cells took up much more drug than their resistant counterparts. The sensitive cells showed predominantly nuclear fluorescence with heavier 'spots' of fluorescence localised within the nuclei (Fig. 3.11). Very little cytoplasmic fluorescence was observed and the plasma membrane was not often discernible. Resistant cells showed a much more diffuse cytoplasmic and nuclear pattern of staining, than the MGH-U1 cells, with similar quantities of MTZ located in the nucleus and cytoplasm. Very intense areas of perinuclear fluorescence were seen in some resistant cells (Fig. 3.12).

Due to the limitations of this instrument, the cells drying out while being viewed and limited fluorescence analysis (also see section 2.B.1.ii), it was decided in future the confocal microscope would be used to visualise the intracellular drug localisation patterns.

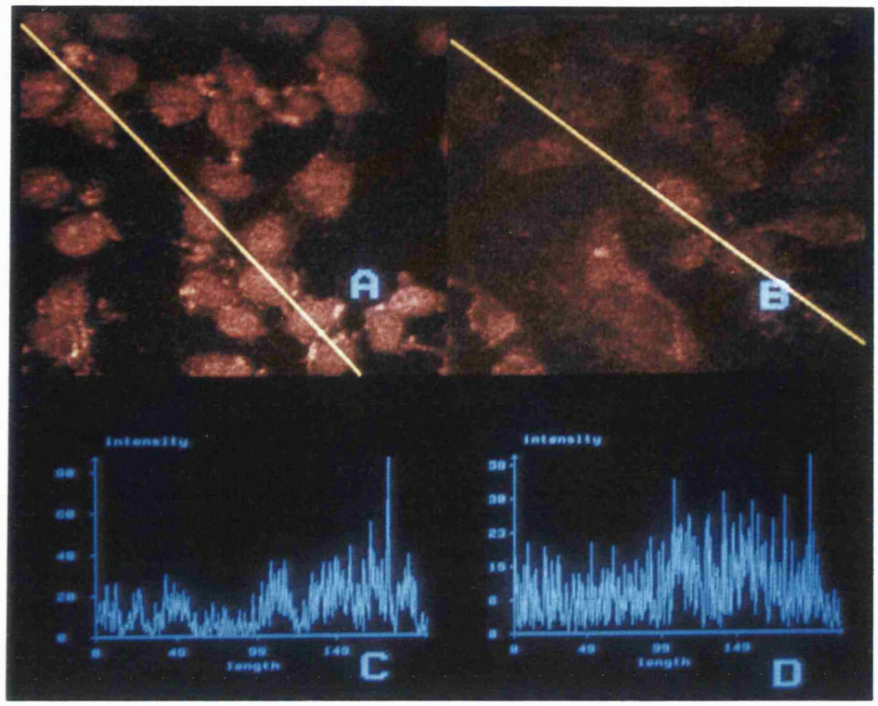

Fig. 3.1. **Patterns of intracellular doxorubicin (10μg/ml) localisation in MGH-U1 and MGH-U1/R cells, detected using the confocal microscope, with corresponding intensity graphs.**
A & C: MGH-U1 cells B & D: MGH-U1/R cells
Nuclear fluorescence can be observed in the sensitive cells, with increased points of fluorescence which may correspond to chromatin or nucleoli.
Nuclear holes and perinuclear fluorescence can be seen in the resistant cells.
(X 300)

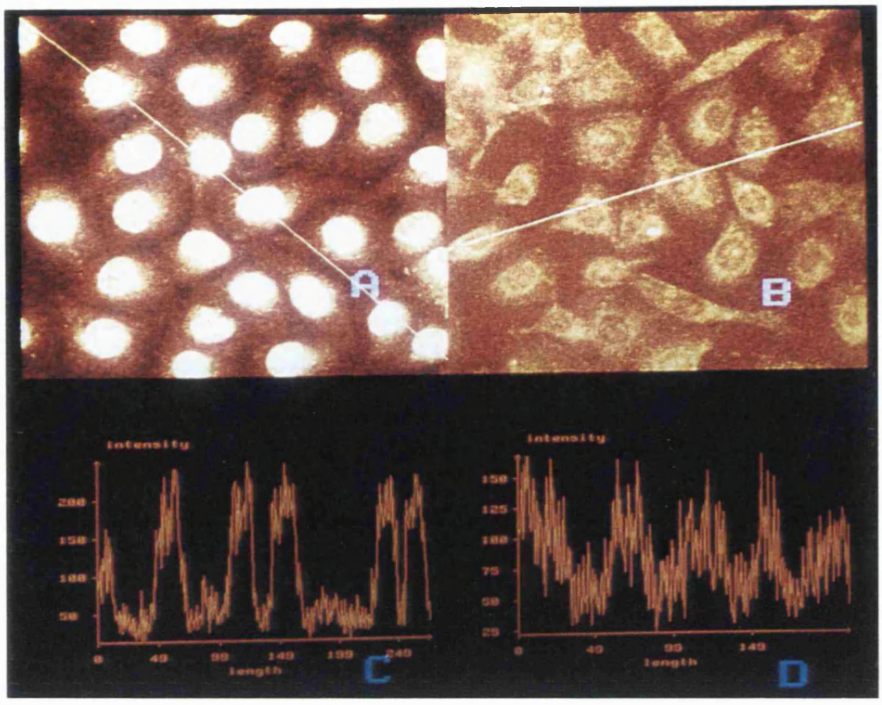

Fig. 3.2. **Patterns of intracellular doxorubicin (20μg/ml) localisation in MGH-U1 and MGH-U1/R cells, detected using the confocal microscope, with corresponding fluorescence intensity graphs.**

A & B: MGH-U1 cells **B & D: MGH-U1/R cells**

Nuclear fluorescence can be observed in the sensitive cells. Nuclear holes and perinuclear fluorescence are visible in resistant cells.

Note: the intensity graphs record the peaks of fluorescence (Pe), in particularly in the nuclei of the sensitive cells, and the troughs of fluorescence (Tr) notably when the line cuts through a) the cytoplasm of the sensitive cells or b) the nuclear holes of resistant cells.

(X 300)

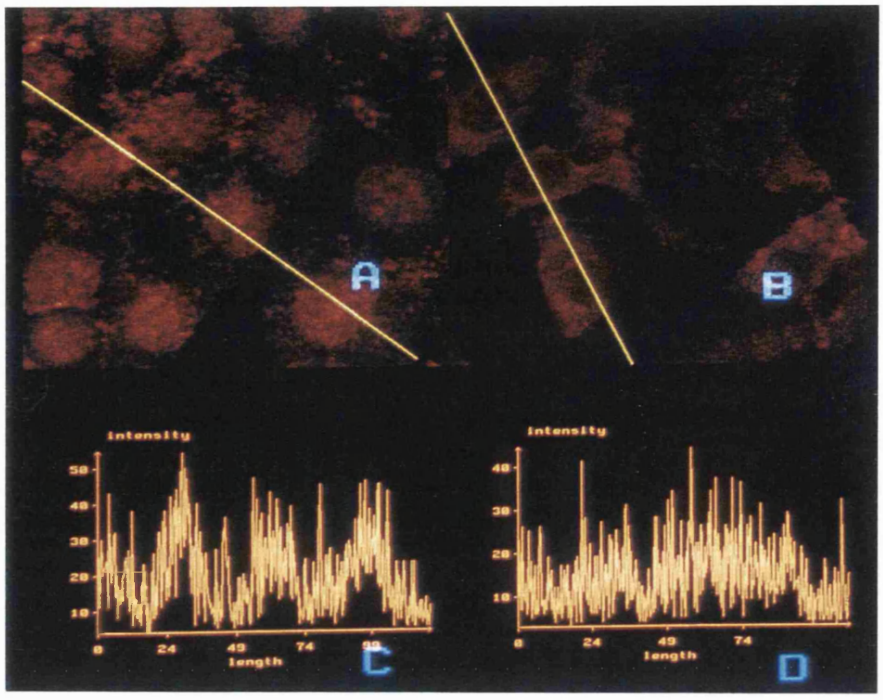

Fig. 3.3. **Patterns of intracellular epirubicin (10μg/ml) localisation in MGH-U1 and MGH-U1/R cells, detected using the confocal microscope, with corresponding intensity graphs.**
A & C: MGH-U1 cells B & D: MGH-U1/R cells
Nuclear fluorescence can be observed in the sensitive cells. Nuclear holes and perinuclear fluorescence are visible in resistant cells.
(X 600)

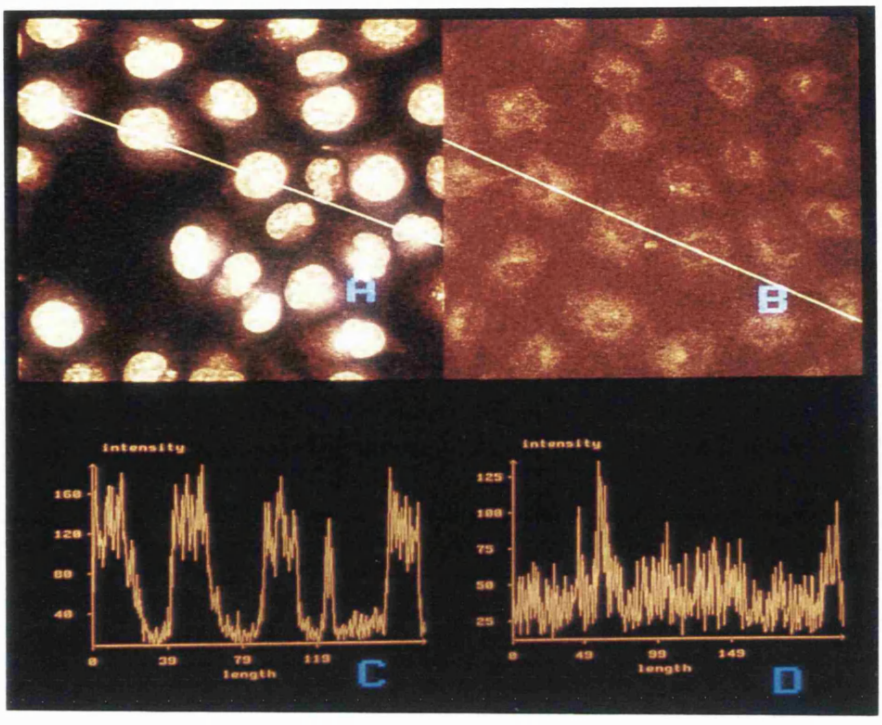

Fig. 3.4. **Patterns of intracellular epirubicin (20μg/ml) localisation in MGH-U1 and MGH-U1/R cells, detected using the confocal microscope, with corresponding intensity graphs.**
A & C: MGH-U1 cells B & D: MGH-U1/R cells
Nuclear fluorescence can be observed in the sensitive cells, with increased points of fluorescence which may correspond to chromatin or nucleoli.
Nuclear holes and perinuclear fluorescence are visible in resistant cells.
(X 300)

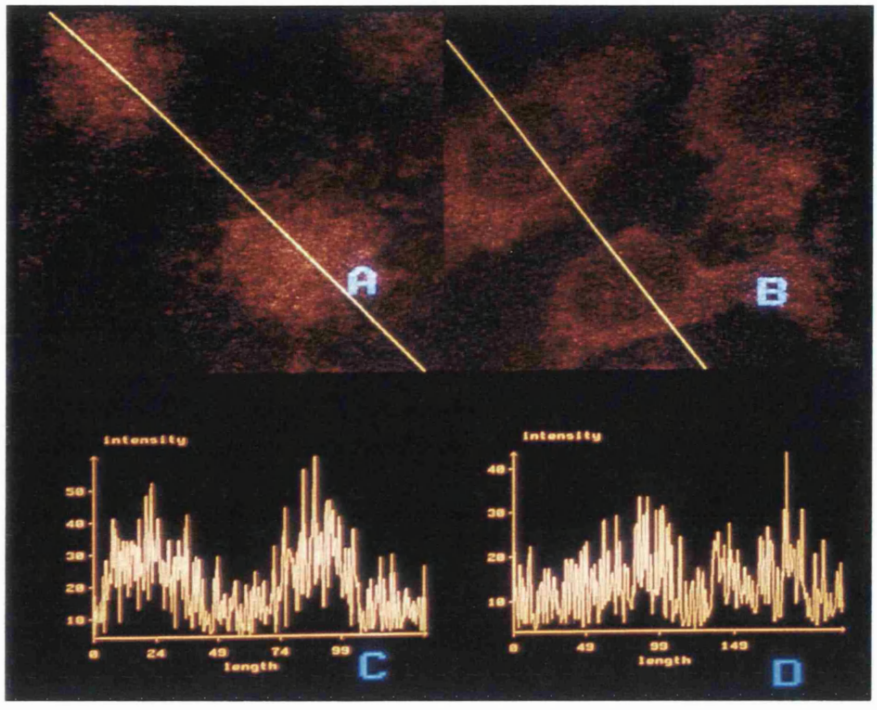

Fig. 3.5. **Intracellular epirubicin distribution (soft zoom from section of fig. 3.3) in MGH-U1 and MGH-U1/R cells, detected using the confocal microscope, with corresponding intensity graphs.**

A & C: MGH-U1 cells **B & D: MGH-U1/R cells**

Nuclear fluorescence can be observed in the sensitive cells. Nuclear holes and perinuclear fluorescence are visible in resistant cells.

(X 900)

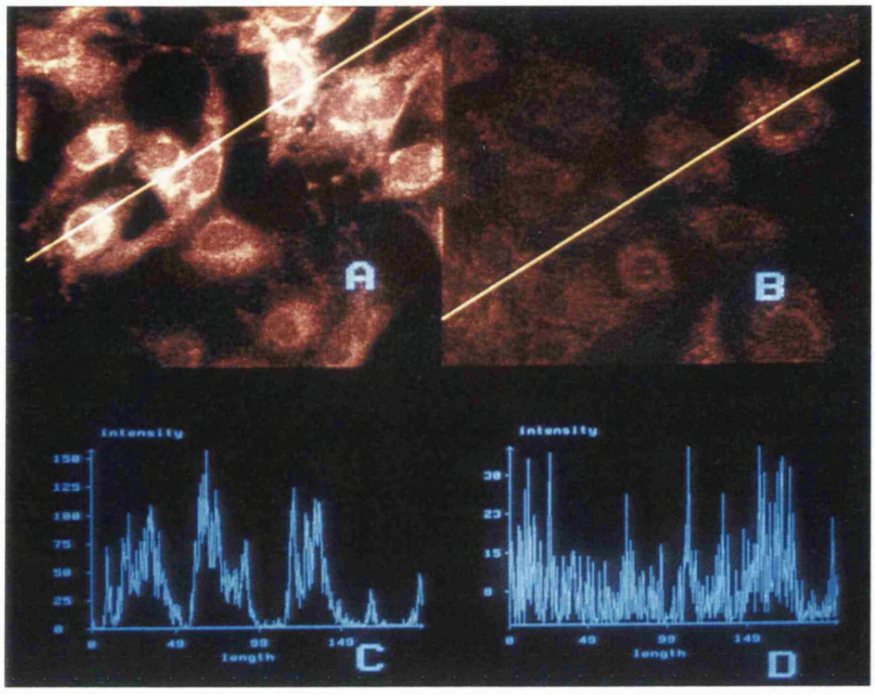

Fig. 3.6. **Patterns of intracellular idarubicin (10μg/ml) localisation in MGH-U1 and MGH-U1/R cells, detected using the confocal microscope, with and corresponding intensity graphs.**

A & C: MGH-U1 cells **B & D: MGH-U1/R cells**

Nuclear holes and perinuclear fluorescence are visible in both sensitive and resistant cells.

(X 300)

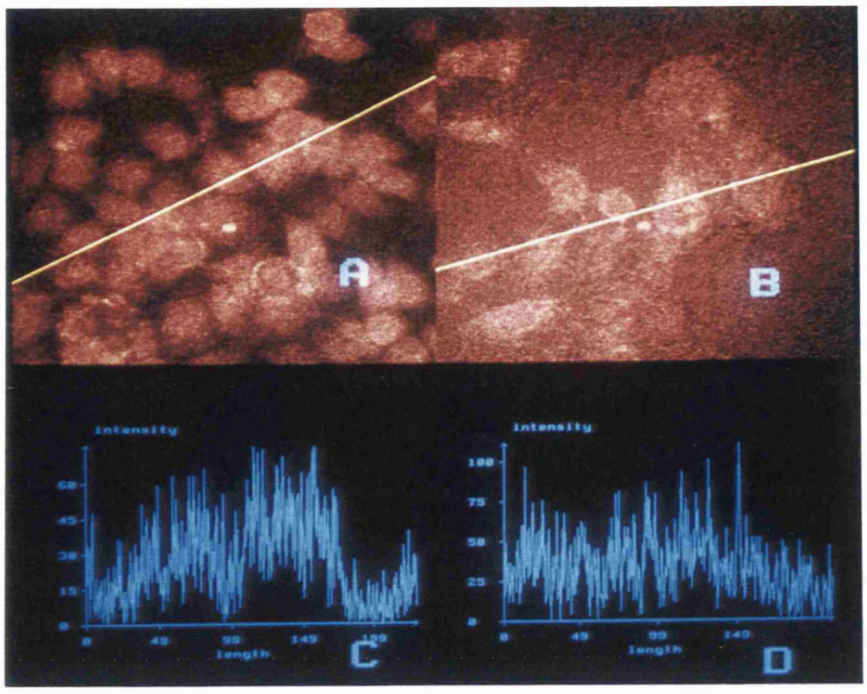

Fig. 3.7. **Patterns of intracellular doxorubicin (10μg/ml) localisation in MCF-7 and MCF-7/R cells, detected using the confocal microscope, with corresponding intensity graphs. A & C: MCF-7 cells B & D: MCF-7/R cells**

Nuclear fluorescence can be observed in the sensitive cells. Nuclear holes and perinuclear fluorescence are visible in resistant cells.

Note: high background fluorescence (b) of the resistant cells, probably due to the drug 'sticking' to the plastic petri dish.

(X 300)

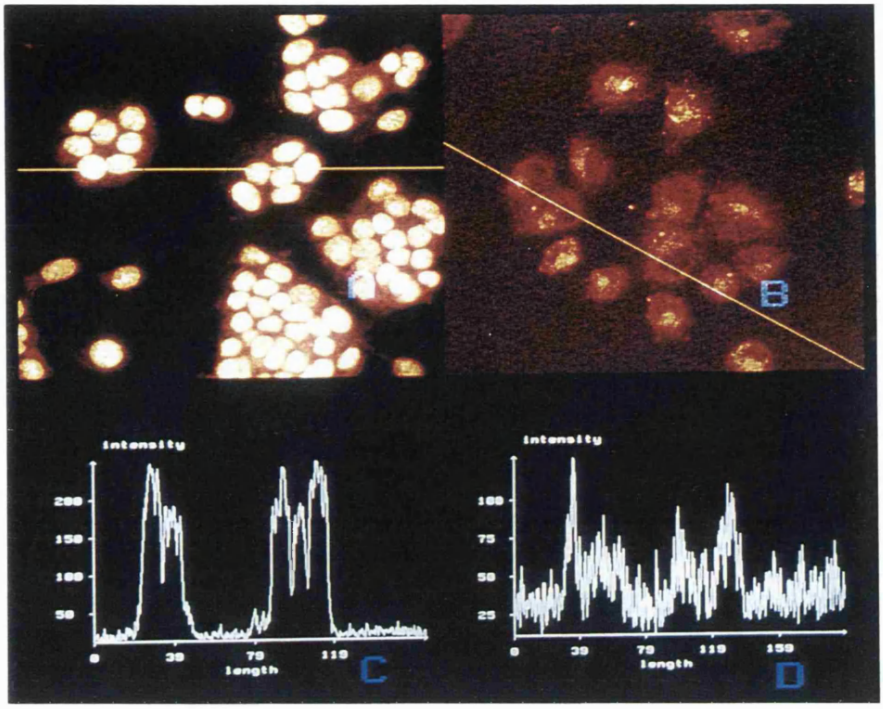

Fig. 3.8. **Patterns of intracellular doxorubicin (20μg/ml) localisation in MCF-7 and MCF-7/R cells, detected using the confocal microscope, with corresponding intensity graphs.**
A & C: MCF-7 cells B & D: MCF-7/R cells
Nuclear fluorescence can be observed in the sensitive cells, with increased points of fluorescence which may correspond to the chromatin or nucleoli.
Nuclear holes and perinuclear fluorescence are visible in resistant cells.
(X 200)

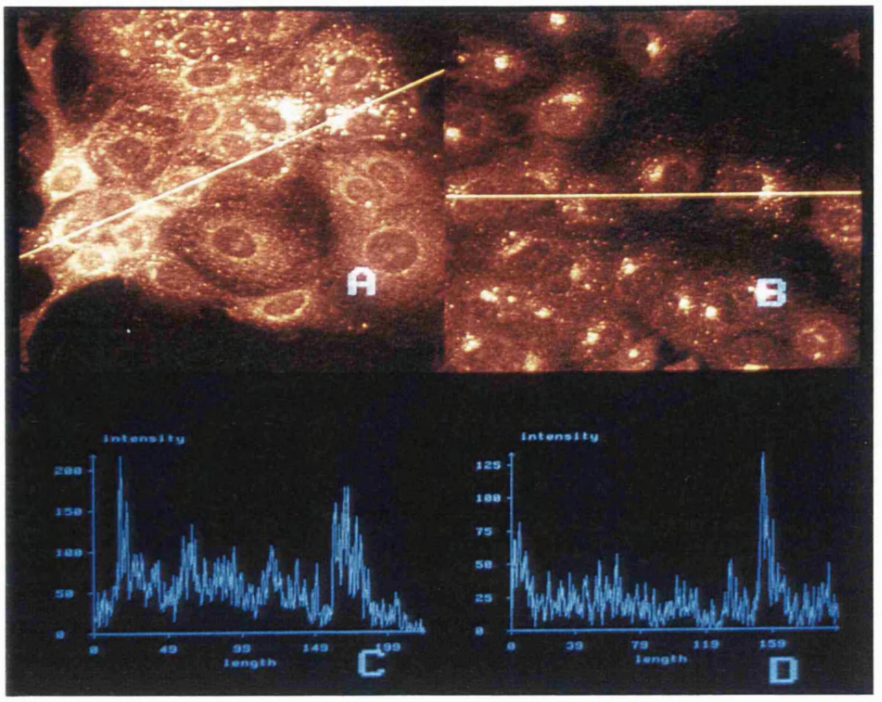

Fig. 3.9. **Patterns of intracellular mitozantrone (10μg/ml) localisation in MCF-7 and MCF-7/R cells, detected using the confocal microscope, with corresponding intensity graphs.**
A & C: MCF-7 cells B & D: MCF-7/R cells
Nuclear holes are visible in both sensitive and resistant cells.
Rings of fluorescence are visible around the nuclei of sensitive cells.
Localised areas of perinulcear fluorescence can be seen in resistant cells.
(X 300)

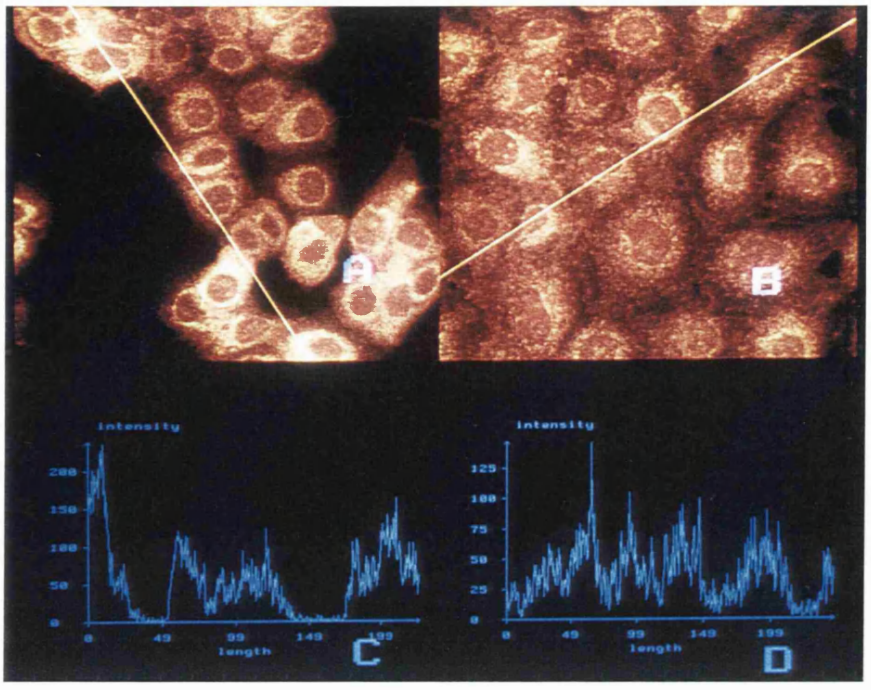

Fig. 3.10. **Patterns of intracellular idarubicin (10μg/ml) localisation in MCF-7 and MCF-7/R cells, detected using the confocal microscope, with corresponding intensity graphs.**
A & C: MCF-7 cells B & D: MCF-7/R cells
Nuclear holes and perinuclear fluorescence are visible in both sensitive and resistant cells.
(X 300)

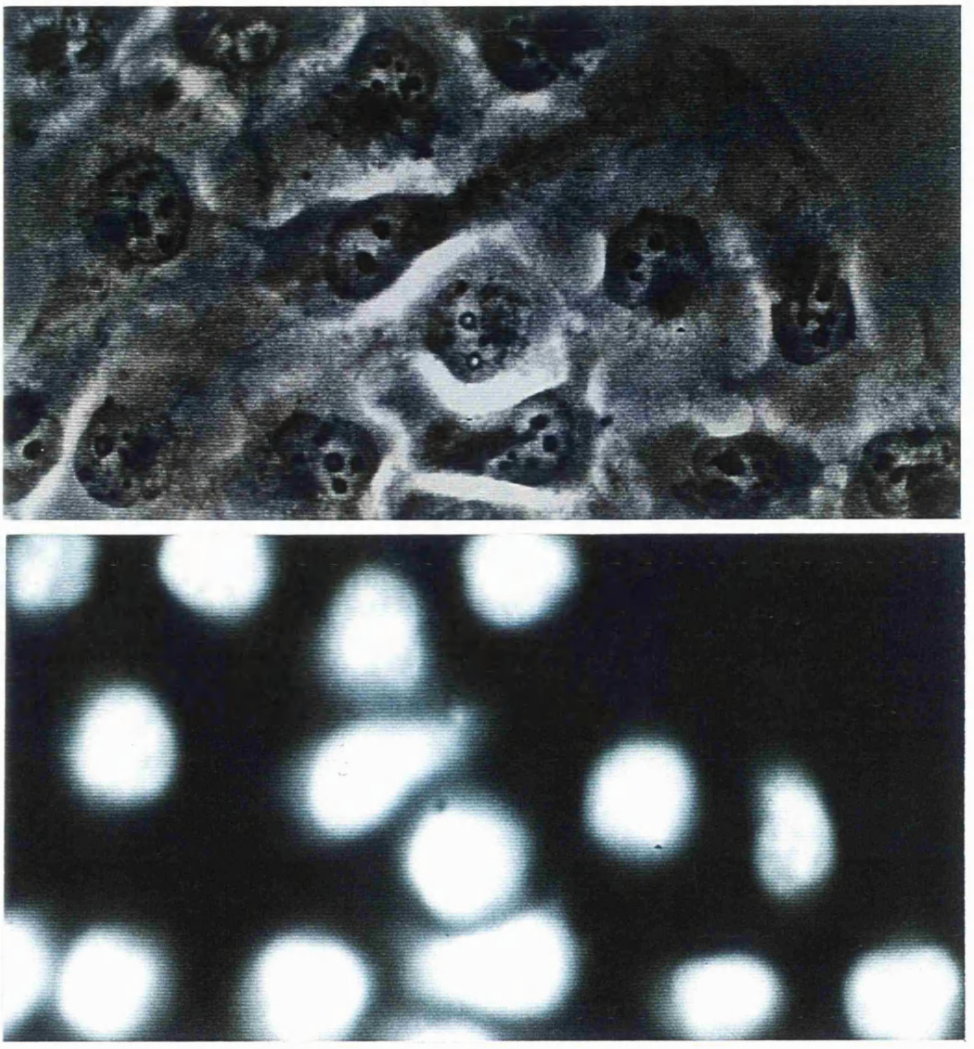

Fig. 3.11. **Patterns of intracellular localisation of MTZ (2μg/ml) in MGH-U1 cells, using the CCD camera. Cells were visualised as phase contrast and fluorescent images.**

Nuclear fluorescence can be observed in the sensitive cells, with heavier points of fluorescence which may correspond to chromatin or nucleoli.

(X 750)

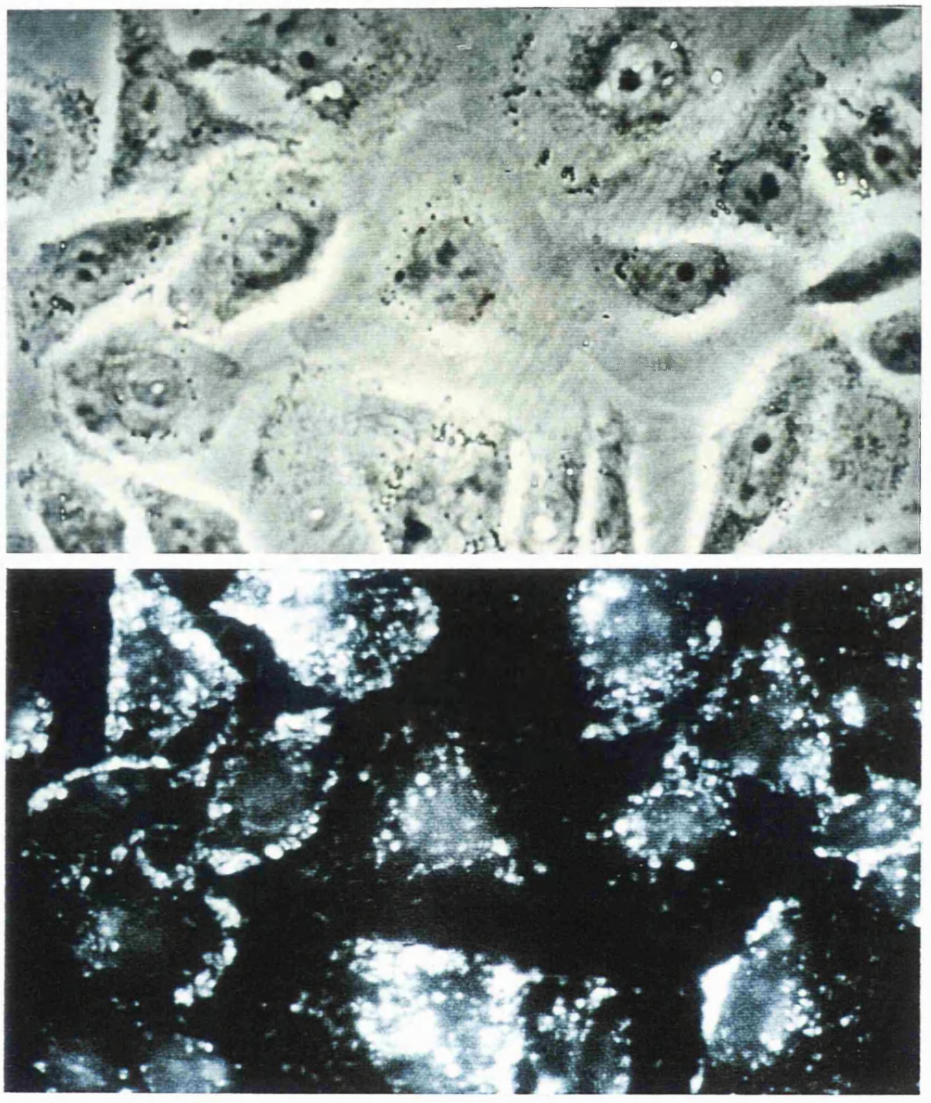

Fig. 3.12. **Patterns of intracellular localisation of MTZ (2μg/ml) in MGH-U1/R cells, using the CCD camera. Cells were visualised as phase contrast and fluorescent images.**

Diffuse nuclear and cytoplasmic fluorescence can be observed in resistant cells.

(X 750)

3.4. EFFECT OF CELL CONFLUENCE ON INTRACELLULAR DRUG DISTRIBUTION

This work addressed the effect the state of confluence of the cells had on drug uptake, by employing both the confocal microscope and the flow cytometer. For flow cytometry, the difference in cellular drug uptake due to the effect of confluence was observed in cells incubated with the drug in suspension and versus cells attached to the flasks. Stages of cell confluence were described as sub-confluent (around 50% of the flask covered with cells), confluent (around 90% of the flask covered with cells) and supra-confluent (cells were allowed to grow until the flask surface was completely covered and the cells became 'heaped' on top of each other). All estimations of the state of confluence were made by eye and corroborated by an independent observer, skilled in culture techniques.

As shown by flow cytometry, when the cells were incubated with drug while in suspension in the same amount of medium, the fewer cells present the more drug they took up. So the higher the number of cells per volume of medium the lower the fluorescence per cell; for example, MGH-U1 cells taking up MTZ when sub-confluent had a mean fluorescence of 246 (arbitrary units) compared to confluent MGH-U1 cells which had a mean fluorescence of 165 (arbitrary units). Both sub-confluent and confluent MGH-U1 cells were incubated in suspension with MTZ in an identical way.

However, when the cells were incubated with drug still attached to each other and to a plastic surface, very confluent cultures took up more drug per cell than cells which were confluent and sub-confluent. In flow cytometry experiments, MTZ uptake by MCF-7/R cells, attached to the flask, produced very similar results regardless of their stage of confluence. The sensitive cells varied with their MTZ uptake depending on their state of confluence, with the cells which were supraconfluent taking up twice as much drug as the confluent or sub-confluent cells at all MTZ concentrations.

Using the confocal microscope not only could the relative amount of intracellular drug, between cell lines, be viewed but also the intracellular localisation of the drug investigated. There were differences with intracellular drug localisation within the same cell line depending on the confluence of the cells. The

confluent and sub-confluent MGH-U1 cell line displayed a typical intracellular DOX distribution pattern with mainly nuclear drug localisation (Fig. 3.13C). However, the supra-confluent cells displayed a similar pattern of DOX localisation to the resistant cells, with nuclear holes evident and rings of bright perinuclear fluorescence (Fig. 3.13A). The confluent and sub-confluent resistant cells had similar patterns of intracellular DOX localisation but the supra-confluent cells appeared have taken up more drug than the sub-confluent cells (Fig. 3.13B and D). The intracellular pattern of IDA distribution did not change when comparing the supra-confluent and confluent / sub-confluent cells of the MGH-U1 and MGH-U1/R cell lines, respectively (Fig. 3.14). The supra-confluent and confluent / sub-confluent sensitive cells had mainly perinuclear fluorescence with little nuclear IDA uptake. The amount of fluorescence within the supra-confluent cells appeared to be more than within the confluent / sub-confluent, but no solid statement can be made as the cells in the supra-confluent cultures were very tightly packed together with little room for their cytoplasm to spread out.

The MCF-7 cells showed similar patterns of IDA uptake but with the supra-confluent cells taking up much more drug than the confluent / sub-confluent cells (Fig. 3.15C and D). However, with MTZ there was a difference in intracellular localisation between supra-confluent and confluent / sub-confluent MCF-7 cells although both had taken up similar levels of the drug (Fig. 3.15A and B). In both sets of cells those on the edge of the colony had taken up more MTZ than the rest. The supra-confluent MCF-7 cells displayed a pattern of MTZ localisation often observed with drug uptake in tumour explants. Unlike sub-confluent cells, there was no definite cytoplasmic localisation of MTZ in the supra-confluent cells. MTZ has not entered many of these cells localising instead between the cells producing a 'pavement effect' of fluorescence (Fig. 3.15A). This may also have occurred with the supra-confluent MCF-7 cells and IDA (Fig. 3.15C), however as the IDA fluorescence was so bright it was not possible to say for certain and the IDA may be intracellular. Different patterns of drug uptake by supra-confluent and confluent / sub-confluent MCF-7 cells was also observed with DOX (Fig. 3.16). Supra-confluent cells show nuclear holes, with the majority of DOX located in the cytoplasm producing intense fluorescence (Fig. 3.16A). In contrast, confluent and sub-confluent MCF-7 cells had low cytoplasmic fluorescence with DOX located

mainly in the nuclei especially within the nucleoli and the nuclear membranes (Fig. 3.16B).

In the majority of these experiments there appeared to be increased drug uptake by supra-confluent cells compared to either the confluent or sub-confluent cells, with the intracellular drug distribution remaining unchanged. A change in the pattern of intracellular drug distribution in supra-confluent and confluent / sub-confluent cells was clearly shown, for example, by MCF-7 cells and DOX.

So in summary, different intracellular patterns of drug uptake were observed supra-confluent cells compared to confluent / sub-confluent. Also, there generally appeared to be more drug taken up by supra-confluent cultures versus confluent / sub-confluent. These experiments led to the decision that all further work be performed on adherent cells when they had grown to a similar stage of confluence judged, by eye, to be around 90% but definitely not supra-confluent. Cultures at different stages of confluence have different percentages of their cell populations at stages in the cell cycle, *e.g.* supra-confluent cultures will have a higher percentage of cells in G_0 of the cell cycle than confluent and sub-confluent cells the majority of which are still dividing. Therefore, the effect that cell cycle may have on cellular drug uptake needs to be taken into account.

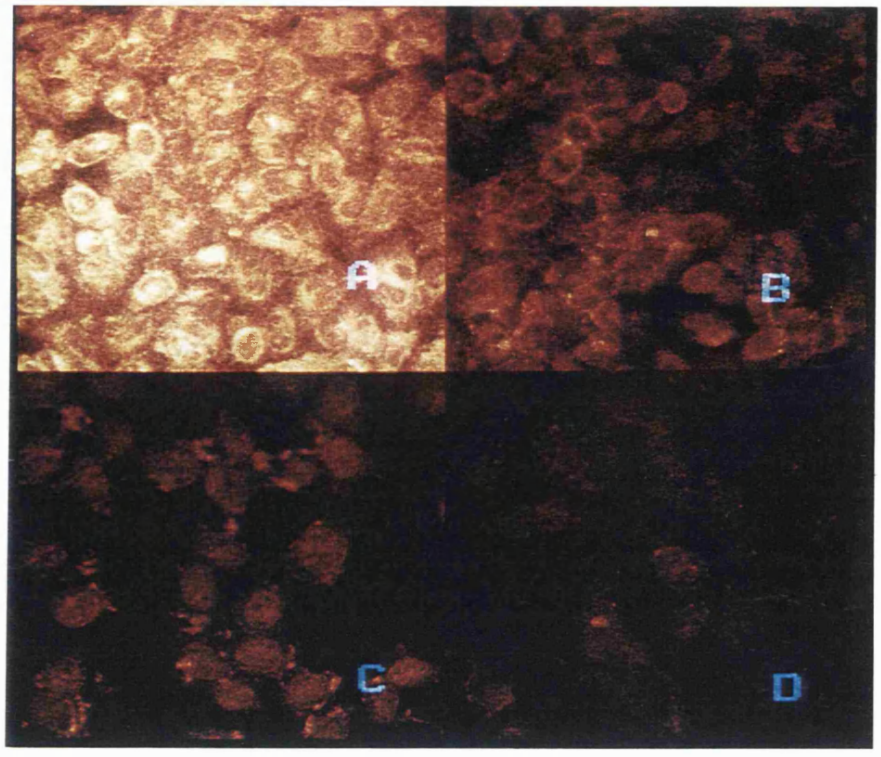

Fig. 3.13. **Intracellular DOX (10μg/ml) localisation in confluent / sub- confluent compared to supra-confluent MGH-U1 and MGH-U1/R cells, detected using the confocal microscope.**

A and C : MGH-U1 cells B and D : MGH-U1/R cells

A and B : supra-confluent C and D : confluent / sub confluent

Nuclear fluorescence can be observed in the confluent / sub-confluent sensitive cells (C).

Nuclear holes with perinuclear fluorescence can be seen in confluent / sub-confluent resistant cells and in both sensitive and resistant supra-confluent cells (A,B & D).

(X 300)

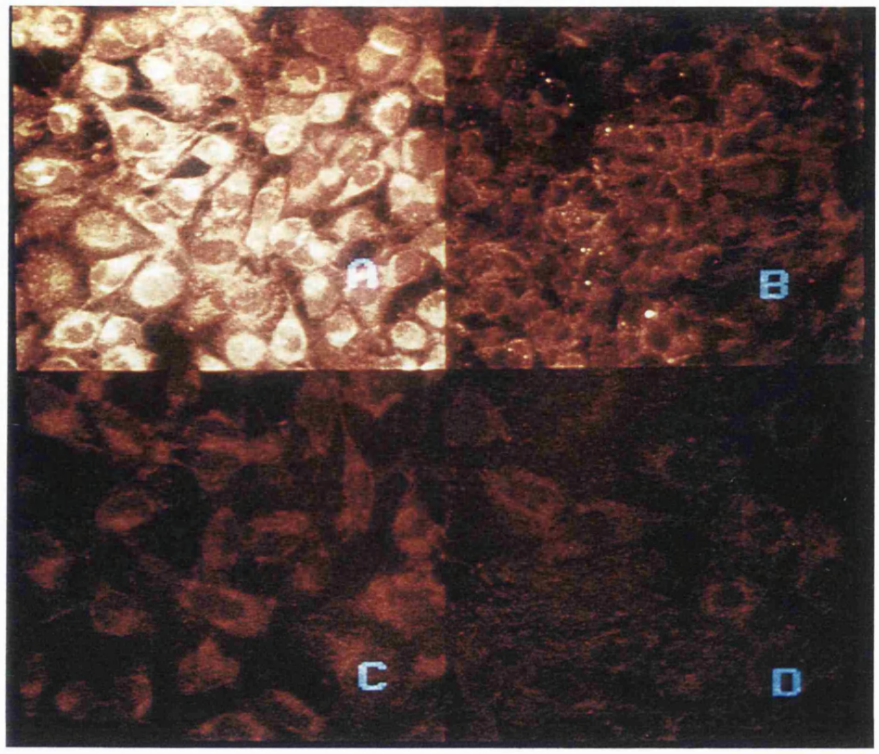

Fig. 3.14. **Intracellular IDA (10μg/ml) localisation in confluent / sub- confluent compared to supra-confluent MGH-U1 and MGH-U1/R cells, detected using the confocal microscope.**

A and C : MGH-U1 cells B and D : MGH-U1/R cells

A and B : supra-confluent C and D : confluent / sub-confluent

Nuclear holes with perinuclear fluorescence can be seen in both sensitive and resistant, confluent / sub-confluent and supra-confluent cells.

(X 300)

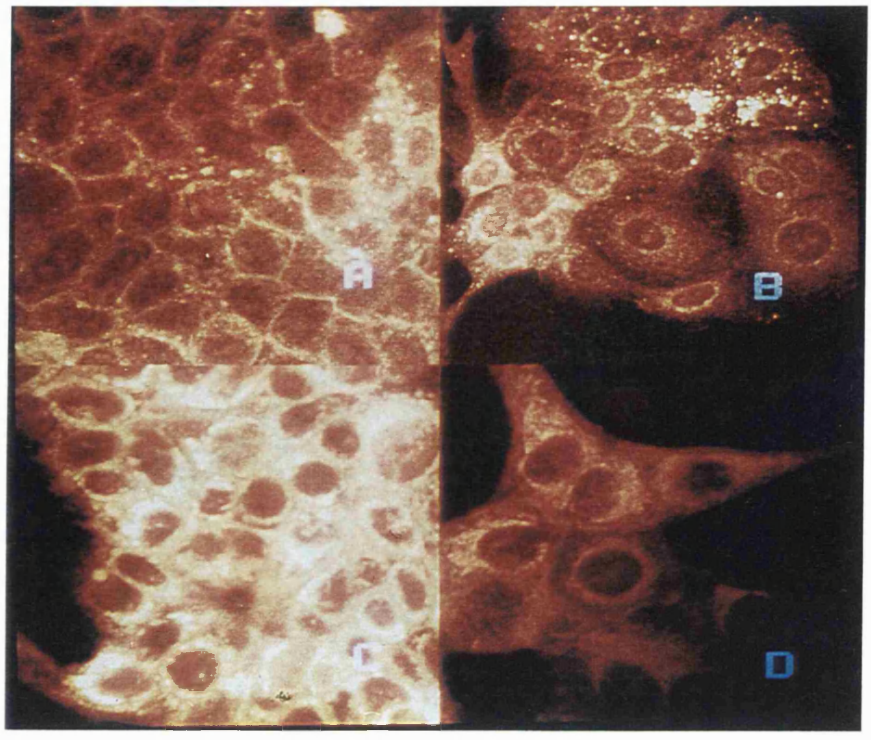

Fig. 3.15. **Intracellular MTZ (10μg/ml) and IDA (10μg/ml) localisation in confluent / sub- confluent compared to supra-confluent MCF-7 cells detected using the confocal microscope.**

A and B : MTZ **C and D : IDA**

A and C : supra-confluent **B and D : confluent / sub-confluent**

Nuclear holes with perinuclear fluorescence can be seen in both sensitive and resistant supra-confluent and confluent / sub-confluent cells for both drugs.

A pavement effect of fluorescence can be observed in supra-confluent sensitive cells with MTZ (A).

(X 300)

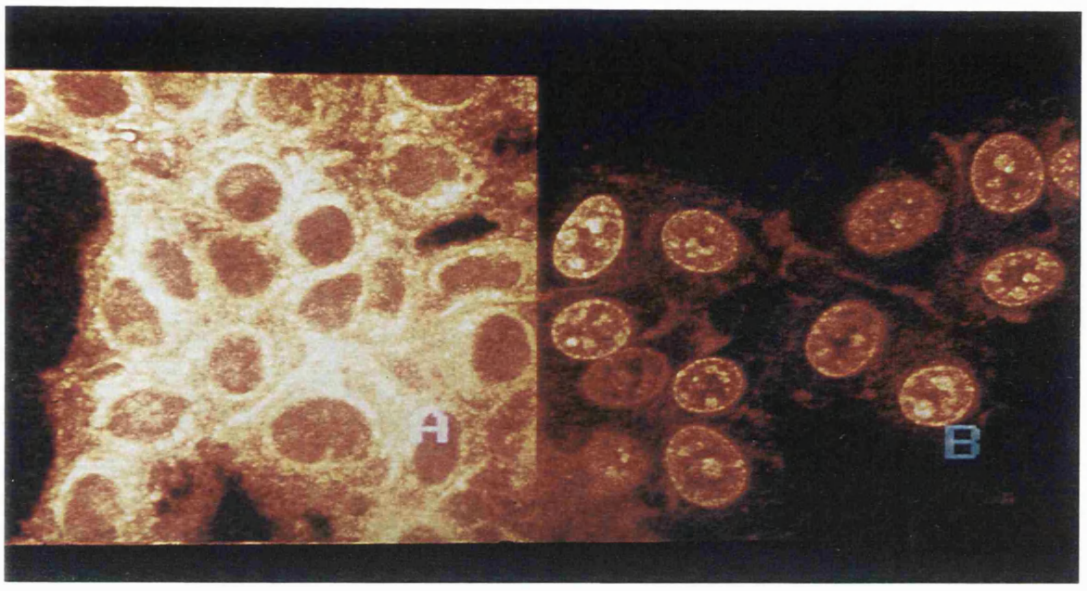

Fig. 3.16. **Intracellular DOX (10μg/ml) localisation in confluent / sub- confluent compared to supra-confluent MCF-7 cells, detected using the confocal microscope.**
A: supra-confluent B: confluent / sub-confluent
Nuclear fluorescence can be observed in the confluent / sub-confluent sensitive cells, with increased areas of fluorescence which correspond to the nucleoli or chromatin and nuclear membranes.
Nuclear holes with perinuclear fluorescence can be seen in sensitive supra-confluent cells.
(X 600)

4. INTRACELLULAR INCORPORATION OF GLA

4.1. GLA UPTAKE IN SENSITIVE AND RESISTANT CELLS

The incorporation of radiolabelled GLA into cells was followed over time using a scintillation counter. In all four cell lines, the uptake of GLA increased over four hours with the largest uptake occurring within the first 30 or 60 min (Graphs 4.1a & b) 32 ± 7.0 for MGH-U1, 22.2 ± 11.0 for MGH-U1/R, 40.7 ± 2.0 for MCF-7 and 30.5 ± 4.0 for MCF-7/R cells, c.p.m $x10^3$. After a period of approximately 1h, the uptake of GLA was not as smooth with the amount of intracellular radioactive GLA fluctuating. The MCF-7 and MGH-U1 sensitive cell lines tended to take up more GLA than their resistant partners but the differences did not reach statistical significance. The amount of GLA entering the cells did not increase much more over the 24h incubation time compared to 4h. However, for convenience and continuity, the cells were incubated with GLA for 24h for all experiments involving this treatment. The amount of carrier GLA did not affect the incorporation of radioactive GLA into MGH-U1 and MGH-U1/R cells.

4.2. PATTERN OF INTRACELLULAR GLA DISTRIBUTION

Cellular uptake of GLA was observed by incubating the four cell lines on chamber slides with radiolabelled GLA, then performing autoradiography on the slides. The cells were counter stained with haematoxylin which made them easier to discern and to locate intracellular radioactive GLA.

Although there was relatively heavy background staining on the slides, particularly within the sensitive cells, the location of the GLA could be clearly observed within all cell lines. As all cell lines displayed similar patterns of intracellular GLA localisation, only the bladder cell lines are shown here (Fig. 4.1 and 4.2). There were distinct areas of black (silver grains) around the majority of cells indicating the presence of radioactive GLA which appeared to be located primarily in the plasma membrane. There also appeared to be varying amounts of GLA taken up by individual cells with some taking up more than others (Fig. 4.2).

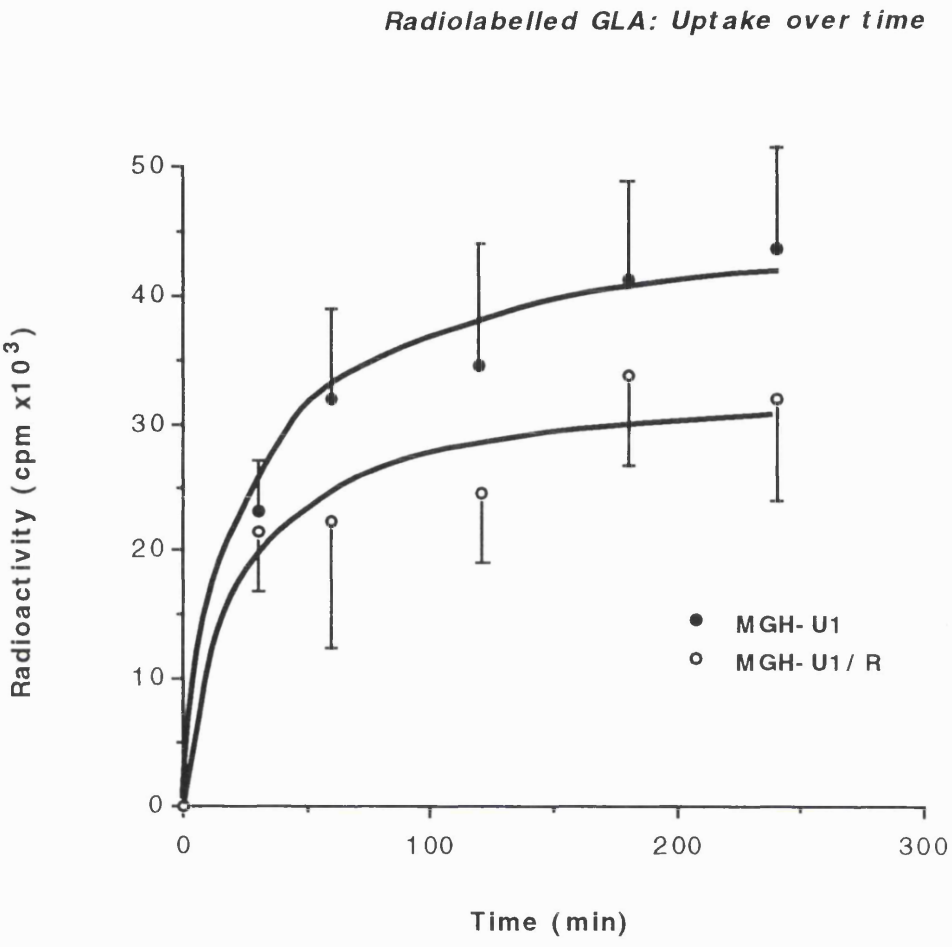

Graph 4.1a. **Incorporation of radiolabelled GLA into MGH-U1 and MGH-U1/R cells over time , measured as counts per minute (c.p.m) ± standard deviations using a scintillation counter. There was no statistically significant difference between GLA uptake in sensitive or resistant cells.**

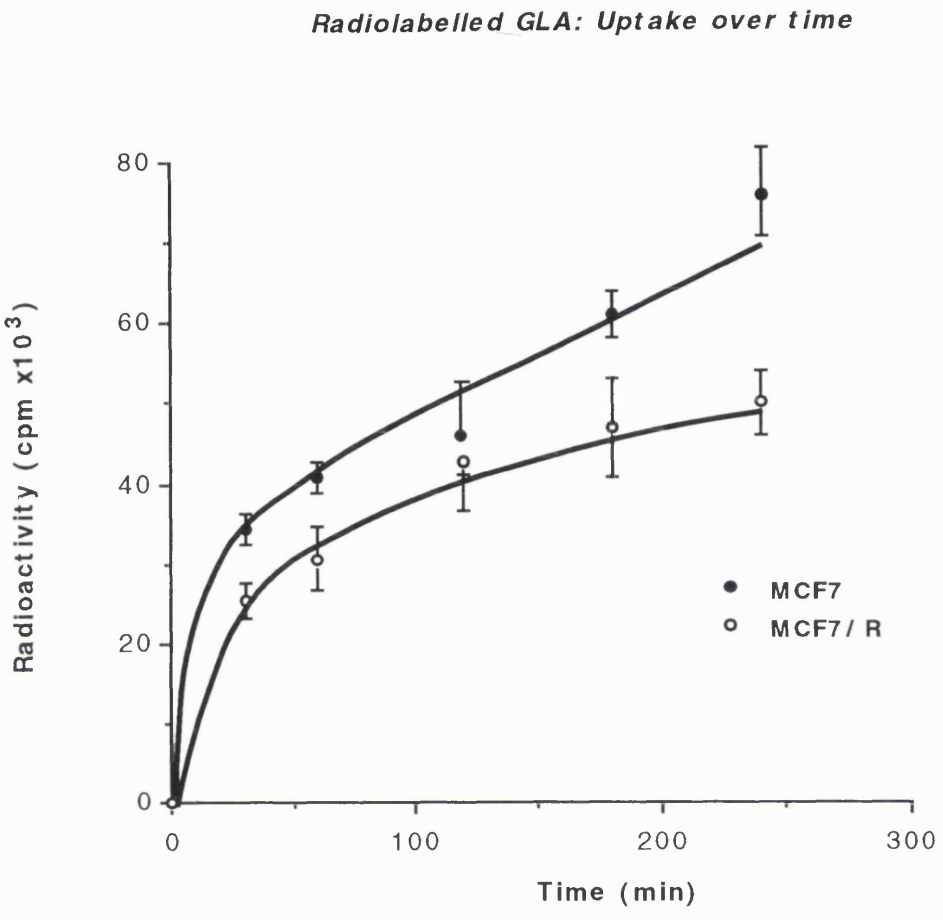

Graph 4.1b. **Incorporation of radiolabelled GLA into MCF-7 and MCF-7/R cells over time , measured as counts per minute (c.p.m) ± standard deviations using a scintillation counter. There was no statistically significant difference between GLA uptake in sensitive or resistant cells.**

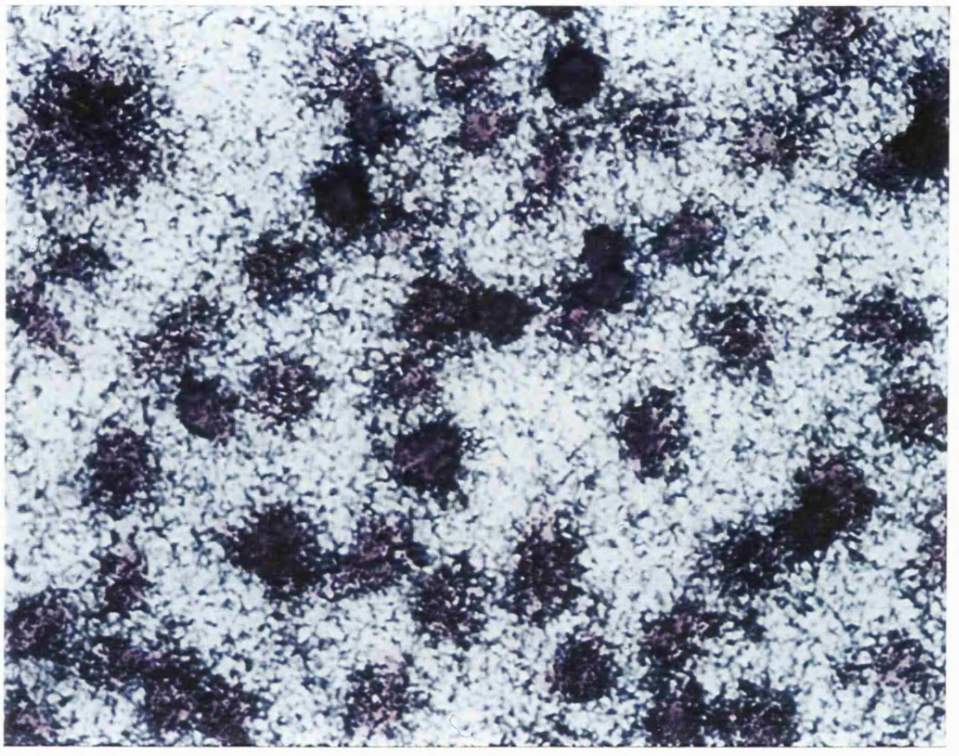

Fig. 4.1. **Pattern of intracellular GLA distribution within MGH-U1 cells.**
GLA can be observed around the cells indicating its location as membranous.
(X 300)

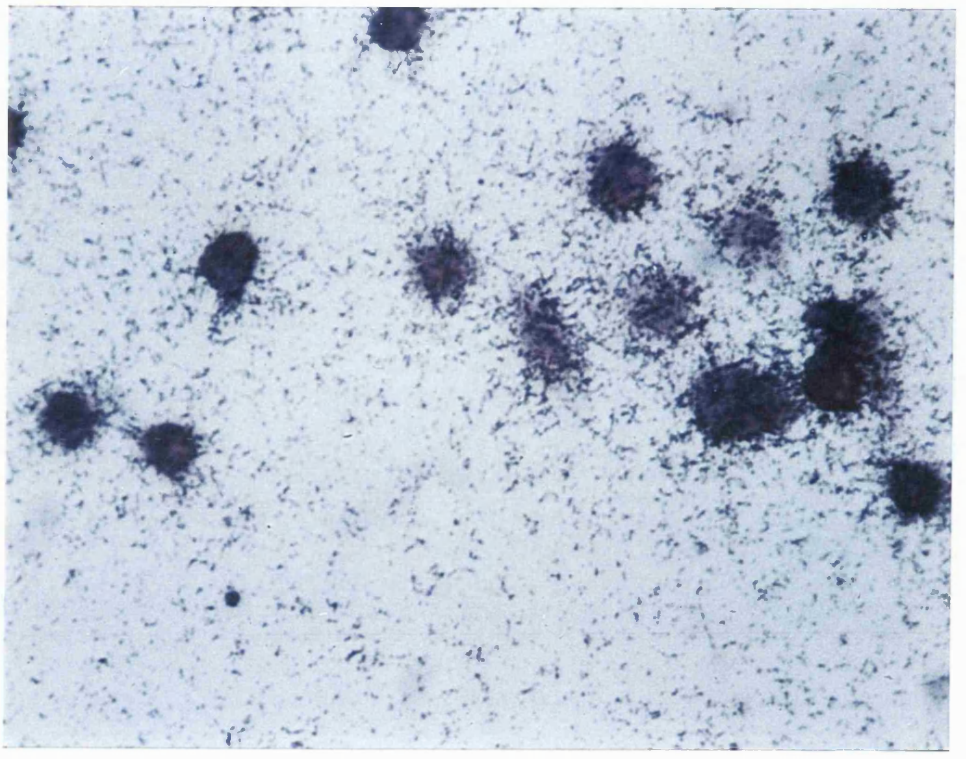

Fig. 4.2. **Pattern of intracellular GLA distribution within MGH-U1/R cells.**
GLA can be observed around the cells indicating its location as membranous.
(X 300)

5. EFFECT OF GLA ON CELLS AND CELLULAR DRUG UPTAKE

5.1. DIRECT CYTOTOXICITY

The cytotoxicity of GLA on cells was measured using the MTT assay after the cells were incubated with various amounts of GLA over different time periods. The optimum concentration and length of time the cells could be incubated with GLA, which did not result in cell death, but still allowed GLA to enter the cells (see section 4.1) was recorded and used for the experiments described in 'indirect cytotoxicity' of GLA (section 5.2).

5.1.i) MGH-U1 AND MGH-U1/R CELLS

GLA was cytotoxic at a concentration of 40μg/ml over 24h and 30μg/ml over 48h (Graph 5.1a and b) in both the resistant and sensitive cells. There was no cytotoxic effect by GLA exerted on the sensitive or resistant cells at 10 or 20μg/ml over either time period.

5.1.ii) MCF-7 AND MCF-7/R CELLS

The cytotoxic effects of GLA, at concentrations of 10-30μg/ml, were investigated for 24, 48 and 72h on these cell lines. GLA was non-cytotoxic to the sensitive MCF-7 cell line at all doses and over all time periods (Fig. 5.1c). However, cell death of the MCF-7/R cells tended to occur at GLA concentrations of 30μg/ml at all time periods (Graph 5.1d).

It was noted that the resistant cells, especially the MCF-7/R cells, were more sensitive to GLA than their non-MDR counterparts. Taking into consideration all the above results the optimum concentration of GLA for the experiments involving 'indirect cytotoxicity' was taken as 20μg/ml GLA over a 24h incubation period. This meant that at 24h GLA had definitely entered all the cells but was not at a sufficient concentration to kill them for the experimental time period.

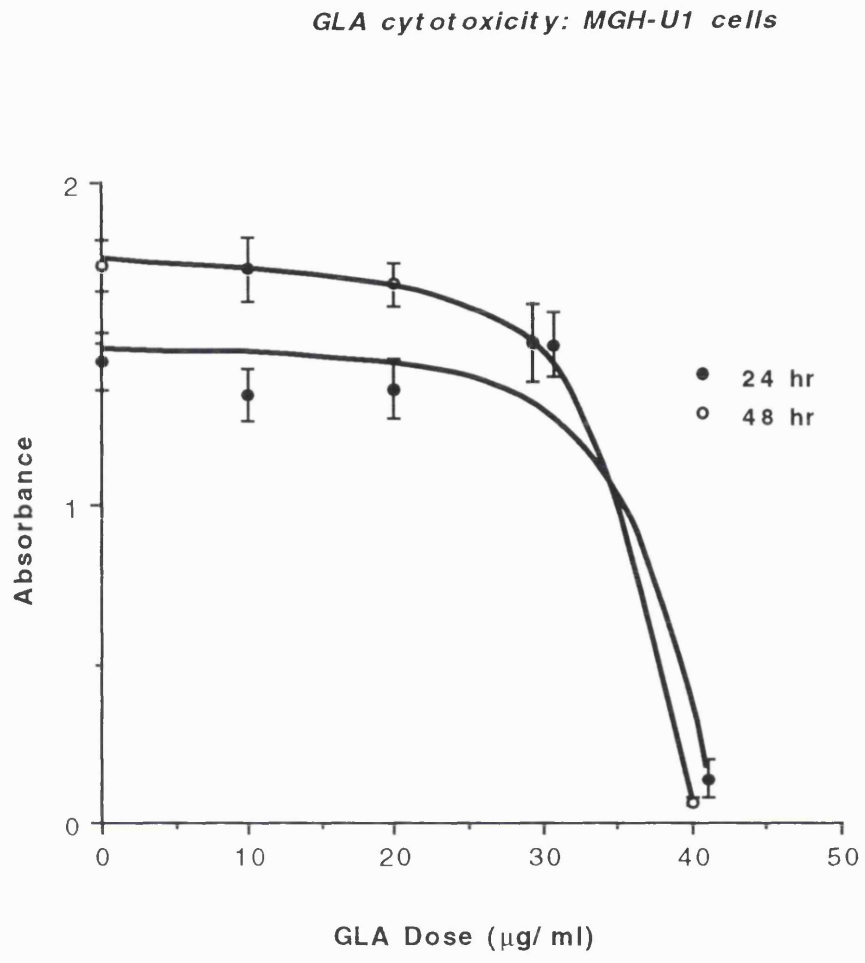

Graph 5.1a. **Cytotoxicity of GLA over different concentrations and time periods in MGH-U1 cells, using the MTT assay. Mean ± standard deviations measured using a spectrophotometer. GLA was cytotoxic at a concentration of 40μg/ml over 24h and 30μg/ml over 48h.**

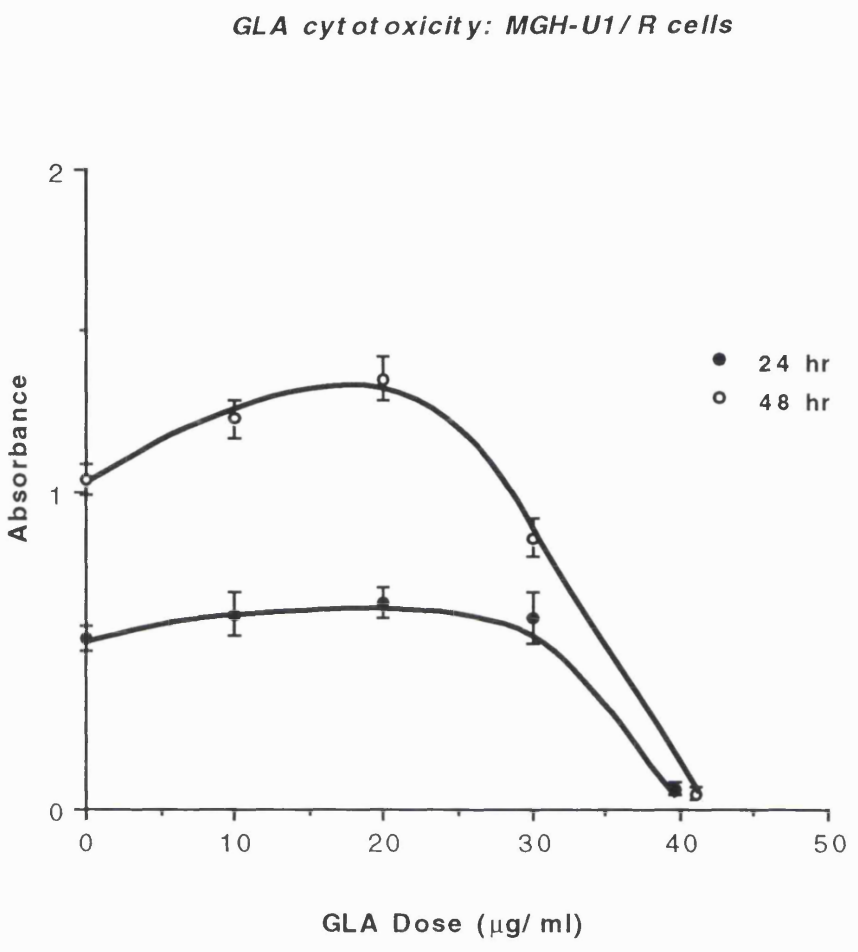

Graph 5.1b. **Cytotoxicity of GLA over different concentrations and time periods in MGH-U/R cells, using the MTT assay. Mean ± standard deviations measured using a spectrophotometer. GLA was cytotoxic at a concentration of 40µg/ml over 24h and 30µg/ml over 48h.**

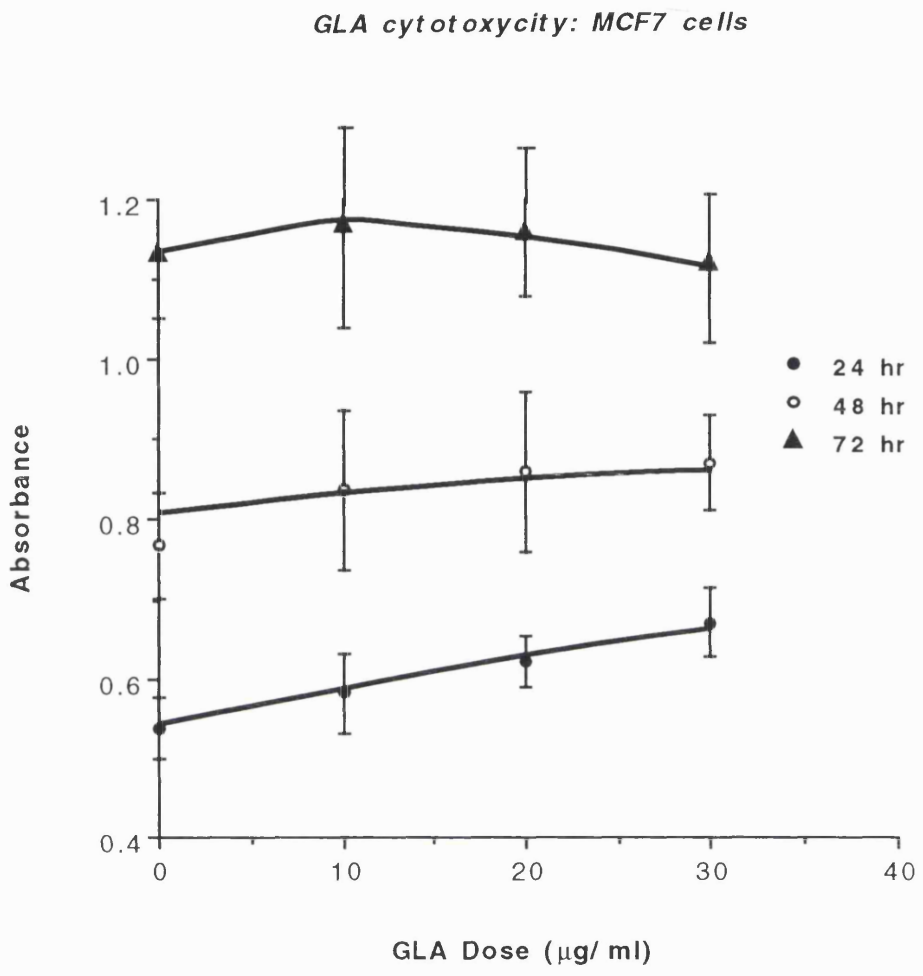

Graph 5.1c. **Cytotoxicity of GLA over different concentrations and time periods in MCF-7 cells, using the MTT assay. Mean ± standard deviations measured using a spectrophotometer. GLA was non-cytotoxic at all concentrations and over all time periods.**

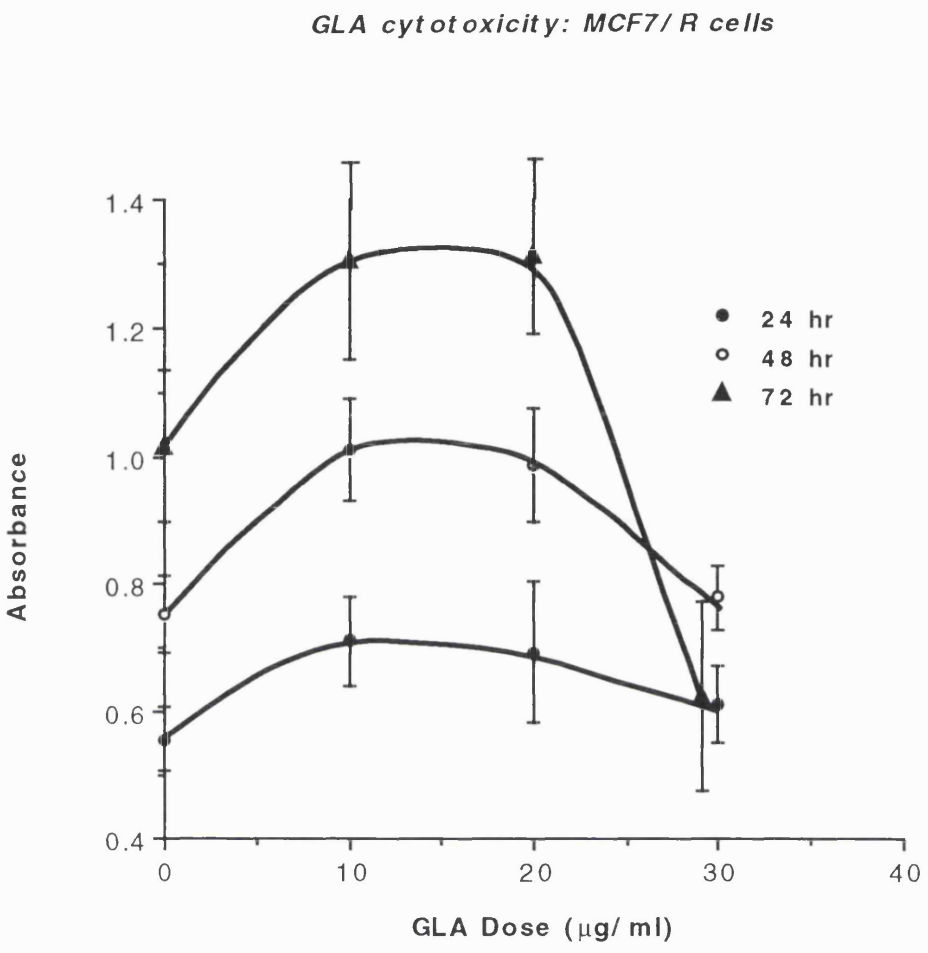

Graph 5.1d. **Cytotoxicity of GLA over different concentrations and time periods in MCF-7/R cells, using the MTT assay. Mean ± standard deviations measured using a spectrophotometer. GLA was non-cytotoxic at all concentrations and over all time periods.**

5.2. INDIRECT CYTOTOXICITY

The hypothesis behind this work is that the incorporation of GLA in cells will result in increases in overall drug uptake and therefore lead to more toxicity. This effect has been named arbitrarily "indirect cytotoxicity". Cells were incubated with GLA for 24h to allow dynamic membrane incorporation of the EFA. The cells were then exposed to the drug (anthracycline) and differences in cellular drug uptake were noted between GLA treated and untreated cells. Indirect cytotoxicity was inferred as the probable outcome of higher cellular drug uptake[129].

5.2.1. CHANGES IN CELLULAR DRUG UPTAKE

This was measured using flow cytometry. All four cell lines cells were incubated with GLA, following this the GLA treated cells were exposed to three different drug doses and the amount of intracellular drug recorded. These were compared with the results gained, using the same method, from untreated cells exposed to the same drug doses at the same time.

i). MGH-U1 AND MGH-U1/R CELLS

There was no change in drug uptake by either cell line due to the incorporation of GLA (Table 5.2I).

ii). MCF-7 AND MCF-7/R CELLS

Again there was no change in drug uptake in either cell line due to incorporation of GLA (Table 5.2I).

There were variations in drug uptake but these were not significant and occurred between experimental repeats.

MGH-U1 & MGH-U1/R				
DRUGS (μg/ml)	SENSITIVE	SENSITIVE + GLA	RESISTANT	RESISTANT + GLA
DOX				
0	0	0	0	0
5	30.8 ± 7.0	14.8 ± 5.0	2.8 ± 0.5	4.0 ± 0.9
10	64.1 ± 6.0	50.0 ± 6.0	4.0 ± 0.8	6.0 ± 0.8
EPI				
0	0	0	0	0
5	42.8 ± 8.0	63.1 ± 13.0	2.4 ± 0.6	3.7 ± 0.7
10	67.1 ± 8.0	70.5 ± 4.0	3.9 ± 0.7	4.7 ± 0.5
IDA				
0	0	0	0	0
5	78.0 ± 15.0	80.6 ± 9.0	3.4 ± 0.6	2.7 ± 0.9
10	130.0 ± 10.0	123.8 ± 11	6.8 ± 1.2	5.2 ± 1.2
MCF-7 & MCF-7/R				
DRUGS (μg/ml)	SENSITIVE	SENSITIVE + GLA	RESISTANT	RESISTANT +GLA
DOX				
0	0	0	0	0
5	9.2 ± 0.5	15.2 ± 5.0	4.7 ± 0.2	4.6 ± 0.6
10	19.5 ± 3.0	27.0 ± 5.0	10.0 ± 0.7	8.8 ± 1.0
MTZ				
0	0	0	0	0
5	19.7 ± 5.6	24.0 ± 6.0	15.2 ± 0.5	14.8 ± 1.6
10	32.4 ± 2.0	23.6 ± 5.0	18.2 ± 1.2	19.9 ± 2.8

Table 5.2I. Intracellular drug uptake by MGH-U1 & MGH-U1/R and MCF-7 & MCF-7/R cell lines due to incorporation of GLA into the cells as shown by flow cytometry.

5.2.2. CHANGES IN THE PATTERNS OF INTRACELLULAR DRUG UPTAKE

The previous section showed that overall drug uptake was not affected significantly by GLA incorporation into cells. Therefore, the possible effect of GLA on changes on intracellular drug localisation was investigated using the confocal microscope. Both GLA treated and untreated cells were incubated with drug in the same manner and the distribution patterns of the drug viewed and compared between cells with and without GLA incorporation.

If after visualisation on the confocal microscope there appeared to be changes in the amount of or location of intracellular fluorescence due to GLA incorporation then semi-quantitation was performed on these picture files. This analysis consisted of free-hand drawing around the cellular compartments, including nucleus, cytoplasm and whole cell, and then recording the mean fluorescence of each compartment (arbritary fluorescence of pixels per area) (Fig. 5.1). The figures and table for this section are presented on pages 122 to 130.

5.2i) MGH-U1 AND MGH-U1/R CELLS

DOXORUBICIN: Both GLA treated and untreated cells showed a nuclear pattern of drug distribution, the GLA treated cells having less intense spots of fluorescence in their nuclei. The sensitive cells appeared to have taken up less DOX after having GLA incorporated into them but this was not significant.

The GLA treated resistant cells also appeared to have taken up less drug than the untreated resistant cells but this was not at a significant level. The pattern of intracellular DOX distribution producing nuclear holes was still visible in both sets of resistant cells (Fig 5.2).

EPIRUBICIN: GLA treated and untreated MGH-U1 cells had similar levels of fluorescent intensity and similar patterns of intracellular localisation of EPI which was mainly located in the nuclei with some cytoplasmic distribution.

There was also no observable affect of GLA on EPI uptake by the MGH-U1/R cells. Both GLA treated and untreated cells appeared to take up similar levels

of EPI and both showed the drug being located in the cytoplasm producing the 'nuclear hole' effect (Fig 5.3).

IDARUBICIN: The confocal picture shows that an increase in IDA uptake occurs after incorporation of GLA into resistant cells (Fig. 5.4). This was shown by an increase in the amount of fluorescence in the GLA treated resistant cells compared to the untreated resistant cells. Semi-quantitation revealed a significant increase in drug uptake in GLA treated resistant cells compared to untreated resistant cells. This increase occurred in all cellular compartments, that is the nuclei, cytoplasm and whole cells (Table 5.2II). This could be regarded as being due to overall higher level of drug uptake in GLA treated cells compared to untreated cells.

Sensitive cells showed similar plots of fluorescent intensity, in the cells cut by the line, regardless of GLA treatment (Fig 5.5).

5.2.ii) MCF-7 AND MCF-7/R CELLS

DOXORUBICIN: There was little difference in DOX uptake or intracellular localisation between sensitive cells with or without incorporated GLA. Both had nuclear DOX accumulation with very little in the cytoplasm.

In resistant cells there was a difference in DOX localisation but not the amount of DOX accumulated between GLA treated and untreated cells. The untreated cells displayed nuclear holes with mainly cytoplasmic fluorescence and very strong perinuclear drug localisation. The GLA treated cells had taken up the DOX mainly into their nuclei, producing a pattern of intracellular drug distribution similar to that observed in sensitive cells. Semi-quantitation of the different cellular compartments within non-treated and GLA treated cells showed no significant difference in drug uptake between the two cell sets (Fig. 5.6).

MITOZANTRONE: Sensitive cells pre-treated with GLA took up less MTZ than their untreated counterparts but there was no significant difference. Both sets of sensitive cells showed nuclear holes of fluorescence with perinuclear rings of MTZ uptake and very punctate bright points of fluorescence (Fig. 5.7).

GLA treated resistant cells had a different pattern of intracellular MTZ distribution than untreated resistant cells. The untreated cells had little nuclear fluorescence with the MTZ mainly distributed in the cytoplasm especially in the perinuclear region. GLA treated resistant cells have nuclear MTZ accumulation with less MTZ in the cytoplasm whilst still retaining an area of very high perinuclear fluorescence (Fig. 5.7). This shift in drug distribution into the nuclei was due to GLA incorporation into MCF-7/R cells and was significant (Table 5.2II). However, there was no significant increase in drug uptake by the whole cells. It should be noted that it was rather difficult to define clearly and precisely the exact compartmentalisation of this particular drug in any of the confocal slices all through these cells. It was believed there was a non-partitioning of the MTZ into cytoplasmic intracellular compartments in MCF-7/R cells after GLA incorporation.

IDARUBICIN: Sensitive cells which have had GLA incorporated into them showed similar intracellular patterns and levels of IDA uptake compared to the untreated sensitive cells (Fig. 5.8).

The resistant cells showed similar patterns of intracellular IDA localisation regardless of whether they had been incubated with GLA or not. However, those resistant cells with GLA incorporated into them produce a higher level of fluorescent intensity with the additional IDA located mainly in the perinuclear region. The perinuclear rings of fluorescence in these GLA treated cells were brighter than those observed in untreated resistant cells (Fig. 5.8). There was a significant increase in IDA uptake by the nuclei of the GLA treated resistant cells compared to the untreated cells but this increase did not occur in other cellular compartments (Table 5.2II). That there was no change in drug uptake by the whole cell was not surprising, considering that the fluorescence was mainly in the peri-nuclear region of the cells. This area was difficult to define in terms of cellular compartments which were nuclear or cytoplasmic. The actual sensitivity of the machine is not good enough to visualise any smaller cellular compartments, such as the Golgi apparatus which are located in the perinuclear area.

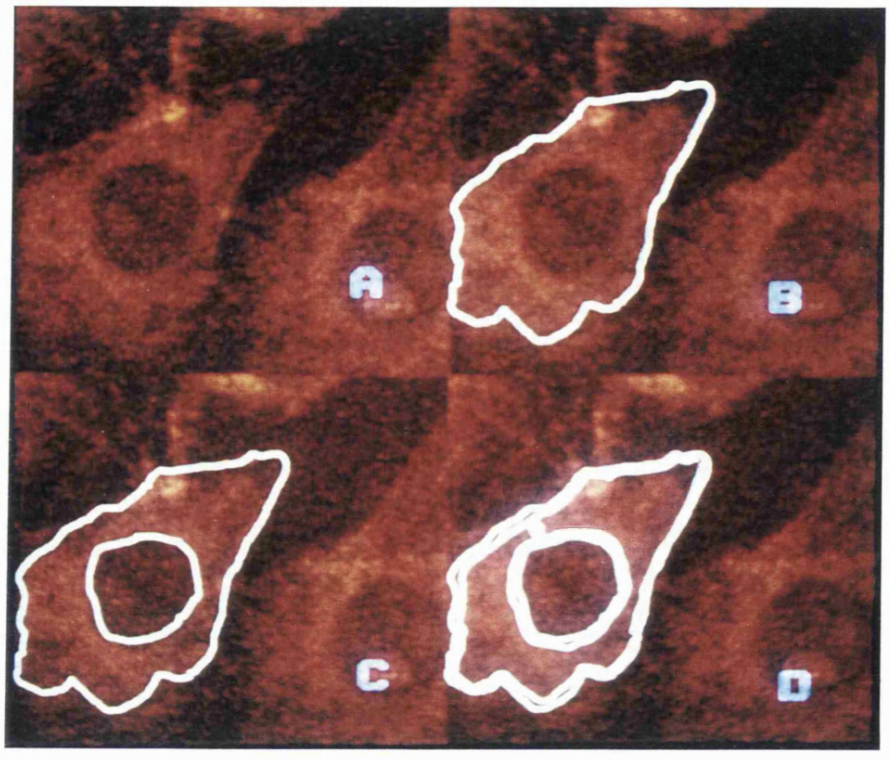

Fig. 5.1. **Analysis of drug uptake in intracellular compartments, using the confocal microscope.**
(X 900)

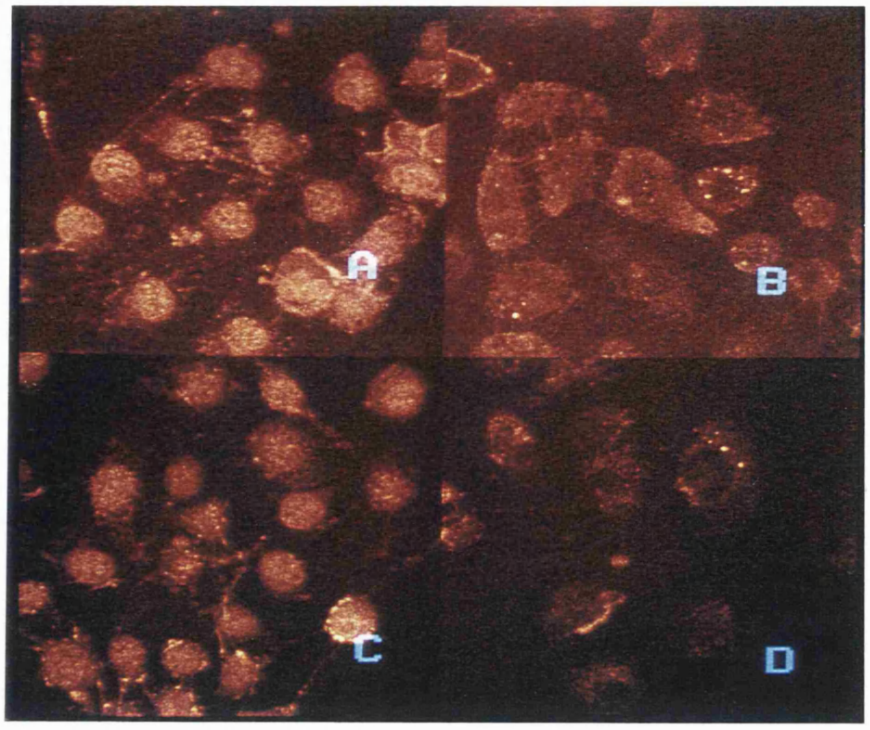

Fig. 5.2. **Patterns of intracellular DOX (10μg/ml) in GLA (20μg/ml) treated and untreated MGH-U1 and MGH-U1/R cells, detected using the confocal microscope.**

A and C : MGH-U1 cells **B and D : MGH-U1/R cells**

A and B : untreated cells **C and D : GLA treated cells**

(X 300)

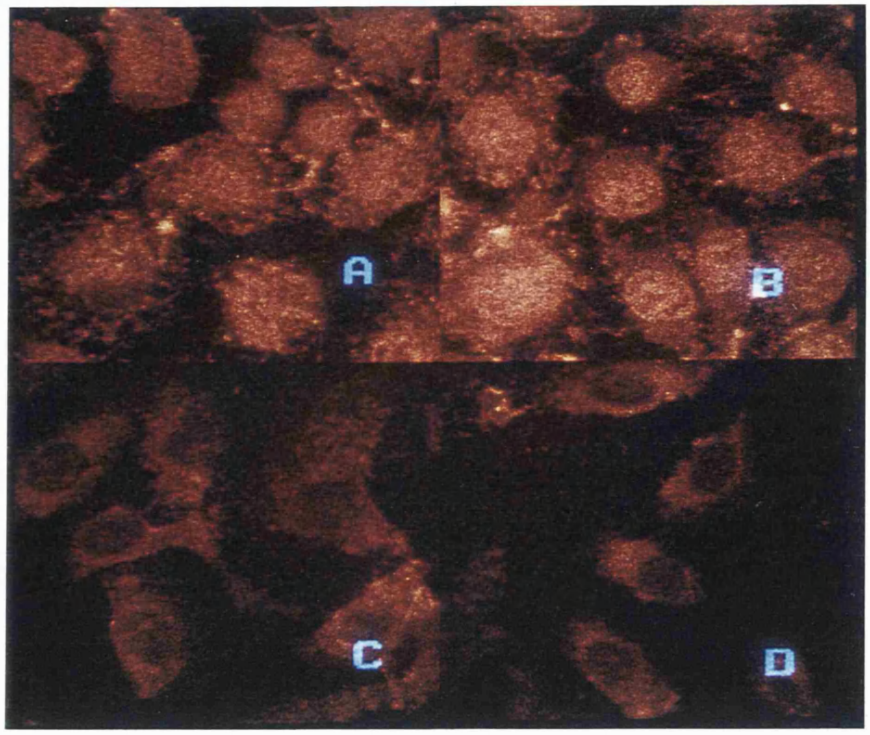

Fig. 5.3. **Patterns of intracellular EPI (10μg/ml) in GLA (20μg/ml) treated and untreated MGH-U1 and MGH-U1/R cells, detected using the confocal microscope.**

A and C : MGH-U1 cells **B and D : MGH-U1/R cells**

A and B : untreated cells **C and D : GLA treated cells**

(X 600)

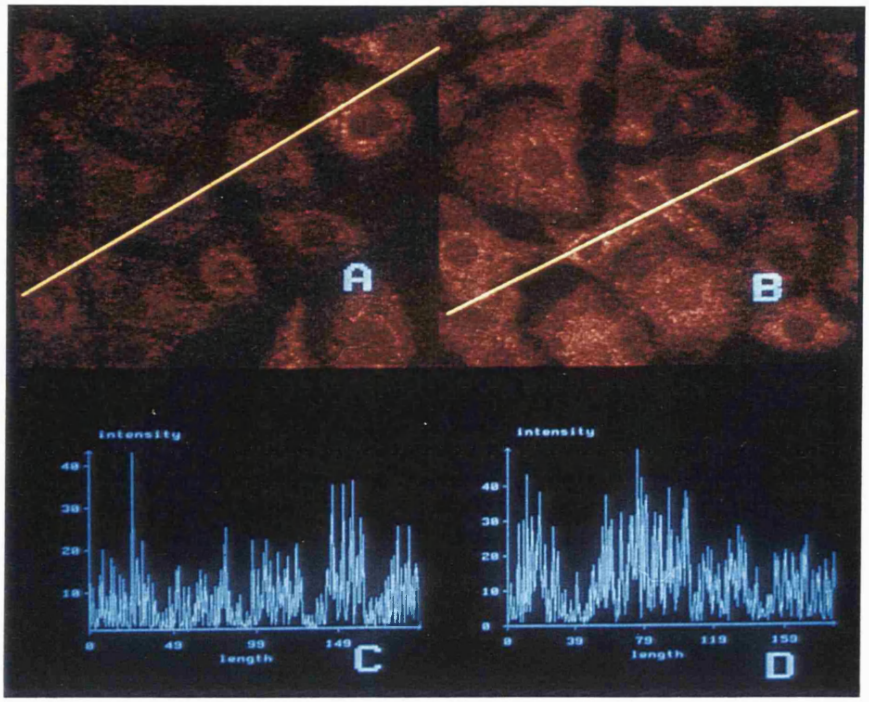

Fig. 5.4. **Patterns of intracellular IDA (10μg/ml) in GLA (20μg/ml) treated and untreated MGH-U1/R cells, detected using the confocal microscope with corresponding intensity graphs.**

A : untreated cells **B : GLA treated cells**

(X 300)

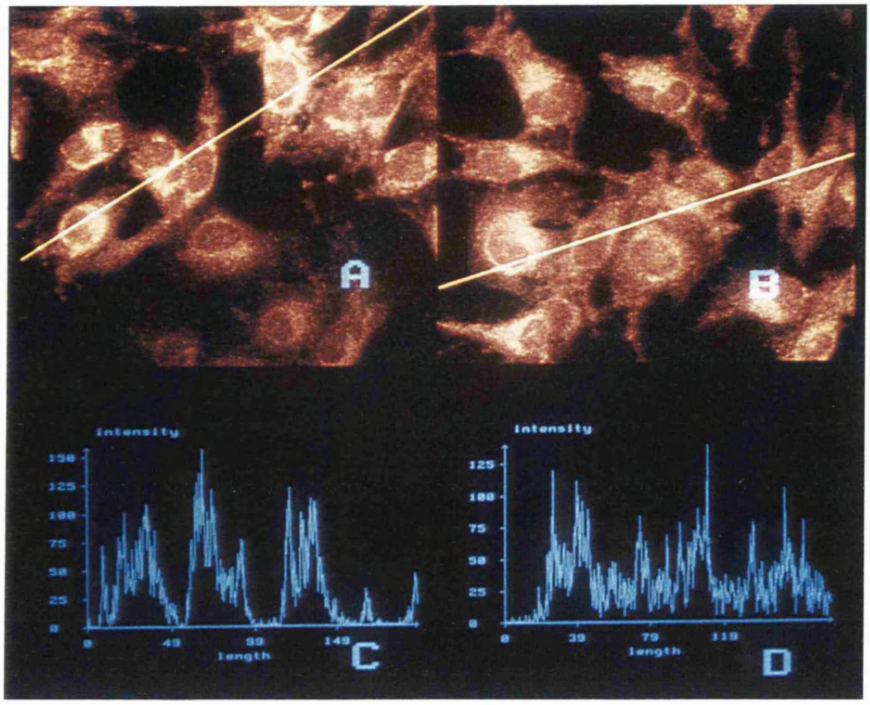

Fig. 5.5. **Patterns of intracellular IDA (10μg/ml) in GLA (20μg/ml) treated and untreated MGH-U1 cells, detected using the confocal microscope with corresponding intensity graphs.**

A : untreated cells **B : GLA treated cells**

(X 300)

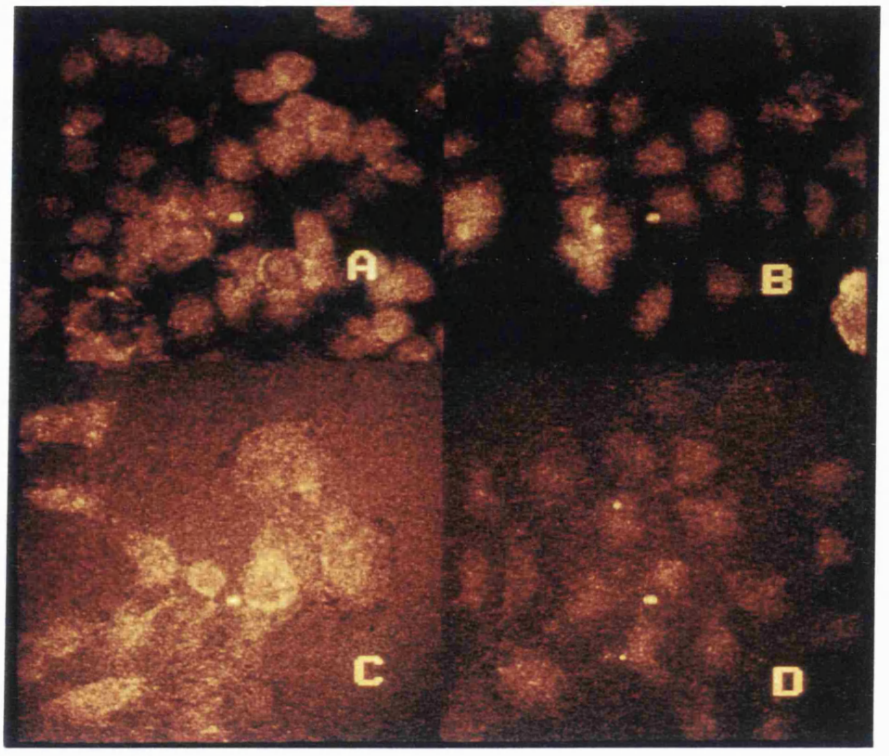

Fig. 5.6. **Patterns of intracellular DOX (10μg/ml) in GLA (20μg/ml) treated and untreated MCF-7 and MCF-7/R cells, detected using the confocal microscope.**
A and C : MCF-7 cells **B and D : MCF-7/R cells**
A and B : untreated cells **C and D : GLA treated cells**
(X 300)

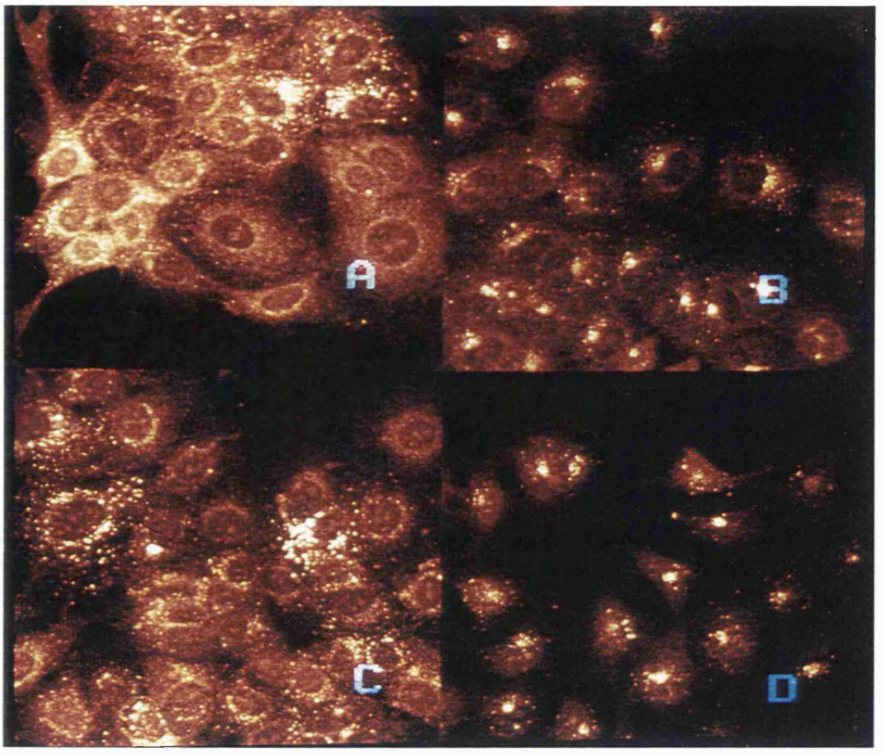

Fig. 5.7. **Patterns of intracellular MTZ (10μg/ml) in GLA (20μg/ml) treated and untreated MCF-7 and MCF-7/R cells, detected using the confocal microscope.**

A and C : MCF-7 cells **B and D : MCF-7/R cells**

A and B : untreated cells **C and D : GLA treated cells**

(X 300)

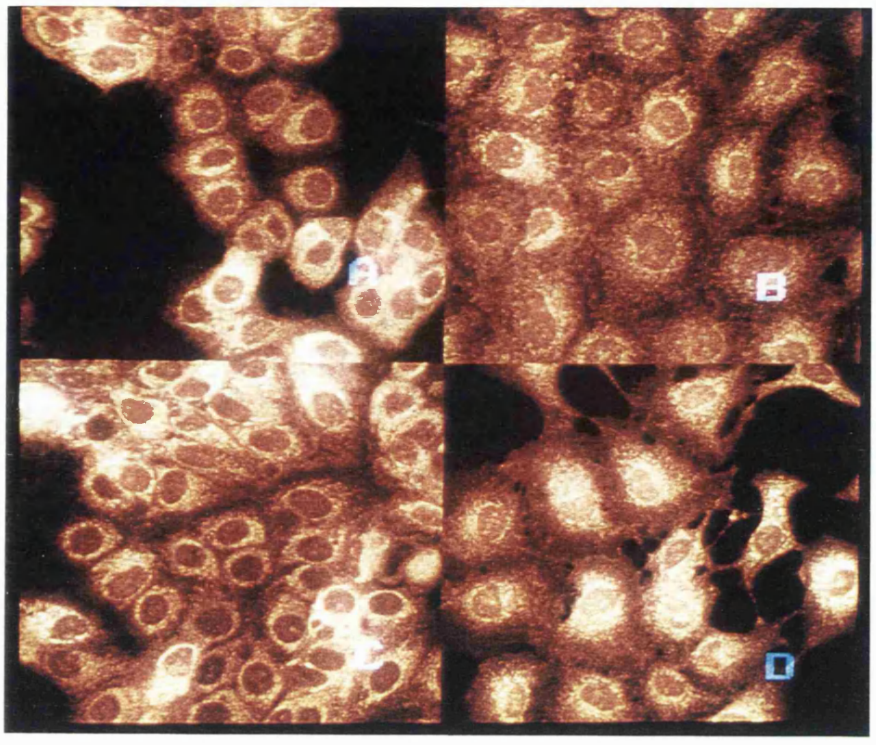

Fig. 5.8. **Patterns of intracellular IDA (10μg/ml) in GLA (20μg/ml) treated and untreated MCF-7 and MCF-7/R cells, detected using the confocal microscope.**

A and C : MCF-7 cells **B and D : MCF-7/R cells**

A and B : untreated cells **C and D : GLA treated cells**

(X 300)

WITHOUT GLA			WITH GLA		
MGH-U1 + DOX					
Nuclei	**Cytoplasm**	**Whole Cell**	**Nuclei**	**Cytoplasm**	**Whole Cell**
41.7 ± 4.3	24.8 ± 3.4	30.9 ± 5.5	28.3 ± 10.9	12.0 ± 10.2	20.1± 6.7
			not significant p < 0.04		
MGH-U1/R + DOX					
40.3 ± 7.4	49.8 ± 7.95	47.6 ± 5.4	29.1 ± 8.6	32.3 ± 8.9	30.2 ± 12.7
			not significant p ≈ 0.04		
MGH-U1/R + IDA					
10.5 ± 1.5	11.8 ± 1.9	12.0 ± 2.0	16.6 ± 3.4	19.3 ± 3.86	19.5 ± 3.7
all display significance p = < 0.01			**p = 0.0002**	**p = 0.0006**	**p = 0.0004**
MCF-7/R + MTZ					
24.9 ± 7.4	22.18 ± 4.6	22.7 ± 3.4	37.2 ± 5.2	18.4 ± 3.4	24.2 ± 3.0
nuclear uptake shows significance			**p < 0.001**	**NS**	**NS**
MCF-7/R + IDA					
51.4 ± 5.1	4.5 ± 10.6	47.1±10.3	71.2 ± 12.7	43.9 ± 8.3	49.2 ± 9.6
nuclear uptake shows significance			**P = 0.002**	**NS**	**NS**

Table 5.2II. Semi-quantitation by confocal microscopy of the changes in intracellular drug localisation in different cellular compartments, *i.e.* nuclei, cytoplasm and whole cell, in MGH-U1, MGH-U1/R and MCF-7/R cells, due to the incorporation of GLA into these cells.

6. PRESENCE AND LOCALISATION OF RESISTANCE PROTEINS

This section is concerned with the presence of resistance proteins and their location within the cells, in particular the resistant cell lines. The detected resistance proteins were used as evidence of the resistance mechanism conferring MDR to those cells. The three proteins stained for were Ppg, LRP and MRP. The proteins were located by using monoclonal antibody indirect staining, and the secondary antibody was mainly conjugated with FITC which was detected under fluorescence. Some experiments were carried out using a Cy3-conjugated secondary antibody, as described in the methods section (2.2).

The antibody used to detect Pgp was called JSB-1 and had been raised against a cytoplasmic epitope of this membrane transporter protein. LRP-56 was the antibody used to locate the cytoplasmic protein LRP. This resistance protein is believed to be a vault protein and associated with the nuclear pore complex, so may be detected around the nuclei. Two monoclonal antibodies raised against MRP were employed to locate this resistance protein; MRPm6 and MRPr1. The protein MRP is cytoplasmic and believed to be involved in vesicular transport of drug out of the cell.

The effect that incubating the cells with GLA had on the presence and location of these proteins was also investigated.

6.1. RESISTANCE PROTEINS WITHOUT GLA

The figures for this section are presented on pages 134 to 142.

6.1.i) MGH-U1 AND MGH-U1/R CELLS

The negative controls (Figs. 6.1A and 6.3A) had very little background or natural fluorescence and were therefore ideal for comparisons with the slides stained for the three antibodies against resistance.

P-GLYCOPROTEIN: There were high levels of Pgp in MGH-U1/R cells indicated by the high levels of fluorescence (Fig. 6.1B). Although some slight fluorescence was present within the cytoplasm of some cells, the location of the protein was obviously in the plasma membrane. This appeared as bright rings of fluorescence around the cells and can be observed more clearly at higher magnification. Here individual points of fluorescence can be seen along the plasma membrane of the cells (Fig. 6.2).

The level of staining due to JSB-1 binding in the MGH-U1 cells (Fig.6.3B) was negligible compared with their negative control (Fig 6.3A). This lack of membrane staining (compared to the control and the MGH-U1/R cells) indicated that no or very little Pgp was present in the sensitive cells.

LUNG RESISTANCE PROTEIN: There was a slight increase in the fluorescence intensity, compared to the negative control after staining for LRP (Fig.6.1C), suggesting a low level of LRP present in these resistant cells. The pattern of specific staining presented as punctate dots of fluorescence around the nuclei and in the perinuclear cytoplasm but was only observed in some cells. This was clearly shown by enlarging the image (Fig. 6.4).

There was no LRP detected in the MGH-U1 cells (Fig. 6.3C).

MULTIDRUG RESISTANCE ASSOCIATED PROTEIN: No MRP was detected in either MGH-U1/R or MGH-U1 cells, using MRPm6 (Fig. 6.1D and 6.3D respectively).

Using the antibody MRPr1 there was again no detection of MRP in either of the cell lines (Fig. 6.5). However, as the controls had such high background fluorescence it was difficult to discern any increase in fluorescence due to antibody binding. Hence the experiments were repeated using a different secondary antibody conjugated with Cy3 (Fig. 6.6); a variety of blocking and pre-blocking procedures were also tried, *e.g.* pre-incubation or antibody dilution with 10% FCS in PBS, 10% human serum (HS) in PBS or rabbit albumin at 2% in PBS. None of these brought the non-specific binding down to really acceptable levels. This suggested a natural 'stickiness' of these cell lines for the secondary antibodies.

ii) MCF-7 AND MCF-7/R CELLS

P-GLYCOPROTEIN: The resistant cells contained Pgp, indicated by the increased level of fluorescence (Fig. 6.7B) compared to the negative control (Fig. 6.7A). The localisation of the protein was membranous as shown clearly by Fig. 6.8. However, most of the cells which stained with the antibody were those layered on top of other cells (Fig. 6.7B); the cells beneath these appear to either have taken up very little antibody or none at all.

The sensitive cells stained for Pgp showed similar levels of fluorescence (Fig. 6.9B) as the negative control (Fig. 6.9A).

LUNG RESISTANCE PROTEIN: In the resistant cells there was a very low level of fluorescence in cells stained for LRP (Fig. 6.7C) similar to the negative control (Fig. 6.7A). The pattern of specific staining due to the presence of LRP presented as sparse punctate dots of fluorescence within the cell's nuclei and cytoplasm.

The sensitive cells had very little LRP with only a couple of cells containing bright dots of fluorescence (Fig. 6.9C). The majority of MCF-7 cells showed similar staining patterns and levels of staining for LRP as their negative controls (Fig. 6.9A).

MULTIDRUG RESISTANCE PROTEIN: There was no specific staining for MRP in the MCF-7/R cells (Fig. 6.7D). Both the stained cells and their negative control showed highly fluorescent nucleoli with very low cytoplasmic or nuclear fluorescence; why the nucleoli alone should bind the secondary antibody so strongly is unknown. The MGH-U1 experiments proved that the secondary antibody was working but that no protein was located in those resistant cells, so no further experiments using different secondary antibodies were performed on the MCF-7 cells.

Again the sensitive cells showed similar patterns of fluorescence in cells stained for MRP (Fig. 6.9D) and their negative controls (Fig. 6.9A).

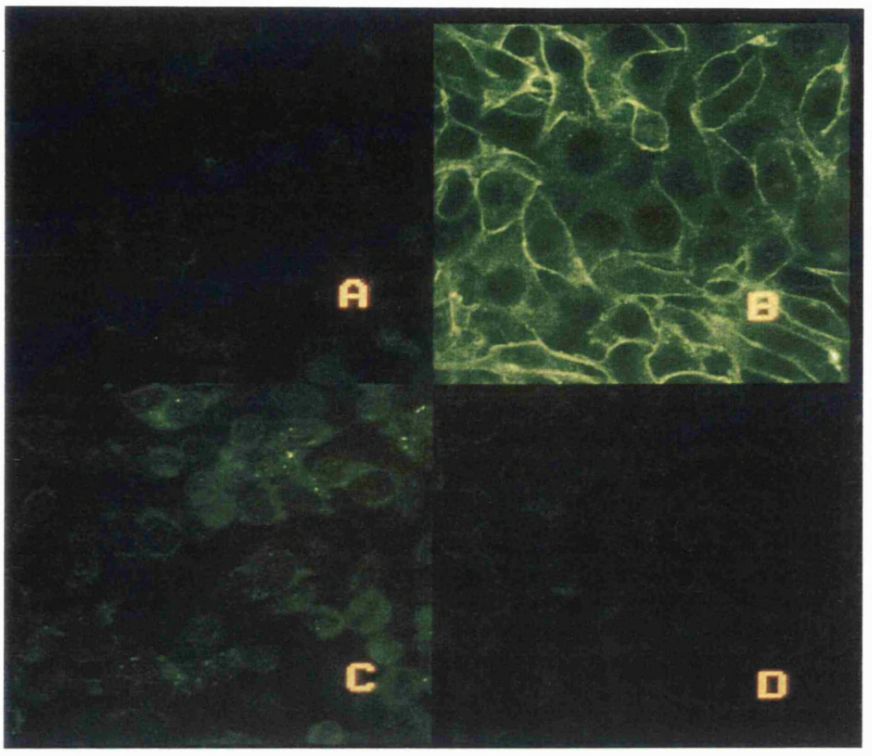

Fig. 6.1. **Immunohistochemical staining for resistance proteins in MGH-U1/R cells, detected by FITC-conjugated secondary antibody and viewed using a fluorescent microscope.**

A : negative control **B : P-glycoprotein**

C : LRP **D : MRPm6**

(X 300)

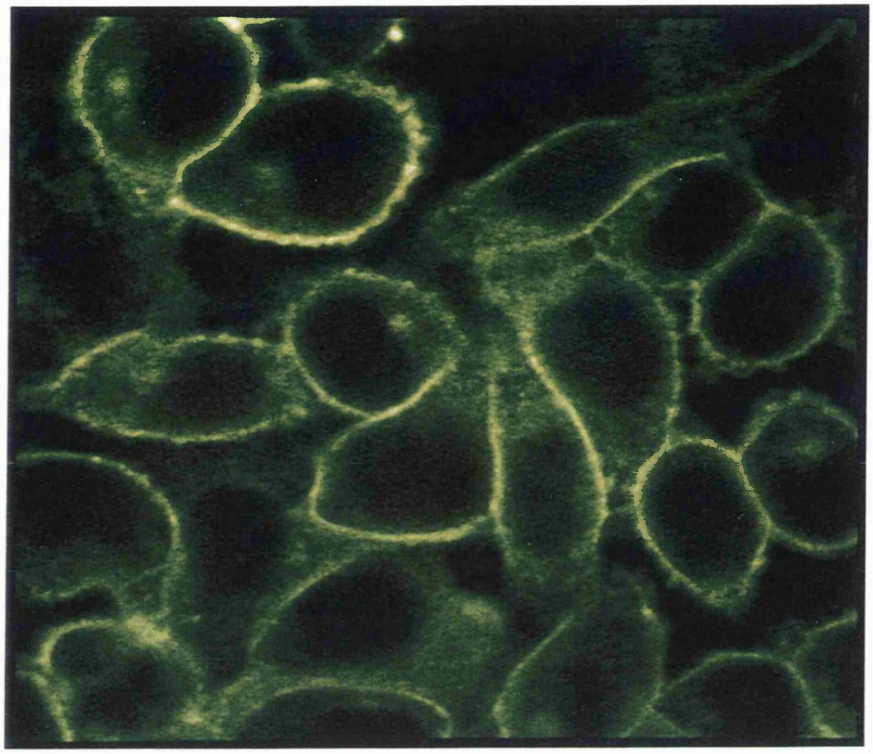

Fig. 6.2. **Immunohistochemical staining for P-glycoprotein in MGH-U1/R cells, detected by FITC-conjugated secondary antibody and viewed using a fluorescent microscope.** (X 900)

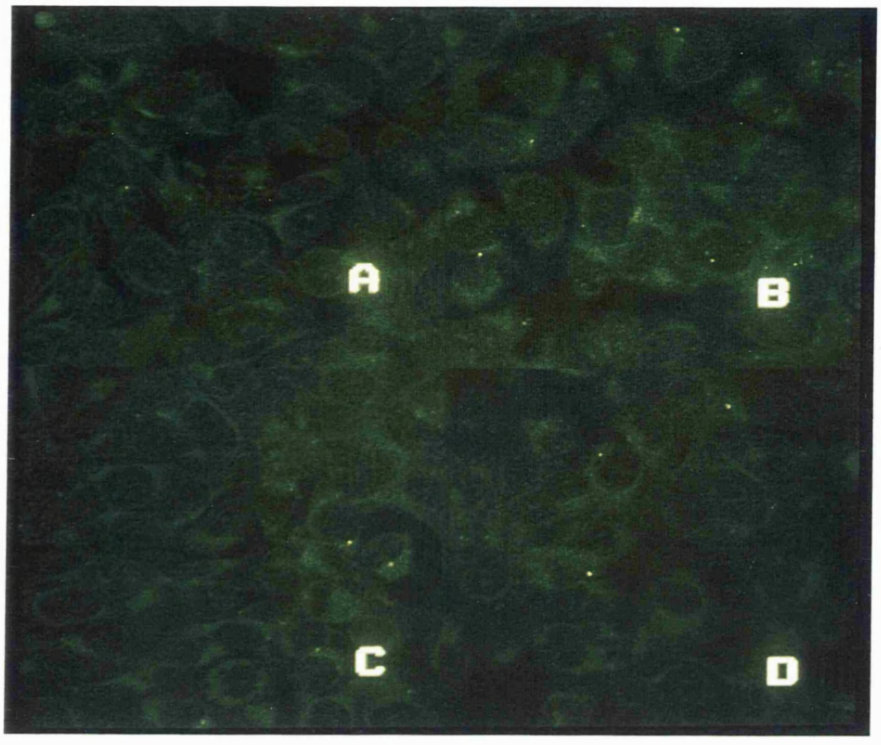

Fig. 6.3. **Immunohistochemical staining for resistance proteins in MGH-U1 cells, detected by FITC-conjugated secondary antibody and viewed using a fluorescent microscope.**

A : negative control **B : P-glycoprotein**

C : LRP **D : MRPm6**

(X 300)

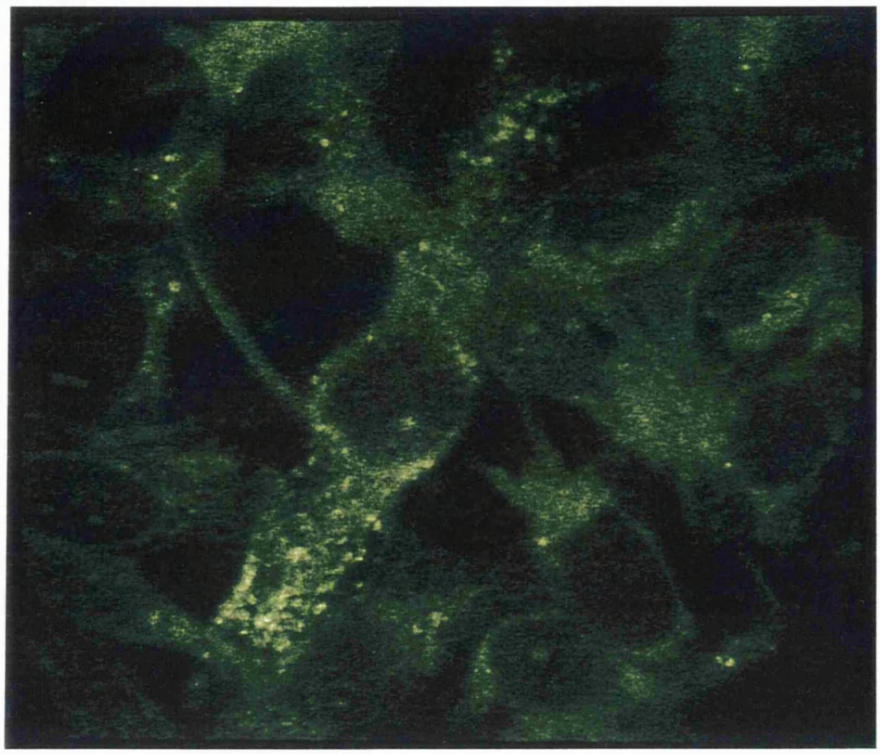

Fig. 6.4. **Immunohistochemical staining for lung resistance protein in MGH-U1/R cells, detected by FITC-conjugated secondary antibody and viewed using a fluorescent microscope.**
(X 900)

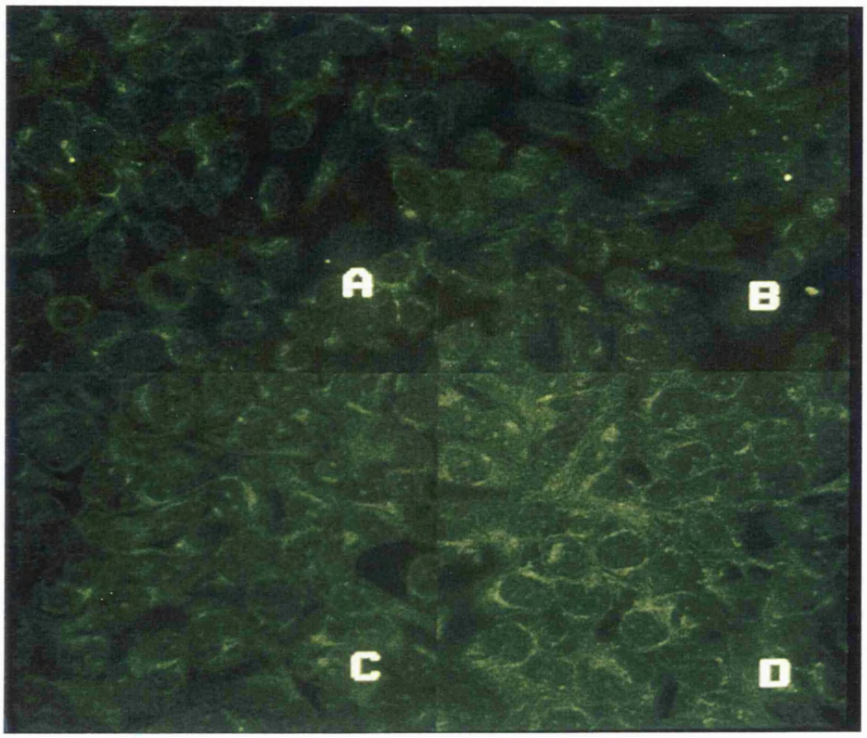

Fig. 6.5. **Immunohistochemical staining for multidrug resistance associated protein using the primary MRPr1 and a secondary FITC-conjugated antibodies in MGH-U1/R and MGH-U1/R cells.**

A and B : MGH-U1/R cells **C and D : MGH-U1 cells**

A and C : negative controls **B and D : MRPr1**

(X 300)

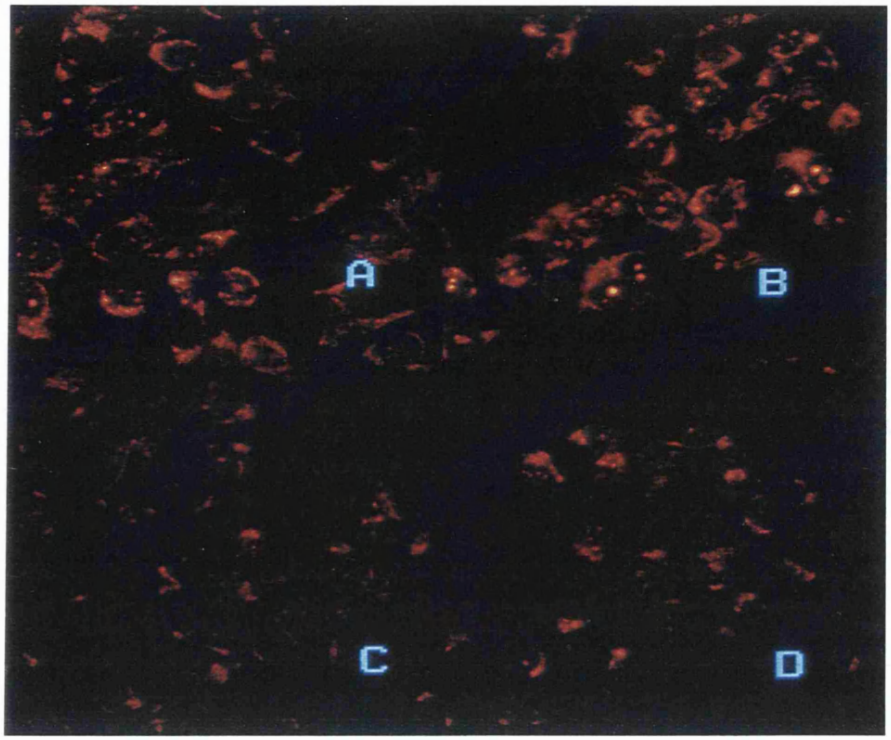

Fig. 6.6. **Immunohistochemical staining for multidrug resistance associated protein using the primary MRPr1 and a secondary Cy3-conjugated antibodies in MGH-U1/R and MGH-U1/R cells.**

A and B : MGH-U1/R cells **C and D : MGH-U1 cells**

A and C : negative controls **B and D : MRPr1**

(X 300)

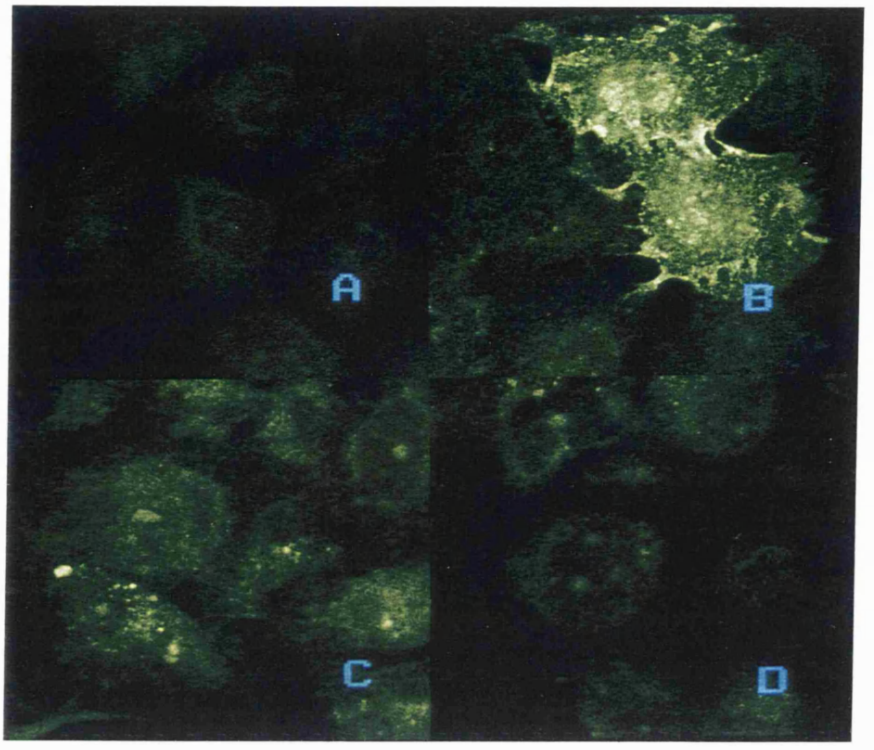

Fig. 6.7. **Immunohistochemical staining for resistance proteins in MCF-7/R cells, detected by FITC-conjugated secondary antibody and viewed using a fluorescent microscope.**

A : negative control **B : P-glycoprotein**

C : LRP **D : MRPm6**

(X 600)

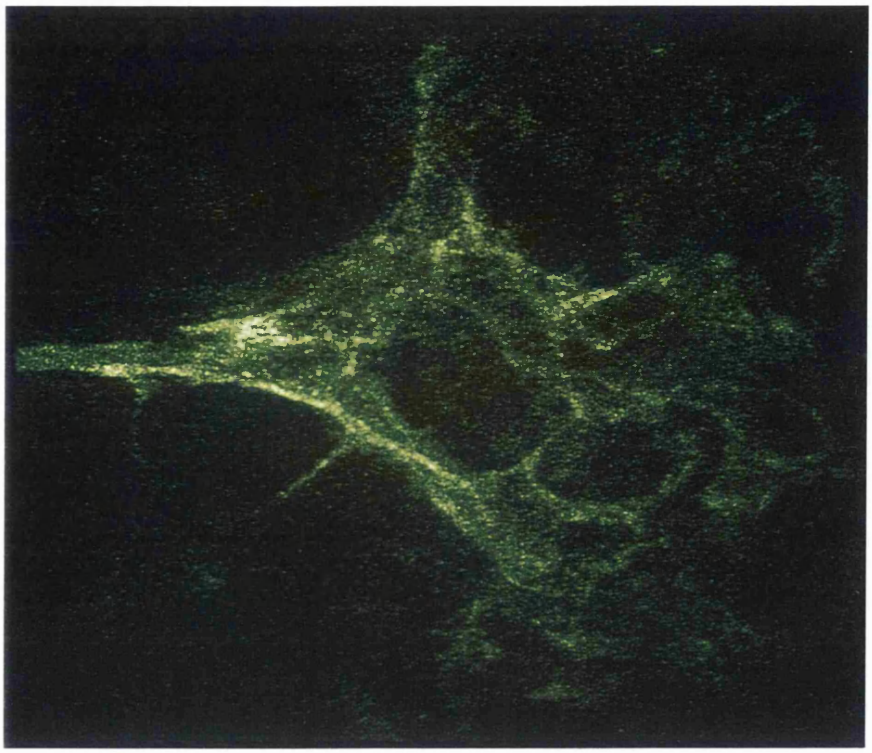

Fig. 6.8. **Immunohistochemical staining for P-glycoprotein in MCF-7/R cells, detected by FITC-conjugated secondary antibody and viewed using a fluorescent microscope.** (X 900)

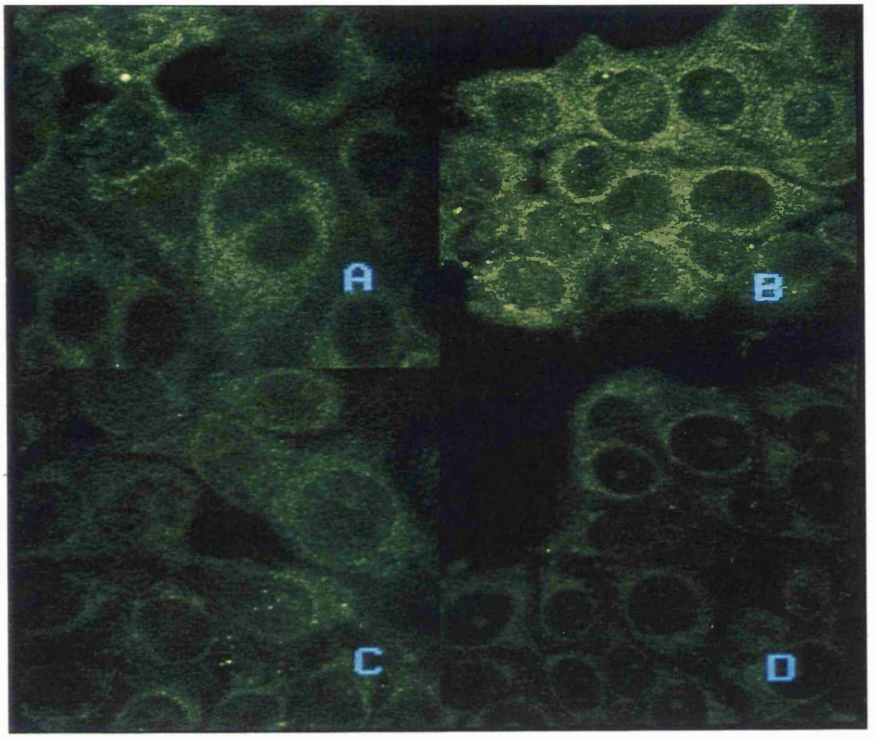

Fig. 6.9. **Immunohistochemical staining for resistance proteins in MCF-7 cells, detected by FITC-conjugated secondary antibody and viewed using a fluorescent microscope.**

A : negative control **B : P-glycoprotein**

C : LRP **D : MRPm6**

(X 600)

6.2. RESISTANCE PROTEINS WITH GLA

As the only resistance proteins detected in either the MGH-U1, MGH-U1/R, MCF-7 and MCF-7/R cells were Pgp and LRP these were the only ones studied in this section to observe if incubation with GLA affected their distribution or level of intensity. The results are presented on pages 145 to 148.

6.2i) MGH-U1 AND MGH-U1/R CELLS

P-GLYCOPROTEIN: In both the GLA treated and untreated cells, the positive antibody JSB-1 staining showed in a membranous pattern, indicating the presence of Pgp in the cell's plasma membrane (Figs. 6.10B&D). In Fig 6.10D there appeared to be a difference in the staining pattern for Pgp compared to that of the untreated cells (Fig. 6.10B). However, on closer inspection the GLA treated cells appear more rounded which could be giving the illusion of a different staining pattern for these cells.

In sensitive cells there was no Pgp detected in either the GLA treated cells or untreated cells, since the fluorescence from the cells stained with JSB was similar to that of their controls.

LUNG RESISTANCE PROTEIN: The characteristic punctate cytoplasmic staining pattern LRP was present in GLA treated cells and non treated cells. There was no change in the number of cells which contained this resistance protein between these two sets of resistant cells (1-5%). However, in the GLA treated cells there were larger points of fluorescence, which may correspond to vesicles which have sequestered antibody, located around the nuclei (Fig. 6.11).

There was no staining for LRP observed in either the GLA treated or non-treated MGH-U1 cells.

ii). MCF-7 AND MCF-7/R CELLS

P-GLYCOPROTEIN: There was no obvious difference between Pgp location or amount of staining in GLA treated or non-treated cells. The figure shown (Fig.

6.12) might appear to have brighter GLA treated cells. However, taking into account that; a) the control of the GLA treated cells had a much higher background fluorescence compared to the control of the untreated cells and b) the brightest cell in picture 6.12D has probably taken up more antibody due to its positioning, *i.e.* on top of the other cells; there is no difference between Pgp staining in GLA treated and non treated cells.

GLA treated and untreated MCF-7 cells showed similar intensities of fluorescence to each other and their controls, therefore, probably had similar amounts of JSB-1.

LUNG RESISTANCE PROTEIN: Again with the resistant cells the background fluorescence was much higher in the control of the GLA treated cells compared to that of the untreated cells (Fig. 6.13A&C). In both the treated and untreated cells, there was distinct staining for LRP by the antibodies but at a very low cell numbers (Fig. 6.13B&D). LRP was detected as bright punctate dots of fluorescence in the cytoplasm around the nuclei of the cells. This localisation of LRP was present in both sets of resistant cells but was perhaps clearest in the GLA treated cells (Fig. 6.13D). As with the MGH-U1/R cell line, the GLA treated MCF-7/R cell line showed larger points of fluorescence compared to the untreated MCF-7/R cells. However, it was a very low percentage (around 1-5%) of cells which stained for LRP making any conclusive observations limited.

In MCF-7 cells there was no difference in the intensity and pattern of staining between cells with or without GLA.

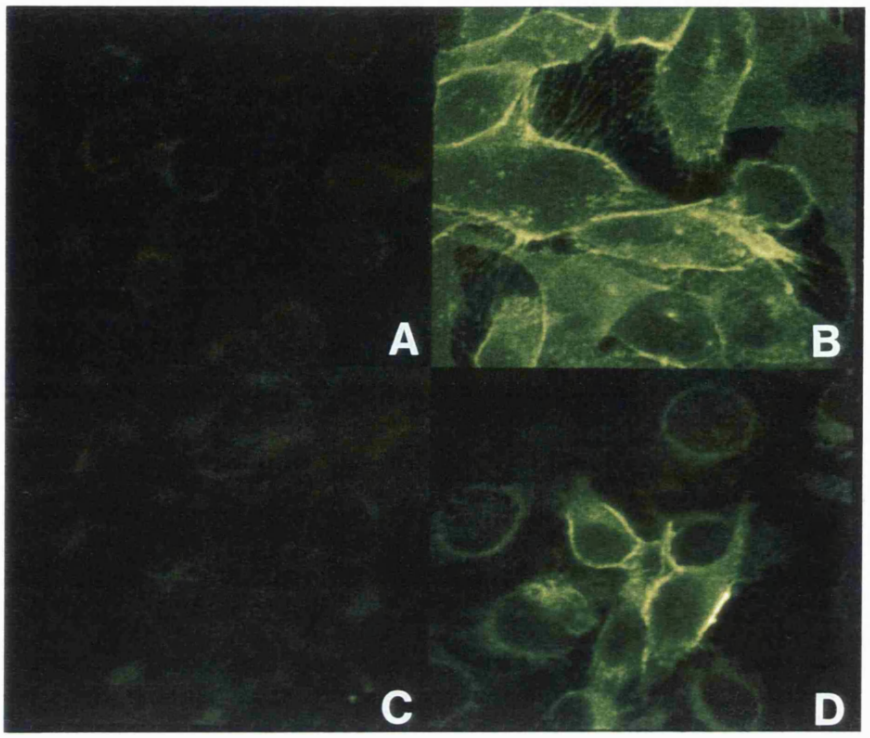

Fig. 6.10. **Immunohistochemical detection of P-glycoprotein in GLA treated and untreated MGH-U1/R cells using a FITC conjugated secondary antibody and viewed by fluorescent microscopy.**

A and C : controls **B and D : P-glycoprotein**

A and B : untreated cells **C and D : GLA treated cells**

(X 600)

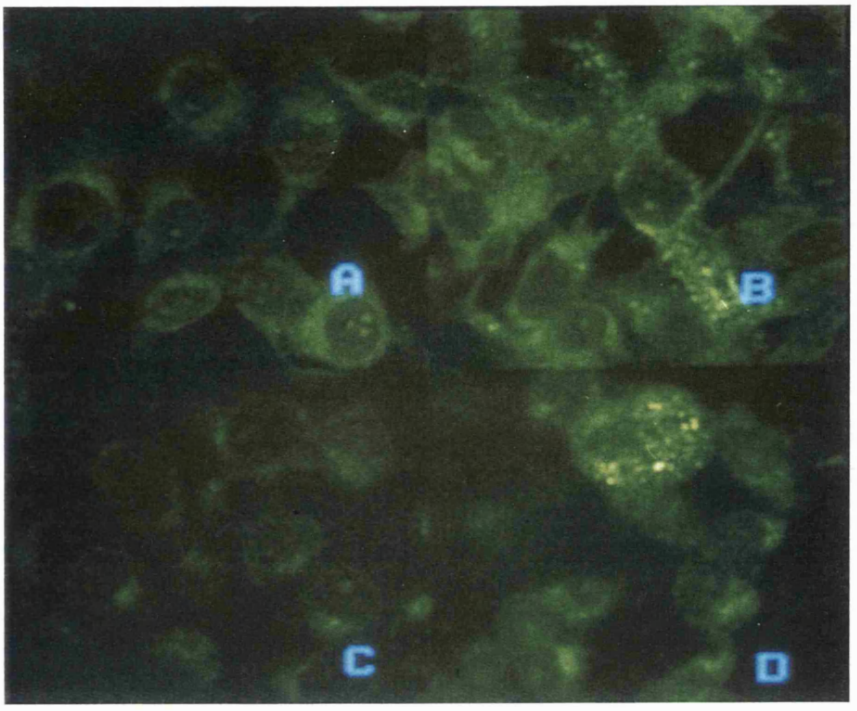

Fig. 6.11. **Immunohistochemical detection of lung resistance protein in GLA treated and untreated MGH-U1/R cells using a FITC conjugated secondary antibody and viewed by fluorescent microscopy.**

A and C : controls **B and D : LRP**

A and B : untreated cells **C and D : GLA treated cells**

(X 600)

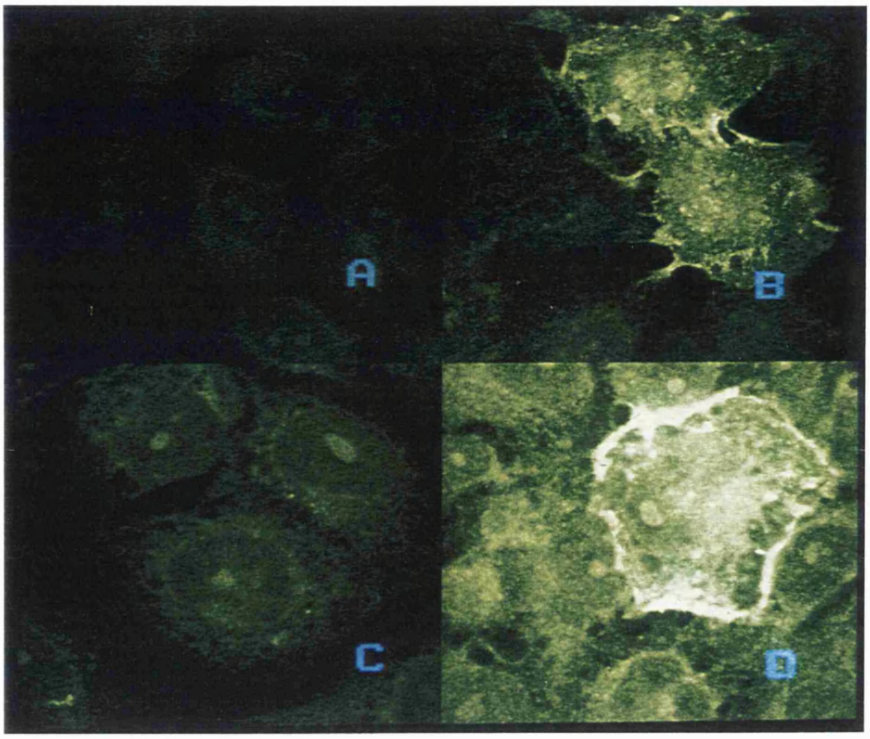

Fig. 6.12. **Immunohistochemical detection of P-glycoprotein in GLA treated and untreated MCF-7/R cells using a FITC conjugated secondary antibody and viewed by fluorescent microscopy.**

A and C : controls **B and D : P-glycoprotein**

A and B : untreated cells **C and D : GLA treated cells**

(X 750)

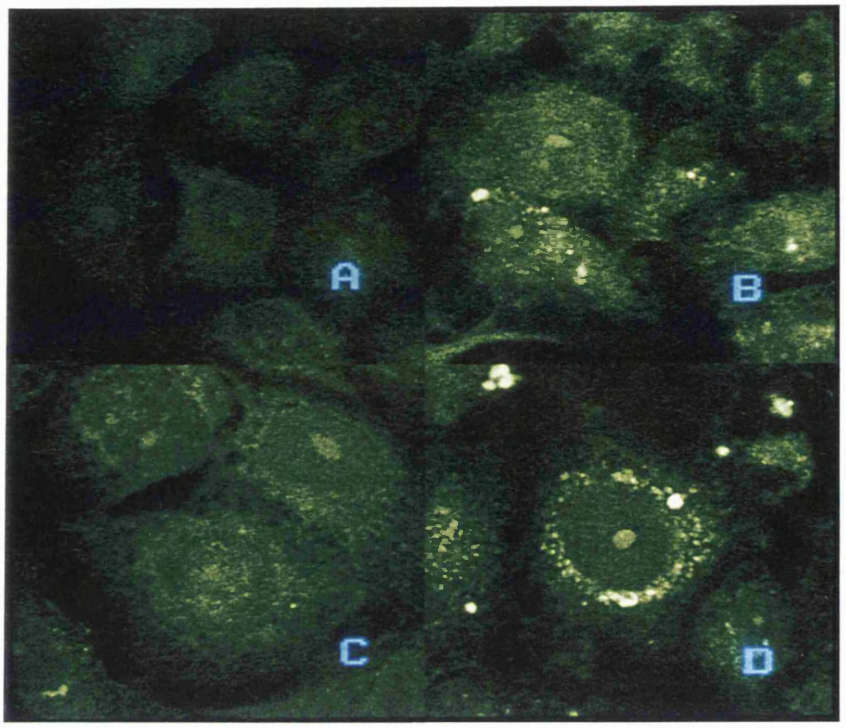

Fig. 6.13. **Immunohistochemical detection of lung resistance protein in GLA treated and untreated MCF-7/R cells using a FITC conjugated secondary antibody and viewed by fluorescent microscopy.**

A and C : controls **B and D : P-glycoprotein**

A and B : untreated cells **C and D : GLA treated cells**

(X 750)

6.3 RESISTANCE PROTEINS IN TISSUE SECTIONS

An additional study on clinical samples was carried out within the department by Irene Chong (an intercalated BSc. student who undertook the work as part of her research project). This study observed the presence and type of resistance proteins in a small number of bladder and breast cancer tissue sections. It is included here to show the applicability of the methodology used in this thesis, to study cell membrane efflux pumps in clinical material.

6.3i). BLADDER CANCER SECTIONS

Five out of the eleven bladder cancers investigated stained positive for Pgp. Fewer bladder cancers (2/11) expressed LRP, which was also observed in a very low percentage (5%) of MGH-U1/R (bladder cancer) cells. In contrast to the MGH-U1/R cell lines investigated, three out of the eleven bladder cancers stained positive for MRP. Two of the five cancers which were positive for Pgp also expressed at least one other resistance protein with one cancer expressing all three. The *in vitro* resistance of cells grown from these bladder cancers was assessed using the confocal microscope to observe intracellular patterns of EPI localisation. These patterns of drug localisation were compared to the characteristic intracellular EPI distribution observed in sensitive and resistant cell lines. The sensitive cells showed mainly nuclear fluorescence and the resistant cells took up less drug which was located in the cytoplasm producing distinctive nuclear holes.

In the *in vitro* experiments, four of the ten tumours analysed displayed total resistance but only two of them expressed Pgp and one expressed MRP as well, the others did not stain positive for any of the resistance proteins. Three of the tumours displayed cells with EPI uptake patterns of both sensitive and resistant characteristics and were deemed to have partial resistance. These three tumours all stained positive for resistance proteins but for different ones (Pgp, LRP and MRP). Of the three cancers which were sensitive *in vitro* one showed no immunopositivity, one stained positive for Pgp and the other expressed all three resistance proteins investigated (Table 6.3I).

In addition to the results from the *in vitro* study described above, information was available as to which patients were exposed to high levels of chemotherapy. The three cancers which had been highly exposed to cytotoxic drugs were all resistant *in vitro*. One of these cancers was positive, and two were negative, for MDR proteins. Of the seven cancers which had not been exposed to high levels of chemotherapy, only one displayed resistance *in vitro* and expressed Pgp. It is possible that this cancer was intrinsically resistant. The above comparisons imply that exposure to high levels of chemotherapy correlates with *in vitro* resistance in this small number of bladder cancers investigated. In contrast, no obvious relationship can be observed between the level of chemotherapy and MDR protein expression.

6.3ii). BREAST CANCER SECTIONS

Ten breast cancers were investigated with one staining positive for Pgp, three for MRP but none for LRP. There was no overlap in the expression of the resistance proteins.

Patient	Resistance Protein Immunopositivity	*In vitro* Resistance	Exposure to Chemotherapy
1	P-glycoprotein	sensitive	
2	MRP	resistant and sensitive (mixed)	
3	____	not assessed	
4	Pgp, MRP ,LRP	sensitive	
5	____	resistant	high exposure
6	____	sensitive	
7	P-glycoprotein	resistant	
8	P-glycoprotein	resistant and sensitive (mixed)	
9	LRP	resistant and sensitive (mixed)	
10	Pgp, MRP	resistant	high exposure
11	____	resistant	high exposure

Table 6.3I. Immunopositivity for Pgp, LRP and MRP, *in vitro* resistance and exposure to chemotherapy of bladder cancers. Any positive staining in the bladder cancer sections was present in less than 40% of the total area stained, in any field.

7. DISCUSSION

7.1 ANTHRACYCLINE UPTAKE AND DISTRIBUTION IN SENSITIVE AND MDR CELL LINES

As already mentioned many cells with the MDR phenotype exhibit impaired drug accumulation compared with their sensitive partners. This accumulation defect along with inefficient drug sequestering completely explained the resistance observed in two MDR cell lines[175]. Hence in our bladder and breast cancer cell lines drug accumulation was regarded as an indicator of cellular MDR and was studied along with the intracellular drug sequestration.

Although the MGH-U1/R cells were produced by being grown in increasing concentrations of DOX this was not the drug to which they were most resistant. The differential multidrug resistance of the resistant cell lines to each drug was determined by comparing drug uptake by resistant cells with drug uptake by their sensitive parental cell line for each drug. The difference in drug uptake between MGH-U1 and MGH-U1/R cells were for DOX 5 fold, for EPI 30 fold and for IDA 6-9 fold, showing that the cells were more resistant to EPI when compared to the sensitive cells' EPI uptake (see appendix 4). The MCF-7/R cell line was also raised against DOX but this cell line showed similar levels of resistance to this drug and MTZ, as shown by comparing drug uptake in resistant cells with drug uptake by sensitive cells: MCF-7 cells took up 2 fold more DOX and 2-3 fold more MTZ than MCF-7/R cells. In the original study assessing the cytotoxicity of DOX and EPI on the MGH-U1 and MGH-U1/R cell lines used in this study the largest differential was again observed with EPI[176]. However, other reports state that the largest differential in cellular accumulation between sensitive and resistant lines was seen for DOX, compared to DNR[177], in human small cell lung cancer cell lines and a murine mammary tumour cell line. Although DNR was shown to be a better substrate for energy-dependent efflux than DOX, with DNR efflux being greater than that of DOX even in resistant cells raised against DOX[177]. This has also been shown in a human leukaemia cell line, P388. Drug efflux experiments were performed by i) preloading the cells with drug then observing them in a drug free medium or ii) by allowing the initial accumulation of drug to be performed in an

energy depleted medium then adding an energy substrate (glucose) and again observing drug movement over time[177]. Unlike the MGH-U1/R cell line, the MCF-7/R cell line was not resistant to IDA since these resistant cells took up the same amount of drug as the sensitive cell line (MCF-7) at various low drug concentrations. At best, the MCF-7 cells took up 0.5 fold more IDA than the MCF-7/R cells. This may be due to IDA being a newer, more potent drug which is more lipophilic and has shown enhanced cellular influx[174] compared to the other anthracyclines. However, the fact that the MCF-7/R cell line was less resistant to DOX compared to the MGH-U1/R cell line should also be taken into account. This observation lead us to suggest that the MGH-U1/R cell line was overall more multidrug resistant than the MCF-7/R cell line.

In the experiments described in this thesis, with all three drugs, the length of time and the concentration of drug the cells were incubated in were very important. Too long an incubation period or too high a drug dose would not only result in inconsistent recordings but also damage the cells, in particular the sensitive cell lines, MGH-U1 and MCF-7. This production of inconsistent readings was also true for too short an incubation time or too low a drug dose. At the early incubation times, there was similar drug uptake by counterpart resistant and sensitive cells for all drugs except for IDA uptake by MGH-U1 and MGH-U1/R cell lines. Rapidly achieved (within 15min) high intracellular drug concentrations in both sensitive and resistant cells have been shown in other human cancer cell lines[178]. In an MDR human large cell lung cancer line, the defect in DOX accumulation was not evident until 1h following drug exposure when compared to drug uptake in the sensitive cell line[179]. This is in contrast to a MDR murine mammary cell line where reduced DOX accumulation was evident at earlier time points[180]. In the experiments described here, at low drug concentrations (1, 2 or 5μg/ml for DOX, EPI and MTZ; 0.1,0.5 or 1μg/ml for IDA) there was less difference between drug uptake by resistant cells, when compared to their sensitive partners, than at higher drug concentrations (10, 15 or 20μg/ml for DOX, EPI and MTZ; 2, 5 or 10μg/ml for IDA). These last points could imply that the effluxing of drug by Pgp (the main resistance protein detected in the MGH-U1/R and MCF-7/R cell lines) occurred only after the drug has been in the cells for a certain length of time, of around 20 minutes, and only at a high enough dose. Therefore there may be a critical time

factor and level of intracellular drug needed for the efflux proteins to work in resistant cells. Hence the drug dose and incubation time were kept at their optimums for the individual drugs and the cell lines. Although these factors, along with cell confluence, were identical for each experimental repeat there were still variations in cellular drug uptake between the runs. This may be due to a natural difference of drug uptake between cells of the same cell line or external influences such as the weather (the cells had to be transported via the outside to the ICRF, therefore, part of the incubation took place at 25°C).

Incubating the cells in suspension with the drug also led to wide variations between identical experiments. The resistant cells tended to take up more drug in suspension, often taking up similar amounts of drug to the sensitive cells, than equivalent cells incubated with drug while attached to flasks. This might have occurred due to the cells rounding up in suspension producing a larger surface area for drug influx, also drug was present all around the cells. When the cells were in a layer attached to the plastic and surrounded by other cells only one surface was likely to be available for drug influx. Also they were in a more realistic situation as in the body epithelial cells are in compact layers surrounded by and attached to other cells. This latter method of drug incubation, also lead to healthier cells during the incubation period which in turn led to more consistent repeatable results.

The state of confluence of the cells in each experiment affected drug uptake in different ways depending on how the cells were incubated with the drug and what type of cells were used. Cells incubated with drug in suspension took up drug indirectly proportional to the number of cells present, so the higher the number of cells the less drug each individual contained. On the other hand cells, incubated with drug when attached to a surface and each other, took up more drug when supra-confluent compared to sub- and confluent cells. This was observed in both MGH-U1 and MCF-7 cell lines. In MCF-7 cells, a change in intracellular DOX and MTZ localisation patterns occurred when cells were supra-confluent compared to sub- and confluent cells. This change was not observed in MGH-U1 cells nor in MCF-7 cells with IDA. The reason that no difference was observed in the intracellular pattern of IDA may be to do with the potency of this drug: that is, the metabolite of this drug is known to accumulate in high levels in both sensitive and drug resistant cells due to enhanced influx compared to other anthracyclines[175].

This is supported by our results where the MCF-7/R cells took up as much IDA as their sensitive parental cell line.

Whether cells in culture are in a proliferative or quiescent state tends to be dependent on environmental factors, such as space and serum deprivation. The percentage of cells in different phases of the cell cycle was also dependent upon the state of confluence of cells. Sub-confluent cells were still dividing and, therefore, going through the stages of the cell cycle. These include mitosis and interphase which consists of S phase (DNA synthesis), G_1 and G_2 (G = gaps). When conditions for cell division are not met, a healthy cell will almost always be delayed in the G_1 phase of the cell cycle[131]. When circumstances change so as to favour cell division, such as more room or additional serum, the cell resumes its progress through the cell cycle[131]. Supra-confluent cells no longer had any room left to divide and were probably deprived of serum and its growth factors. Therefore, these cells were likely to be impeded in the G_1 phase of the cell cycle. If this starvation of growth factors continued halting division of the cells, they would be arrested in a quiescent or G_0 state. A G_0 cell, besides being quiescent with respect to the chromosome cycle, generally has an altered balance of protein synthesis and degradation compared with a proliferative cell. Anthracyclines are able to insert themselves into membranes of any phospholipid composition[118] and therefore the membrane of the cells are permeable to them. A non dividing cell, with a static membrane may therefore be more susceptible to passive drug diffusion[118] allowing increased drug uptake. Furthermore, as the anthracyclines main cellular target is DNA, dividing cells may attract drug to the nuclei whilst non-dividing cells (i.e. the supra-confluent ones) contain the majority of drug in the cytoplasm. There may also be some factor missing or altered in quiescent cells stopping drug from entering the nucleus.

The observed increased drug uptake in supra-confluent cells compared to confluent and sub-confluent cells contradicts the theory of confluence dependent resistance (CDR), which is a mechanism by which tumour cells resist anthracyclines[181]. CDR causes a lowering of drug uptake in cancer cells and is thought to be mediated by cell-cell contact which increases the fraction of non-proliferating resistant cells in a post confluence monolayer[181]. In the majority of these experiments there appeared to be increased drug uptake by supra-confluent

cells compared to either the confluent or sub-confluent cells. The main difference between confluent or sub-confluent cells compared with supra-confluent cells appeared to be the change in intracellular drug distribution pattern clearly shown by MCF-7 cells and DOX. DOX uptake in sub- and confluent cells was as expected with predominantly nuclear localisation of the drug, whilst supra-confluent cells showed mainly cytoplasmic DOX localisation with very little entering the nuclei. This difference in intracellular DOX localisation due to the state of confluence of the cells was also observed in the MGH-U1 cell line. A change in the pattern of intracellular drug distribution in supra-confluent compared to sub- and confluent cells was also shown by MCF-7 cells and MTZ. Increased MTZ was taken up by supra-confluent cells, compared to confluent / sub-confluent cells, however, MTZ in these cells was mainly located between the cells rather than entering the cytoplasm as it did in confluent / sub-confluent MCF-7 cells. This redistribution of drug within supra-confluent cells may be connected to resistance by stopping the drug reaching its main site of action, the nucleus. It also needs to be considered that the drug is not actually entering some of these supra-confluent cells but building up between the cells which could lead to lowered cellular toxicity. These factors led to the decision that all experiments were performed when the cells had grown to a similar stage of confluence, around 90% confluence.

In some of the intracellular drug distribution experiments there was a difference in drug uptake between individual cells in a single experiment. This was particularly found in the sensitive cell lines where individual cells took up different amounts of drug. The MCF-7 cell line can be separated into several different sub-populations with different characteristics, including rate of growth and DNA synthesis[166]. The MGH-U1 cell line is also multiclonal. The non-uniform cellular drug uptake observed in these two cell lines may be due to this heterogeneity. Another interpretation is connected to the cell cycle. Cells which took up more drug may have been in a different phase of the cycle, such as G_1, compared to those cells which took up less drug, which would be in S-phase or undergoing mitosis. The former explanation is most likely as this phenomenon was not really observed in resistant cell lines, at a similar stage of confluence. Also the resistant cells were grown as clones selectively derived from the parental cell lines.

In this report confocal microscopy was employed to investigate the

intracellular retention of anthracyclines in two drug sensitive (MGH-U1 and MCF-7) and two corresponding multidrug resistant (MGH-U1/R and MCF-7/R) cell lines. Confocal microscopy is useful for measuring the intracellular accumulation of fluorescent drugs, such as the anthracyclines. It is a non-invasive technique which is able to delineate the subcellular distribution pattern of the drug and does not require high cell numbers. Furthermore, the anthracyclines appeared to be relatively resistant to photobleaching by the laser compared to other compounds[182].

In the following paragraph the individual drugs will be discussed separately for both sensitive and resistant cell lines.

From the results, the pattern of intracellular DOX localisation did not appear to be dependent on the type of cell line, *i.e.* bladder or breast cells but rather on whether the cell line was resistant or sensitive. Although some minor differences in intracellular DOX localisation occurred, the overall patterns of DOX distribution were similar between bladder and breast cancer cells. Doxorubicin in both sensitive cell lines displayed predominantly nuclear localisation, especially at the higher drug concentration where there was very little DOX in the cytoplasm. The intracellular drug distribution was easier to discern at 20μg/ml. At this dose, the MGH-U1 cells had more DOX cytoplasmic fluorescence compared to the MCF-7 cells but this could be due to the different growth arrangements of the two cell lines. The MGH-U1 cells grew spread out over the petri dishes showing more visible cytoplasm than the MCF-7 cells which tended to grow as compact colonies with less cytoplasm visible. These DOX localisation patterns seen in the sensitive cells were reported by other researches in different sensitive cell lines, including human large cell lung cancer cell line and a uterine sarcoma cell line. In these cell lines there was intense fluorescence in the nuclei and a progressive decrease in fluorescence in the perinuclear area and the cytoplasm[182, 183]. Distinct spots of fluorescence were reported to be visible within the nuclei, presumed to be chromosomal DNA. The nuclear envelope was easily discernible. Small regions of less intense fluorescence were also observed within the cytoplasm and believed to be consistent with the localisation of drug in vesicles[182]. These bright spots of fluorescence in the nuclei were present in MCF-7 cells but could not be seen in the MGH-U1 cells. However, spots of fluorescence were observed in the cytoplasm of MGH-U1 cells but mainly in the perinuclear region. For both cell lines, the plasma

membrane of the cells was barely discernible.

In the resistant cells, DOX was distributed within the cytoplasm with lesser amounts entering the nucleus. This pattern of intracellular DOX localisation led to the appearance of nuclear holes particularly visible in the MGH-U1/R cells. Both resistant cells lines showed an area of increased DOX staining in the perinuclear region compared to its uptake in the rest of the cytoplasm. The MCF-7/R cells had particularly bright spots of perinuclear fluorescence whereas the fluorescence in the MGH-U1/R cells was less intense and more diffuse encircling the nuclei. Some sensitive and resistant cell lines have been reported as having similar patterns of intracellular DOX distribution but with the resistant cells having less fluorescence[183]. At the lower DOX dose of 10μg/ml, the pattern of drug uptake between sensitive and resistant cells, in both cell lines, did appear similar. This could be due to the very low fluorescent intensity of the resistant cells; which would not allow a clear picture of nuclear holes if such existed. Other resistant cell lines had a different DOX localisation pattern compared to their parental cell lines[182, 184], similar to those observed in this study at the higher drug dose. Hindenburg *et al* noted that their parental human myeloid cells only distributed the drug to the nuclei at concentrations lethal to the sensitive cells and that these cells and their resistant counterparts had similar patterns of drug distribution when exposed to lower concentrations of the drug[69].

Epirubicin produced similar patterns of intracellular localisation as DOX, with the majority of the drug located in the nuclei of the MGH-U1 cells and the cytoplasm of MGH-U1/R cells. The resistant cells showed nuclear holes where EPI had not entered the nuclei, with bright spots of fluorescence in the perinuclear region. These patterns of EPI uptake by resistant and sensitive cells were observed at both 10 and 20μg/ml drug concentrations. The two drugs, DOX and EPI are very similar in structure and mechanism of cytotoxicity. They are very closely related anthracyclines with EPI being the stereoisomer of DOX and both are related to DNR, making comparisons of the intracellular distributions of these drugs feasible.

In the majority of sensitive cell lines, such as human leukaemia and human lung cancer, nuclear fluorescence has been reported, following exposure to DOX[29, 182, 183, 185]. Not all the reports mentioned the bright spots of intense fluorescence noted in this study but those which do suggest that it was chromosomal staining[182].

This fits in with the drugs exerting their effect on the DNA and causing compaction of the chromatin in the nucleus[118].

Generally, drug uptake by resistant cells has been shown to be very different compared to sensitive cells. The pattern of drug distribution tended to be cytoplasmic with little or no nuclear fluorescence. The cytoplasmic fluorescence may be present as distinct regions of punctate fluorescence[182] or as diffuse fluorescence with intense areas of perinuclear fluorescence (observed in human myeloid leukaemia and human large cell lung cancer cell lines)[29, 182] or with both, as in KB carcinoma cells[96]. The spots of fluorescence observed in the cytoplasm may be vesicles[182] involved in drug transport or lysosomes[96] which will break the drug down.

Unlike the two drugs above, the intracellular distribution of MTZ and IDA was mainly cytoplasmic with both sensitive and resistant cell lines displaying nuclear holes. This difference between DOX and MTZ uptake in drug sensitive cells has been observed by others in SV-40 transformed fibroblasts and murine cell lines[186]. Whereas DOX displayed intense staining within the nucleus, nuclear membrane and perinuclear regions, MTZ was primarily located in cytoplasmic inclusions with overall cytoplasmic staining. The nuclear membrane and nucleoli were observed to have attracted MTZ in drug sensitive transformed human fibroblasts[186]. The pattern of MTZ intracellular distribution in MCF-7 cells was mainly in cytoplasmic inclusions with additional perinuclear and nuclear membrane fluorescence in some of the cells present. Although nuclear fluorescence was low, compared with the cytoplasm and the rings of perinuclear fluorescence, some cells contained visibly bright nucleoli. This is in contrast to the results achieved using the CCD camera, where MTZ in MGH-U1 cells showed a different pattern of staining. Here the sensitive cells showed predominantly nuclear fluorescence with heavier 'spots' of fluorescence localised within the nuclei. By comparing the phase-contrast with the fluorescent photographs, these high nuclear 'spots' of fluorescence corresponded to the positioning of the nucleoli. This preferential location of fluorescence within nucleolar-like structures perhaps reflects the proposed base pair preference (G-C) of the intercalator (MTZ)[187] and the GC-rich nature of nucleolar DNA[186]. The resistant cells showed similar low levels of cytoplasmic fluorescence and nuclear holes, compared to the sensitive cells, but

small bright spots of fluorescence which were located in the cytoplasm particularly in the perinuclear region. This punctate pattern of cytoplasmic staining was recorded for both the MCF-7/R and MGH-U1/R cell lines, using the confocal microscope and the CCD camera respectively. The nature of these cytoplasmic structures corresponded in size and location to the Golgi and to lysosomes[96] as seen with DOX and EPI localisation in these cell lines.

All four cell lines showed similar patterns of intracellular IDA localisation with very little nuclear distribution of the drug but with most of the drug staying in the cytoplasm. The cytoplasmic fluorescence in both resistant cell lines was more granular than that seen in the sensitive cells which may indicate vesicles with drug. In the MCF-7, MCF-7/R and MGH-U1 cell lines, some of the cells displayed nuclear membrane staining. This staining pattern of the perinuclear and nuclear membrane regions may indicate drug sequestration. Other studies have confirmed that the MGH-U1 and MGH-U1/R cell lines show similar patterns of IDA intracellular localisation. Both the sensitive and resistant bladder cancer cell lines displayed little nuclear fluorescence with the IDA mainly localised within the perinuclear region of the cytoplasm[188].

It is a generally accepted that MDR leads to a lowering of intracellular drug within resistant cells[29, 69, 96, 182, 183, 185,]. This is often accompanied by a change in the intracellular distribution of drug within resistant cells when compared to their sensitive counterparts, as demonstrated in human large cell lung cancer and a uterine sarcoma[182, 183, 185, 69]. These altered drug distributions are believed to be a general phenomenon associated with MDR cell lines regardless of their Pgp status[29, 182]. Although lowered drug accumulation was observed in our resistant cells for all drugs studied, changes in their intracellular drug distributions did not always occur. Whereas DOX, EPI and MTZ all showed different patterns of intracellular localisation between sensitive and resistant cells, IDA showed similar patterns of drug distribution in all four cell lines.

The perinuclear fluorescence of DOX, EPI and MTZ often observed in resistant cells is believed to correspond to the position of the Golgi apparatus[96] and be involved in trafficking the drug away from the nucleus as drug located in the nucleus of resistant cells is rapidly removed[185]. Resistant cells were loaded with drug (DNR) in an energy depleted environment. These cells were then added to

media containing glucose and the movement of drug away from the nuclei, across and out of the cells observed[185]. Other areas of bright fluorescence observed in the cytoplasm of resistant cell are believed to correspond anatomically to vesicles[182] and/or lysosomes[96]. It may be that all three of these subcellular organelles are involved at different stages of drug removal from the resistant cells. The drug passing from the Golgi to vesicles, for exocytosis from the cell, and to lysosomes for destruction. These routes of drug removal could work separately or in conjunction with the protein efflux pumps, in particular Pgp, present in resistant cells. Intracellular pathways for trafficking substances around and out of the cell have been described and hypothesised to be involved in MDR. The most generally accepted hypothesis for the transport of drug out of MDR cells is via Pgp. The latter is an ATP driven efflux pump which either transports drug out of the cell or works as a 'flippase' to extrude chemotherapeutic drugs from the plasma membrane bilayer of MDR cells[12]. This protein is also located on the luminal side of the Golgi stack membranes, as demonstrated in a human carcinoma cell line KB 3-1[28]. This would account for drug removal from the nucleus into the perinuclear region where high drug levels are often observed in MDR cells, probably located in the Golgi. However, as the other subcellular structures in which the drugs accumulate in, *i.e.* endocytotic vesicles and lysosomes, do not contain Pgp[28] another mechanism must be involved. The Golgi, lysosomes and endocytotic vesicles are very acidic cell compartments and this pH concentration gradient may additionally cause the cationic drugs to accumulate in them[96]. Intracellular trafficking between the Golgi and endocytotic vesicles has been demonstrated using fluorescent lipids[30]. Gervasoni hypothesises that a perinuclear structure termed the prelysosomal sorting compartment (PLC) is where the chemotherapeutic drug first localises and is then redistributed into organelles which receive lipid vesicles, such as lysosomes and the plasma membrane[30]. Once in the plasma membranes the drug would be effluxed out of the cell. In support of this drug transportation theory, increased membrane traffic (recycling) from intracytoplasmic compartments to the plasma membrane has been shown to occur in resistant cells compared to sensitive cells, in Ehrlich ascites tumour cells[32]. Thus the resistant cells remove drug so that a high cytoplasmic concentration is never achieved and nuclear accumulation cannot occur[96]. This hypothesis appears to be particularly applicable for MCF-7/R cells

with MTZ which had a very punctate pattern of intracellular drug localisation. This could indicate vesicular transport of drug away from the nucleus by binding to cytoplasmic organelles such as the Golgi or vesicles.

This drug sequestration away from the nucleus into the perinuclear region was not only observed in resistant cells but also in sensitive cells for the drugs MTZ and IDA. There was observed maintenance of highly fluorescent cytoplasmic inclusions in both MCF-7 and MCF-7/R cells which may indicate sequestration of MTZ into a drug pool. Smith *et al* have demonstrated that mitotic transformed human fibroblast cells showed a reduced level of cytoplasmic MTZ fluorescence compared with the bright fluorescence of the condensed chromatin which was homogeneously stained. Hence it is possible that the sequestered cytoplasmic MTZ pool was released upon entry into mitosis resulting in efficient cell kill due to unimpeded access to chromatin[186] and peak levels of target enzyme DNA topoII[189]. In the case of MDR cells, any sequestered drug would be rapidly removed from the cell resulting in progression through mitosis and a reduced drug burden for daughter cells[186]. The intracellular IDA localisation patterns observed in all, four cell lines may also represent drug sequestration. The IDA staying in the perinuclear and nuclear membrane region until the cells undergo mitosis[186] when IDA will enter the nuclei and intercalate with the DNA. This nuclear membrane binding was not observed in MGH-U1/R cells which were shown by flow cytometry to be resistant to IDA, unlike the MCF-7/R cell line. The noted lower resistance factor of IDA compared to that of other anthracyclines was not due to the inability of the Pgp to export IDA from the cells[190].

Also to be taken into account is whether any other resistance proteins were present and functional within the resistant cells, such as LRP and MRP. LRP is believed to be the major human vault protein[80] and is associated with vesicles, being located primarily within the cytoplasm of cells in a coarsely granular fashion[79]. The vault proteins are similar to the structure proposed for the transporter of the nuclear pore complex and have been located in association with the nuclear membrane[82]. This evidence of subcellular position leads to the theory that LRP / vaults mediate drug resistance through vesicular and nucleocytoplasmic transport[81, 82] of drugs[9]. In the MGH-U1/R and MCF-7/R cell lines, LRP expression is very low being present in less than 5% of the cells. However, it could

still be functional as a drug transport mechanism in these resistant cells to contribute to the observed intracellular distribution and lowered drug accumulation. MRP is primarily located in the endoplasmic reticulum with lower levels in the plasma membranes of resistant cells[64]. This protein may participate directly in the active transport of drugs into subcellular organelles or influence drug distribution indirectly, by altering cytoplasmic or intraorganelle pH *via* ion transport[66]. However, no MRP was found to be located in any populations of our resistant cells. (Also see Introduction 1.1.3 and Discussion 7.4).

To conclude this part of the discussion, comparisons of anthracycline uptake as recorded by flow cytometry and confocal microscopy are highlighted. Different results were gained regarding IDA uptake using the flow cytometer or the confocal microscope. Using the flow cytometer IDA uptake by MCF-7 and MCF-7/R cells were very similar but this was not shown by the confocal microscope where the sensitive cells appeared to take up more IDA than the resistant cells. However, the IDA dose for the confocal was 10μg/ml, the highest concentration used in the flow experiments where it produced the largest difference in uptake by resistant and sensitive cells. Also the semi-quantitation performed by the confocal microscope did not show large differences in IDA uptake between the two cell lines. The discrepancies between flow cytometry and confocal microscopy could have occurred for two reasons: firstly semi-quantitation on the confocal is performed in one plane, flow cytometry measures the amount of drug in 3-dimensional cells. Secondly, for the flow cytometry experiments, the cells were transported to the ICRF and had to be trypsinised off the flasks, thus had a harsher treatment than those viewed under the confocal microscope.

7.2. GLA AS A DIRECT CYTOTOXIC AGENT

The extent of an EFA's cytotoxic effects, such as GLA, are influenced by the source and concentration of serum and depend upon cell density, fatty acid concentration, the type of cell and the particular fatty acid[133]. The albumin contained in serum binds the EFA reducing its cytotoxicity. Several reports have taken into account the inhibitory effects of serum on the toxicity of EFA by using

serum / albumin free medium[146, 147]. However, Begin *et al* found that the percentage of dead cells, due to FA toxicity, was maximal when the cultures were challenged in the presence of 10% FCS. The extent of cytotoxic effects decreased with increasing serum concentrations[133]. This report also indicated that the extent of induced killing of tumour cells decreased with cell density, depending on cell line and fatty acid. For example, lung cancer cells lost their sensitivity to AA, LA and GLA but not EPA (all at 20μg/ml) with increasing cell density. Hence, all our experiments were carried out using the same cell seeding density and 10% FCS.

EFA's are selectively cytotoxic to human cancer cells compared to normal human cells *in vitro*. The most selective cytotoxic effects were obtained from fatty acids containing 3, 4, or 5 double bonds, including GLA[133, 136]. The cytotoxicity of GLA has also been demonstrated in animal models where evening primrose oil, which contains a high percentage of GLA, suppressed tumour growth by 51% of the mean control weight. This study also showed that fish oil, containing high levels of n = 3 fatty acids, limited tumour growth compared to the control[129]. Other reports suggest that n=6 fatty acids stimulate cancer cell growth[146, 147] and that only n = 3 inhibit tumour cell growth *in vitro*[145, 155]. LA (n = 6) stimulated proliferation of human breast cancer cells whereas DHA (n = 3) inhibited cell growth[147]. The results from our cytotoxicity assays confirmed that n = 6 fatty acids were cytotoxic to human breast cancer cells above certain threshold levels. All doses of GLA below and including 20μg/ml incubated with the cells for up to 48h showed no cytotoxic effects on any of the four cell lines. However, there may be cytostatic effects exerted on the cell at longer times of incorporation, such as inhibition of mitosis. As all experiments involving the incorporation of GLA were performed immediately, after 24 or 48 hours incorporation, the longer term effects of GLA were not considered. Evaluating PUFA-induced toxic effects on cells by methods of comparing total amounts of cells after only 3 days may underestimate the differentials between normal and tumour cells. Small changes in the conditions influencing the extent of cytotoxicity may either result in total loss of selectivity or complete inhibition of selectivity[133], but this consideration was not necessary for our work. The results showed that cell death in all cell lines occurred after 72h at all GLA doses and after 24h at the high doses of GLA 30μg/ml and above.

The exact mechanism of EFA cytotoxicity is not fully understood but

various theories have been suggested. It is known that transformed cells cannot produce the prostaglandin PGE1 due to loss of the delta-6-saturase enzyme. This loss may be a critical change in malignancy in many forms of cancer. Malignant prostatic tissue had reduced concentrations of desaturated metabolites of LA[144] due to this reduced activity of delta-6-saturase, which converts LA into GLA[142, 143] and then into various PGs. Thus, incubating cancer cells with additional GLA was believed to lead to restoration of PGE1 synthesis by-passing the blocked delta-6-saturase, aiding normalisation of the malignant cells and reversing cancer growth[129, 142]. However, fatty acid desaturase activity was reported to be independent of cell division in malignant tissue and part of a single, more fundamental change in cell structure and function[143]. The decreased level of LA metabolites in malignant tissues, compared to normal or benign tissues, may be due to increased cellular metabolism, *via* the lipoxygenase and cyclooxygenase pathways to produce higher concentrations of eicosanoids (including PGE1), rather than an impairment in desaturase activity *in situ*[144].

The contribution of lipid peroxidation to the killing of human cancer cells by EFAs has been examined. PUFAs and EFAs containing several double bonds are unstable molecules and are readily oxidised by non-specific and specific lipoxygenase and cyclooxygenase enzyme systems to yield free radical lipids and peroxides which are toxic to cells[129]. It was found that the cytotoxic potential varied with the ability of the EFAs to stimulate production of superoxide radicals, GLA being highly cytotoxic. The addition of GLA to human breast cancer cells *in vitro* was found to stimulate the initiation of its own peroxidation by increasing the amount of free radicals and by increasing the substrate available for lipid peroxidation. Consequently, cancer cells were thought to be killed as a result of an elevation of toxic peroxidation products generated by the PUFAs[136]. This theory is supported by the detection of peroxide degradation products and the ability of antioxidants, such as Vitamin E, which scavenge free radicals to block the PUFAs cytotoxic effects[129, 136]. The effect of GLA on human neuroblastoma cells in cultures was inhibited by antioxidants and associated with superoxide lipid peroxidation[136]. However, whether the structural change in the cancer cell membranes were responsible for the change in biological properties or whether the fatty acids simply acted as substrates for other intermediates to exert the effect is

unknown[129]. The cytotoxic effect may be due to an oxidative process other than lipid peroxidation or one specific metabolite formed by lipid peroxidation. Also, the *in vivo* effects of PUFAs are likely to be more complex and influenced by other factors[139].

7.3. GLA AS AN INDIRECT CYTOTOXIC AGENT

Appreciable changes in cellular lipid composition after the addition of fatty acids have been observed *in vivo*[153] and *in vitro*, detected using gas chromatography[153, 157] and electron spin resonance probes[154]. Lipid modification of the cells produced by diet or supplementation of the medium were associated with changes in the plasma membrane fatty acid composition. There was an increase, almost 2 fold, in the polyenoic (that is the polyunsaturated) fatty acids (with more than one double carbon bond) in the phospholipid fraction of the plasma membrane. This increase was shown in murine leukaemic cells, taken from mice fed a diet high in polyunsaturated sunflower oil [154]. However, there was no change in the cholesterol content, or phospholipid head composition or fatty acid chain length, or protein content[140, 154]. The cells appeared to compensate for the increase in membrane polyenoic acids by altering the saturated acid content of their phopholipids[153, 154]. Membrane fluidity is determined by the degree of unsaturation of the fatty acid residues in the component phospholipids and by the cholesterol content. The fluidity of the membrane increased with the degree of unsaturation of the component fatty acids[164]. Therefore, cells enriched with polyunsaturated fatty acids, in the phospholipid component of the membranes, had increased fluidity of their membranes. This would explain the changes observed in membrane physical properties and certain cellular functions, including carrier mediated transport, receptor binding[140] and increased diffusion of drugs entering the cell by passive diffusion, such as DOX and MTZ[157, 160, 161].

Modification of cellular sensitivity by EFA incorporation should enhance the toxic action of the chemotherapeutic agents by increased drug uptake. Hence, it has been suggested that pre-treatment of the cells with PUFAs would lead to increased cancer cell kill by increased cytotoxic drug uptake. This increased cell

death could be due to either increased drug uptake, with the PUFA changing the membrane fluidity, or to the additive effects of the cytotoxicity of the PUFA and the drug.

GLA was shown to incorporate into our cell lines, presumably into the plasma membrane, using radioactive LiGLA, the uptake of which could be followed over time (section 4.1). This incorporation should have, in turn led to an increase in membrane fluidity and increased drug uptake. However, there was no increase in cellular uptake of the chemotherapeutic agents studied using flow cytometry. Although many other studies have described increased cellular uptake of various cytotoxic drugs due to prior incubation of the cells with an EFA[157-162], including GLA[159] on MCF-7 cells increasing the uptake of DOX[162]. The systems used were *in vitro* cultures of mammalian cancer cells, such as human lung cancer, incubated with an EFA for 24-48h and then exposed to a cytotoxic drug, such as DOX[157,158,160-162]. However, none of these reports used flow cytometry but various types of cell viability assays or spectrophotometry.

In our experiments, the use of GLA to enhance the cytotoxic action of anthracyclines by increasing drug uptake was investigated using concentrations of GLA which were non-cytotoxic to the cells. Although no increased drug uptake was recorded for any drug in any of the four cell lines using flow cytometry (section 5.1), when confocal microscopy was employed (section 5.2) one drug appeared to have increased uptake in the resistant cell lines due to GLA incorporation.

For DOX, MTZ and EPI, no significant change in drug uptake was visible in any of the cell lines due to GLA treatment. Although from semi-quantitation performed using the confocal microscope, there was a decrease in DOX uptake in MGH-U1/R cells incubated with GLA compared to non-treated MGH-U1/R cells, this was non-significant. An enhancement in IDA uptake was observed in both resistant cell lines after 24h incubation with GLA but this was not accompanied with a change in intracellular IDA distribution. The GLA-treated MGH-U1/R and MCF-7/R cell lines had significantly increased IDA uptake compared to IDA uptake in these untreated cells. The GLA treated sensitive cell lines showed no difference in IDA uptake or intracellular localisation compared to the untreated cells. Why equivalent experiments using flow cytometry and confocal microscopy

should record differing results is uncertain. Of the two techniques flow cytometry may be more accurate at recording the amount of intracellular drug as it records amount of drug fluorescence per cell whereas the confocal microscope can only semi-quantitate the amount of drug per cell. However, for flow cytometry the cells have to be trypsinised from the flasks after drug incubation prior to being put through the machine which is an unnecessary step for the confocal microscope. This trypsination may have some effect on the cells causing a change in the intracellular IDA content. For the other drugs, there was no change in drug uptake, recorded by either method. The increase in IDA uptake in resistant cells after GLA incorporation actually correlates to results gained from IDA uptake experiments using flow cytometry with the cells in suspension (section 3.2.1). This may be due to the increased lipophilicity of IDA compared to the other anthracyclines. The slightest change in membrane fluidity might result in an observable increase in IDA uptake. Although this increase in drug uptake was arithmetically significant it is unsure whether it is biologically significant. Preliminary cytotoxicity assays were performed to ascertain if using GLA and an anthracycline led to increased cell death. These showed a slight decrease in cellular residual viable biomass due to the use of both agents compared to GLA alone.

It was believed that this enhancement of drug uptake due to membrane fluidity modification by cellular PUFA incorporation may not only increase drug uptake but could be used to modulate multidrug resistance in cancer cells, both on their own as cytotoxic agents and in conjunction with anthracycline therapy. Evidence for the former is that human multidrug resistant cancer cells were more sensitive to EFAs, such as GLA, than their non-MDR counterparts[163]. This was also found to be true for our MCF-7/R cell line. The latter modulation of MDR with EFAs followed by treatment with anthracyclines was done using sub-lethal doses of EFAs. A change in the resistance due to GLA incorporation was observed in the MGH-U1/R and MCF-7/R cell lines, as mentioned above. This change was also visible after GLA treatment using the same cell lines but with MTZ and the CCD camera (section 3.3.1). The difference here was that the GLA used in these experiments was the di-ethyl ester rather than the LiGLA salt used clinically and in the rest of our experiments.

Apart from the change in membrane fluidity, the effect of long chain

PUFAs may predispose the cell to injury and could be attributed to an increased oxidative potential[158]. Although it is generally believed that anthracyclines, such as DOX, exert their cytotoxic effects by binding to DNA, several observations suggest that it may also have a direct effect on cell membranes[157]. Evidence indicates that DOX need not enter the cell in order to exert its cytotoxic effect[122] . This was demonstrated by covalently attaching Adriamycin to large, insoluble polymeric beads which stopped the drug penetrating into the cytoplasm or nucleus of the cell. This immobilised Adriamycin reduced the survival of murine leukaemia cells, the polymeric beads being non-cytotoxic. Although all membrane binding sites of this drug have not been identified, binding to spectrin[191] and cardiolipin has been identified[192]. This latter substance is of interest as an increased cardiolipin content in membranes appears to be a shared characteristic of malignant cells and cardiac mitochondria leading to speculation that this is why anthracyclines cause damage to cardiac tissue[192]. Hence, an explanation for increased cellular sensitivity to DOX may be that incorporation of large amounts of EFA into the membrane alters the interaction between drug and a critical membrane target[157] increasing drug effect at the membrane level. The insertion of DOX into the cells membrane would also increase membrane fluidity[118] self potentiating the enhanced passive diffusion of drug into the cell. Anthracyclines have the ability to trigger the formation of free radicals. The drugs are reduced by enzymes to semiquinones which in turn reduce molecular oxygen to the superoxide ion[123]. DOX stimulated superoxide formation is both exo- and endo-cellular with both playing a role in the ability of DOX to kill human cancer cells, including the MCF-7 cell line[156]. This combined oxidative potential of the drug and the fatty acid may in part explain the increased cell death observed in cells treated with EFAs prior to cytotoxic drugs. This suggests that there is no modulation of drug uptake in either drug sensitive or resistant cells due to EFAs treatment, and that the effect observed was due to additive toxicity[164]. This would fit in with our results that at sub-lethal doses of GLA no increase in drug uptake or modulation of resistance was observed, except for IDA.

For DOX, EPI and IDA there was no change in the intracellular drug distribution patterns as a result of GLA treatment in any of the cell lines. This was also true for the MCF-7 cell line and MTZ but not for the MCF-7/R cell line with this drug. There was a change in the intracellular MTZ localisation pattern in GLA

treated MCF-7/R cells compared to untreated cells. This was observed as an increase in the amount of nuclear fluorescence but there was no overall increase in MTZ uptake. MTZ is believed to be sequestered in cytoplasmic pools of drug so it could be that the GLA releases this sequestering. GLA may also affect the nuclear membrane allowing MTZ to enter the nucleus.

Another effect of EFA treatment of cancer cells is the ability to inhibit both motility and invasiveness, shown on human colon cancer cells using GLA. This may occur due to modification of the cell-surface adhesion molecules[193]. Treatment of cells with GLA for 24h leads to an increased expression of E-cadherin in lung, colon, breast, melanoma and liver cancer cells, but not in fibroblasts. The increased expression of E-cadherin was correlated with reduced *in vitro* invasion and increased cellular aggregation, indicating that the increased E-cadherin expression induced by GLA was biologically active. The up-regulation of E-cadherin expression in human cancer cells may contribute to the anticancer properties of GLA[194].

Whether the enhanced cytotoxicity is due to increased drug uptake alone or the additive effects of drug and EFA on the cell is unknown. Many of the reports stating increased cell death are unclear on whether the PUFA used was at concentrations which were directly cytotoxic. However, whatever the mechanism, the results are still the same with increased cancer cell death. This still makes the clinical use of EFAs beneficial but at doses where the fatty acids are themselves cytotoxic. This increased cell death although not modulating resistance could still improve cell death in these cancers, for as yet there are no reports of tumours resistant to the cytotoxic effects of the EFAs.

As mentioned before, the use of EFAs *in vivo* may present problems arising from trying to target the fatty acid to the tumour cells. These include the binding of the FA to blood albumin which may be overcome by complexing the FA to albumin prior to addition[146] or introducing the FA directly to the malignant tissue. The best results have been achieved where the tumours can be in direct contact with the EFA, such as the bathing the tumour bed after surgical removal or tumours in more accessible places *e.g.* the bladder. Clinical trials are already in place for such use of EFAs and these would provide a better answer to the desirability of using these agents successfully *in vivo*.

7.4. RESISTANCE PROTEINS WITHIN THE CELL LINES

The MGH-U1/R cells produced and expressed the membrane efflux pump, Pgp, unlike their sensitive counterpart which did not stain for the protein. This indicates that one of the mechanism for MDR in these resistant cells was by Pgp removing the drug from the cells. This mechanism ties in with the lowered drug uptake observed, for all drugs studied in MGH-U1/R cells compared to MGH-U1 cells. MCF-7/R cells were shown to contain Pgp but not to the same magnitude as MGH-U1/R cells. This would fit with the MDR bladder cancer cell line being more resistant to drug uptake (compared to its sensitive partner) compared to the breast cancer cell lines.

Pgp has been found on many MDR cancer cell lines from different histological backgrounds, including breast[55], bladder and colon[56] and was first described in Chinese Hamster Ovary cells[4]. This drug transporter has been located, using immunopathological studies, on a wide variety of human tumours, most commonly in colon, renal and adrenal carcinomas[40]. Other tumours, such as breast[47] and bladder[48], tend to express Pgp during a course of chemotherapy due to acquired MDR[2]. Pgp or the gene encoding for the protein, MDR1, has been found in normal tissues, including liver, epithelial cells of the kidney and the mucosal surface of the colon and jejunum[37-39]. Hence, it is mainly found in specialised cells with excretory or secretary functions. This suggests that it is used as an extrusion mechanism transporting substances out of the cells and into luminal cavities[39, 41].

Pgp has been shown to be capable of both reducing drug influx and increasing drug efflux[2]. A proposed mechanism of outward transport of drugs by Pgp involves this transporter molecule forming a channel for drug transport. The main function of the multidrug transporter is to detect drug within the plasma membrane and extrude it, *via* a channel-like structure, from the cell in an energy-dependent fashion[2]. Increased membrane trafficking from intracellular compartments to the plasma membrane occurs more in resistant cells compared to sensitive cells. This increased trafficking may be connected with the increased active drug extrusion from resistant cells[32]. As well as being located on the plasma

membrane Pgp is present on intracellular membranes, such as the Golgi stacks but not in vesicles or lysosomes[28]. This means drug could be pumped into the Golgi for transport to the plasma membrane, or lysosomes, by vesicles which are known to be involved in intracellular trafficking. The extrusion of the drug in vesicles may also help explain the very high background fluorescence observed in the confocal experiments using DOX. The use of vesicles suggests the drug would not dissipate into the medium but most likely stay adhered to the plastic of the petri-dish rather than free drug.

After incubating the cells with GLA there was no change in the membranous staining of Pgp in either MGH-U1/R or MCF-7/R cells. However, the rounding up of MGH-U1/R cells after incubation with GLA made the pattern of staining appear different. Due to this change in cellular shape the membrane was more condensed (rounder) and there appeared heavier membrane antibody staining encroaching in to the cytoplasm. As there was no change in the positioning or amount of Pgp in these MDR cells after incubation with GLA any increase in cellular drug uptake must be due to a different mechanism of the EFA.

It has been hypothesised that a general Pgp-independent type of defence of mammalian cells against certain anticancer agents may precede Pgp expression in early DOX resistance. This was demonstrated in *in vitro* experiments using human lung cancer cells serially exposed to DOX[195]. As mentioned before, the MGH-U1/R cells are more resistant and contain more Pgp compared to the MCF-7/R cells. This may be because the MCF-7/R cells are at an early point in the development of their MDR than the MGH-U1/R cells. In resistant cells believed to be preceding Pgp production, there was a lowering of drug uptake with lower nuclear than cytoplasmic drug uptake[195]. Such mechanisms preceding Pgp production may include LRP. From transfectants studies, LRP was shown to be insufficient to confer MDR to sensitive lines and may only contribute to the resistance observed[9].

There is also evidence that LRP may be involved in drug effluxing in the MGH-U1/R and MCF-7/R cell lines, as a minority of them (1-5% of cells in each cell line) contained this protein. LRP was detected as bright punctate dots of fluorescence around the nuclei and over the cytoplasm of the cells containing this protein. The staining of the antibody in this coarsely, granular fashion indicated

that it reacted with a molecule (LRP) closely associated with vesicular / lysosomal structures[79]. After treatment with GLA, the positive staining by the LRP-56 antibody appeared to be slightly changed within the resistant cell lines. Both cell lines showed larger spots of punctate fluorescence in the GLA treated cells than in the untreated cells. This may not be an indication that GLA has effected the resistance conferred to the cells by this protein but may result from other factors. The spots of staining appear to be of vesicle size and may be vesicles or droplets of the EFA that concentrated antibody in an opportunistic fashion. The MCF-7/R cells showed these spots of fluorescence mainly around the nuclei. This type of staining correlates to that observed in cells using fluorescent lipids. The latter produce spots of fluorescence (about the same size as those observed in the GLA treated resistant cells) as lipid droplets around the nuclei[30]. However, GLA has not been reported as a fluorescent lipid. It should be noted that the GLA treated MGH-U1/R cells which stained for LRP did not appear as healthy as other cells in the field of view, in other words their nuclei were distorted. Cell death is often associated with an increase in vesicles and lysosomes and these intracellular components may bind to the antibody producing larger points of bright fluorescence. Another explanation for the LRP staining appearing in such a low percentage of cells in both GLA treated and untreated cells is that it is only present in cells which are or have just undergone mitosis. As mitosis involves a change in the membrane of cells, it may be that Pgp becomes inactive, so as an MDR mechanism, the cells increase LRP production solely in these cells for a short period of time.

LRP has been detected in a number of MDR lines of different origins, such as small cell and non small cell lung cancer and breast cancer and myeloma[79]. Although most resistant cell lines only display one type of resistance protein either Pgp or LRP, in certain instances MDR cell lines known to express Pgp (MCF-7/D40) were also shown to stain positively with LRP-56[79]. The above mentioned resistant MCF-7 cell line was raised to DOX; however, another derivative of MCF-7 which had been raised against MTZ did not display Pgp but was believed likely to contain LRP. This cell line was reported by Taylor *et al* and compared to a MDR MCF-7 cell line raised to DOX. Both showed reduced drug accumulation secondary to enhanced drug efflux. The MCF-7/R line raised to DOX

overproduced Pgp while the MCF-7/R line raised to MTZ was Pgp negative[57]. Scheper reports that LRP was located in MCF-7/R raised against DOX, and MCF-7 cells, but only partial staining was observed. However, no LRP was present in our MCF-7 cells and very little in MCF-7/R cells. Such discrepancies between results may be due to the use of antibodies of different origins and epitope specificity. LRP expression in normal tissue was most pronounced in epithelial cells and tissues with high exposure to xenobiotics and potentially toxic agents, such as bronchial cells, cells lining the intestines and kidney tubules[79].

LRP has been predicted to be the human major vault protein showing 87.7% amino acid sequence homology with the rat major vault protein. The structure of the major vault protein is similar to that proposed for the transporter of the nuclear pore complex (NPC) and vaults have been shown to associate with the nuclear envelope and more specifically with the NPC[82]. For MDR cancer cells containing LRP this could account for the presence of drug free nuclei with LRP extruding the drug into the cytoplasm. This along with the granular cytoplasmic staining of the protein indicates that LRP/vaults mediate drug resistance through vesicular and nucleocytoplasmic transport of drugs[83]. Due to the nature of the vault it should be present in all of our cell lines as it is present in all eukaryotic cells. However, the sensitive cell lines did not show any staining for LRP.

The other MDR protein investigated, MRP, was not present in either of the resistant cell lines, although Scheper records partial MRP in MCF-7/DOX and MCF-7 cells. In the drug resistant cell line H69AR which contained MRP, major differences in net drug accumulation or efflux were not observed and did not appear to be part of the resistance phenotype of these MDR cells[65]. This raised the possibility that the intracellular sequestration of drugs was modified so the cytotoxic agents were less able to reach their intracellular sites of action in MDR cell lines producing this protein[68-70]. MRP has been shown to be primarily located in the endoplasmic reticulum, with lower levels in the plasma membrane[64], the Golgi and lysosomes[67-69]. This positioning of the protein may represent the transport pathway away from the prime site of action for chemotherapy drugs, the nucleus, to lysosomes or out of the cell[67-69].

In summary, the sensitive cells did not appear to contain any of the resistance proteins, showing negative staining for all four antibodies. The resistant

cell lines had positive staining for Pgp, the MGH-U1/R cells staining strongly with 100% of the cells containing the protein. MCF-7/R cells did stain for Pgp but not as strongly as the MGH-U1/R cells and the protein was only detected in about 50% of the cells. Both the resistant cell lines had limited LRP, which was present in 1-5% of each cell line. MRP was not detected in either of the resistant cell lines. MDR is a complex phenomenon, so although a protein may be present within a resistant cell there is no indication that the protein is functioning as a drug efflux pump or that it is even active.

7.5 RESISTANCE PROTEINS WITHIN CANCER TISSUE SECTIONS

In the bladder cancers analysed, Pgp was present in the majority of totally and partially resistant cancers but was also detected in two cancers which were sensitive to anthracyclines *in vitro*. In two of the cancers, more than one resistance protein was detected: MRP and Pgp were detected in one resistant cancer and in a sensitive cancer Pgp was detected along with MRP and LRP. LRP and MRP were detected separately in two other cancers both showing partial resistance to anthracyclines. These results correspond to those found with the bladder cancer cells lines where the resistant cells stained positive for Pgp with only 1-5 % staining for LRP. High exposure of the tumours to chemotherapy correlated with *in vitro* drug resistance but no obvious relationship was observed between exposure to chemotherapy and the presence of MDR proteins. The expression of Pgp in these cancers may reflect the extent of their progression, since high grade tumours have been previously shown to express higher levels of MDR1 mRNA than low grade tumours[42]. As no previous studies have systematically investigated the presence of LRP in bladder cancers its significance in drug resistance of this cancer is still circumspect. MRP mediated multidrug resistance in bladder cancer was found to be induced after chemotherapy, more frequently by high doses (300mg) than low doses (less than 300mg). In this study MRP was found to be co-expressed in 18% of patients after chemotherapy, however, no significant correlation between positive Pgp expression before chemotherapy and clinical outcome was found[54]. It may be that resistance proteins can be detected immunohistochemically before

biological (*in vitro*) resistance is evident. These resistance proteins may be detected in a small population of cancer cells already MDR; this would lead to biological resistance as these cells survive and multiply while the drug sensitive cells are killed during chemotherapy. Cancers, which were resistant *in vitro* but not immunohistochemically resistant, may owe their resistance to other mechanisms and not Pgp, LRP or MRP.

In the breast cancer sections only four out of the ten stained positive for any resistance proteins, one for Pgp and three for MRP. As for the bladder cancers no studies have systematically investigated the presence of MRP and LRP in breast cancer. Although one study investigated the expression of MRP and LRP in relation to chemotherapy in different groups of breast cancer patients. They concluded that neither of the two proteins predicted response to chemotherapy in breast cancer[53].

However, various studies have detected Pgp in breast cancer and have found a correlation between the presence of this protein with a) *in vitro* resistance to chemotherapy drugs belonging to the MDR group[47, 50, 196] and b) shorter periods of progression free survival[50]. In one study high intensity expression of Pgp was observed more frequently in chemotherapy treated cancers than in untreated tumours (40% vs 9%) although no relationship between Pgp and type of clinical treatment was observed. This observed increase in resistance following chemotherapy may be due to selection of initially drug resistant cells, *i.e.* acquired resistance. To study *in vitro* resistance, $1mm^3$ fragments of tumour, from different areas of the whole tumour, were treated *in vitro* with drug for 3h. Drug activity was expressed as the ability to inhibit the incorporation of a radioactively labelled precursor. Simultaneous resistance was observed in all those Pgp positive and 56% of Pgp negative tissue thus not all Pgp negative tumours were drug sensitive[47]. Although studies have found a significant relationship between Pgp expression and *in vitro* doxorubicin resistance, evaluated by metabolic or proliferative assays, no correlation was found between Pgp positivity and *in vitro* resistance to cisplatin, a drug not included in the MDR phenotype[196]. Another study found that Pgp was more frequently expressed in premenopausal and metastatic breast cancer patients compared to primary breast cancers, leading to speculation that Pgp may be an indicator of the aggressiveness of the tumour[49, 50]. In a study investigating 17

locally advanced tumours and three confirmed metastases, strong Pgp staining was detected in the majority of tumours and this correlated with no initial response to chemotherapy and with shorter progression free survival. However, not only were the majority of these tumours locally advanced they were also aggressive. Also the monoclonal antibody used to test for Pgp status was C494 which bound to a different epitope than C219 and JSB-1[50], the anti-Pgp antibodies more commonly used.

Double immunostaining of cytoplasmic membrane Pgp expression and nuclear accumulation of p53 has shown that they often occur concomitantly in the same breast tumour cells. A correlation between p53 and Pgp expression found in tissues from 50 breast cancers had a p value of $P = 0.003$ using Fishers exact test. Pgp expression by itself, nuclear p53 accumulation by itself and coexpression of p53 and Pgp were more frequently observed in locally advanced breast cancers than in operable breast cancers, with coexpression of Pgp and p53 being a strong prognostic factor for shorter survival. This implies that the MDR1 gene could be activated during tumour progression associated with mutations in p53[51]. It has been speculated that the site of p53 gene mutation may be necessary for the ability of the mutant p53 to stimulate the MDR1 promotor[197].

Whether Pgp and the other resistance proteins could be used as predictors for tumour response to chemotherapy is still debatable. Detection of these proteins in tumours prior to chemotherapy did not always lead to that tumour displaying the MDR phenotype. However, it is likely that expression of Pgp, especially, but also the other proteins are indicators of the aggressiveness of the tumour and how far it has progressed. It may be possible that a more extensive panel of resistance proteins or mechanisms will be tested on a variety of tumours and will provide a more comprehensive picture of the resistance status of patients. Such a variety of tests would include not only staining or *in vitro* assays for Pgp, MRP and LRP but would extend to p53, topoII and other resistance mechanisms. Eventually, applying this to clinical practice might help indicate appropriate choices for cancer therapy.

7.6. SUMMARY

Both the breast and bladder cancer MDR cell lines exhibited lowered drug accumulation compared to their sensitive counterparts with all drugs. The sole exception was IDA with the breast cancer cell lines; the MCF-7 and MCF-7/R cells took up similar amounts of this drug. There was also a difference in the pattern of intracellular drug sequestration between the sensitive and resistant cells. Again this held with all drugs except IDA. Generally, DOX and EPI showed mainly nuclear localisation in the sensitive cells with little in the cytoplasm. There were increased points of drug accumulated within the nuclei which probably corresponded to chromatin or nucleoli. The resistant cells had mainly cytoplasmic drug distribution with little in the nuclei but intense areas of perinuclear drug localisation. Although the MCF-7 cells did not take up MTZ into the nucleus the pattern of intracellular distribution was different in sensitive compared to resistant breast cancer cells. The pattern of intracellular IDA was similar in both resistant and sensitive cells. All four cell lines had mainly cytoplasmic IDA localisation with little nuclear distribution. The difference observed with IDA compared to the other drugs may be because IDA is a newer, more lipophilic drug compared to the other anthracyclines investigated. MTZ, like IDA, is a synthetic drug and this may in part explain the difference in intracellular localisation compared to the naturally occurring anthracyclines.

Incorporation of LiGLA into the cells should have led to an increase in membrane fluidity which could have resulted in increased cellular drug uptake. There was no significant increase in cellular uptake of the chemotherapeutic agents, DOX, MTZ and EPI, in any of the cell lines due to GLA treatment. An enhancement in IDA uptake was observed in both resistant cell lines after 24h incubation with GLA but this was not accompanied with a change in intracellular IDA distribution. A change in intracellular MTZ localisation but not overall uptake was observed in GLA treated MCF-7/R cells.

This study concentrated mainly on cellular MDR and efflux pumps but it is conceivable that many different mechanisms are working together to confer resistance on these cells. This scenario is probably true for the clinical situation which will complicate the design of resistance avoidance or reversing protocols.

9. REFERENCES

1. Moscow JA, Schneider E and Cowan KH. Multidrug Resistance. Chapt. 8 Cancer Chemotherapy and Biological Response Modifiers Annual 14. 1993.
2. Gottesman MM. How cancer cells evade chemotherapy: Sixteenth Richard and Hinda Rosenthal Foundation Award Lecture. Cancer Research 53: 747-754,1993.
3. Rhoads, CP. Nitrogen mustards in the treatment of neoplastic diseases. JAMA 131: 656-658, 1946.
4. Biedler JL and Riehm H. Cellular resistance to Actinomycin D in Chinese Hamster cells *in vitro*: Cross-resistance, radioautographic and cytogenetic studies. Cancer Research 30: 1174-1184, 1970.
5. Simon SM and Schindler M. Cell biological mechanisms of multidrug resistance in tumours. Proc. Natl. Acad. Sci. 91:3497-3504, 1994.
6. Riordan JR and Ling V. Purification of P-glycoprotein from plasma membrane vesicles of Chinese Hamster Ovary cell mutants with reduced colchicine permeability. J.Biol. Chem. 254:12701-5 1979.
7. Cole SPC, Bhardwaj G, Gerlach JH, Mackie JE, Grant CE, Almquist KC, Stewart AJ, Kurz EU, Duncan AMV and Deeley RG. Overexpression of a transporter gene in a multidrug-resistant human lung cancer cell line. Science 258:1650-1653, 1992.
8. Zaman GJR, Flens MJ, van Leusden MR, de Haas M, Mulder HS, Lankelma J, Pinedo HM, Scheper RJ, Baas F, Broxtrman HJ and Borst P. The human multidrug resistance-associated protein MRP is a plasma membrane drug-efflux pump. Proc. Natl. Acad. Sci. USA 91:8822-8826, 1994.
9. Scheffer GL, Wijngaard PLJ, Flens MJ, Izquierdo MA, Slovak ML, Pinedo HM, Meijer CJLM, Clevers HC and Scheper RJ. The drug resistance-related protein LRP is the major vault protein. Nature Medicine 1 (6): 578-582, 1995.
10. Scheper R. Transporter molecules in multidrug resistance. International Meeting on Drug Resistance in Cancer. ETCS. Dublin City University, Sept. 1995.
11. Juliano, RL and Ling, V. A surface glycoprotein modulating drug permeability in Chinese Hamster Ovary cell mutants. Biochem Biophys. Acta 455:152-162,

1976.

12. Danø K. Active outward transport of daunomycin in resistant Ehrlich ascites tumour cells. Biochim. Biophys. Acta. 323:466-483, 1973.

13. Inaba M, Kobayashi H, Sakurai Y and Johnson RK. Active efflux of daunorubicin and adriamycin in sensitive and resistant sublines of P388 leukemia. Cancer Research 39:2200-2203, 1979.

14. Deuchars KL, Duthie M and Ling V. Identification of distinct P-glycoprotein gene sequences in rat. Biochim. Biophys. Acta 1130 (2): 157-165, 1992.

15. Wu CT, Budding M, Griffin MS and Croop JM. Isolation and characterisation of Drosophila multidrug resistance gene homologs. Mol. Cell. Biol. 11(8): 3940-3948, 1991.

16. Giulfoile PG and Hutchinson CR. A bacterial analog of the mdr gene of mammalian tumour cell is present in *Streptomyces peucetius,* the producer of daunorubicin and doxorubicin. Proc. Natl. Acad. Sci. USA. 88(19): 8553-8557, 1991.

17. Choi K, Chen C, Kriegler M and Roninson IB. An altered pattern of cross-resistance in multidrug resistant human cells results from spontaneous mutations in the *mdr* (P-glycoprotein) gene. Cell 53: 519-529, 1988.

18. Lincke CR, Smit JJ, van de Velde Koerts T and Boerst P. Structure of the human MDR3 gene and physical mapping of the human MDR locus. J. Biol. Chem. 266(8): 5303-5310, 1991.

19. Ueda K, Cardarelli C, Gottesman MM and Pastan I. Expression of a full-length cDNA for the human 'MDR1' gene confers resistance to colchicine, doxorubicin and vinblastine. Proc. Natl. Acad. Sci. USA. 84(9): 3004-3008, 1987.

20. Schinkel AH, Roelofs EM and Borst P. Characterisation of the human MDR3 P-glycoprotein and its recognition by P-glycoprotein specific monoclonal antibodies. Cancer Research 51(10): 2628-2635, 1991.

21. Smit JJ, Schinkel AH, Mol CA, Majoor D, Mooi WJ, Jongsma AP, Lincke CR and Borst P. Tissue distribution of the human MDR3 P-glycoprotein. Comment in: Lab Invest. 71(5): 617-620, 1994.

22. Chin JE, Soffir R, Noonan KE, Choi K and Roninson IB. Structure and expression of the human MDR (P-glycoprotein) gene family. Mol. Cell. Biol. 9(9): 3808-3820, 1989.

23. Smit JJ, Schinkel AH, Oude Elferink RPJ, Groen AK, Wagenaar, van Deemter L, Mol CA, Ottenhoff R, van der Lugt NMT, van Roon MA, van der Valk MA, Offerhaus GJA, Berns AJM and Borst P. Homozygous disruption of the murine *mdr*2 P-glycoprotein gene leads to a complete absence of phospholipid from bile and to liver disease. Cell 75: 451-462, 1993.

24. Chen CJ, Chin JE, Ueda K, Clark DP, Pastan I, Gottesman MM and Roninson IB. Internal duplication and homology with bacterial transport proteins in the mdr1 (P-glycoprotein) gene from multidrug-resistant human cells. Cell 47(3): 381-389, 1986.

25. Chambers TC, Zheng B and Kuo JF. Regulation by the phorbol ester and protein kinase C inhibitors and by a protein phosphatase inhibitor (okadaic acid), of P-glycoprotein phosphorylation and relationship to drug accumulation in multidrug-resistant human KB cells. Mol. Pharmacol. 41(6): 1008-1015, 1992.

26. Germann UA, Pastan I and Gottesman MM. P-glycoproteins: mediators of multidrug resistance. Seminars in Cell Biol. 4:63-76, 1993.

27. Personal Communication (Lecture) from LM Fisher, 1995.

28. Willingham MC, Richert ND, Cornwell MM, Tsururo T, Hamada H, Gottesman MM and Pastan IH. Immunocytochemical localisation of P170 at the plasma membrane of multidrug-resistant human cells. J. Histochem. Cytochem. 35(12): 1451-1456, 1987.

29. Gervasoni JE, Fields SZ, Krishna S, Baker MA, Rosado M, Thuraisamy K, Hindenburg AA and Taub RN. Subcellular distribution of daunorubicin in P-glycoprotein positive and negative drug resistant cell lines using laser-assisted confocal microscopy. Cancer Research 51:4955-4963, 1991.

30. Pagano RE and Sleight RG. Defining lipid transport pathways in animal cells. Science 229: 1051-1056, 1985.

31. Koval M and Pagano RE. Lipid recycling between the plasma membrane and intracellular compartments: Transport and metabolism of fluorescent sphingomyelin analogues in cultured fibroblasts. J. Cell Biology. 108: 2169-2181, 1989.

32. Sehested M, Skovasgaard T, van Deurs B and Winther-Neilsen H. Increase in nonspecific absorptive endocytosis in anthracycline- and vinca alkaloid-resistant Ehrlich ascites tumour cell lines. J. Natl. Ca. Inst. 78(1): 171-177, 1987.

33. Demant EJF, Sehested M and Jensen PB. A model for computer simulation of

P-glycoprotein and transmembrane ΔpH-mediated anthracycline transport in multidrug resistant tumour cells. Biochim. Biophys. Acta 1055: 117-125, 1990.

34. Roepe PD. Analysis of the steady-state and initial rate of doxorubicin efflux from a series of multidrug-resistant cells expressing different levels of P-glycoprotein. Biochemistry 31: 12555-12564, 1992.

35. Naito M and Tsuruo T. Competitive inhibition by verapamil of ATP-dependent high affinity vincristine binding to the plasma membrane of multidrug-resistant K562 cells without calcium ion involvement. Cancer Research 49(6): 1452-1455, 1989.

36. Kohno K, Sato S, Takano H, Matsuo K and Kuwano M. The direct activation of human multidrug resistance gene (MDR1) by anticancer agents. Biochem. Biophys. Res. Commun. 165(3): 1415-1421, 1989.

37. Nooter K and Herweijer H. Multidrug resistance (*mdr*) genes in human cancer. Br. J. Cancer 63:663-669, 1991.

38. Fojo AT, Ueda K, Slamon DJ, Poplack DG, Gottesman MM and Pastan I. Expression of a mutidrug-resistance gene in human tumours and tissues. Proc. Natl. Acad. Sci. USA 84:265-269, 1987.

39. Thiebaut F, Tsuruo T, Hamada H, Gottesman MM, Pastan I and Willingham MC. Cellular localisation of the multidrug-resistance gene product P-glycoprotein in normal human tissues. Proc. Natl. Acad. Sci. USA 84(21): 7735-7738, 1987.

40. Cordon-Cardo C, O'Brien JP, Boccia J, Casals D, Bertino JR and Melamed MR. Expression of the multidrug resistance gene product (P-glycoprotein) in human normal and tumour tissues. J. Histochem. Cytochem. 38(9): 1277-1287, 1990.

41. Klohs WD and Steinkampf RW. Possible link between the intrinsic drug resistance of colon tumours and a detoxification mechanism of intestinal cells. Cancer Research 48: 3025-3030, 1988.

42. Clifford SC, Neal DE and Lunec J. High level expression of the multidrug resistance (MDR1) gene in the normal bladder urothelium: a potential involvement in protection against carcinogens? Carcinogenesis 17(3): 601-604, 1996.

43. Gottesman MM and Pastan I. Biochemistry of multidrug resistance mediated by the multidrug transporter. Ann. Rev. Biochem. 62:385-427, 1993.

44. Baldini N. Multidrug resistance- a multiplex phenomenon. Nature Medicine 3(4): 447-450,1997.

45. Chin KV, Ueda K, Pastan I and Gottesman MM. Modulation of activity of the promoter of the human *MDR*1 gene by Ras and p53. Science 255, 459-462, 1992.

46. Ogretmen B and Safa AR. Expression of the mutated p53 tumour suppressor protein and its molecular and biochemical characterization in multidrug resistant MCF-7/Adr human breast cancer cells. Oncogene14(4): 499-506, 1997.

47. Sanfillipo O, Ronchi E, De Marco C, Di Fronzo G and Silvestrini R. Expression of P-glycoprotein in breast cancer tissue and *in vitro* resistance to doxorubicin and vincristine. Eur. J. Cancer 27(2): 155-159, 1991.

48. Nezasa S, Fujihiro S, Deguchi T, Kawada Y, Kawamoto S, Tamaki M, Yamada S and Okano M. Analysis of induction of MDR1 gene expression by anticancer chemotherapy in bladder cancer. Hinyokika Kiyo 43(9): 629-636, 1997.

49. Giaccone G, Linn SC and Pinedo HM. Multidrug resistance in breast cancer: mechanisms and strategies. Eur. J. Cancer 31A (suppl. 7):S15-S17, 1995.

50. Verrelle P *et al.* Clinical relevance of immunohistochemical detection of MDR P-glycoprotein in breast carcinoma. J. Natl. Cancer. Inst. 83(2):111-116,1991.

51. Linn SC *et al.* P53 and P-glycoprotein are co-expressed and are associated with poor prognosis in breast cancer. Br. J. Cancer 74(1): 63-68, 1996.

52. Trock BJ, Leonessa F and Clarke R. Multidrug resistance in breast cancer: a meta-analysis of MDR1/gp170 expression and its possible functional significance. J. Natl. Cancer Inst. 89(13): 917-931, 1997.

53. Linn SC, Pinedo HM, van Ark-Otte J, van der Valk P, Hoekman K, Honkoop AH, Vermorken JB and Giaconne G. Expression of drug resistance proteins in breast cancer, in relation to chemotherapy. Int. J. Cancer 71(5): 787-795, 1997.

54. Nakagawa M, Emoto A, Nasu N, Hanada T, Kuwano M, Cole SP and Nomura Y. Clinical significance of multi-drug resistance associated protein and P-glycoprotein in patients with bladder cancer. Journal of Urology 157(4): 1260-1264, 1997.

55. Molinari A, Cianfriglia M, Meschini S, Calcabrini A and Arancia G. P-glycoprotein expression in the Golgi apparatus of multi-drug resistant cells. Int. J. Cancer. 59(6): 789-795, 1994.

56. Peters WHM and Roelofs HMJ. Biochemical characterisation of resistance to mitoxantrone and adriamycin in Caco-2 human colon adenocarcinoma cells: a possible role for glutathione S-transferases. Cancer Research 52: 1886-1890, 1992.

57. Taylor CS, Dalton WS, Parrish PR, Gleason MC, Bellamy WT, Thompson FH, Roe DJ and Trent JM. Different mechanisms of decreased drug accumulation in doxorubicin and mitoxantrone resistant variants of the MCF-7 human breast cancer cell line. Br. J. Cancer 63: 923-929, 1991.

58. Nakagawa M, Schneider E, Dixon KH, Horton J, Kelley K, Morrow C and Cowan KH. Reduced intracellular drug accumulation in the absence of P-glycoprotein (*mdr*1) overexpression mitoxantrone-resistant human MCF-7 breast cancer cells. Cancer Research 52: 6175-6181, 1992.

59. Zaman GJR, Versantvoort CHM, Smit JJM, Eijdems EW, de Haas M, Smith AJ, Broxterman HJ, Mulder NH, de Vries EG, Baas F and Borst P. Analysis of the expression of *MRP*, the gene for a putative transmembrane drug transporter, in human multidrug resistant lung cancer cell lines. Cancer Research 53: 1747-1750, 1993.

60. Cole SPC and Deeley RG. Multidrug resistance-associated protein: Sequence correction. Science 260: 879, 1993.

61. Hyde SC, Emsley P, Hartshorn MJ, Mimmack MM, Gileadi U, Pearce SR, Gallagher MP, Gill DR, Hubbard RE and Higgins CF.. Structural model of ATP-binding proteins associated with cystic fibrosis, multidrug resistance and bacterial transport. Nature 346:362-365, 1991.

62. Oulette M, Fase-Fowler F and Borst P. The amplified H circle of methotrexate-resistant *Leishmania tarentolae* contains a novel P-glycoprotein gene. EMBO 9(4): 1027-1033, 1990.

63. Center M. Studies on multidrug resistance in HL-60/ADR cells overexpressing the MRP gene. International Meeting on Drug Resistance in Cancer. ETCS. Dublin City University, Sept. 1995.

64. Krishnamachary N and Center MS. The MRP gene associated with a non-P-glycoprotein multidrug resistance encodes a 190-kDa membrane bound glycoprotein. cancer Research 53: 3658-36661, 1993.

65. Cole SPC, Chanda ER, Dicke FP, Gerlach JH and Mirski SEL. Non-P-glycoprotein-mediated multidrug resistance in a small cell lung cancer cell line:

Evidence for decreased susceptibility to drug-induced DNA damage and reduced levels of topoisomerase II. Cancer Research 51: 3345-3352, 1991.

66. Sehested M, Skovsgaard T, van Deurs B and Winther-Nielsen H. Increased plasma membrane traffic in daunorubicin resistant P388 leukaemic cells. Effects of daunorubicin and verapamil. Br. J. Cancer 56: 747-751, 1987.

67. Barrand MF, Rhode T, Center MS and Twentyman PR. Chemosensitisation and drug accumulation. Effects of Cyclosporin A, PSC – 833 and verapamil in human multidrug resistant large cell lung cancer cells expressing a 190k membrane protein distinct from Pgp . Eur. J. Cancer. 29A (3): 408-415, 1993.

68. Marquardt D and Center MS. Drug transport mechanisms in HL60 cells isolated for resistance to adriamycin: Evidence for nuclear drug accumulation and redistribution in resistant cells. Cancer Research 52: 3157-3163, 1992.

69. Hindenburg AA, Gervasoni JE, Krishna S, Stewart VJ, Rosado M, Lutzky J, Bhalla K, Baker MA and Taub RN. Intracellular distribution and pharmacokinetics of daunorubicin in anthracycline sensitive and resistant HL60 cells. Cancer Research 49: 4607-4614, 1989.

70. Breuninger LM, Paul S, Gaughan K, Miki T, Chan A, Aaronson SA and Kruh GD. Expression of multidrug resistance associated protein in NIH/3T3 cells confers multidrug resistance associated with increased drug efflux and altered intracellular drug distribution. Cancer Research 55: 5342-5347, 1995.

71. Cole SPC, Downes HF and Slovak ML. Effect of calcium antagonists on the chemosensitivity of two multidrug-resistant tumour cell lines which do not overexpress P-glycoprotein. Br. J. Cancer 59:42-, 1989.

72. Cole SPC, Sparks KE, Fraser K, Loe DW, Grant CE, Wilson GM and Deeley RG. Pharmacological characterisation of multidrug resistant MRP-transfected human tumour cells. Cancer Research 54: 5902-5910, 1994.

73. Baas F, Jongsma APM, Broxterman, Arceci RJ, Housman D, Scheffer GL, Riethorst, van Groenigen M, Nieuwint AWM and Joenje H. Non-P-glycoprotein mediated mechanism for multidrug resistance precedes P-glycoprotein expression during *in vitro* selection for doxorubicin resistance in a human lung cancer cell line. Cancer Research 50: 5392-5398, 1990.

74. Slapak CA, Mizunuma N and Kufe DW. Expression of the multidrug resistance associated protein and P-glycoprotein in doxorubicin-selected human myeloid leukemia cells. Blood 84(9): 3113-3121, 1994.

75. Paul S, Breuninger LM, Tew KD, Shen H and Kruh GD. ATP-dependent uptake of natural product cytotoxic drugs by membrane vesicles establishes MRP as a broad specificity transporter. Proc. Natl. Acad. Sci. USA 93: 6929-6934, 1996.

76. Nooter K, Brutel de la Riviere G, Look MP, van Wingerden KE, Henzen-Logmans SC, Scheper RJ, Flens MJ, Klijn JG, Stoter G and Foekens JA. The prognostic significance of expression of the multidrug resistance-associated protein (MRP) in primary breast cancer. Br. J. Cancer 76(4): 486-493,1997.

77. Hasegawa S, Abe T, Naito S, Kotoh S, Kumazawa J, Hipfner DR, Deeley RG, Cole SP and Kuwano M. Expression of multidrug resistance-associated protein (MRP), MDR1 and DNA topoisomerase II in human multi-drug resistant bladder cancer cell lines. Br. J. Cancer 71(5): 907-913, 1995.

78. Schneider E, Horton JK, Yang CH, Nakagawa M and Cowan KH. Multidrug resistance-associated protein gene overexpression and reduced drug sensitivity of topoisomerase II in a human breast carcinoma MCF-7 cell line selected for etoposide resistance. Cancer Res. 54(1): 152-158, 1994.

79. Scheper RJ, Broxterman HJ, Scheffer GL, Kaaijk P, Dalton WS, van Heijningen THM, van Kalken CK, Slovak ML, de Vries EGE, van der Valk P, Meijer CJ and Pinedo HM. Overexpression of a M_r 110,000 vesicular protein in non-P-glycoprotein-mediated multidrug resistance. Cancer Research 53: 14475-1479, 1993.

80. Rome LH. Multidrug resistance locked in the vault? Nature Medicine 1(6): 527, 1995.

81. Rome L, Kedersha N and Chugani D. Unlocking vaults: organelles in search of a function. Trends in Cell Biol. 1: 47-50, 1991.

82. Chugani DC, Rome LH and Kedersha NL. Evidence that vault ribonucleoprotein particles localise to the nuclear pore complex. J. Cell Sci. 106: 23-29, 1993.

83. Izquierdo MA. Role of LRP in anticancer drug resistance: from the laboratory to clinic. ECC Newsletter. 12-14.

84. Morrow CS and Cowan KH. Multidrug resistance associated with altered topoisomerase II activity- Topoisomerase II as targets for rational drug design. J. Natl. Ca. Inst. 82(8): 38-39, 1990.

85. Wang JC. Recent studies of DNA topoisomerases. Biochim. Biophys. Acta

909:1-9, 1987.

86. Giaccone G. DNA topoisomerases and topoisomerase inhibitors. PathBiol 42 (4): 346-352, 1994.

87. Glisson B, Gupta R, Hodges P and Ross W. Cross-resistance to intercalating agents in an Epipodophyllotoxin-resistant Chinese Hamster Ovary cell line: Evidence for a common intracellular target. Cancer Research 46: 1939-1942, 1986.

88. de Jong S, Zijlstra JG, de Vries EGE and Mulder NH. Reduced DNA topoisomerase II activity and drug-induced DNA cleavage activity in an adriamycin-resistant human small cell lung carcinoma cell line. Cancer Research 50: 304-309, 1990.

89. Drake FH, Zimmerman JP, McCabe FL, Bartus HF, Per SR, Sullivans DM, Ross WE, Mattern MR, Johnson RK, Crooke ST and Mirabelli CK. Purification of topoisomerase II from amsacrine-resistant P388 leukemia cells. Biol. Chem. 262: 16739-16747, 1987.

90. Patel S and Fisher LM. Novel selection and genetic characterisation of an etoposide-resistant human leukaemic CCRF-CEM cell line. Br. J. Cancer 67: 456-463, 1993.

91. D'Incali M. Mechanisms of resistance to alkylating agents. International Meeting on Drug Resistance in Cancer. ETCS. Dublin City University, Sept. 1995.

92. Ravdin PM. Anthracycline resistance in breast cancer: clinical applications of current knowledge. Eur. J. Cancer 31A (suppl. 7): S11-S14, 1995.

93. Batist G, Tulpule A, Sinha BK, Katki AG, Myers CE and Cowan KH. Overexpression of a novel anionic glutathione transferase in multidrug-resistant human breast cancer cells. J. Biol. Chem. 261(33): 15544-15549, 1986.

94. Ciocca DR, Fuqua SAW, Lock-lim S, Toft DO, Welch WJ and Mcguire WL. Responses of human breast cancer cells to heat shock and chemotherapeutic drugs. Cancer Research 52: 3648-3654, 1992.

95. Consoli U, Priebe W, Ling Y-H, Mahadevia R, Griffin M, Zhao S, Perez-Soler R and Andreef M. The novel anthracycline annamycin is not affected by P-glycoprotein-related multidrug resistance: Comparison with idarubicin and doxorubicin in HL60 leukemia cell lines. Blood 88(2): 633-644, 1996.

96. Willingham MC, Cornwell MM, Cardarelli C, Gottesman MM and Pastan I.

Single cell analysis of daunomycin uptake and efflux in multidrug-resistant and sensitive KB cells: Effects of verapamil and other drugs. Cancer Research 46: 5941-5946, 1986.

97. Merlin J-L, Marchal S, Ramacci C, Dieterlen A, Schultz, Lucas C, Poullain MG and Berlion M. Influence of S9788, a new modulator of multidrug resistance, on the cellular accumulation and subcellular distribution of daunorubicin in P-glycoprotein-expressing MCF7 human breast adenocarcinoma cells. Cytometry 20: 315-323, 1995.

98. Le Bot MA, Kernaleguen D, Robert J, Berlion M and Riche C. Modulation of anthracycline accumulation and metabolism, in rat hepatocytes in culture by three revertants of multidrug resistance. Cancer Chemother. Pharmacol. 35(1): 53-58, 1994.

99. Foxwell BMJ, Mackie A, Ling V and Ryffel B. Identification of the multidrug resistance-related P-glycoprotein as a cyclosporine binding protein. Molecular Pharmacol. 36: 543-546, 1989.

100. Kessel D. Interactions among membrane transport systems: anthracyclines, calcium antagonists and anti-estrogens. Biochem. Pharmacol. 35(16): 2825-2826, 1986.

101. Sachs CW, Ballas LM, Mascarella SW, Safa AR, Lewin AH, Loomis C, Carroll FI, Bell RM and Fine RL. Effects of sphingosine stereoisomers on P-glycoprotein phosphorylation and vinblastine accumulation in multidrug-resistant MCF-7 cells. Biochem. Pharmocol. 52(4): 603-612, 1996.

102. Versantvoort CHM, Schuurius GJ, Pinedo HM, Eekman CA, Kuiper CM, Lankelma J and Broxterman HJ. Genistein modulates the decreased drug accumulation in non-P-glycoprotein mediated multidrug resistant tumour cells. Br. J. Cancer 68:939-946, 1993.

103. Tew KD. The mechanism of action of estramustine. Seminars in Oncol. 10 (suppl.3): 21-26, 1983.

104. Speicher LA, LR, Chapman AE, Hudes, Laing N, Smith CD and Tew KD. P-glycoprotein binding and modulation of the resistant phenotype by estramustine. J. Natl. Ca. Inst. 86(9): 688-694,1994.

105. Deutsch HF, Tsukada Y and Hirai H. Cytotoxic effects of daunomycin-fatty acid complexes on rat hepatoma cells. Cancer Research 43:2668-2672, 1983.

106. Cuvier C, Roblot-Treupel L, Millot JM, Lizard G, Chevillard S, Manfait M,

Couvreur P and Poupon MF. Doxorubicin-loaded nanospheres bypass tumour cell multidrug resistance. Biochem. Pharmacol. 44(3): 509-51, 1992.

107. Hu YP, Henry-Toulme N and Robert J. Failure of liposomal encapsulation of doxorubicin to circumvent multidrug resistance in an *in vitro* model of rat glioblastoma cells. Eur. J. Cancer. 31A (3): 389-394, 1995.

108. Callaghan R, Stafford A and Epand RM. Increased accumulation of drugs in a multidrug resistant cell line by alteration of membrane biophysical properties. Biochim. Biophys. Acta 1175: 277-282, 1993.

109. Robert J and Gianni L. Pharmacokinetics and metabolism of anthracyclines. Cancer Surveys 17:219-251, 1993.

110. Launchbury P. Anticancer drugs: Research, development and production. Lecture notes for Tumour Biology Course, Intercalated BSc, UCLMS 1995.

111. Booser DJ and Hortobagyi GN. Anthracycline antibiotics in cancer therapy: Focus on drug resistance. Drugs 47(2): 223-258, 1994.

112. Young RC, Ozols RF and Myers CE. The anthracycline antineoplastic drugs. The New England Journal of Medicine 305(3): 139-153.

113. Arcamone A. Properties of antitumour anthracyclines and new developments in their application: Cain Memorial Award Lecture. Cancer Research 45: 5995-5999, 1985.

114. Kuffel MJ, Reid JM and Ames MM. Anthracyclines and their C-13 alcohol metabolites: growth inhibition and DNA damage following incubation with human tumour cells in culture. Cancer Chemother. Pharmacol. 30(1): 51-57, 1992.

115. Smith PJ, Morgan SA, Fox ME and Watson JV. Mitoxantrone-DNA binding and the induction of topoisomerase II associated DNA damage in multidrug resistant small cell lung cancer cells. Biochem. Pharmacol. 40(9): 2069-2078, 1990.

116. Lederle Laboratories, Fareham Road,Gosport, Hampshire, UK. Novantrone™ Injection. Mitozantrone information sheet.

117. Silvestrini R, Di Marco A and Dasdia T. Interference of Daunomycin with metabolic events of the cell cycle in synchronised cultures of rat fibroblasts. Cancer Research 30:966-973, 1970.

118. Brown JR and Imam SH. Recent studies on doxorubicin and its analogues. Progress in Med. Chem. 21: 170-213, 1984.

119. Zunino F, Gambetta R and Di Marco A. The inhibition *in vitro* of DNA and RNA polymerases by daunomycin and adriamycin. Biochem. Pharmacol. 24: 309-311, 1975.

120. Bhushan A, Kermode JC, Posada J and Tritton TR. Anthracycline resistance. Cancer Treat. Res. 48: 55-72, 1989.

121. Cornarotti M, Tinelli S, Willmore E, Zunino F, Fisher LM, Austin CA and Capranico G. Drug sensitivity and sequence specificity of human recombinant DNA topoisomerases IIα (p170) and IIβ(p180). Molecular Pharmacol. 50: 1463-1471, 1996.

122. Tritton TR and Yee G. The anticancer agent adriamycin can be actively cytotoxic without entering cells. Science 217: 248-250, 1982.

123. Handa K and Sato S. Generation of free radicals of quinone group-containing anti-cancer chemicals in NADPH-microsome system as evidenced by initiation of sulfite oxidation. Gann 66:43-47, 1975.

124. Myers CE, McGuire WP, Liss RH, Ifrim I, Grotzinger K and Young RC. Adriamycin: The role of lipid peroxidation in cardiac toxicity and tumour response. Science 197:165-169, 1977.

125. Smith PJ. Topoisomerase inhibitors: New twists to anticancer drug action. Oncology Today 3:4-9, 1991.

126. Vaage JV, Donovan D, Loftus T, Abra R, Working P and Huang A. Chemoprevention and therapy of mouse mammary carcinomas with doxorubicin encapsulated in sterically stabilised liposomes. Cancer 73(9): 2366-2371, 1994.

127. Forssen EA and Tokes ZA. Improved therapeutic benefits of doxorubicin by entrapment in anionic liposomes. Cancer Research 43: 546-550, 1983.

128. Gunstone FD. Gamma linolenic acid – Occurrence and physical and chemical properties. Prog. Lipid Res. 31(2): 145-161, 1992.

129. Pritchard GA, Jones DL and Mansel RE. Lipids in breast carcinogenesis. Br. J. Surg. 76: 1069-1073, 1989.

130. Begin ME. Effects of polyunsaturated fatty acids and of their oxidation products on cell survival. Chemistry and Physics of Lipids 45: 269-313, 1987.

131. Alberts B, Bray D, Lewis J, Raff M, Roberts K and Watson JD. Molecular biology of the cell, 2nd Ed. Garland Publishing Inc, New York and London. Chapt. 6: The Plasma membrane p277, 1989.

132. Begin ME, Das UN, Ells G and Horrobin DF. Selective killing of human

cancer cells by polyunsaturated fatty acids. Prostaglandins. Leuko. Med. 19(2): 177-186, 1985.

133. Begin ME, Ells G, Das UN and Horrobin DF. Differential killing of human carcinoma cells supplemented with n-3 and n-6 polyunsaturated fatty acids. J. Natl.Ca. Inst. 77(5): 1053-1062, 1986.

134. Begin ME and Ells G. Effects of C18 fatty acids on breast carcinoma cells in culture. Anticancer Research 7(2): 215-217, 1987.

135. Das UN, Huang YS, Begin ME, Ells G and Horrobin DF. Uptake and distribution of cis-unsaturated fatty acids and their effect on free radical generation in normal and tumour cells *in vitro.* Free Radic. Biol. Med. 3(1): 9-14, 1987.

136. Begin ME, Ells G and Horrobin DF. Polyunsaturated fatty acid-induced cytotoxicity against tumour cells and its relationship to lipid peroxidation. J. Natl. Cancer. Inst. 80: 188-194, 1988.

137. Kappus H. Lipid peroxidation: Mechanisms, Analysis, Enzymology and Biological Relevance. In: Sies H, ed. Oxidative stress. New York: Academic Press, 1985:273-310.

138. Cantrill RC, Ells G, Chisholm K and Horrobin DF. Concentration-dependent effect of iron on gamma-linolenic acid toxicity in ZR-75-1 human breast tumour cells in culture. Cancer Letters 72(1-2): 99-102, 1993.

139. Falconer JS, Ross JA, Fearon KCH, Hawkins RA, O'Riordain MG and Carter DC. Effect of eicosapentaenoic acid and other fatty acids on the growth *in vitro* of human pancreatic cancer cell lines. Br. J. Cancer 69: 826-832, 1994.

140. Spector AA and Burns CP. Biological and therapeutic potential of membrane lipid modification in tumors. Cancer Research 47:4529-4537, 1987.

141. Lanson M, Bougnoux P, Besson P, Lansac J, Hubert B, Couet C and Le Floch O. n-6 polyunsaturated fatty acids in human breast carcinoma phosphatidylethanolamine and early relapse. Br. J. Cancer 61: 776-778, 1990.

142. Horrobin DF. The reversibility of cancer: the relevance of cyclic AMP, calcium, essential fatty acids and prostaglandin E1. Med. Hypothesis 6(5): 469-486, 1980.

143. Chiappe LE, De Tomas ME and Mercuri O. In vitro activity of Δ6 and Δ9 desaturases in hepatomas of different growth rates. Lipids 9(7): 489-490, 1974

144. Chaudry A, McClinton S, Moffat LEF and Wahle KWJ. Essential fatty acid

distribution in the plasma and tissue phospholipids of patients with benign and malignant prostatic disease. Br. J. Cancer 64: 1157-1160, 1991.

145. Grammatikos SI, Subbaiah PV, Victor TA and Miller WM. n-3 and n-6 fatty acid processing and growth effects in neoplastic and non-cancerous human mammary epithelial cell lines. Br. J. Cancer 70: 219-227, 1994.

146. Hussey HJ and Tisdale MJ. Effect of polyunsaturated fatty acids on the growth of murine colon adenocarcinomas *in vitro* and *in vivo.* Br. J. Cancer 70: 6-10, 1994.

147. Rose DP and Connolly JM. Effects of fatty acids and inhibitors of eicosanoid synthesis on the growth of a human breast cancer cell line in culture. Cancer Research 50: 7139-7144, 1990.

148.Hubbard NE and Erickson KL. Enhancement of metastasis from a transplantable mouse mammary tumour by dietary linolenic acid. Cancer Research 47: 6171-6175, 1987.

149. Rose DP and Connolly JM. Effects of dietary omega-3 fatty acids on human breast cancer growth and metastases in nude mice. J. Natl. Cancer. Inst. 85(21): 1743-1747, 1993.

150. Rose DP, Connolly JM, Rayburn J and Coleman M. Influence of diets containing eicosapentanoic or docosahexaenoic acid on growth and metastasis of breast cancer cells in nude mice. J. Natl. Cancer. Inst. 87(8): 587-592, 1995.

151. Chen YQ, Duniec ZM, Liu B, Hagmann W, Gao X, Shimoji K, Marnett LJ, Johnson CR and Honn KV. Endogenous 12 (S) – HETE production by tumour cells and its role in metastasis. Cancer Research 54: 1574-1579.

152. Sakaguchi M, Rowley S, Kane N, Imray C, Davies A, Jones C, Newbold M, Keighley MRB, Baker P and Neoptolemos. Reduced tumour growth of the human colonic cancer cell lines COLO-320 and HT-29 *in vivo* by dietary n-3 lipids. Br. J. Cancer 62: 742-747, 1990.

153. Awad AB and Spector AA. Modification of the fatty acid composition of Ehrlich ascites tumour cell membranes. Biochim. Biophys. Acta. 426: 7223-731, 1976.

154. Burns CP, Luttenegger DG, Dudley DT, Buettner GR and Spector AA. Effect of modification of plasma membrane fatty acid composition on fluidity and methotrexate transport in L1210 murine leukemia cells. Cancer Research 39: 1726-1732, 1979.

155. Burns CP and Wagner BA. Effects of exogenous lipids on cancer and cancer chemotherapy: Implications for treatment. Drug Safety 8(1): 57-68, 1993.

156. Sinha BK, Katki AG, Batist G, Cowan KH and Myers CE. Differential formation of hydroxyl radicals by adriamycin in sensitive and resistant MCF-7 human breast tumour cells: Implications for the mechanism of action. Biochemistry 26: 3776-3781, 1987.

157. Guffy MM, North JA and Burns CP. Effect of cellular fatty acid alteration on adriamycin sensitivity in cultured L1210 murine leukemia cells. Cancer Research 44:1863-1866, 1984.

158. Kinsella JE and Black JM. Effects of polyunsaturated fatty acids on the efficacy of antineoplastic agents toward L5178Y lymphoma cells. Biochem. Pharmacol. 45(9): 1881-1887, 1993.

159. Sangeetha Sagar P and Das UN. Gamma-linolenic acid and eicosapentaenoic acid potentiate the cytotoxicity of anti-cancer drugs on human cervical carcinoma (HeLa) cells *in vitro.* Med. Sci. Res. 21: 457-459, 1993.

160. Burns CP, Haugstad BN, Mossman CJ, North JA and Ingraham LM. Membrane lipid alteration: effect on cellular uptake of mitoxantrone. Lipids 23(5): 393-397, 1988.

161. Timmer-Bosscha H, Hospers GAP, Meijers C, Mulder NH, Muskiet FAJ, Martini IA, Uges DRA and de Vries EGE. Influence of docosahexanoic acid on cisplatin resistance in a human small cell lung carcinoma cell line. J. Natl. Cancer. Inst. 81: 1069-1075, 1989.

162. Neades GT, Jones DL and Hughes LE. Effect of polyunsaturated fatty acids on doxorubicin sensitivity in MCF-7 cells. (SRS Abstract) Br. J. Surg. 78(6): 749, 1991.

163. Weber JM, Sircar S and Begin ME. Greater sensitivity of human multidrug-resistant (mdr) cancer cells to polyunsaturated fatty acids than their non-mdr counterparts. J. Natl. Cancer. Inst. 86(8): 638-639, 1994.

164. Plumb JA, Luo W and Kerr DJ. Effect of polyunsaturated fatty acids on the drug sensitivity of human tumour cell lines resistant to either cisplatin or doxorubicin. Br. J. Cancer 67: 728-733, 1993.

165. European Collection of Animal Cell Culture Catalogue. 4thEdition. European Collection of Animal Cell Cultures, Porton Down, Salisbury, UK.

166. Masters JRW, Hepburn PJ, Walker L, Highman WJ, Trejdosiewicz LK,

Povey S, Parkar M, Hill BT, Riddle PR and Franks LM. Tissue culture model of transitional cell carcinoma: characterisation of twenty-two human urothelial cell lines. Cancer Research 46: 3630-3636, 1986.

167. McGovern F, Kachel T, Vijan S, Schiff S, Lin CW and Prout, Jr GR. Establishment and characterisation of a doxorubicin-resistant human bladder cancer cell line (MGH-U1R). J. Urol. 140: 410-414, 1988.

168. Becton-Dickinson FACScan manual. LYSIS™ II Software users guide. 1992.

169. Lackie P. A Practical Introduction to Confocal Microscopy. Confocal Course Manual. EM Unit, Southampton General Hospital, 1996.

170. Bedwell J, MacRobert AJ, Phillips D and Bown SG. Fluorescence distribution and photodynamic effect of ALA-induced PP IX in the DMH rat colonic tumour model. Br. J. Cancer 65: 818-824, 1992.

171. Freshney RI. Culture of Animal Cells. A Manual of Basic Technique. Third Edition. Chapt. 19. Pg. 297, Wiley-Liss, Inc. New York.1994.

172. Monaghan P and Moss D. An introduction to immunochemistry. Microscopy and Analysis. Sept. 1995, 17-19.

173. Bogush T and Robert J. Comparative evaluation of the intracellular accumulation and DNA binding of idarubicin and daunorubicin in sensitive and multidrug resistant human leukaemia K562 cells. Anticancer Research 16: 365-368, 1996.

174. Schuurius GJ, Broxterman HJ, Cervantes A, van Heijningen THM, de Lange JHM, Baak JPA, Pinedo HM and Lankelma J. Quantitative determination of factors contributing to doxorubicin resistance in multidrug resistant cells. J Natl. Cancer. Inst. 81(24): 1887-1892, 1989.

175. Popert RJM, Masters JRW, Coptcoat M and Zupi G. Relative cytotoxicities of adriamycin and epirubicin in combination with ionidamine against human bladder cancer cell lines. Urol. Res. 22: 367-372, 1995.

176. Coley HM, Twentyman PR and Workman P. The efflux of anthracylines in multidrug resistant cell lines. Biochem. Pharmacol. 46(8): 1317-1326, 1993.

177. Tapiero H, Nguyen BG and Lampidis TJ. Cross resistance relevance of the chemical structure of different anthracyclines in multidrug resistant cells. Pathl. Biol. Paris 42(4): 328-337, 1994.

178. Coley HM, Workman P and Twentyman PR. Retention of activity by

selected anthracyclines in a multidrug resistant human large cell lung carcinoma line without P-glycoprotein. Br. J. Cancer 63: 351-357, 1991.

179. Coley HM, Twentyman PR and Workman P. Improved cellular accumulation is characteristic of anthracyclines which retain high activity in multidrug resistant cell lines, alone or in combination with verapamil or cyclosporin A. Biochem. Pharmacol. 38(24): 4467-4475, 1989.

180. Dimanche-Boitrel MT, Genne P, Duchamp O and Chauffert B. Confluence dependent resistance (CDR) to doxorubicin and E-cadherin expression in murine mammary cells. Cancer Letters 85(2): 171-176, 1994.

181. Resnicoff M, Medrano EE, Podhajcer OL, Bravo AI, Bover L and Mordoh J. Subpopulations of MCF-7 cells separated by Percoll gradient centrifugation: A model to analyse the heterogeneity of human breast cancer. Proc. Natl. Acad. Sci. USA 84: 7295-7299, 1987.

182. Coley HM, Amos WB, Twentyman PR and Workman P. Examination by laser scanning confocal fluorescence imaging microscopy of the subcellular localisation of anthracyclines in parent and multidrug resistant cell lines. Br. J. Cancer 67: 1316-1323, 1993.

183. Lau DHM, Duran GE and Sikic BI. Analysis of intracellular retention of morpholinyl anthracyclines in multidrug resistant cancer cells by interactive laser cytometry. Int. J. Oncol. 5: 1273-1277, 1994.

184. Meschini S, Molinari A, Calcabrini A, Citro G and Arancia G. Intracellular localisation of the antitumour drug adriamycin in living cultured cells: a confocal microscope study. Journal of Microscopy 176(3): 204-210, 1994.

185. Marquardt D and Center MS. Drug transport mechanisms in HL60 cells isolated for resistance to adriamycin: Evidence for nuclear drug accumulation and redistribution in resistant cells. Cancer Research 52: 3157-3163, 1992.

186. Smith PJ, Sykes HR, Fox ME and Furlong IJ. Subcellular distribution of the anticancer drug mitoxantrone in human and drug-resistant murine cells analyzed by flow cytometry and confocal microscopy and its relationship to the induction of DNA damage. Cancer Research 52: 4000-4008, 1992.

187. Lown JW and Hanstock CC. High field ^{1}H-NMR analysis of the 1:1 intercalation complex of the antitumour agent mitoxantrone and the DNA duplex $[d(CpGpCpG)]_2$. J. Biomol. Struct. Dyn. 2 (6): 1097-1106, 1985.

188. Duffy PM, Hayes MC, Cooper A and Smart CJ. Confocal microscopy of

idarubicin localisation in sensitive and multidrug-resistant bladder cancer cell lines. Br. J of Cancer 74: 906-909, 1996.

189. Heck MMS, Hillelman WN and Earnshaw WC. Differential expression of DNA topoisomerase I and II during the eukaryotic cell cycle. Proc. Natl. Acad. Sci. USA 85: 1086-1090, 1988.

190. Mulder HS, Dekker H, Pinedo HM and Lankelma J. The P-glycoprotein-mediated relative decrease in cytosolic free drug concentration is similar for several anthracyclines with varying lipophilicity. Biochem. Pharmacol. 50(7): 967-974, 1995

191. Mikkelson RB, Lin PS and Wallach DFH. Interaction of adriamycin with human red blood cells: a biochemical and morphological study. J. Mol. Med. 2: 33-40, 1977.

192. Tritton TR, Murphree SA and Sartorelli AC. Adriamycin: a proposal on the specificity of drug action. Biochem. Biophys. Res. Commun. 84(3): 802-808, 1978.

193. Jiang WG, Hiscox S, Hallett MB, Scott C, Horrobin DF and Puntis MCA. Inhibition of hepatocyte growth factor-induced motility and *in vitro* invasion of human colon cancer cells by gamma-linolenic acid. Br. J. Cancer 71: 744-752, 1995.

194. Jiang WG, Hiscox S, Hallett MB, Horrobin DF, Mansel RE and Puntis MCA. Regulation of the expression of E-cadherin on human cancer cells by γ-Linolenic acid (GLA). Cancer Research 55: 5043-5048, 1995.

195. Schuurhius GJ, Broxterman HJ, de Lange JHM, Pinedo HM, van Heijningen THM, Kuiper CM, Scheffer GL, Scheper RJ, van Kalken CK, Baak JPA and Lankelma J. Early multidrug resistance, defined by changes in intracellular doxorubicin distribution, independent of P-glycoprotein. Br. J. Cancer 64: 857-861, 1991.

196. Veneroni S, Zaffaroni N, Daidone MG, Benini R, Villa R and Silvestrini R. Expression of P-glycoprotein and *in vitro* and *in vivo* resistance to doxorubicin and cisplatin in breast and ovarian cancers. Eur. J Cancer 30A(7): 1002-1007,1994.

197. Greenblatt MS, Bennett WP, Holstein M and Harris CC. Mutations in the p53 tumour suppressor gene: Clues to cancer etiology and molecular pathogenesis. Cancer Research 54 (18): 4855- 4878, 1994.

198. Fairchild CR, Ivy PS, Kao-Shan C-S, Whang-Peng J, Rosen N, Israel MA, Melera PW, Cowan KH and Goldsmith ME. Cancer Research 47: 5141, 1987.
199. Personal communication from Betty Swann-Taylor and John Masters at the Institute of Urology, University College London.

9. APPENDICES

9.1. APPENDIX 1

CELLULAR DRUG UPTAKE SHOWN BY USING THE FACSCAN

The raw data for the cellular drug uptake of one drug by the cell lines are shown in this appendix. Epirubicin uptake over time and dose response histograms along with the effect of GLA incorporation by MGH-U1 and MGH-U1/R cells. The MCF-7 and MCF-7/R cells are shown for the similar experiments using DOX (Fig. 9.1). This work is presented over pages 199 to 222.

9.2. APPENDIX 2

FLOW CYTOMETRY METHODOLOGY EXPERIMENTS

THE USE OF INCLUSION / EXCLUSION GATES

The dot plots produced from the cell lines were often very spread out especially for the sensitive cells, in particular the MCF-7 cell line. This may be due to cellular heterogeneity in shape and size, doublets and clusters of cells and dead cells. The resistant cells appeared to be more homogenous in shape and size producing a tighter dot plot of cell population. All cell lines had debris either from the medium or cellular debris probably from the trypsinisation process. This debris was observed with all cell lines regardless of their method of drug incubation, *i.e* in cellular suspension or attached to the flasks. The debris is typically smaller than the cells and appears on the dot plots as a cluster in the bottom left hand corner. In the pilot experiments these were excluded from the recordings using an exclusion gate. At this stage they were the only particles in the cell suspension to be excluded (Fig. 9.2).

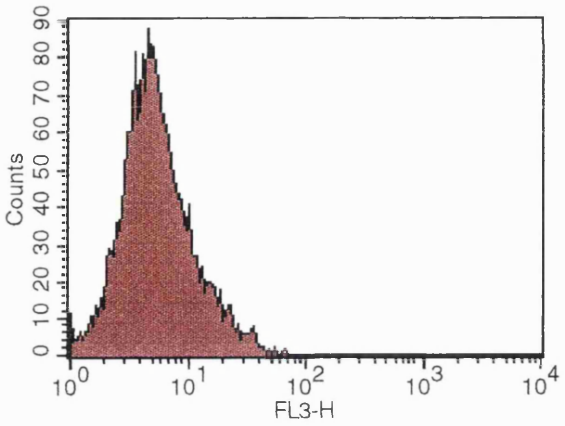

Geo Mean	Median
5.33	5.00

MGH-U1 S CONTROL

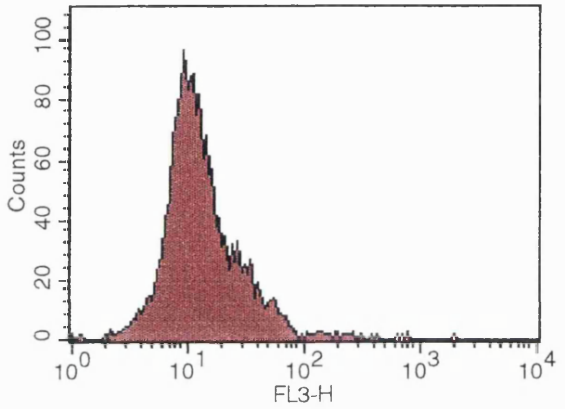

Geo Mean	Median
12.52	11.14

MGH-U1 S EPI 10'

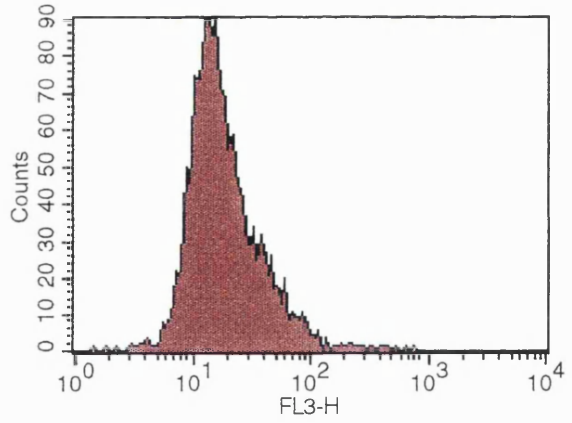

Geo Mean	Median
17.42	15.54

MGH-U1 S EPI 20'

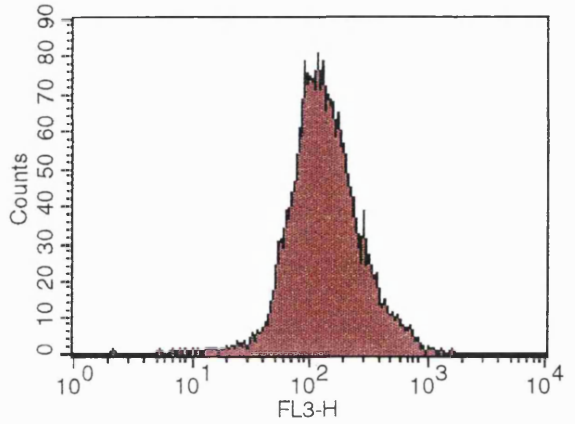

Geo Mean	Median
127.75	121.88

MGH-U1 S EPI 40'

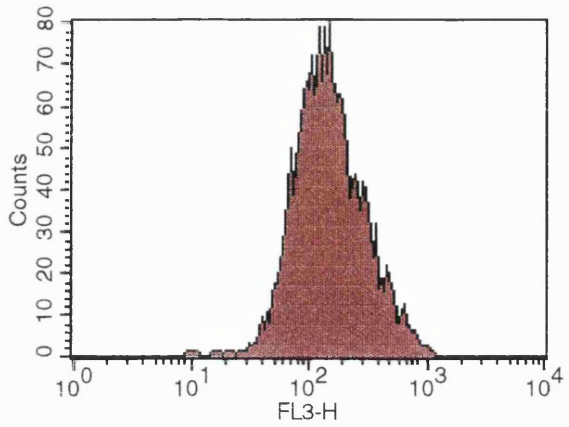

Geo Mean	Median
141.27	134.56

MGH-U1 S EPI 60'

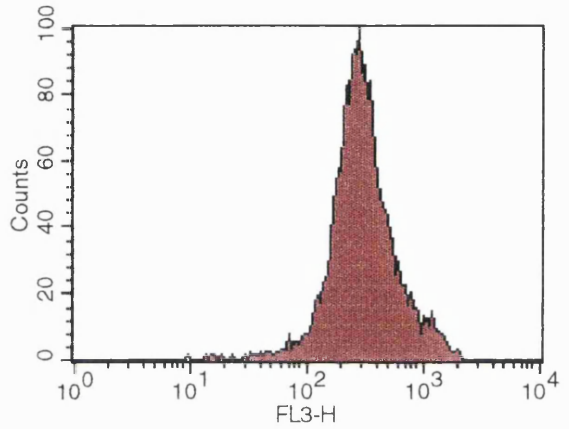

Geo Mean	Median
283.77	271.39

MGH-U1 S EPI 90'

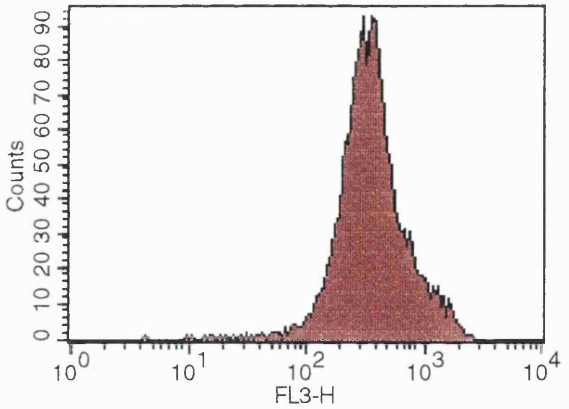

Geo Mean	Median
344.22	330.77

MGH-U1 S EPI 120'

Fig. 9.1a. **Histograms of EPI uptake over time in MGH-U1 cells. Mean of intracellular drug fluorescence as arbritary units from the FACScan.**

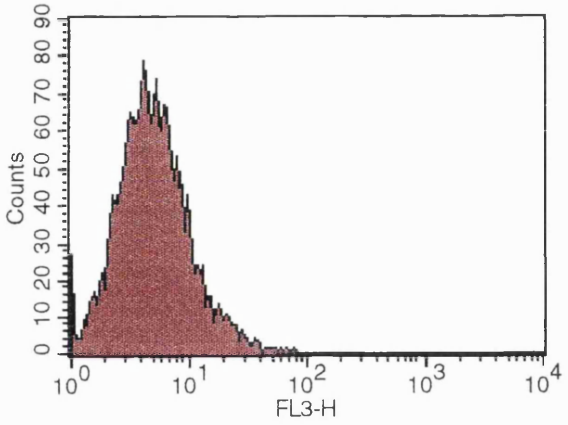

Geo Mean	Median
4.84	4.70

MGH-U1 R CONTROL

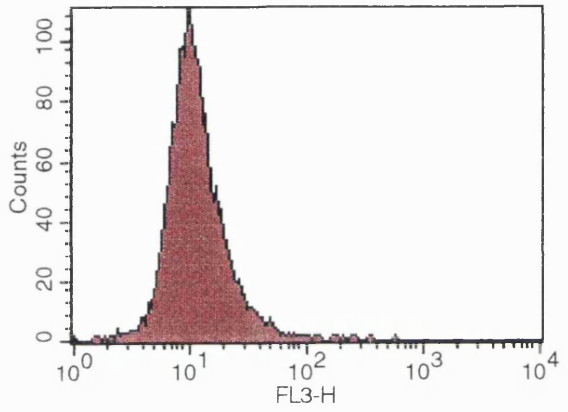

Geo Mean	Median
10.86	10.27

MGH-U1 R EPI 10'

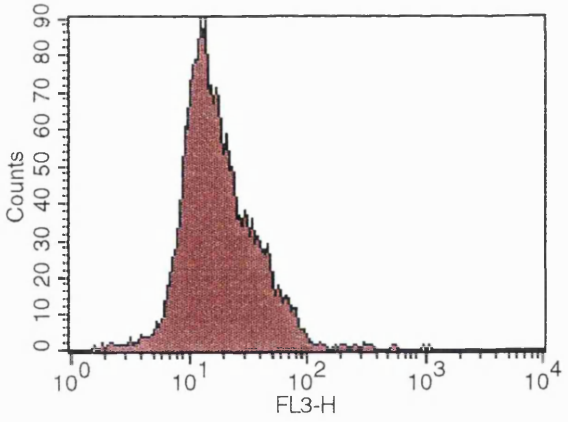

Geo Mean	Median
17.16	15.40

MGH-U1 R EPI 20'

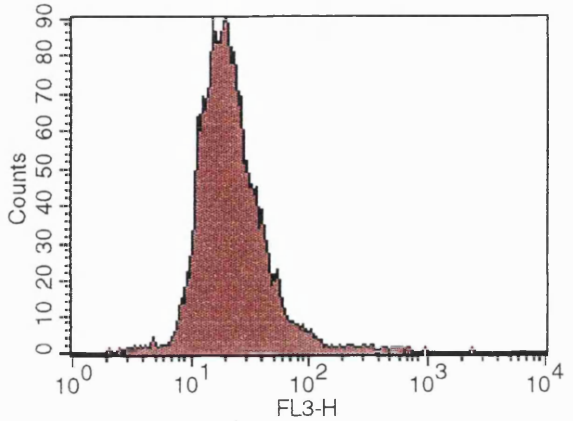

Geo Mean	Median
20.98	19.46

MGH-U1 R EPI 40'

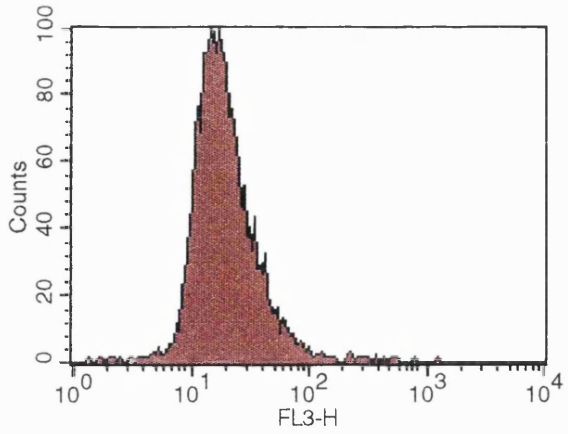

Geo Mean	Median
18.38	17.00

MGH-U1 R EPI 60'

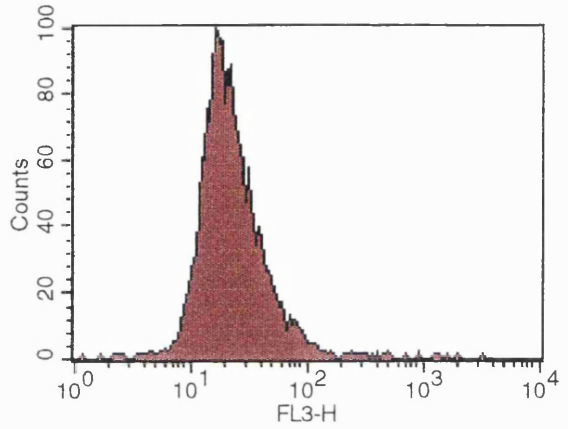

Geo Mean	Median
21.07	19.46

MGH-U1 R EPI 90'

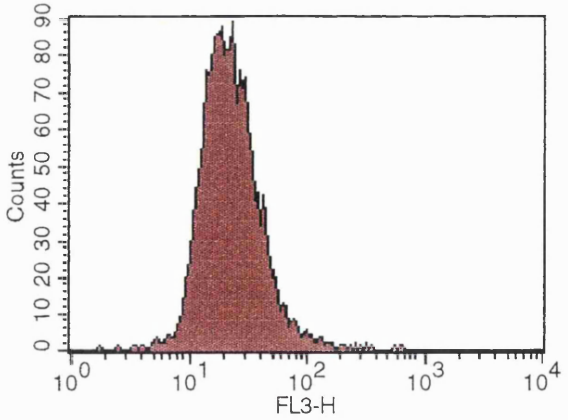

Geo Mean	Median
21.66	20.91

MGH-U1 R EPI 120'

Fig.9.1b. **Histograms of EPI uptake over time in MGH-U1/R cells. Mean of intracellular drug fluorescence as arbitrary units from the FACScan.**

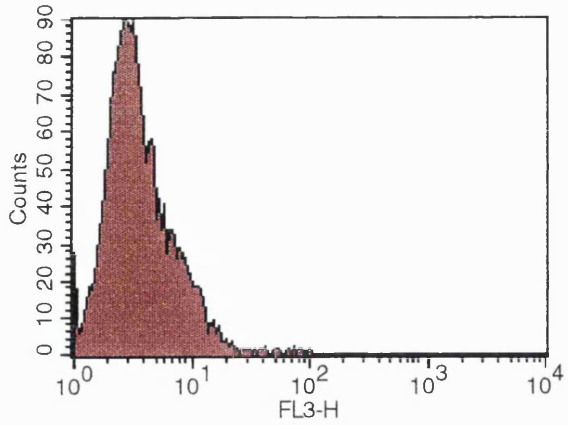

Geo Mean	Median
3.49	3.16

MGH-U1 S Control

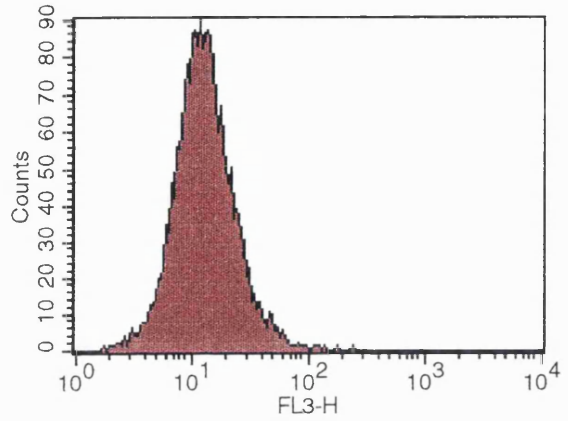

Geo Mean	Median
12.38	12.08

MGH-U1 S EPI 1µg/ml

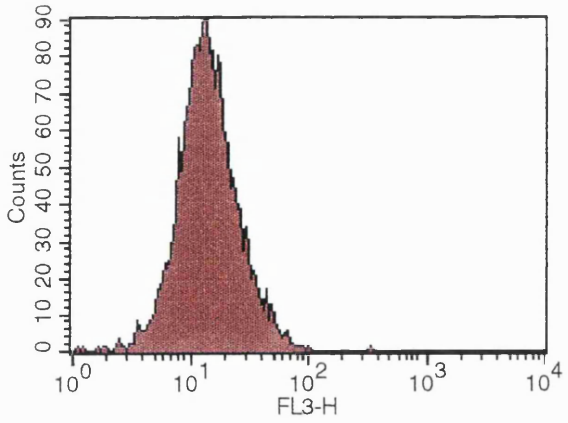

Geo Mean	Median
13.92	13.58

MGH-U1 S EPI 2µg/ml

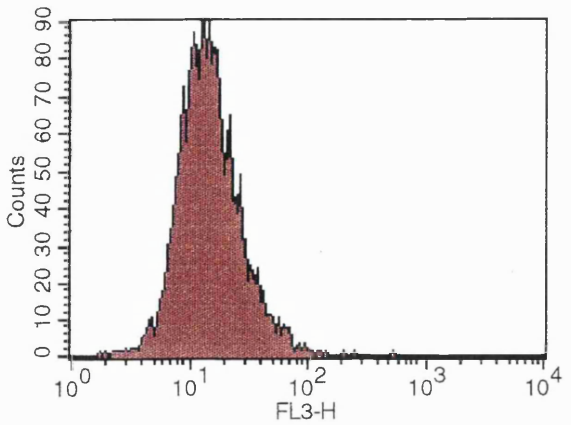

Geo Mean	Median
14.41	13.70

MGH-U1 S EPI 5µg/ml

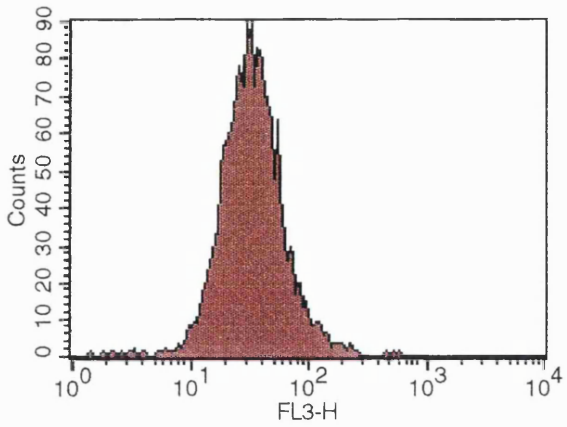

Geo Mean	Median
32.18	31.91

MGH-U1 S EPI 10µg/ml

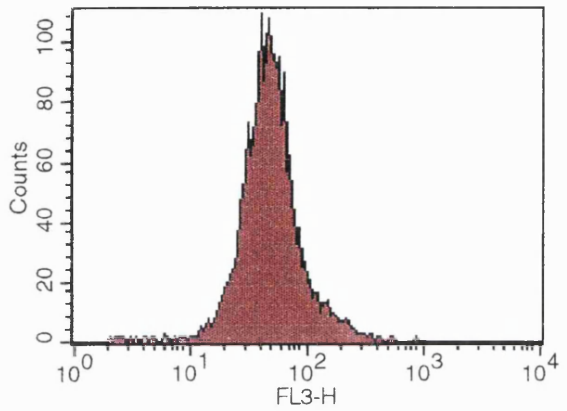

Geo Mean	Median
45.98	44.91

MGH-U1 S EPI 15µg/ml

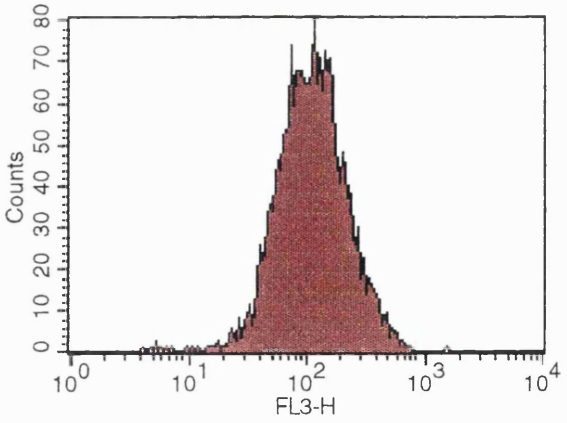

Geo Mean	Median
106.33	105.54

MGH-U1 S EPI 20µg/ml

Fig. 9.1c. **Histograms of EPI dose response in MGH-U1 cells. Mean of intracellular drug fluorescence as arbitrary units from the FACScan.**

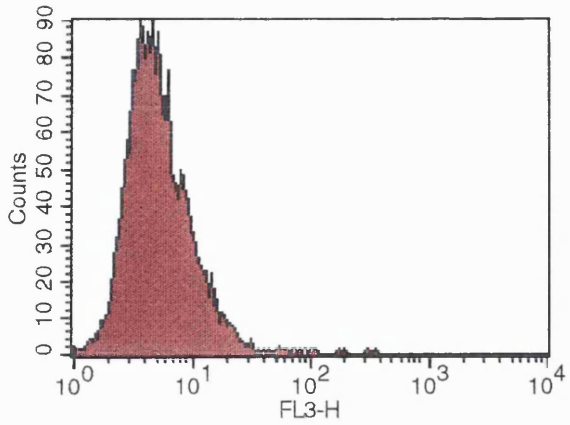

Geo Mean	Median
4.92	4.53

MGH-U1 R Control

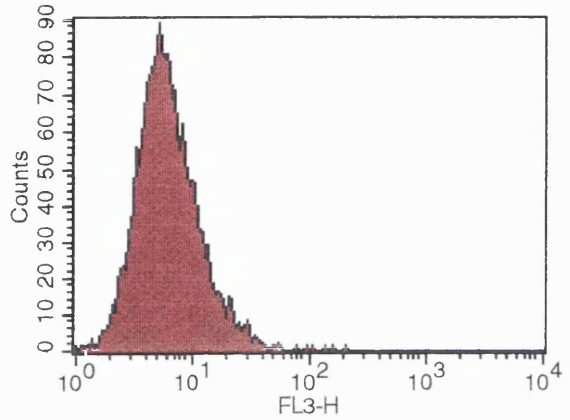

Geo Mean	Median
5.95	5.62

MGH-U1 R EPI 1μg/ml

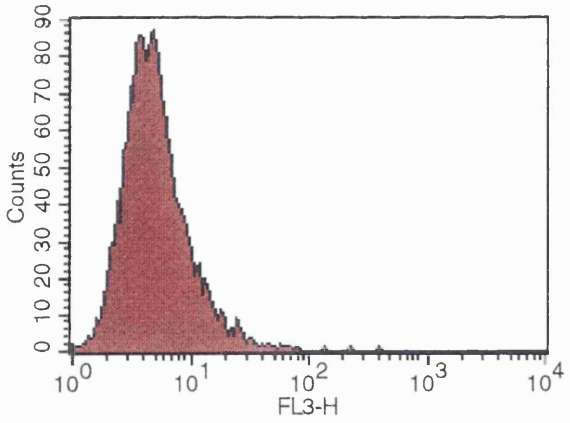

Geo Mean	Median
4.88	4.53

MGH-U1 R EPI 2μg/ml

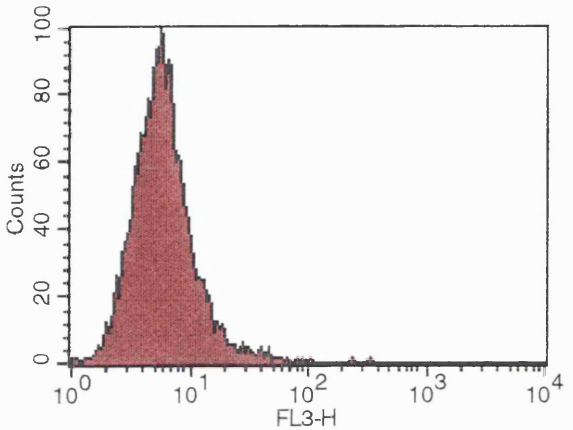

Geo Mean	Median
5.69	5.47

MGH-U1 R EPI 5μg/ml

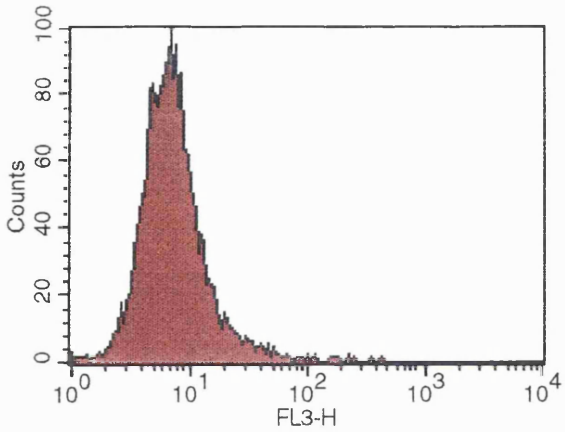

Geo Mean	Median
6.99	6.67

MGH-U1 R EPI 10µg/ml

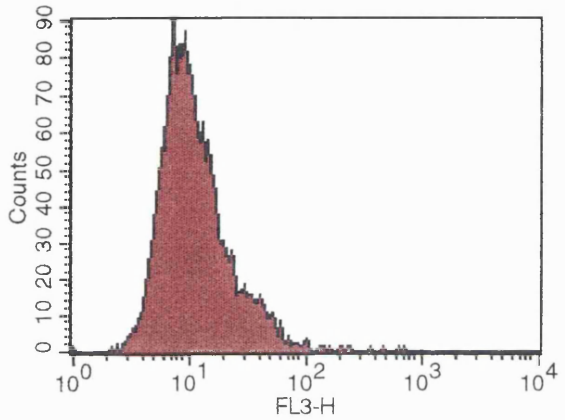

Geo Mean	Median
10.35	9.39

MGH-U1 R EPI 15µg/ml

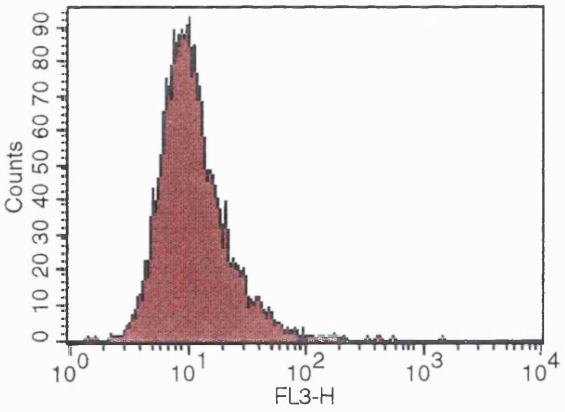

Geo Mean	Median
10.50	9.73

MGH-U1 R EPI 20µg/ml

Fig. 9.1d. **Histograms of EPI dose response in MGH-U1/R cells. Mean of intracellular drug fluorescence as arbitrary units from the FACScan.**

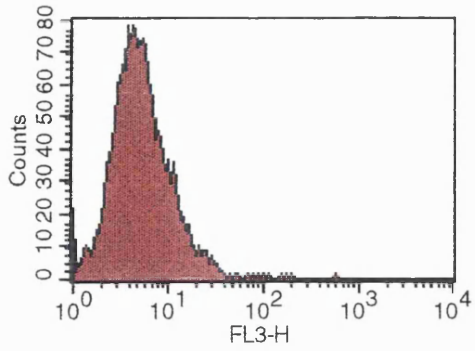

Geo Mean	Median
5.09	4.78

MGH-U1/S Control

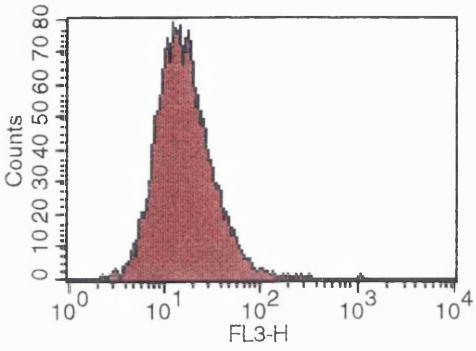

Geo Mean	Median
15.24	14.46

MGH-U1/S EPI 5µg/ml

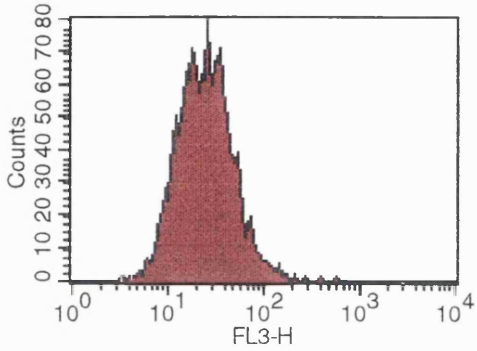

Geo Mean	Median
23.14	23.08

MGH-U1/S EPI 5µg/ml

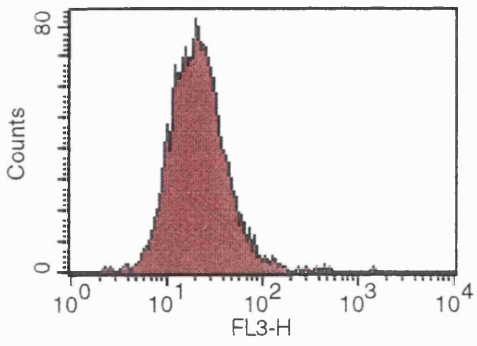

Geo Mean	Median
20.33	19.81

MGH-U1/S EPI 10µg/ml

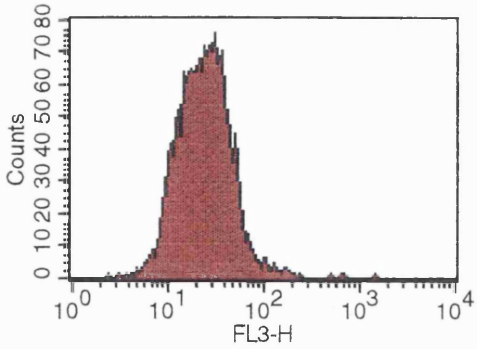

Geo Mean	Median
22.88	23.08

MGH-U1/S EPI 10µg/ml

Fig. 9.1e. **Histograms of EPI uptake in GLA untreated MGH-U1 cells. Mean of intracellular drug fluorescence as arbitrary units from the FACScan.**

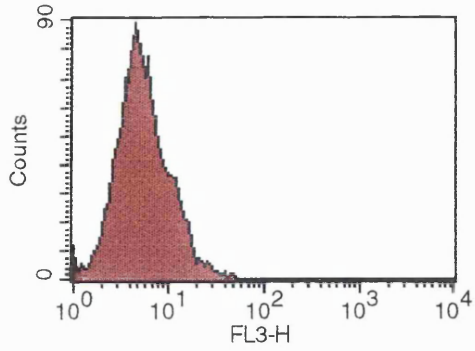

Geo Mean	Median
5.28	5.05

MGH-U1/S + GLA Control

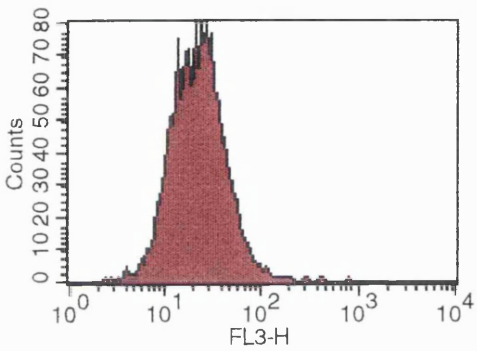

Geo Mean	Median
20.86	20.54

MGH-U1/S + GLA EPI 5µg/ml

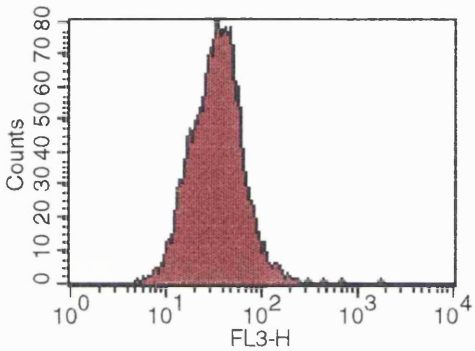

Geo Mean	Median
31.78	32.49

MGH-U1/S + GLA EPI 5µg/ml

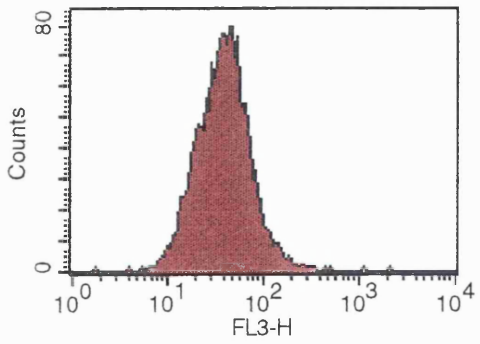

Geo Mean	Median
36.43	37.18

MGH-U1/S + GLA EPI 10µg/ml

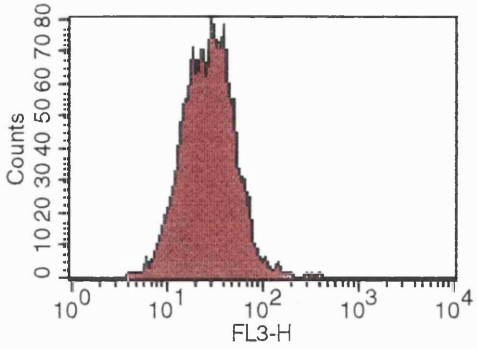

Geo Mean	Median
25.73	26.18

MGH-U1/S + GLA EPI 10µg/ml

Fig. 9.1f. **Histograms of EPI uptake in GLA treated MGH-U1 cells. Mean of intracellular drug fluorescence as arbitrary units from the FACScan.**

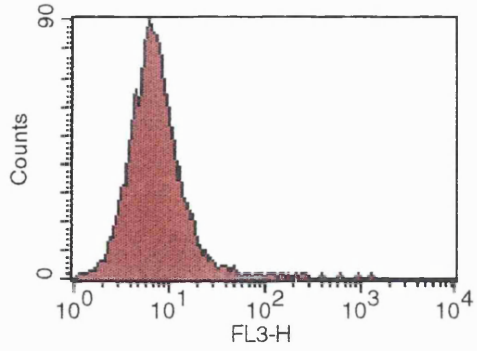

Geo Mean	Median
6.88	6.67

MGH-U1/R Control

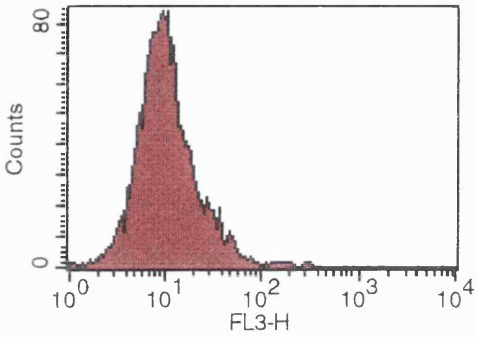

Geo Mean	Median
9.70	9.14

MGH-U1/R EPI 5μg/ml

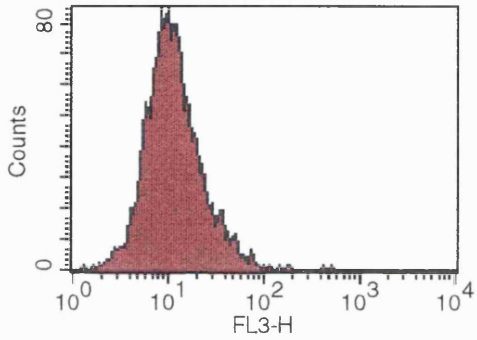

Geo Mean	Median
10.99	10.37

MGH-U1/R EPI 5μg/ml

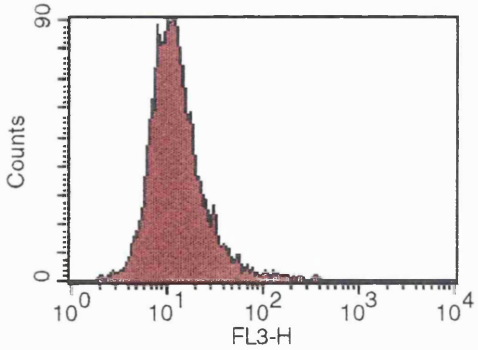

Geo Mean	Median
11.75	11.09

MGH-U1/R EPI 10μg/ml

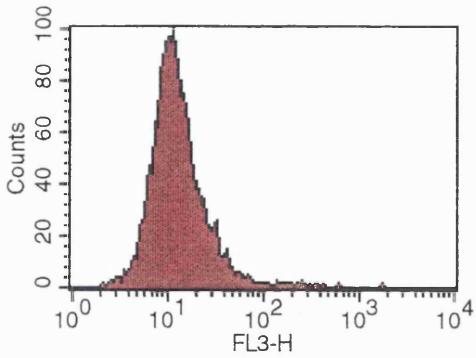

Geo Mean	Median
11.95	11.24

MGH-U1/R EPI 10μg/ml

Fig. 9.1g. **Histograms of EPI uptake in GLA untreated MGH-U1/R cells. Mean of intracellular drug fluorescence as arbitrary units from the FACScan.**

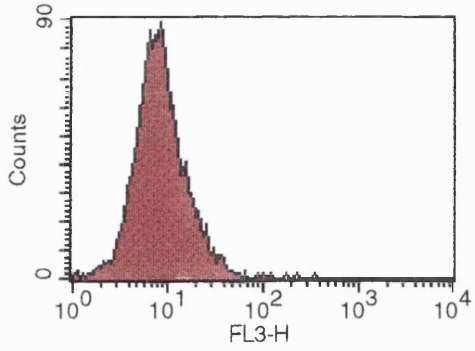

Geo Mean	Median
8.22	7.91

MGH-U1/R +GLA Control

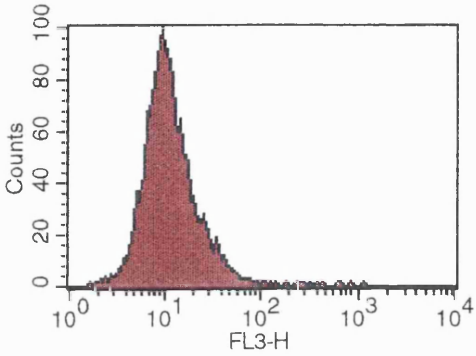

Geo Mean	Median
10.55	9.91

MGH-U1/R +GLA EPI 5µg/ml

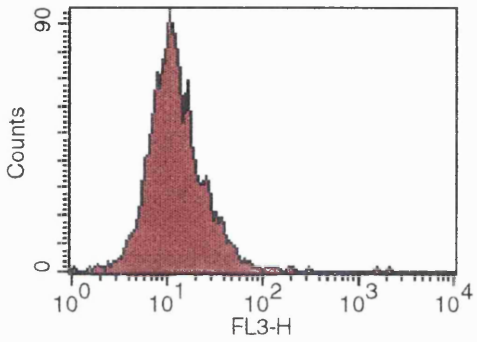

Geo Mean	Median
11.71	11.04

MGH-U1/R +GLA EPI 5µg/ml

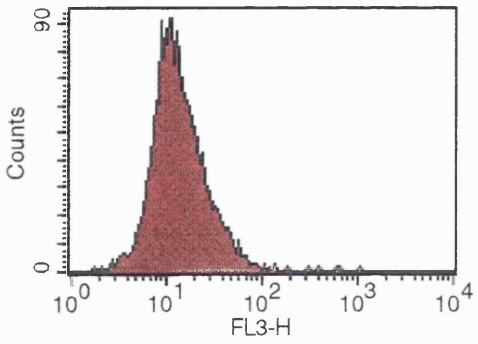

Geo Mean	Median
13.07	12.19

MGH-U1/R +GLA EPI 10µg/ml

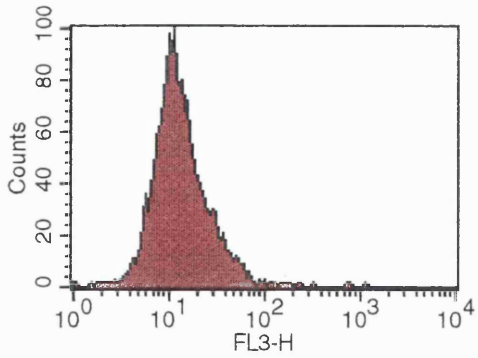

Geo Mean	Median
12.53	11.76

MGH-U1/R +GLA EPI 10µg/ml

Fig. 9.1h. **Histograms of EPI uptake in GLA treated MGH-U1/R cells. Mean of intracellular drug fluorescence as arbitrary units from the FACScan.**

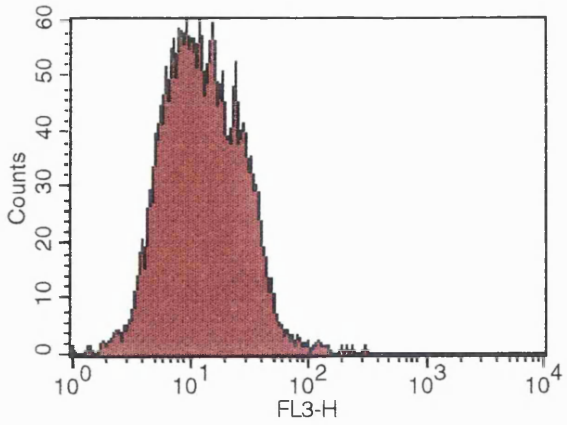

Geo Mean	Median
12.13	11.55

MCF7 S Control

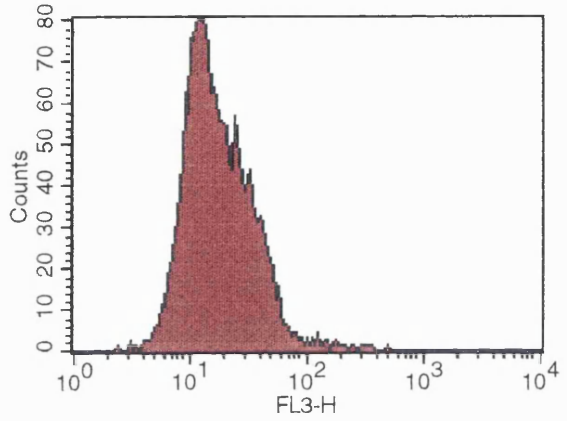

Geo Mean	Median
16.51	14.99

MCF7 S DOX 10'

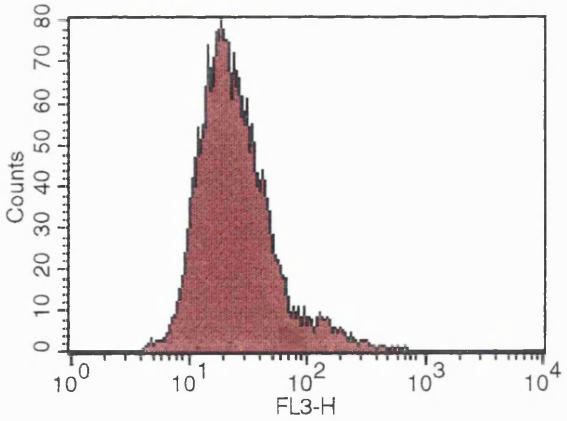

Geo Mean	Median
23.49	21.48

MCF7 S DOX 20'

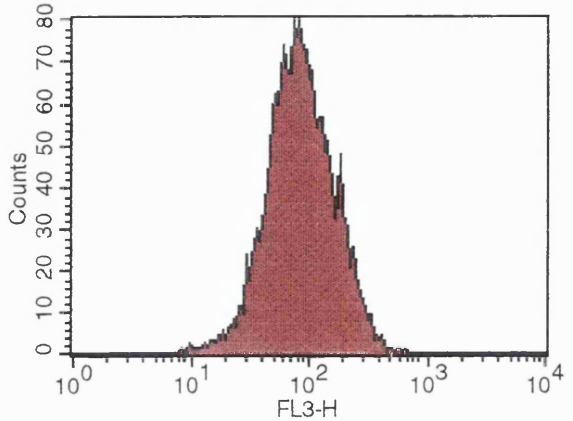

Geo Mean	Median
81.78	80.58

MCF7 S DOX 40'

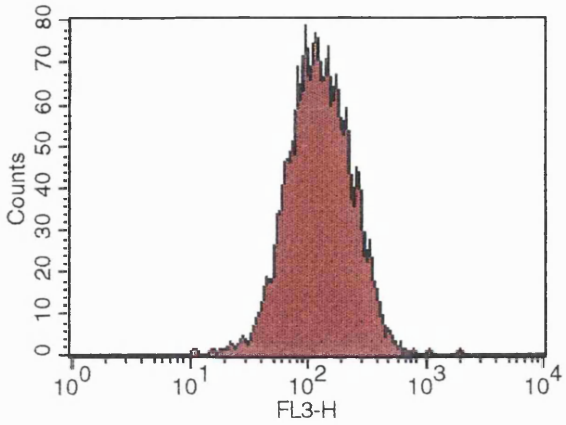

Geo Mean	Median
119.93	118.64

MCF7 S DOX 60'

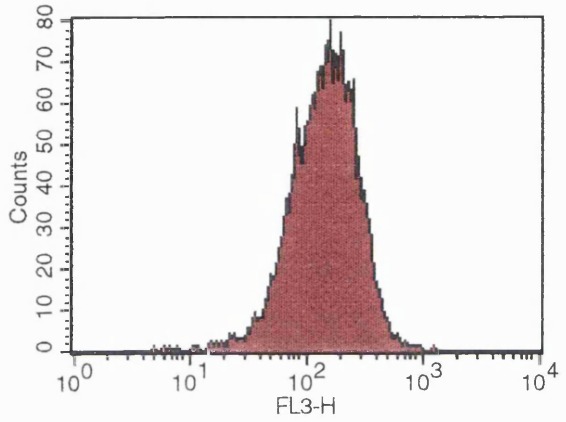

Geo Mean	Median
134.67	139.49

MCF7 S DOX 90'

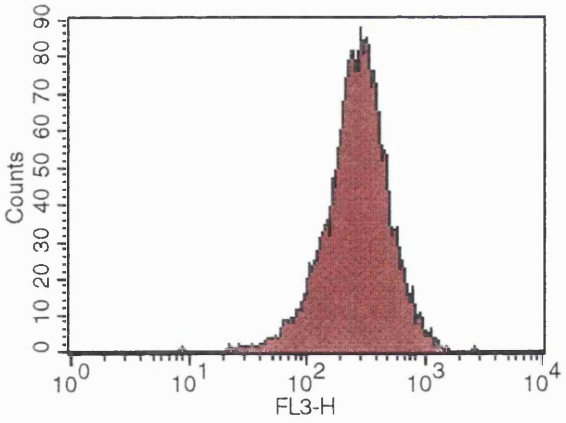

Geo Mean	Median
256.93	264.16

MCF7 S DOX 120'

Fig. 9.1i. **Histograms of DOX uptake over time in MCF-7 cells. Mean of intracellular drug fluorescence as arbitrary units from the FACScan.**

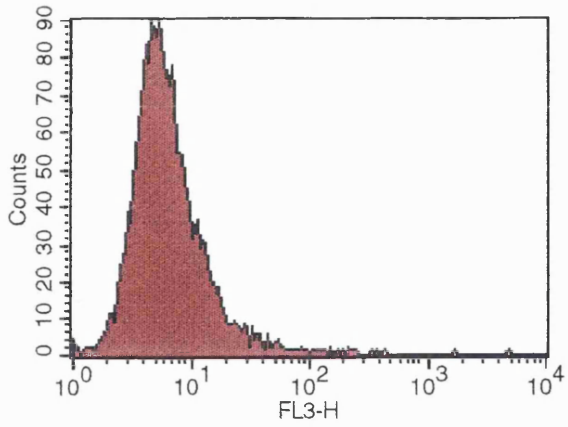

Geo Mean	Median
6.09	5.57

MCF7 R Control

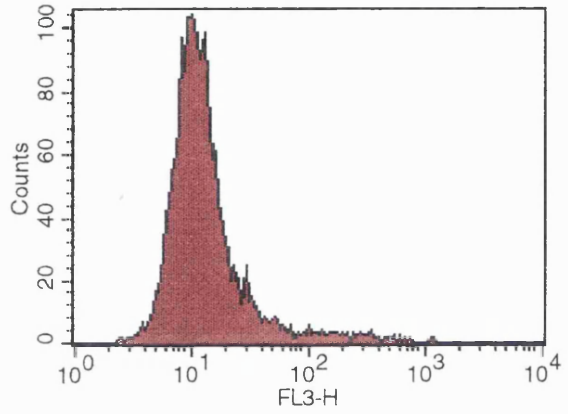

Geo Mean	Median
11.80	10.65

MCF7 R DOX 10'

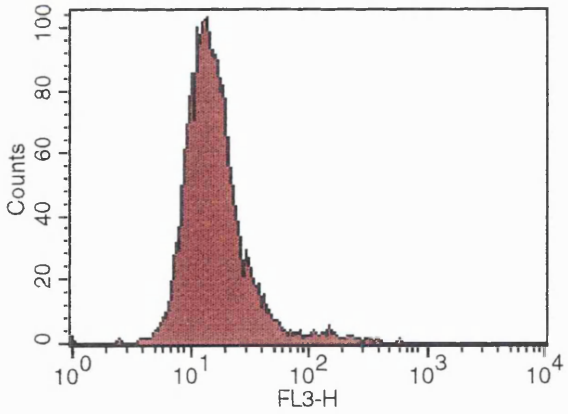

Geo Mean	Median
15.41	14.33

MCF7 R DOX 20'

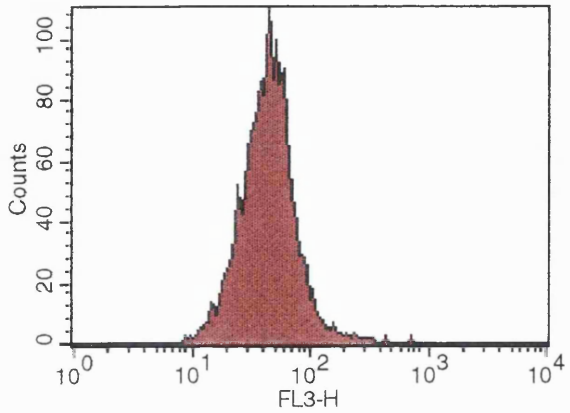

Geo Mean	Median
42.22	42.94

MCF7 R DOX 40'

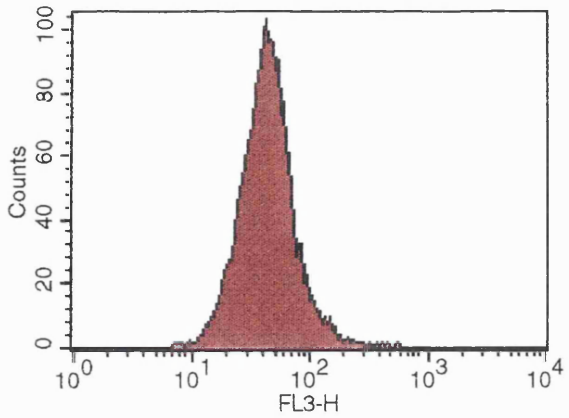

Geo Mean	Median
41.77	42.17

MCF7 R DOX 60'

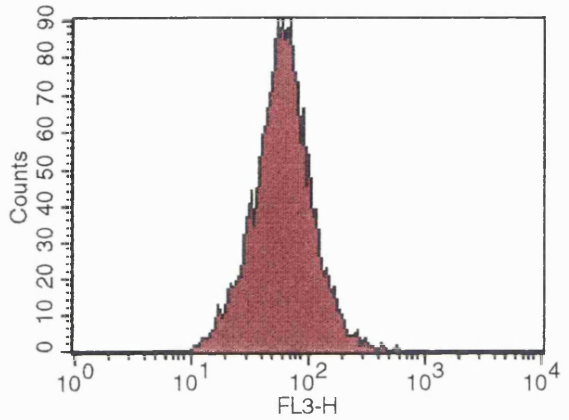

Geo Mean	Median
57.70	58.29

MCF7 R DOX 90'

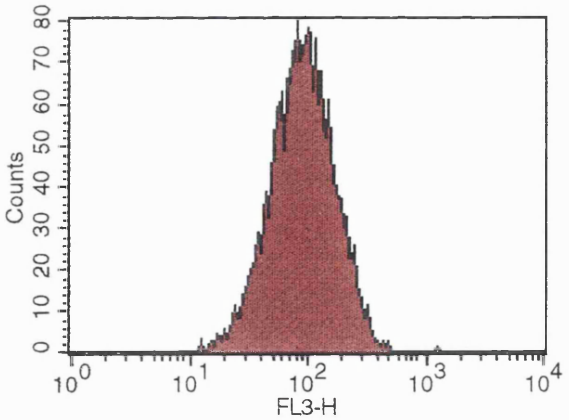

Geo Mean	Median
85.90	86.60

MCF7 R DOX 120'

Fig. 9.1j. **Histograms of DOX uptake over time in MCF-7/R cells. Mean of intracellular drug fluorescence as arbitrary units from the FACScan.**

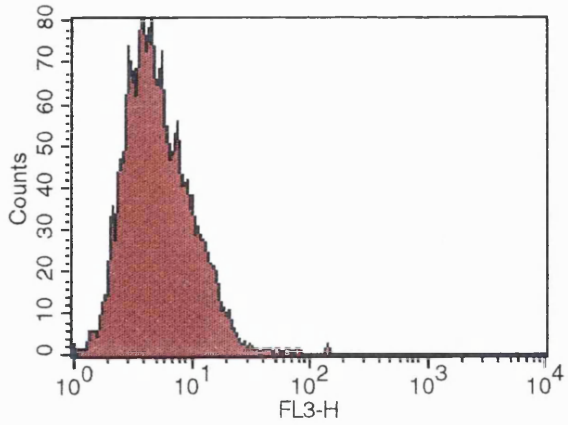

Geo Mean	Median
5.08	4.70

MCF7/S Control

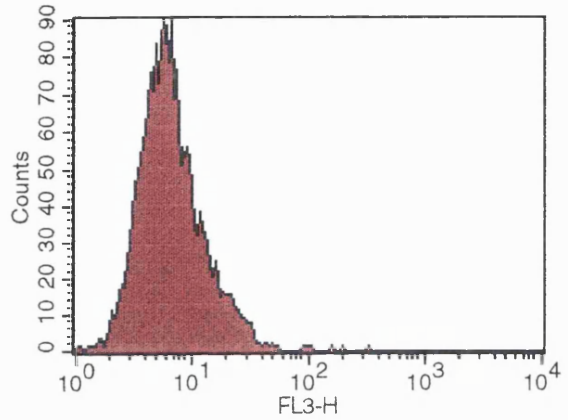

Geo Mean	Median
6.43	5.99

MCF7/S DOX 1µg/ml

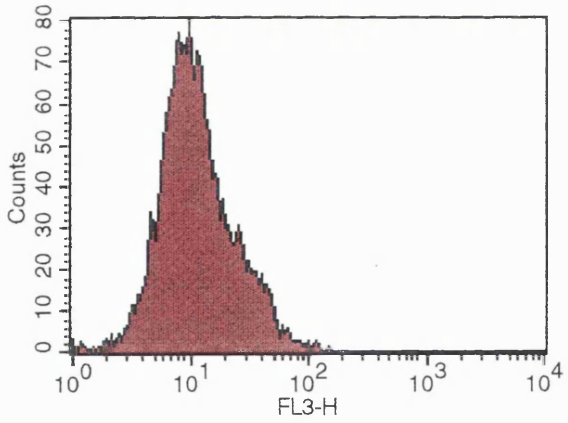

Geo Mean	Median
11.08	10.27

MCF7/S DOX 2µg/ml

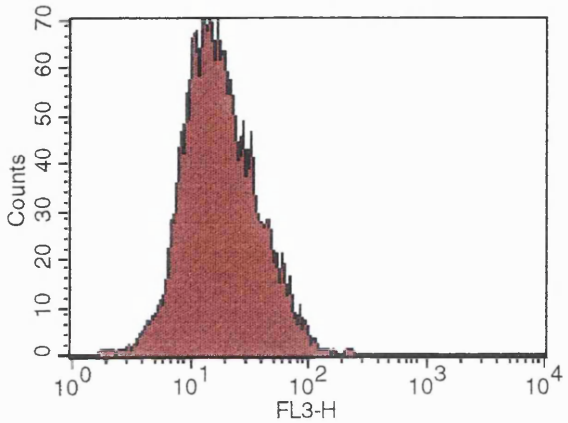

Geo Mean	Median
17.40	16.40

MCF7/S DOX 5µg/ml

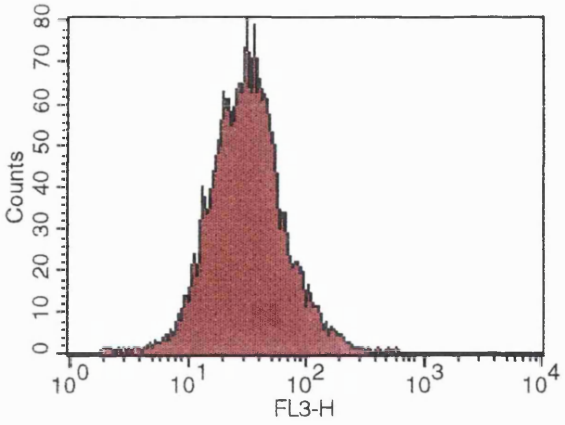

Geo Mean	Median
30.72	30.23

MCF7/S DOX 10µg/ml

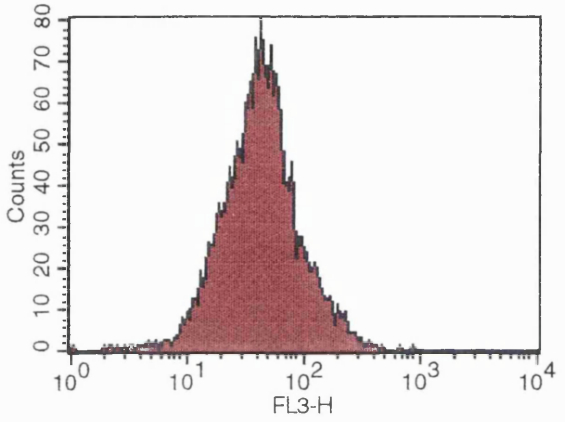

Geo Mean	Median
40.94	40.32

MCF7/S DOX 15µg/ml

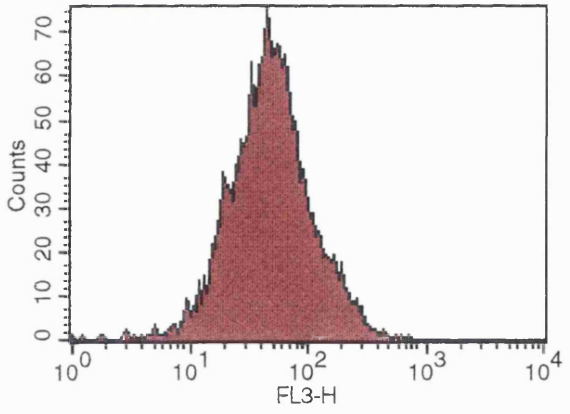

Geo Mean	Median
46.30	46.14

MCF7/S DOX 20µg/ml

Fig. 9.1k. **Histograms of DOX dose response in MCF-7 cells. Mean of intracellular drug fluorescence as arbitrary units from the FACScan.**

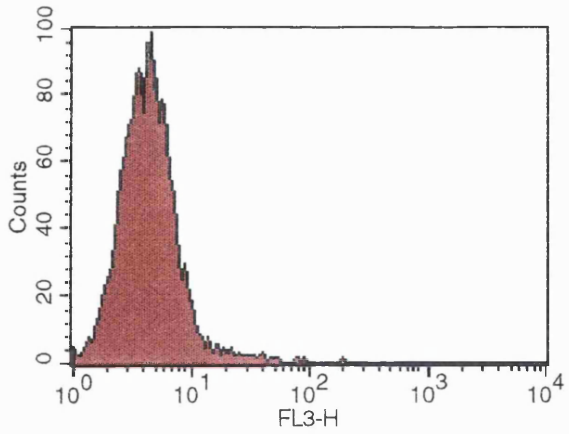

Geo Mean	Median
4.23	4.18

MCF7/R Control

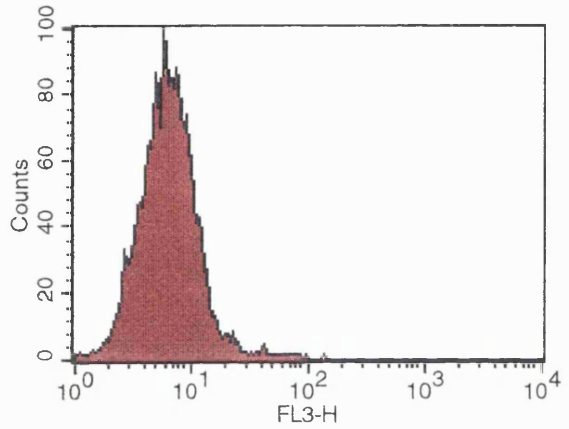

Geo Mean	Median
6.13	6.15

MCF7/R DOX 1μg/ml

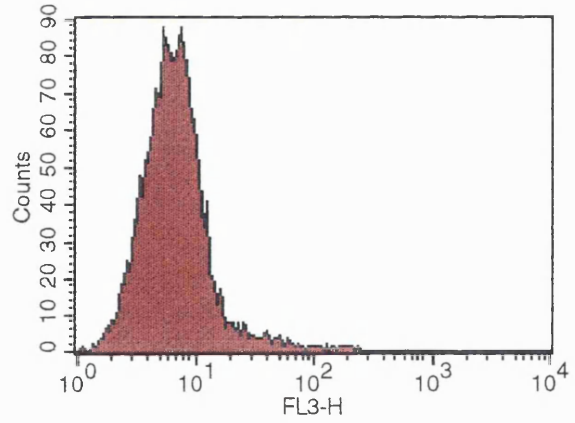

Geo Mean	Median
6.37	6.26

MCF7/R DOX 2μg/ml

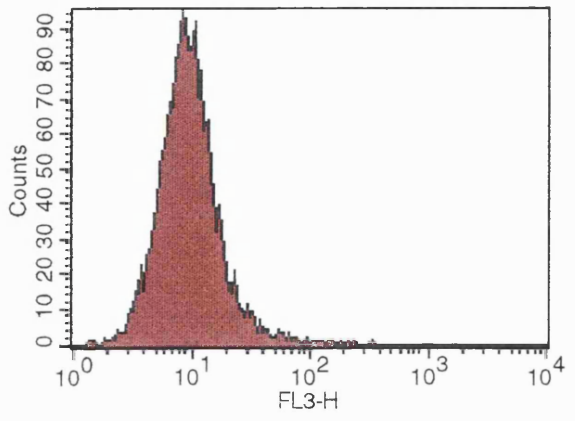

Geo Mean	Median
9.12	8.90

MCF7/R DOX 5μg/ml

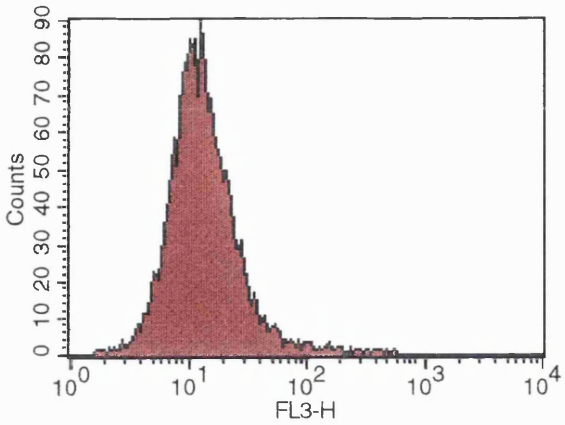

Geo Mean	Median
12.65	12.08

MCF7/R DOX 10µg/ml

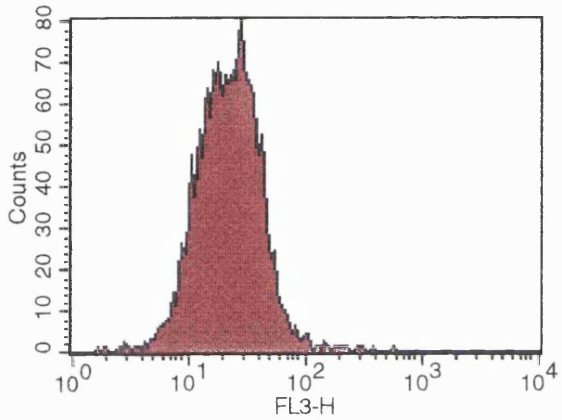

Geo Mean	Median
21.12	21.29

MCF7/R DOX 15µg/ml

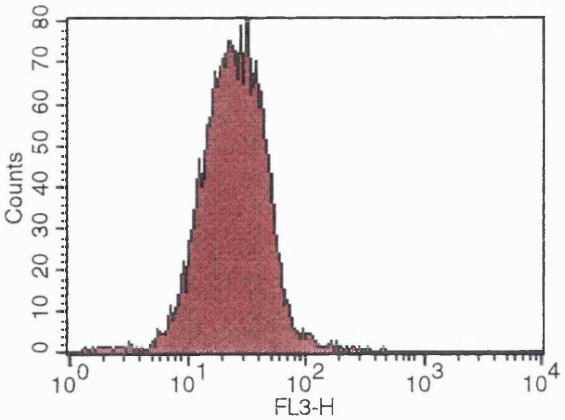

Geo Mean	Median
23.89	24.14

MCF7/R DOX 20µg/ml

Fig. 9.11. **Histograms of DOX dose response in MCF-7/R cells. Mean of intracellular drug fluorescence as arbitrary units from the FACScan.**

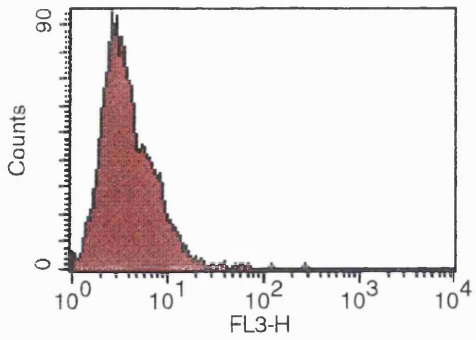

Geo Mean	Median
3.66	3.34

MCF-7/S Control

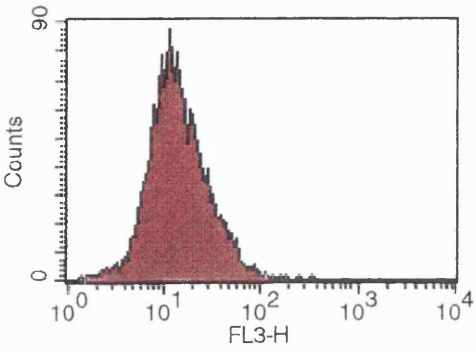

Geo Mean	Median
13.26	12.52

MCF-7/S DOX 5µg/ml

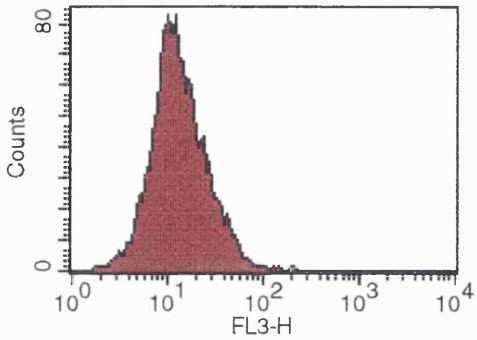

Geo Mean	Median
12.54	11.97

MCF-7/S DOX 5µg/ml

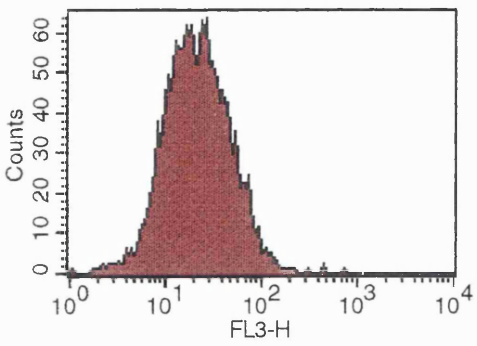

Geo Mean	Median
20.61	20.17

MCF-7/S DOX 10µg/ml

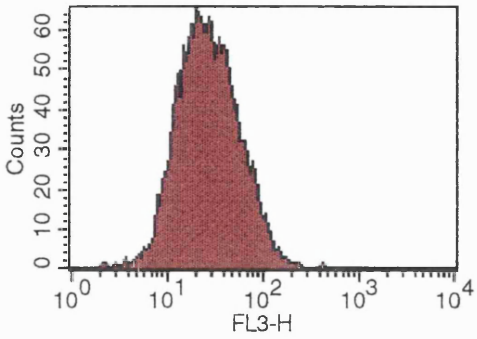

Geo Mean	Median
25.67	25.03

MCF-7/S DOX 10µg/ml

Fig. 9.1m. **Histograms of DOX uptake in GLA untreated MCF-7 cells. Mean of intracellular drug fluorescence as arbitrary units from the FACScan.**

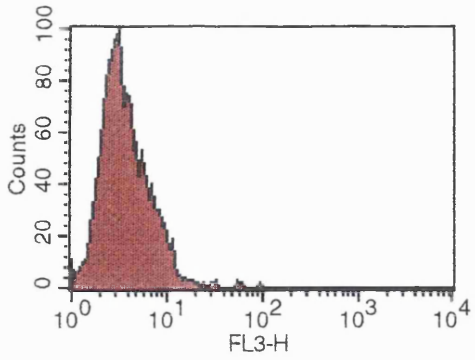

Geo Mean	Median
3.54	3.28

MCF-7/S +GLA Control

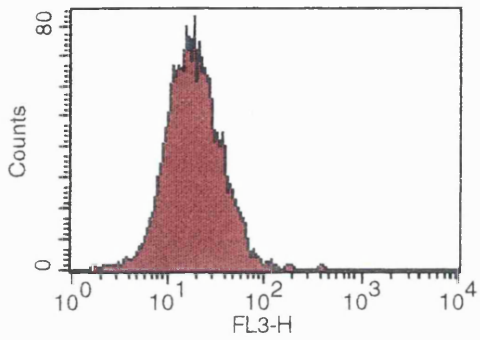

Geo Mean	Median
17.68	17.31

MCF-7/S +GLA DOX 5µg/ml

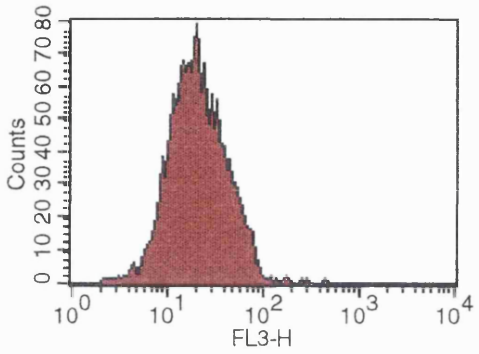

Geo Mean	Median
19.80	19.11

MCF-7/S +GLA DOX 5µg/ml

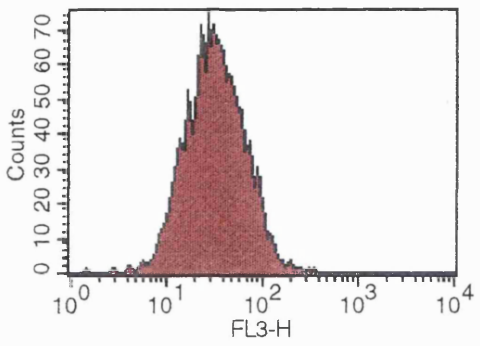

Geo Mean	Median
30.99	30.51

MCF-7/S +GLA DOX 10µg/ml

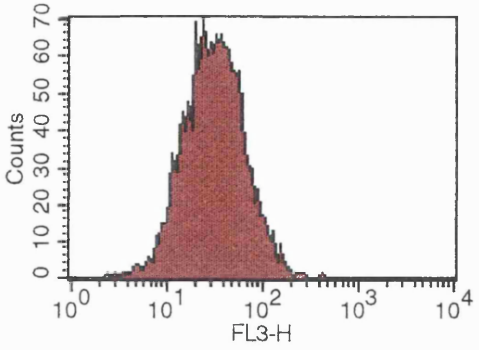

Geo Mean	Median
30.15	30.51

MCF-7/S +GLA DOX 10µg/ml

Fig. 9.1n. **Histograms of DOX uptake in GLA treated MCF-7 cells. Mean of intracellular drug fluorescence as arbitrary units from the FACScan.**

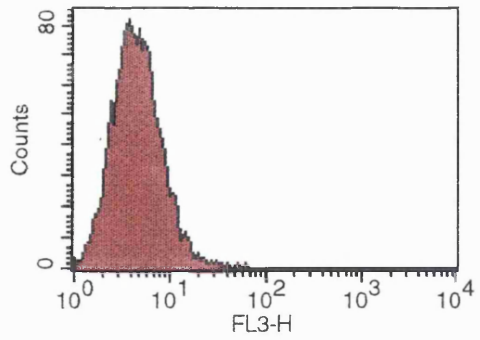

Geo Mean	Median
4.45	4.37

MCF-7/R Control

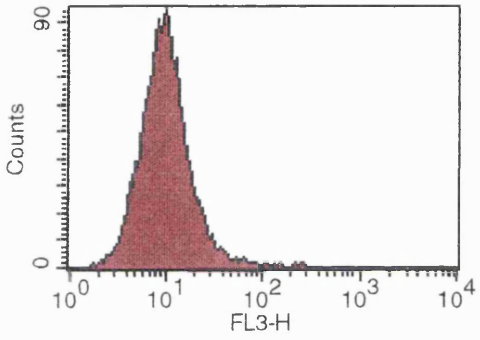

Geo Mean	Median
9.25	9.14

MCF-7/R DOX 5μg/ml

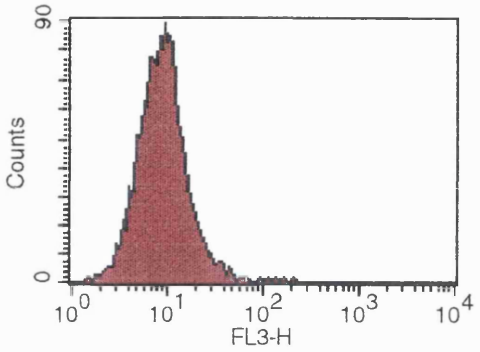

Geo Mean	Median
8.60	8.58

MCF-7/R DOX 5μg/ml

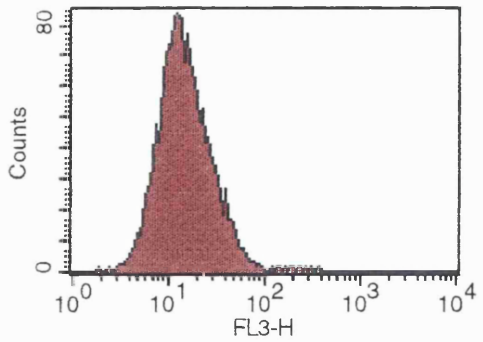

Geo Mean	Median
13.99	13.46

MCF-7/R DOX 10μg/ml

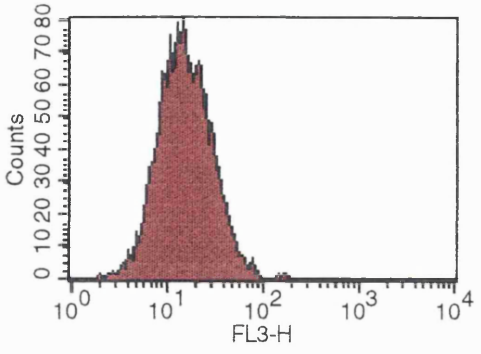

Geo Mean	Median
14.97	14.59

MCF-7/R DOX 10μg/ml

Fig. 9.1o. Histograms of DOX uptake in GLA untreated MCF-7/R cells. Mean of intracellular drug fluorescence as arbitrary units from the FACScan.

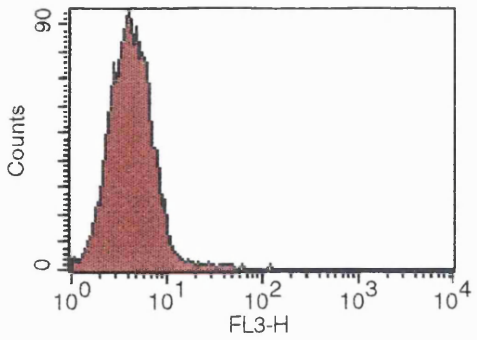

Geo Mean	Median
4.08	4.03

MCF-7/R +GLA Control

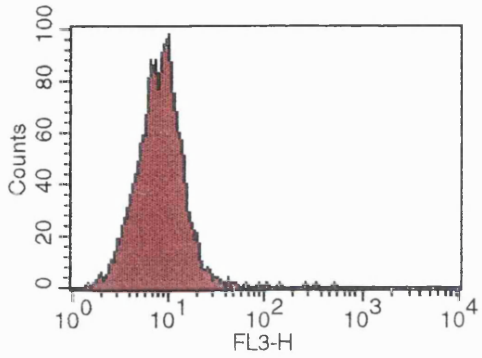

Geo Mean	Median
7.73	7.84

MCF-7/R +GLA DOX 5µg/ml

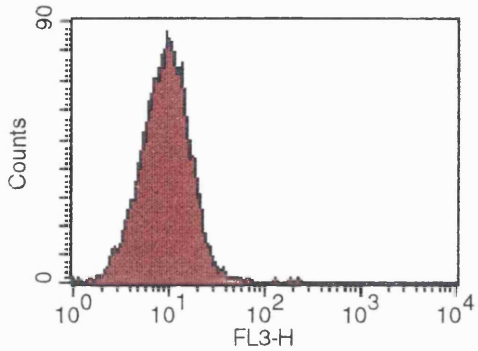

Geo Mean	Median
8.96	9.22

MCF-7/R +GLA DOX 5µg/ml

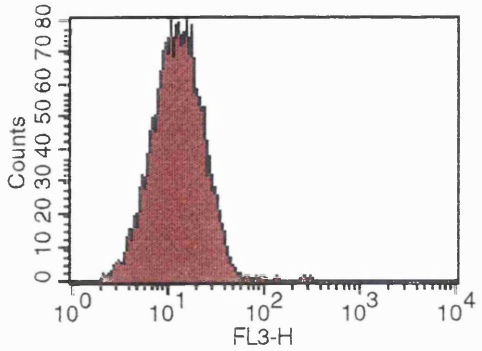

Geo Mean	Median
12.15	12.30

MCF-7/R +GLA DOX 10µg/ml

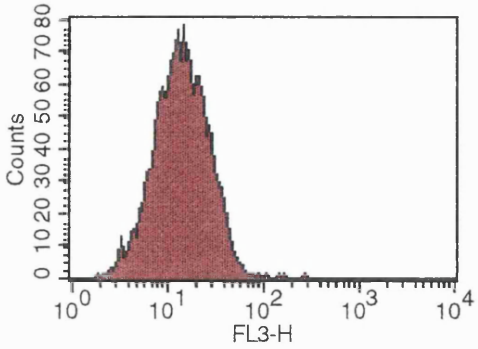

Geo Mean	Median
13.65	13.70

MCF-7/R +GLA DOX 10µg/ml

Fig. 9.1p. **Histograms of DOX uptake in GLA treated MCF-7/R cells. Mean of intracellular drug fluorescence as arbitrary units from the FACScan.**

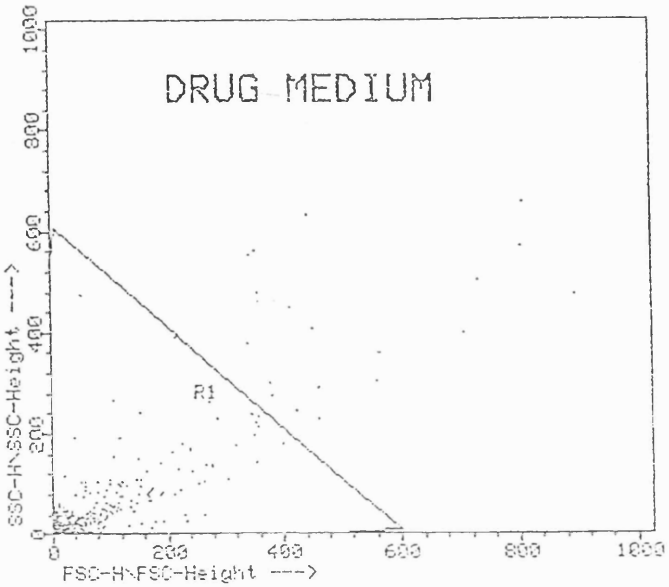

Fig. 9.2.
Dot plot to show exclusion gate originally used in flow cytometry experiments.

It was noted that the dot plots of the four cell lines all contained a main population of cells which were very similar in size and shape. By using an inclusion gate instead of an exclusion gate many of the dead cells and clusters of cells would not be recorded, but only main population of cells which made up the majority of the cell line (Fig. 9.3). Recording the intracellular drug uptake of dead cells and clusters of cells led to an increased reading of mean drug fluorescence since both these groups of cells take up more drug than live cells. This was demonstrated by dividing one population of cells, *i.e.* one flask of MCF-7/R cells into equal portions so that cellular uptake of MTZ could be run in conjunction with a fluorescent marker of cell viability, such as FDA (fluorescein diacetate) which stains live cells. (Figs. 9.4). The population of cells which took up the most MTZ was that which took up little FDA and probably mainly consisted of dead cells. Dead cells take up more drug than live cells probably due to permeablisation of the plasma membrane. This increased drug uptake by dead cells was confirmed by confocal microscopy were dead MGH-U1/R were visualised taking up more EPI then live cells. The pattern of drug uptake in dead resistant cells was similar to that for live sensitive cells (Fig. 9.5).

MCF-7 cells were in this study the most likely to be grouped in clusters and fragile to the various experimental techniques. This meant that they did not go into single cell suspension easily necessary for flowing through the FACScan. The

above properties contributed to producing some very poor dot plots for the MCF-7 cell line. In the end, regardless of cell type or their propensity to form clusters, inclusion gates for only single, similarly sized cells was the chosen method for recording cellular drug uptake as fluorescence per cell, on the flow cytometer.

Finally even using inclusion gates the cells were not always homogenous in their cellular drug uptake, with some cells taking up more drug than others. This difference between drug uptake in cells showed on the histograms as uneven peaks often with 'shoulders', whilst the main population of cells shows a tight typical population of cells (Fig. 9.6).

EFFECT OF DIFFERENT MEDIUMS ON CELLULAR DRUG UPTAKE

When the cells were being incubated with the drug in suspension there was a higher level of cell death than that observed from incubating the cells with drug while attached to the flasks. To minimise the amount of cell death the cells, whether in suspension or on flasks, were incubated in drug medium using an air-buffered medium, L-15. This medium maintained its pH considerably longer than the DMEM used previously which turned alkaline very quickly. This stability of pH led to increased cell integrity and life. As the L-15 medium was obviously more beneficial for the cells it was used in the balk of all future drug uptake experiments where the cells were attached to the flasks.

HEALTH OF CELLS

The health of cells could be observed by changes in cellular appearance and could only really be judged after acquiring knowledge of the cell lines. Unhealthy cells produced 'messy' dot plots with a high percentage of dead cells, leading to poor histograms and unreliable data, such as the mean fluorescence, *ie* the amount of intracellular drug accumulation.

Once the above criteria and the confluence of the cells were judged to be at an optimum the cells were than used for flow experiments and the data analysed then converted into graphs.

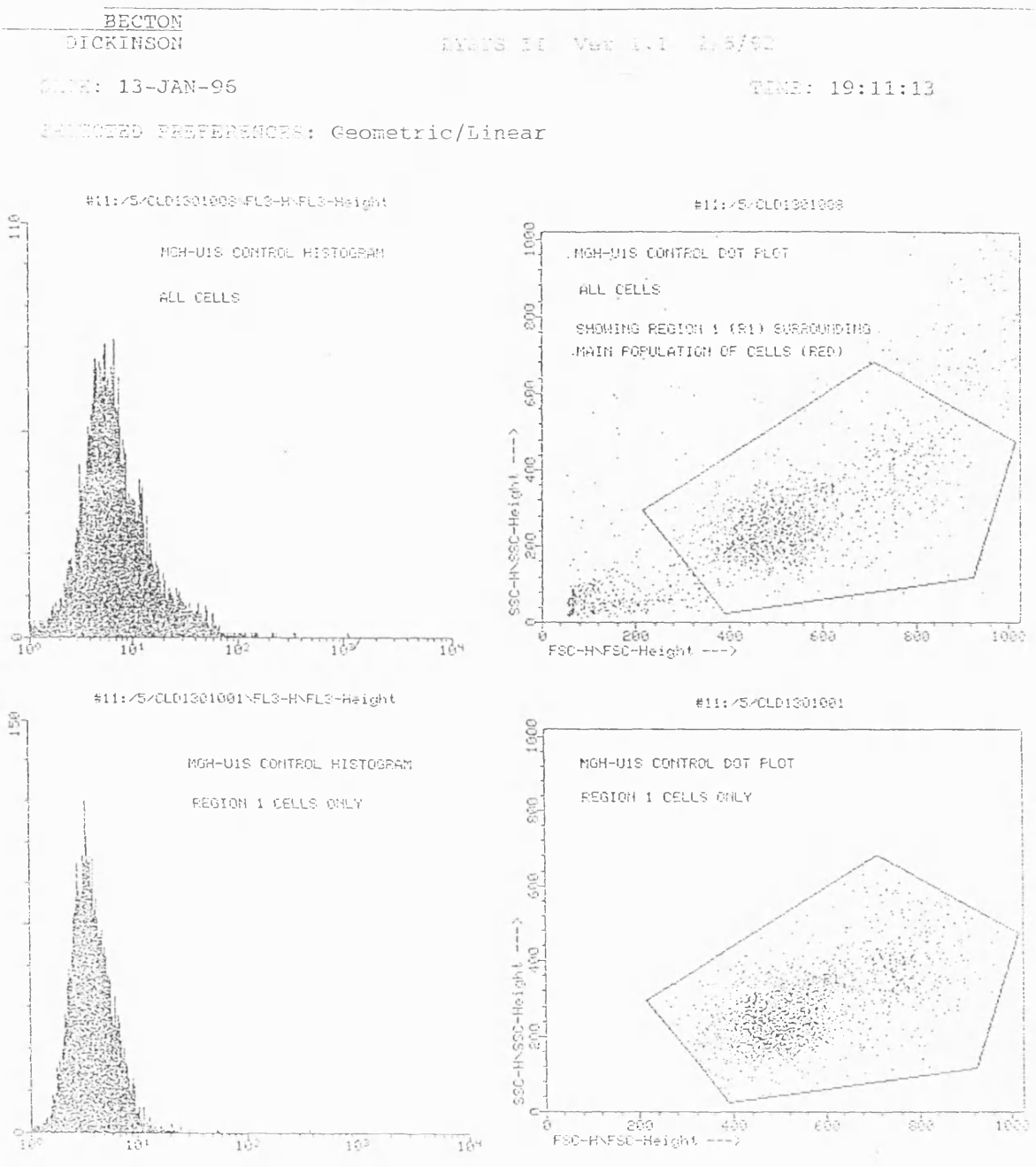

Fig. 9.3a. **Example of an inclusion gate used to record the intracellular drug fluorescence from the main population of MGH-U1 cells during flow cytometry experiments.**

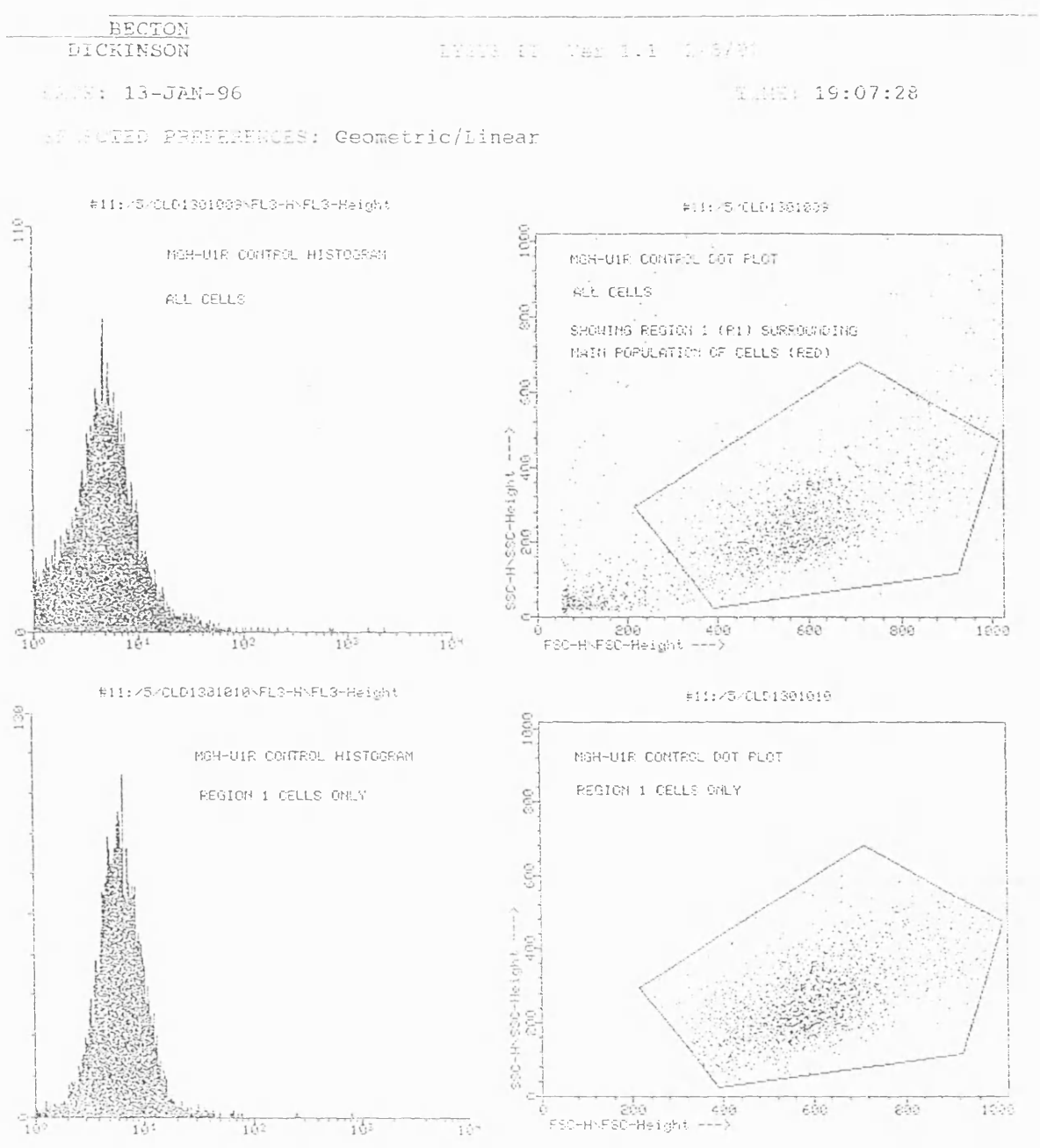

Fig. 9.3b. **Example of an inclusion gate used to record the intracellular drug fluorescence from the main population of MGH-U1/R cells during flow cytometry experiments.**

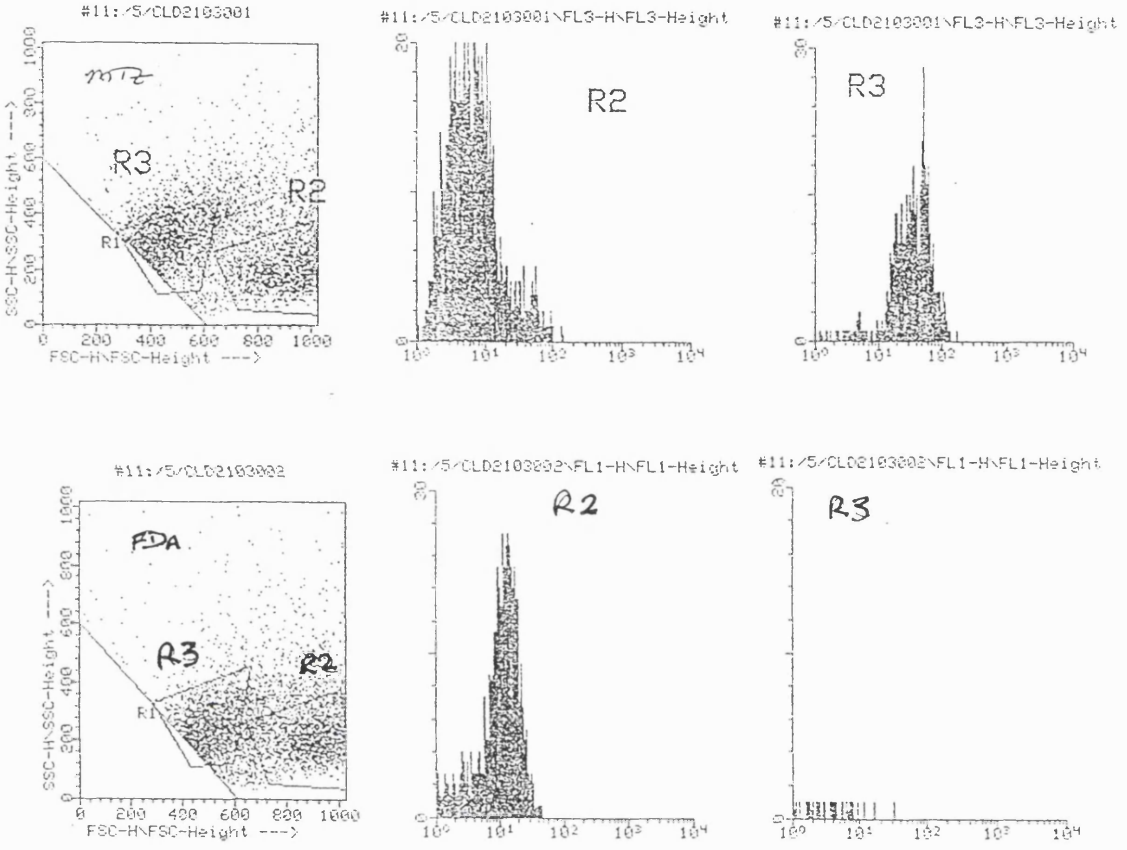

Fig. 9.4. **Use of cell viability marker FDA to show that dead cells take up more MTZ in MCF-7/R cells. Both dot plots indicated two main populations of cells, ringed as R2 and R3. By using FDA the R2 population was found to take up the marker and fluoresce so contained mainly live cells. While the R3 population of cells showed little FDA fluorescence on the histogram and contained mainly dead cells. The equivalent area on the MTZ dot plot containing the R3 dead cell population took up more MTZ than the R2 live cell population.**

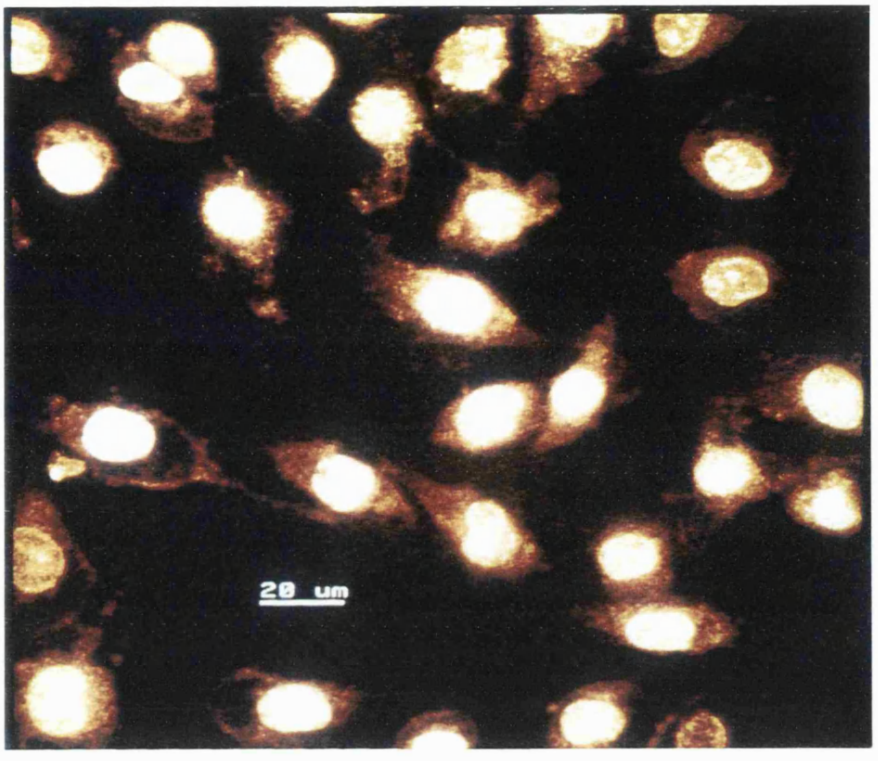

Fig. 9.5. **DOX uptake in dead MGH-U1/R cells detected using the confocal microscope. The intracellular pattern of drug uptake is very similar to that observed in sensitive cells with the nuclei containing most fluorescence.**
(X 600)

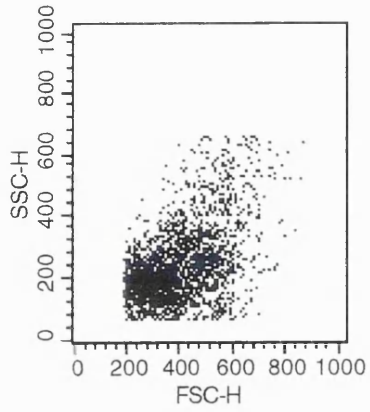

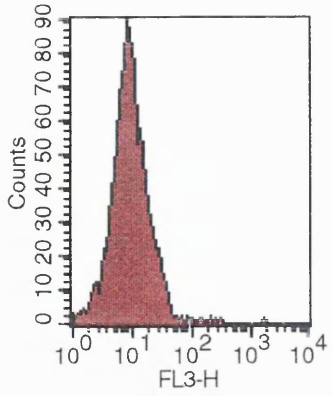

Geo Mean	Median
8.96	8.66

MGH-U1/R Control

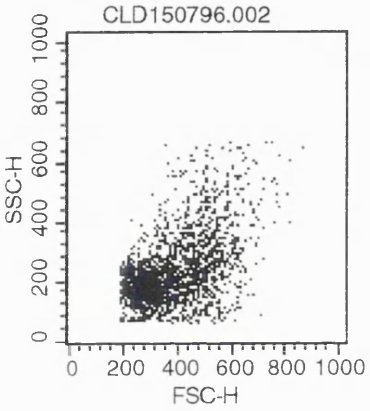

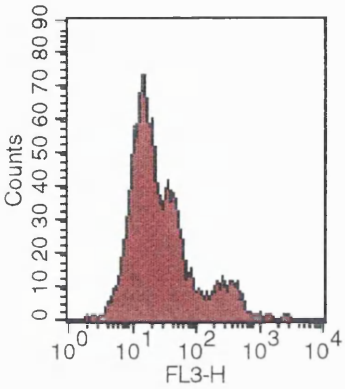

Geo Mean	Median
23.81	18.60

MGH-U1/R DOX 1µg/ml

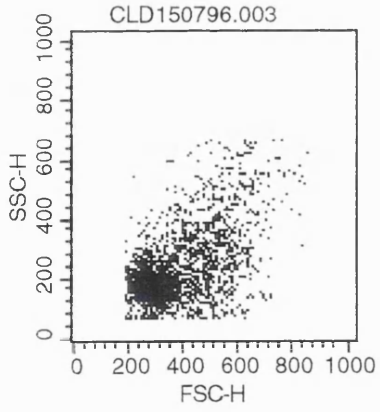

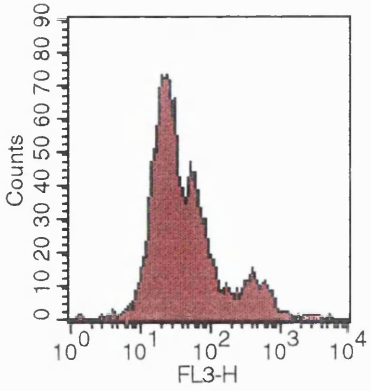

Geo Mean	Median
38.34	29.16

MGH-U1/R DOX 2µg/ml

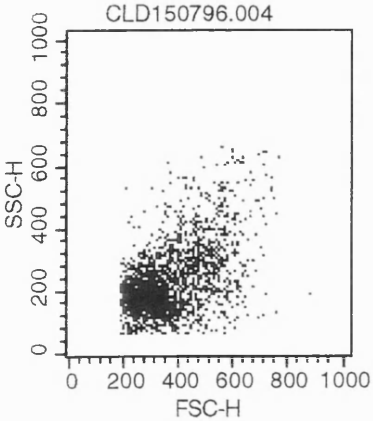

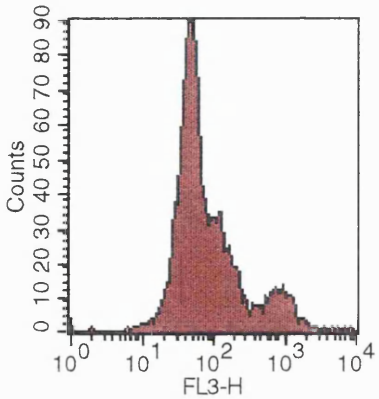

Geo Mean	Median
69.57	51.86

MGH-U1/R DOX 5µg/ml

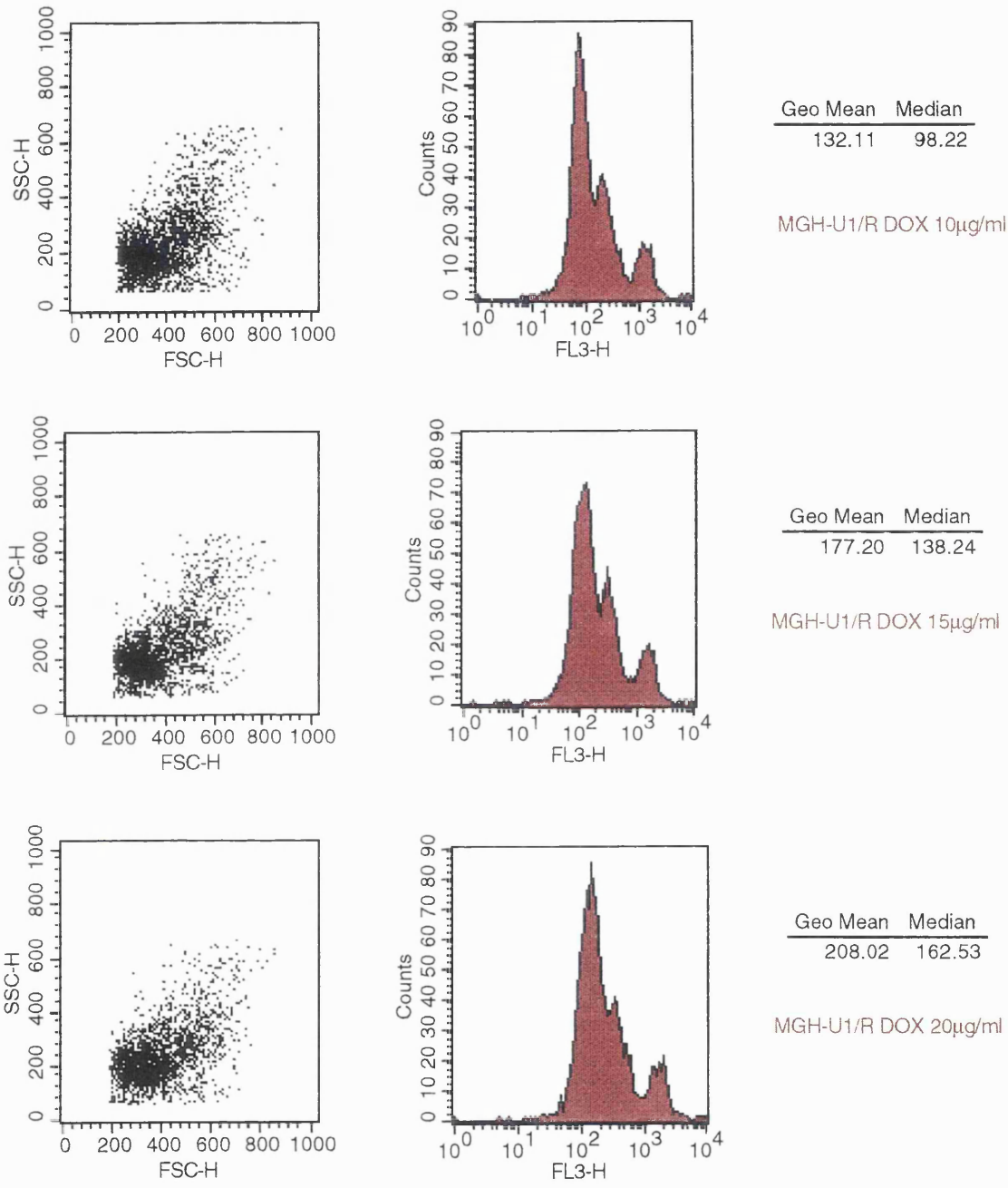

Fig. 9.6. **Difference in DOX uptake within the main poulation of cells recorded using the inclusion gate, shown as two peaks recorded on the histogram, the main peak with a 'shoulder'.**

9.3. APPENDIX 3

USE OF THE FACSCAN TO MEASURE THE DIRECT CYTOTOXICITY OF GLA

As flow cytometry can be used to discern dead cells from live with the use of fluorescent cell viability dyes it was believed that the direct cytotoxicity of GLA could be measured using this technique. The viability markers propidium iodide (PI), which stains dead cells and fluorescein diacetate (FDA) which stains live cells were used. PI enters dead cells in a non-specific manner if their membranes are damaged but fluorescence from FDA is only generated by cellular hydrolysis of this molecule by viable cells. Hence, PI will not enter the cell as the membrane is not damaged however fluorescence from FDA should have occurred if the cells were still viable. However no change in the uptake of the dyes by live or dead cells was observed, although a change in the position of the cells on the dot plots, for example a number of cells appearing in other regions apart from that containing the main population of cells were recorded. There was no real change in the dot plots or histograms of the MCF-7/R cells incubated without GLA or with varying doses of GLA. From Figs. 9.7 the region M1 represented the percentage of cells staining for FDA of PI, depending on the FACScan setting. For the control cells with FDA 97% of the cells fluoresced meaning that 97% of the cellular population was alive. Also 3% of these control cells stained positive for PI again showing that 97% of cells were alive (Fig. 9.7a). These percentages of staining did not significantly change at any dose of GLA. This was considered unusual as GLA was known to affect cells at the concentrations used so the experiments were repeated using spectophotometry. This latter method showed cell death occurring as a result of GLA addition.

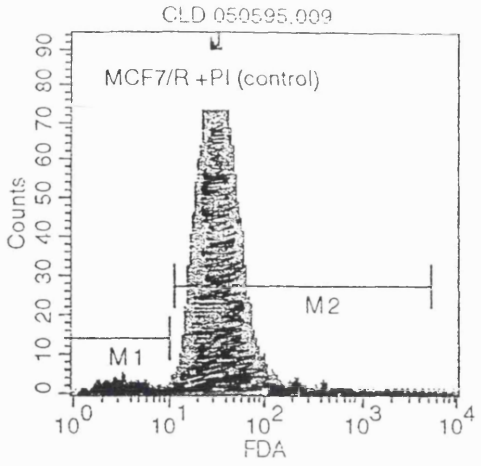

Marker	Left, Right	Events	% Gated
All	1, 9910	10000	100.00
M1	1, 10	222	2.22
M2	11, 5328	9748	97.48

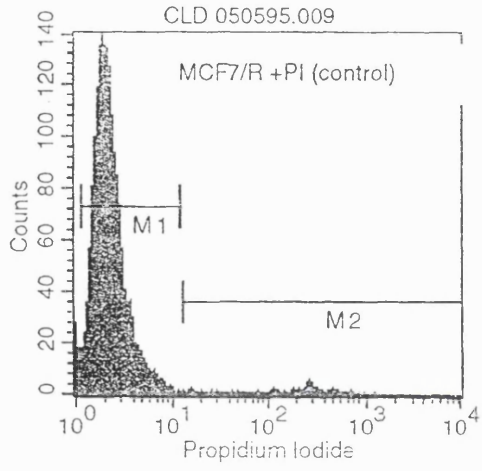

Marker	Left, Right	Events	% Gated
All	1, 9910	10000	100.00
M1	1, 12	9624	96.24
M2	13, 9910	284	2.84

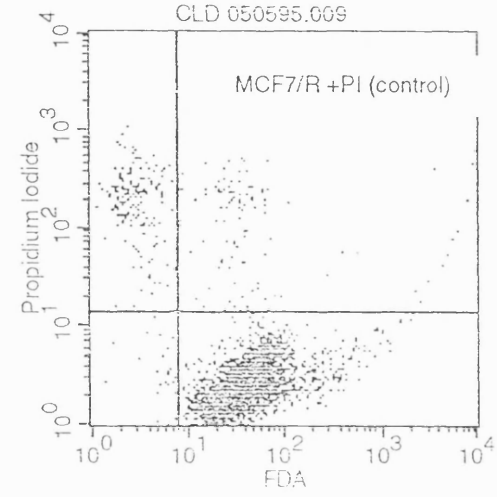

Quad	Events	% Gated
UL	173	1.73
UR	107	1.07
LL	28	0.28
LR	9692	96.92

Fig. 9.7a. Use of the FACScan to analyse the cytotoxicity of GLA on MCF-7/R cells, untreated control population.

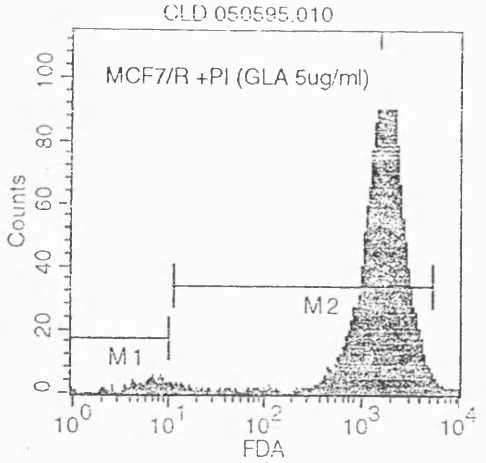

Marker	Left, Right	Events	% Gated
All	1, 9910	10000	100.00
M1	1, 10	149	1.49
M2	11, 5328	9798	97.98

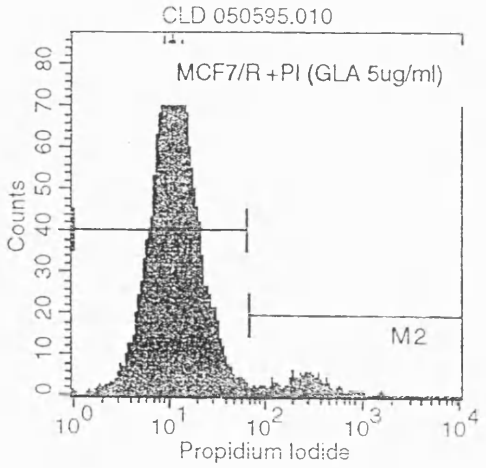

Marker	Left, Right	Events	% Gated
All	1, 9910	10000	100.00
M1	1, 63	9708	97.08
M2	67, 9910	290	2.90

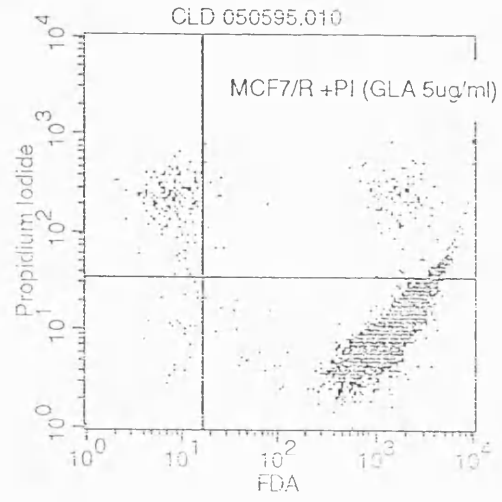

Quad	Events	% Gated
UL	177	1.77
UR	282	2.82
LL	25	0.25
LR	9516	95.16

Fig. 9.7b. Use of the FACScan to analyse the cytotoxicity of GLA on MCF-7/R cells, GLA dose of 5μg/ml.

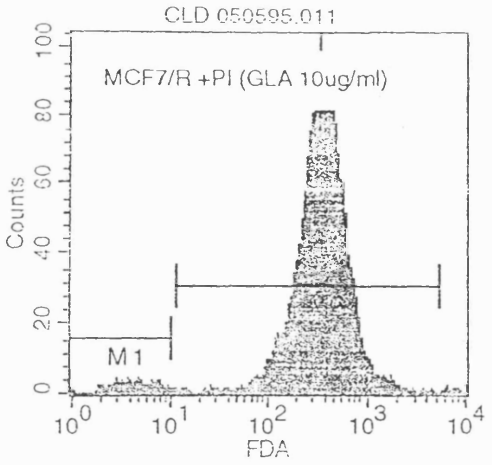

Marker	Left, Right	Events	% Gated
All	1, 9910	10000	100.00
M1	1, 10	161	1.61
M2	11, 5328	9823	98.23

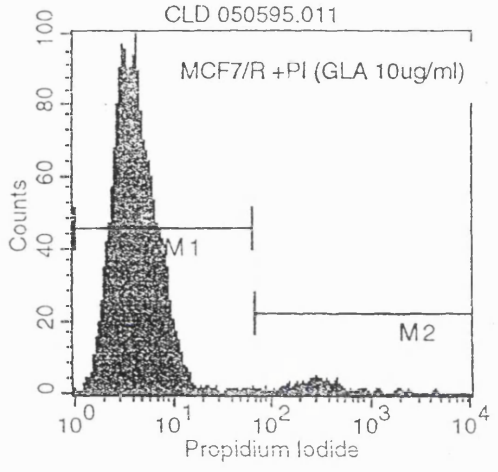

Marker	Left, Right	Events	% Gated
All	1, 9910	10000	100.00
M1	1, 63	9778	97.78
M2	67, 9910	220	2.20

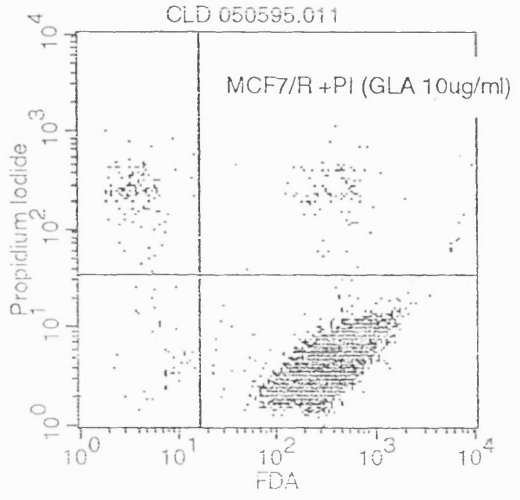

Quad	Events	% Gated
UL	132	1.32
UR	103	1.03
LL	40	0.40
LR	9725	97.25

Fig. 9.7c. Use of the FACScan to analyse the cytotoxicity of GLA on MCF-7/R cells, GLA dose of 10μg/ml.

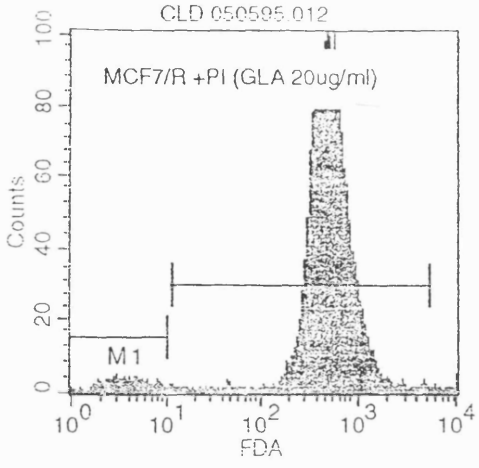

Marker	Left, Right	Events	% Gated
All	1, 9910	10000	100.00
M1	1, 10	239	2.39
M2	11, 5328	9732	97.32

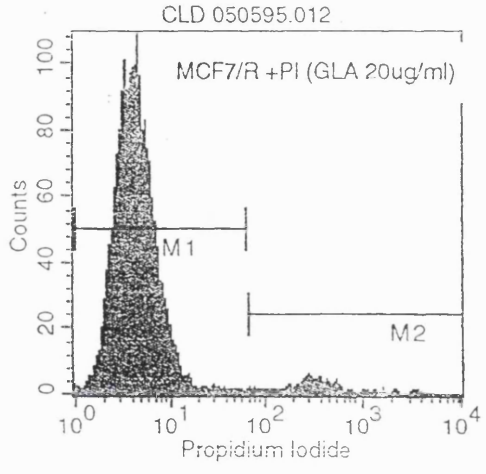

Marker	Left, Right	Events	% Gated
All	1, 9910	10000	100.00
M1	1, 63	9697	96.97
M2	67, 9910	300	3.00

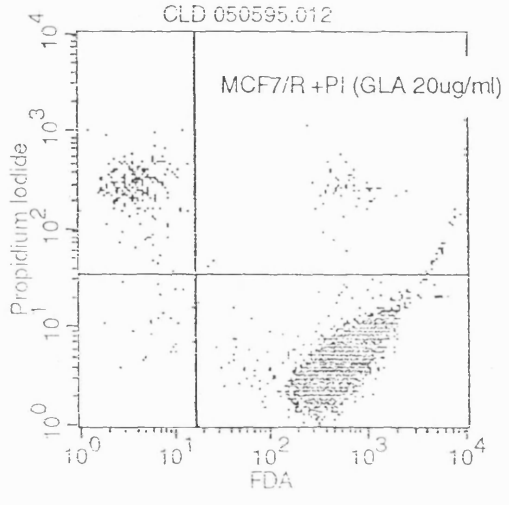

Quad	Events	% Gated
UL	231	2.31
UR	88	0.88
LL	23	0.23
LR	9658	96.58

Fig. 9.7d. Use of the FACScan to analyse the cytotoxicity of GLA on MCF-7/R cells, GLA dose of 20μg/ml.

9.4 APPENDIX 4

CHARACTERISATION OF THE CELL LINES

The MGH-U1/R cell line was obtained from Dr. John Masters at the Institute of Urology, University College London who originally obtained them from Dr. CW Lin at the Massachusetts General Hospital in Boston. The MGH-U1/R cell line was established by exposing the parental MGH-U1 cells to progressively higher concentrations of DOX over twelve months. Sensitive cells were plated at 10,000 / 100mm dish in McCoys SA medium supplemented with 5% FCS. 24h later 0.01μg/ml DOX in the same medium was added to the cells. The cells continued to grow and were fed biweekly with medium containing 0.01μg/ml of the drug. After one month, the surviving cells reached confluency and were passaged with trypsin/ EDTA. Over the next six weeks, the cells were passaged four times. Three times into medium containing DOX at 0.01μg/ml and once into medium containing DOX at 0.02μg/ml. The cells were then passaged into medium without drug and 48h later exposed to 1μg/ml DOX for 1h. DOX was removed and replaced with fresh medium without drug. When the surviving cells again reached confluency, which occurred 17 days later, the cells were exposed to 2μg/ml of DOX for 1h. The drug was removed and 7 days later, the cells passaged. 24h later 0.05μg/ml of DOX was added to the medium and the cells allowed to grow with continual exposure to the drug at this concentration. Two passages (2.5 months later) later, the drug concentration was increased to 0.1μg/ml. The cells were maintained at this drug concentration for one more month (2 passages). DOX was increased to 0.4μg/ml at which concentration the cells continued growing and multiplying. It was shown that 1% of MGH-U1/R cells were able to survive and grow at 50μg/ml of DOX[167].

The MCF-7 DOX resistant cell line was selected by growing wild type MCF-7 cells in minimum essential medium (MEM), supplemented with 5% FCS, containing 0.01μM DOX. The drug concentration was increased 1.5 fold whenever the cells were able to grow to confleuncy. The resistant MCF-7 cells were selected to grow in the presence of 10μM DOX[198].

The relative cytotoxicities of DOX and EPI against MGHU-1, MGHU-1/R, MCF-7 and MCF-7/R cells are displayed in table 9.1, showing the mean and standard errors, from a minimum of three separate experiments, of the concentration of each drug to reduce colony-forming ability by 50% (IC_{50})[175]. The only exception being the IC_{50} of DOX against MCF-7 and MCF-7/R cells which related to the ability of this drug to inhibit control growth of these cells by 50%[198]. The Topo II mRNA levels, also displayed in Table 9.1, are expressed in terms of integrated optical density values from scanned autoradiographs, each corrected according to a GADPH loading control[199].

CELL LINE	IC_{50} (μM)		mRNA LEVELS (arbitrary units)		
	DOX	EPI	TopoIIα	TopoIIβ-1	TopoIIβ-2
MGH-U1/R	3.2	4.9	9.3	14.8	2.0
MGH-U1	0.008	0.007	23.7	14.1	1.9
Ratio of MGH-U1/R : MGH-U1	400	700	0.39	1.0	1.0
MCF-7/R	4.8	0.57	1.7	2.5	1.5
MCF-7	0.025	0.018	14.5	19.3	4.1
Ratio of MCF-7/R : MCF-7	192	31.6	0.18	0.13	0.37

Table 9.1. Characterisation of the MGH-U1, MGH-U1/R, MCF-7 and MCF-7/R cell lines.